

Baseline Study of Kendal Power Station

By

DIRK MOOLMAN

Submitted in fulfilment of the requirements of the degree

Magister Scientiae

In the Faculty of Natural and Agricultural Sciences

Institute for Groundwater Studies

University of the Free State

May 2011

Study Leader: Dr P.D. Vermeulen

DECLARATION

I hereby declare that this dissertation, submitted for a Masters degree in the Faculty of Natural and Agricultural Sciences, Department of Geohydrology, University of the Free State, Bloemfontein, South Africa, is my own work and has not been submitted to any other institution of higher education. I further declare that all sources cited or quoted are indicated and acknowledged by means of a list of references.

D. Moolman

May 2011

ACKNOWLEDGEMENTS

This project was made possible by the co-operation of many individuals and institutions. I wish to record my sincere thanks to the following:

- GHT consulting for funding and support of the project;
- Mr L.J. van Niekerk for granting me the opportunity to carry out this project at GHT;
- Mr J.J.H. Hough at GHT for his assistance with the project and his leadership;
- Dr Vermeulen, in particular, for his continuous assistance; and
- Special thanks to my mother and sisters for their prayers and support during my studies.

And finally to my Lord and Saviour Jesus Christ for carrying me through the good and the bad times.

- TABLE OF CONTENTS -

1	INTRODUCTION TO THESIS	9
1.1	OBJECTIVE OF THE STUDY	9
1.2	METHODS OF INVESTIGATION	9
1.3	STRUCTURE OF THE THESIS	10
2	FLY ASH AND ITS EFFECTS	11
2.1	INTRODUCTION	11
2.2	EXISTING COAL-FIRED POWER STATIONS IN SOUTH AFRICA.....	11
2.3	CURRENTLY MOTHBALLED POWER STATIONS BEING RE-COMMISSIONED IN SOUTH AFRICA.....	12
2.4	FLY ASH IN AUSTRALIA	12
2.5	FLY ASH IN CHINA	13
2.5.1	<i>Water pollution at China power stations</i>	<i>14</i>
2.5.2	<i>Improving coal ash pollution management legislation</i>	<i>14</i>
2.6	FLY ASH IN EUROPEAN COUNTRIES	15
2.6.1	<i>Utilisation.....</i>	<i>18</i>
2.6.2	<i>Transfrontier movements (only for recovery operations)</i>	<i>20</i>
2.6.3	<i>Ecotoxicity.....</i>	<i>20</i>
2.6.4	<i>Environmental Compatibility</i>	<i>21</i>
2.7	ASH DISPOSAL.....	22
2.7.1	<i>Ash disposal methods</i>	<i>22</i>
2.7.1.1	<i>Above-ground ashing.....</i>	<i>22</i>
2.7.1.2	<i>Sub-surface ashing.....</i>	<i>23</i>
2.7.2	<i>Ash and effluents</i>	<i>24</i>
2.7.3	<i>Dry ash disposal</i>	<i>25</i>
2.7.4	<i>Wet ash disposal</i>	<i>26</i>
2.8	COMPARISON BETWEEN EUROPEAN COUNTRIES, CHINA AND SOUTH AFRICA’S FLY ASH PROBLEMS	26
3	BASELINE STUDY CONDUCTED AT KENDAL POWER STATION - PHYSICAL GEOGRAPHY AND DRAINAGE	28
3.1	INTRODUCTION	28
3.2	RAINFALL DATA	28
3.3	SURFACE TOPOGRAPHY AND DRAINAGE.....	29
3.3.1	<i>Impacts upon receiving waterbodies</i>	<i>32</i>
3.3.1.1	<i>Heuwelfontein spruit.....</i>	<i>32</i>
3.3.1.2	<i>Schoongezicht spruit.....</i>	<i>32</i>
3.3.1.3	<i>Leeuwfontein spruit.....</i>	<i>32</i>
3.3.1.4	<i>Zondagsfontein spruit.....</i>	<i>32</i>
3.3.2	<i>Sub-catchments</i>	<i>32</i>
3.3.2.1	<i>Sub-catchment B20F – A.....</i>	<i>32</i>
3.3.2.2	<i>Sub-Catchment B20E – A</i>	<i>33</i>
3.4	GEOLOGY.....	33
3.5	GEOPHYSICS	35
3.5.1	<i>Geophysical Investigations.....</i>	<i>35</i>
3.5.2	<i>Results of magnetometer survey</i>	<i>37</i>
3.5.3	<i>Drilling results</i>	<i>42</i>
3.5.4	<i>Conclusions</i>	<i>43</i>
4	RISK ASSESSMENT	44
4.1	INTRODUCTION	44
4.2	IDENTIFYING POLLUTION SOURCES.....	46
4.3	GROUNDWATER QUALITY-INORGANIC PARAMETERS	48
4.3.1	<i>Discussion of groundwater qualities</i>	<i>55</i>
4.3.2	<i>Pollution index tables.....</i>	<i>57</i>
4.3.3	<i>Indicator elements</i>	<i>61</i>
4.3.4	<i>Pollution index results.....</i>	<i>62</i>
4.3.5	<i>Monitoring boreholes exceeding average concentrations of hydrocensus boreholes.</i>	<i>62</i>
4.3.6	<i>Conclusions</i>	<i>68</i>
4.4	AERIAL MAGNETIC INTERPRETATION	69
4.5	GENERATING WATER LEVELS	71

4.6	CALCULATING POLLUTION MIGRATION DISTANCES	74
4.6.1	<i>Calculated gradients</i>	74
4.6.2	<i>Slug test method</i>	78
4.6.3	<i>Calculation of hydraulic conductivity</i>	79
4.6.4	<i>Slug test results</i>	79
4.6.5	<i>Conclusions</i>	85
4.7	COMPARING METHODS TO EVALUATE RISK ASSESSMENT	90
4.7.1	<i>Ogata Banks</i>	90
4.8	BACKTRACKING	91
4.9	EFFECTS OF KENDAL POWER STATION ON LEEUWFontein AND SCHOONGEZICHT SPRUIT	93
4.9.1	<i>Leeuwfontein Spruit</i>	93
4.9.2	<i>Schoongezicht Spruit</i>	94
4.9.3	<i>Stiff diagrams</i>	99
4.9.4	<i>Conclusions</i>	102
4.10	GROUNDWATER POLLUTION MIGRATION FROM ASH STACK TO LEEUWFontein AND SCHOONGEZICHT SPRUIT.	103
4.10.1	<i>Seepage Velocity calculations</i>	104
4.10.2	<i>Conclusions</i>	106
5	AQUIFER VULNERABILITY	107
5.1	INTRODUCTION	107
5.2	UNSATURATED ZONE CHARACTERISTICS.....	108
5.2.1	<i>Soil hydraulic parameters results</i>	112
5.3	VULNERABILITY OF GROUNDWATER AQUIFER DUE TO HYDROGEOLOGICAL CONDITIONS	112
5.4	CLASSIFYING AQUIFER VULNERABILITY WITHIN DIFFERENT AREAS RELATIVE TO THE SATURATED ZONE	113
5.4.1	<i>Coal Stockyard Area</i>	113
5.4.2	<i>Ash stack</i>	116
5.4.3	<i>Power station</i>	119
6	CONCLUSIONS	123
6.1	RECOMMENDATIONS	124
7	REFERENCES	126
8	APPENDICES	128

- LIST OF FIGURES -

FIGURE 1.	PRODUCTION OF COAL FLY ASH IN 1997 (SOURCE: ECOBA).	17
FIGURE 2.	PRODUCTION AND UTILIZATION OF COAL FLY ASH IN EUROPE (SOURCE ECOBA)	17
FIGURE 3.	RECOVERY AND DISPOSAL OF COAL FLY ASH IN EUROPEAN COUNTRIES (SOURCE ECOBA).	19
FIGURE 4.	UTILISATION OF COAL FLY ASH IN EUROPEAN COUNTRIES IN 1997 (SOURCE ECOBA).	19
FIGURE 5.	CONVEYOR BELT ASH DISPOSAL.	26
FIGURE 6.	AVERAGE RAINFALL RECORDED AT WEATHER STATION 0477 695 (OVER A PERIOD OF 70 YEARS).	29
FIGURE 7.	1:50 000 TOPOGRAPHY MAP.	30
FIGURE 8.	DRAINAGE REGIONS, SUB-CATCHMENT AREAS AND SURFACE RUNOFF.	31
FIGURE 9.	GEOLOGY MAP.	34
FIGURE 10.	GEOPHYSICAL TRAVERSE AND NEWLY DRILLED BOREHOLES.	36
FIGURE 11.	W-E MAGNETIC PROFILE OF TRAVERSE 1.	37
FIGURE 12.	S-N MAGNETIC PROFILE OF TRAVERSE 2.	38
FIGURE 13.	S-N MAGNETIC PROFILE OF TRAVERSE 3.	38
FIGURE 14.	W-E MAGNETIC PROFILE OF TRAVERSE 4.	39
FIGURE 15.	S-N MAGNETIC PROFILE OF TRAVERSE 5.	40
FIGURE 16.	NW-SE MAGNETIC PROFILE OF TRAVERSE 6.	40
FIGURE 17.	NW-SE MAGNETIC PROFILE OF TRAVERS 7.	41
FIGURE 18.	NW-SE MAGNETIC PROFILE OF TRAVERSE 8.	42
FIGURE 19.	POLLUTION SOURCES.	47
FIGURE 20.	SO ₄ CONCENTRATIONS OF MONITORING BOREHOLES.	53
FIGURE 21.	EC CONCENTRATIONS OF MONITORING BOREHOLES.	53
FIGURE 22.	CA CONCENTRATIONS FOR MONITORING BOREHOLES.	54
FIGURE 23.	CL CONCENTRATIONS FOR MONITORING BOREHOLES.	54
FIGURE 24.	NA CONCENTRATIONS FOR MONITORING BOREHOLES.	55
FIGURE 25.	HYDROCENSUS AND MONITORING BOREHOLES.	59
FIGURE 26.	BOREHOLES EXCEEDING AVERAGE CA CONCENTRATIONS OF HYDROCENSUS BOREHOLES.	63
FIGURE 27.	BOREHOLES EXCEEDING AVERAGE CL CONCENTRATIONS OF HYDROCENSUS BOREHOLES.	64
FIGURE 28.	BOREHOLES EXCEEDING AVERAGE ELECTRICAL CONDUCTIVITY OF HYDROCENSUS BOREHOLES.	65
FIGURE 29.	BOREHOLES EXCEEDING AVERAGE NA CONCENTRATIONS OF HYDROCENSUS BOREHOLES.	66
FIGURE 30.	BOREHOLES EXCEEDING AVERAGE SO ₄ CONCENTRATIONS OF HYDROCENSUS BOREHOLES.	67
FIGURE 31.	AERIAL MAGNETIC MAP.	70
FIGURE 32.	CORRELATION BETWEEN TOPOGRAPHY AND GROUNDWATER LEVEL.	72
FIGURE 33.	GROUNDWATER FLOW.	73
FIGURE 34.	POLLUTION DISTANCES (COAL STOCKYARD.)	75
FIGURE 35.	SLUG TEST DATA ANALYSED BY MEANS OF THE BOWER AND RICE METHOD (BOREHOLE AB16).	80
FIGURE 36.	SEEPAGE VELOCITY, COAL STOCKYARD TO HYDROCENSUS BOREHOLES	84
FIGURE 37.	POLLUTION MIGRATION DISTANCES; BAR CHART.	84
FIGURE 38.	POLLUTION MIGRATION WHEN COMPARING HYDROCENSUS BOREHOLES FBB32 AND FBB38.	86
FIGURE 39.	WATER DIVIDE INFLUENCING POLLUTION MIGRATION.	89
FIGURE 40.	RAPID ESTIMATION OF GROUNDWATER FLUX TOWARDS BOREHOLE FBB38.	90
FIGURE 41.	BACKTRACKING.	92
FIGURE 42.	COAL MINE NEXT TO SAMPLING SITE R01.	93
FIGURE 43.	SULPHATE CONCENTRATIONS AT MONITORING SITES IN LEEUWFORTEIN SPRUIT.	94
FIGURE 44.	ADDITIONAL CONCENTRATIONS AT MONITORING SITES IN LEEUWFORTEIN SPRUIT.	94
FIGURE 45.	ARRANGEMENT OF DIRTY AND CLEAN WATER DAMS AT KENDAL POWER STATION (SOURCE FDI HODGSON ET AL.,1998)	95
FIGURE 46.	SITES R03 AND PP05 SULPHATE CONCENTRATIONS.	97
FIGURE 47.	1991 TO 2010 RAINFALL.	97
FIGURE 48.	SULPHATE CONCENTRATIONS AT LEEUWFORTEIN AND SCHOONGEZICHT SPRUIT.	98
FIGURE 49.	CURRENT CONCENTRATIONS (2009).	99
FIGURE 50.	JANUARY 2008 CONCENTRATIONS.	100
FIGURE 51.	JULY 2003 CONCENTRATIONS.	100
FIGURE 52.	NOVEMBER 2002 CONCENTRATIONS.	101
FIGURE 53.	JULY 2000 CONCENTRATIONS.	101
FIGURE 54.	2010 SIMULATED SO ₄ POLLUTION PLUME CONTOURS. (SOURCE: GROUNDWATER PLUME INVESTIGATIONS 2009)	103
FIGURE 55.	GRADIENT LINES FROM ASH STACK TO SCHOONGEZICHT AND LEEUWFORTEIN SPRUIT.	105
FIGURE 56.	AUGER HOLE AD09 DRILLED AT ASH STACK.	108
FIGURE 57.	SIEVE PERMEABILITY AND SOPROP CALCULATIONS FOR PD02-A.	109

FIGURE 58.	SIEVE PERMEABILITY AND SOPROP CALCULATIONS FOR PD02-B.	110
FIGURE 59.	AUGER HOLES DRILLED FOR SIEVE ANALYSIS.	111
FIGURE 60.	BOREHOLES AND AUGER HOLES IN THE COAL STOCKYARD AREA.	114
FIGURE 61.	BOREHOLES AND AUGER HOLES LOCATED IN THE ASHING AREA.	117
FIGURE 62.	BOREHOLES AND AUGER HOLES LOCATED IN THE POWER STATION AREA.	120

- LIST OF TABLES -

TABLE 1.	AVERAGE RAINFALL RECORDED AT TWO WEATHER STATIONS WITHIN RAINFALL ZONE B2B.	29
TABLE 2.	TABLE SHOWING LOCAL LITHOLOGICAL MAKE UP WITH CHRONOLOGICAL TIME CONSTRAINTS.....	33
TABLE 3.	SUMMARY OF DRILLING RESULTS.	43
TABLE 4.	HYDROCENSUS BOREHOLE INFORMATION.	45
TABLE 5.	GLOSSARY OF CHEMISTRY ABBREVIATIONS.	48
TABLE 6.	SANS 241:2006 EDITION 6.1.	49
TABLE 7.	WATER QUALITY TABLES OF MONITORING BOREHOLES.....	50
TABLE 8.	WATER QUALITY TABLES OF HYDROCENSUS BOREHOLES.....	51
TABLE 9.	WATER QUALITY TABLES OF POLLUTED DAMS.	52
TABLE 10.	AVERAGE PARAMETER VALUES.....	60
TABLE 11.	CURRENT CONCENTRATION OF INDICATOR ELEMENTS.....	61
TABLE 12.	POLLUTION INDEX RESULTS.	62
TABLE 13.	CALCULATED HYDROCENSUS BOREHOLES WATER LEVELS.	71
TABLE 14.	CALCULATED POLLUTION SOURCE WATER LEVELS.	74
TABLE 15.	CALCULATED GRADIENTS.	76
TABLE 16.	DISTANCES BETWEEN HYDROCENS BOREHOLES AND POLLUTION SOURCES AND ADDITIONAL INFORMATION.	77
TABLE 17.	SLUG TEST RESULTS.	81
TABLE 18.	EFFECTIVE POROSITY TABLE. (SOURCE: MULLER, J. 1994).	81
TABLE 19.	DARCY AND SEEPAGE VELOCITY CALCULATION; COAL STOCKYARD TO HYDROCENSUS BOREHOLES.	83
TABLE 20.	POLLUTION MIGRATION DISTANCE; COAL STOCKYARD TO HYDROCENSUS BOREHOLES.	83
TABLE 21.	DISTANCES TO HYDROCENSUS BOREHOLES AND DISTANCES TRAVELLED OVER 10 YEARS.	87
TABLE 22.	YEARS FOR CONTAMINATION TO REACH DOWN GRADIENT HYDROCENSUS BOREHOLES.	87
TABLE 23.	OGATA BANKS RESULTS.	91
TABLE 24.	GRADIENT CALCULATIONS.....	104
TABLE 25.	SEEPAGE VELOCITY CALCULATIONS.....	104
TABLE 26.	VULNERABILITY OF GROUNDWATER AQUIFER DUE TO HYDROGEOLOGICAL CONDITIONS (GROUNDWATER PROTOCOL VERSION 2, 2003).	107
TABLE 27.	AVERAGE AND GEOMETRIC MEAN OF HYDRAULIC CONDUCTIVITY AT SOIL SAMPLES.	112
TABLE 28.	VULNERABILITY OF GROUNDWATER AQUIFER DUE TO HYDROGEOLOGICAL CONDITIONS.	113
TABLE 29.	COAL STOCKYARD BOREHOLE DATA.....	115
TABLE 30.	COAL STOCKYARD AUGER HOLE DATA.	115
TABLE 31.	VULNERABILITY OF GROUNDWATER AQUIFER AT COAL STOCKYARD.....	116
TABLE 32.	ASH STACK BOREHOLE DATA.....	118
TABLE 33.	ASH STACK AUGER HOLE DATA.	118
TABLE 34.	VULNERABILITY OF GROUNDWATER AQUIFER AT ASH STACK.	119
TABLE 35.	POWER STATION BOREHOLE DATA.	121
TABLE 36.	POWER STATION AUGER HOLE DATA.	121
TABLE 37.	VULNERABILITY OF GROUNDWATER AQUIFER AT POWER STATION.	122

LIST OF APPENDICES

Appendix A - Newly drilled boreholes

Appendix B - Pollution sources

Appendix C - Slug tests

Appendix D - Calculations

Appendix E - Sieve analysis results

Appendix F - Ogata Banks results

Appendix G - Borehole logs

- GLOSSARY OF GEOHYDROLOGICAL DEFINITIONS -

Geological term	Definition
Aquifer	Water bearing geological formation.
Fractured rock aquifer	Groundwater occurring in within and fissures in hard-rock formations. Groundwater: Refers to water filling the pores and voids in geological formations below the water table
Groundwater flow	The movement of water through openings and pore spaces in rock below the water table i.e. in the saturated zone. Groundwater naturally drains from higher lying areas to low lying areas such as rivers, lakes and oceans. The rate of flow depends on the slope of of the water table and the transmissivity of the geological formations.
Hydraulic conductivity	The hydraulic conductivity is the constant of proportionally in Darcy's law. It is defined as the volume of water that will move threw a porous medium in a unit time under a unit hydraulic gradient through a unit area measured at right angles to the direction of flow.
Hydrocensus	A field survey by which all relevant information regarding groundwater is amassed. This typically includes yields, borehole equipment, groundwater levels, casing height /diameter, WGS84 coordinates, potential pollution risks, photos etc.
Permeability	The ease with which a fluid can pass threw a porous medium and is defined as the volume of fluid discharged from a unit area of a aquifer under unit hydraulic gradient in unit time (expressed as m ³ /m ² or m/d). It is an intrinsic property of the porous medium and is independent of the properties of the saturated fluid; not to be confused with hydraulic conductivity, which relates specifically to the movement of water.
Pollution	The introduction into the environment of any substance by the action of man that is, or results in, significant harmful effects to man or the environment.
Porosity	The porosity of a rock is its property of containing pores or voids. With consolidated rocks and hard rocks, a distinction is usually made between primary porosity, which is present when the rock is formed and secondary porosity , which develops later as result of solution of fracturing.
Recharge	Groundwater recharge or deep drainage or deep percolation is a hydraulic process where water moves downward from surface water to groundwater. This process usually occurs in the vadose zone below plant roots and is often expressed as a flux to the water table surface. Recharge occurs both naturally (through the water cycle) and anthropogically (i.e. "artificial groundwater recharge "), where rainwater and or reclaimed is touted to the subsurface.
Saturated zone	The subsurface zone below the water table where interstices are filled with water under pressure greater than that of the atmosphere.
Unsaturated zone	The part of the geological stratum above the water table where interstices and voids contain a combination of air and water, synonymous with zone of aeration or vadose zone.
Water table	The upper surface of the saturated zone of an unconfined aquifer at which pore pressure is at the atmospheric pressure, the depth to which many fluctuate seasonally.

1 INTRODUCTION TO THESIS

A hydrological and geohydrological baseline study was conducted at Kendal Power Station. In order to evaluate the aquifer vulnerability and risk assessment study, additional tests had to be performed and further interpretation of existing data had to be carried out.

1.1 OBJECTIVE OF THE STUDY

The following tasks were performed during this project:

- Evaluating the surface topography;
- Describing the geology and determine aquifer parameters (aquifer physics – slug tests);
- Describing the hydrology and geohydrology;
- Pollution source investigation;
- Risk assessment regarding pollution migration and effects of the ash stack on the surface and groundwater; and
- Aquifer vulnerability assessment.

1.2 METHODS OF INVESTIGATION

A hydrocensus was conducted to generate the necessary data to describe the baseline conditions in terms of groundwater elevations and groundwater qualities. In terms of existing data the following were available:

- Geological data (borehole logs);
- Geophysical data;
- Chemistry data;
- Slug test data; and
- Water levels.

In terms of required data the following tasks were performed to obtain the data.

- Soil hydraulic parameters (auger holes drilled);
- Generating water levels for entire study area; and

- Utilizing data for risk assessment.

Geophysical investigations were performed to detect and delineate geological features that may be associated with preferential pathways for groundwater migration and contaminant transport and to upgrade the monitoring system with new boreholes.

Slug tests were conducted at the boreholes of Kendal Power Station to determine the K (hydraulic conductivity) values of the boreholes.

Risk assessment was performed in order to calculate possible pollution migration in the groundwater.

Auger holes were drilled at possible pollution sources for sieve test analysis to characterise the soil properties for evaluation of the aquifer vulnerability assessment.

1.3 STRUCTURE OF THE THESIS

- Chapter 2 is a discussion of fly ash and its effects and how power stations impact the groundwater and environment in different countries;
- Chapter 3 discusses the area drainage, geology and the drilling phase conducted to upgrade the monitoring system;
- Chapter 4 is a discussion of the risk assessment and all of the tests performed at Kendal Power Station to evaluate the risk assessment; and
- Chapter 5 discusses and evaluate the aquifer vulnerability of Kendal Power Station and the difference if aquifer vulnerability is evaluated within different areas.

2 FLY ASH AND ITS EFFECTS

2.1 INTRODUCTION

South Africa's power supply mainly relies on coal fired power stations which releases large quantities of fly ash into the environment. It is required that ash management must be up to standard to prevent groundwater pollution from these fly ash deposits into the environment.

Coal-fired power generation is a principal energy source throughout the world. Approximately 70–75% of coal combustion residues are fly ash and its utilization worldwide is only slightly above 30%. The remainder is disposed of in landfills and fly ash basins. It is desirable to revegetate these sites for visual purposes, to stabilize the surface ash against wind and water erosion and to reduce the quantity of water leaching through the deposit. (R.J. Haynes, 2009) Since large scale coal firing for power generation began in the 1920s, many millions of tonnes of ash and related products have been produced worldwide. Today, 52% of the capacity for generation of electricity in USA alone is from coal and the consumption of coal worldwide is projected to increase by 36% between 2000 and 2020 (Jala and Goyal, 2006).

2.2 EXISTING COAL-FIRED POWER STATIONS IN SOUTH AFRICA

The following was taken from Source Watch (www.sourcewatch.org) to indicate the number of coal-fired power stations in South Africa.

- Arnot Power Station: 2,140 MW installed capacity comprising 4 X 350 MW units and 2 X 370 MW units. The power station is located in Middelburg, Mpumalanga; Eskom plans to commission 60 MW upgrades in 2008, a further 60 megawatts in each of 2009 and a further 30 MW in 2010.
- Duvha Power Station: 3,600 MW installed capacity comprising 6 X 600 MW units. The power station is located in Witbank, Mpumalanga.
- Hendrina Power Station: 2,000 MW installed capacity comprising 10 X 200 MW units. The power station is located in Hendrina, Mpumalanga.
- Kendal Power Station: 4,116 MW installed capacity comprising 6 X 686 MW units. The power station is located in Witbank, Mpumalanga.

- Kriel Power Station: 3,000 MW installed capacity comprising 6 X 500 MW units. The power station is located in Kriel, Mpumalanga.
- Lethabo Power Station: 3,708 MW installed capacity comprising 6 X 618 MW units. The power station is located in Sasolburg, Free State.
- Majuba Power Station: 4,110 MW installed capacity comprising 3 X 657 MW units and 3 X 713 MW units. The power station is located in Volksrust, Mpumalanga.
- Matimba Power Station: 3,990 MW installed capacity comprising 6 X 665 MW units. The power station is located in Ellisras, Limpopo Province.
- Matla Power Station: 3,600 MW installed capacity comprising 6 X 600 MW units. The power station is located in Kriel, Mpumalanga.
- Tutuka Power Station: 3,654 MW installed capacity comprising 6 X 609 MW units. The power station is located in Standerton, Mpumalanga.

2.3 CURRENTLY MOTHBALLED POWER STATIONS BEING RE-COMMISSIONED IN SOUTH AFRICA

- Camden Power Station: 1,580 MW installed capacity comprising 6 X 200 MW units and 2 X 190 MW units. The power station is located in Ermelo, Mpumalanga. In 2007 Eskom re-commissioned 390 megawatts. Plans were made to re-commission a further 390 megawatts in 2008.
- Grootvlei Power Station: 1,200 MW installed capacity comprising 6 X 200 MW units. The power station is located in Balfour, Mpumalanga. Eskom planned to re-commission 585 megawatts in 2008 and 2009 respectively.
- Komati Power Station: 1 000 MW installed capacity comprising 5 X 100 MW units and 4 X 125 MW units. The power station is located in Middelburg, Mpumalanga. Eskom planned to re-commission 120 megawatts in 2008, 240 megawatts in 2009, 320 megawatts in 2010 and 285 megawatts in 2011.

2.4 FLY ASH IN AUSTRALIA

Coal-fired power generation in Australia during 2005, for example, with an installed capacity of just over 29,000 MW, produced some 14.55 Mt of ash (Ness and Heeley, 2007). In the absence of flue gas desulphurisation due to use of low-sulphur coals, most of this material (85–90%) is represented by fine (essentially silt sized) fly ash particles and the remainder by coarser aggregates typically described as bottom ash. Around 2 Mt of the ash is sold per year,

mainly for use in the cement and concrete industries, and a further 4 Mt is used for other beneficial purposes, such as structural fill, road construction and mine backfill (Ness and Heeley, 2007). The remainder, representing around 7 Mt per year, is stored as a resource for possible future use, either under water in ash ponds (lagoons) or above the water table in dry disposal emplacements. Overall levels of environmentally-significant trace elements in Australian fly ashes are generally low compared to those produced from Chinese or European power stations (Liu et al., 2004; Moreno et al, 2005).

Nevertheless, there is still some community concern that the emplacement of these ashes might lead to the release of potentially environmentally harmful leachates to the surrounding ground and surface waters over time (Ward et al, 2009).

2.5 FLY ASH IN CHINA

The following section was abbreviated from “The true cost of coal, 2010” p4. Coal ash production has grown by 2.5 times in the eight years since 2002, when China began to rapidly expand its installed capacity of coal-fired plants. Coal ash is now the country’s single largest source of solid industrial waste. In 2009, China produced in excess of 375 million tons of coal ash, equivalent to more than twice that year’s urban waste production. The total volume came to 424 million cubic meters (m³). Greenpeace estimates that the total coal ash waste produced by China’s coal power sector each year contains 358.75 tons of cadmium, 10,054.25 tons of chromium, 9,410 tons of arsenic, 4.25 tons of mercury and 5,345.5 tons of lead. Altogether, that is 25,000 tons of heavy metals (Yang Ailun et al, 2010)

China has long been over-dependent on coal for its energy needs. Currently, more than 70% of China’s energy is generated by burning coal, and as the economy continues to grow at a fast rate, so too does its coal consumption. The power sector is one of the largest consumers of coal, with more than half of national coal consumption going towards electricity generation. Coal ash is the inevitable waste product from coal combustion. Generally speaking, every four tons of coal burned produce one ton of coal ash. In 2009, China consumed more than three billion tons of coal, more than half of which was used to generate electricity. If not dealt with properly, such enormous quantities of coal ash pose a dangerous threat to China’s environment and public health. (Yang Ailun et al, 2010) (The true cost of coal 2010 p7)

2.5.1 Water pollution at China power stations

The following information was obtained from “The true cost of coal, 2010” p7. If the impoundment is not properly secured against leakages, pollutants in coal ash can leach into the groundwater. This is especially common at wet ash ponds, where the coal ash is mixed with water. As the coal ash soaks in the water, the heavy metals and other harmful substances can leach out into the earth, ultimately seeping into the groundwater. This can cause the contamination of local water sources, the discharge of suspended matter into drinking wells, the fluoridation and alkalization of water and so on. Coal ash can also be blown by the wind into rivers and lakes. (Yang Ailun et al, 2010)

The following section was abbreviated from “The true cost of coal, 2010” p13. Surface water samples taken from four power stations out of six showed concentrations of pollutants that exceeded levels stipulated in the “Environmental Quality Standards for Surface Water” and “Standards for Irrigation Water Quality”. Water samples from Douhe Power Plant had traces of fluorides 233% higher than the concentration allowed by the “Environmental Quality Standards,” while water samples from Chifeng Thermal Power Plant contained fluoride at concentrations 187% higher than that allowed. In terms of the “Standards for Irrigation Water Quality,” water samples from Douhe Power Plant contained fluoride at concentrations of 67% over the maximum, while the Chifeng Power Plant’s water sample showed boron at concentrations of 29% over the maximum and fluorides at 43% over the maximum. At Fengzhen Power Plant, boron exceeded maximum concentrations by 400%, and at Datong Number Two Power Plant, boron exceeded concentrations by 17%. Of the samples of underground well water taken from near eight power stations, three of them contained concentrations of pollutants that exceeded levels set by the “Sanitary Standards for Drinking Water.” At Douhe Power Plant, the concentration of nitrates was 36% over the maximum; at Chifeng Thermal Power Plant, boron was found in concentrations 80% over the maximum; at Yuanbaoshan Power Plant, boron concentrations exceeded the maximum by 270%, molybdenum concentrations by 103%, nitrate concentrations by 74%, and fluoride concentrations by 180%. (Yang Ailun et al, 2010)

2.5.2 Improving coal ash pollution management legislation

In order to promote the guiding principle of paying equal attention to the twin problems of utilizing coal ash and managing its environmental pollution, China should learn from the experiences of the U.S, the E.U. and other developed countries in handling coal ash environmental pollution. This includes the careful selection of coal-fired plant and ash impoundment locations, the planning and setting of standards for environmental impact

assessments, as well as methods for public participation. Based on the above proposed “Measures,” China should draw up a complete new set of corresponding environmental standards on pollution prevention, or make existing voluntary standards mandatory, and ensure that each key part of the provisions has clear operational specifications and requirements (Yang Ailun et al, 2010) “The true cost of coal” p25.

The relevant legislation should increase the number of specialized provisions on coal ash treatment in order to break down tasks on coal ash pollution prevention and control and incorporate it into law. The following relevant laws are currently in the legislative process: “Land Management Law” (revised), “Air Pollution Prevention and Control Law” (revised), “Energy Law,” “Law on Nature Reserves,” “Environmental Protection Law,” “Coal Law”(revised), and “Soil Pollution Prevention and Control Law,” etc. (Yang Ailun et al, 2010) “The true cost of coal” p25.

In the revision of the “Measures on the Comprehensive Utilization of Coal Ash,” the experiences of the EU and other developed countries should be used as a reference point to explore the ways in which China can improve its handling of pollution prevention in coal ash utilization, implement a wide ranging set of regulations to monitor the overall utilization production process, and fill the pollution and control legislative gap on coal ash utilization. The MEP should be more actively involved in the revision of “Measures on the Comprehensive Utilization of Coal Ash” and other related legislation in order to ensure that pollution prevention and control objectives are reflected adequately in all policy legislation. (Yang Ailun et al, 2010) (The true cost of coal p25)

China should take the next step in improving the coal pricing system through introducing a carbon tax, a resource tax or other relevant policies as ways to internalize the external costs of coal. At the same time, China should make great efforts to improve energy efficiency and develop renewable energy. The government should promote the optimization of the national energy mix, and gradually move away from its over-dependency on coal as a sure-fire means of controlling coal ash pollution at its source. (Yang Ailun et al, 2010) “The true cost of coal” p25.

2.6 FLY ASH IN EUROPEAN COUNTRIES

In the 13 member countries of the European Union and the Czech Republic, approximately 45 million tonnes of coal fly ash were produced in 1997 (Figure 1). No significant variations

were observed in the quantities produced by the European Countries from 1993 to 1997. (Figure 2), W.S Kyte et al (1999) "Fly Ash from Coal Fired Power Plants" p2.

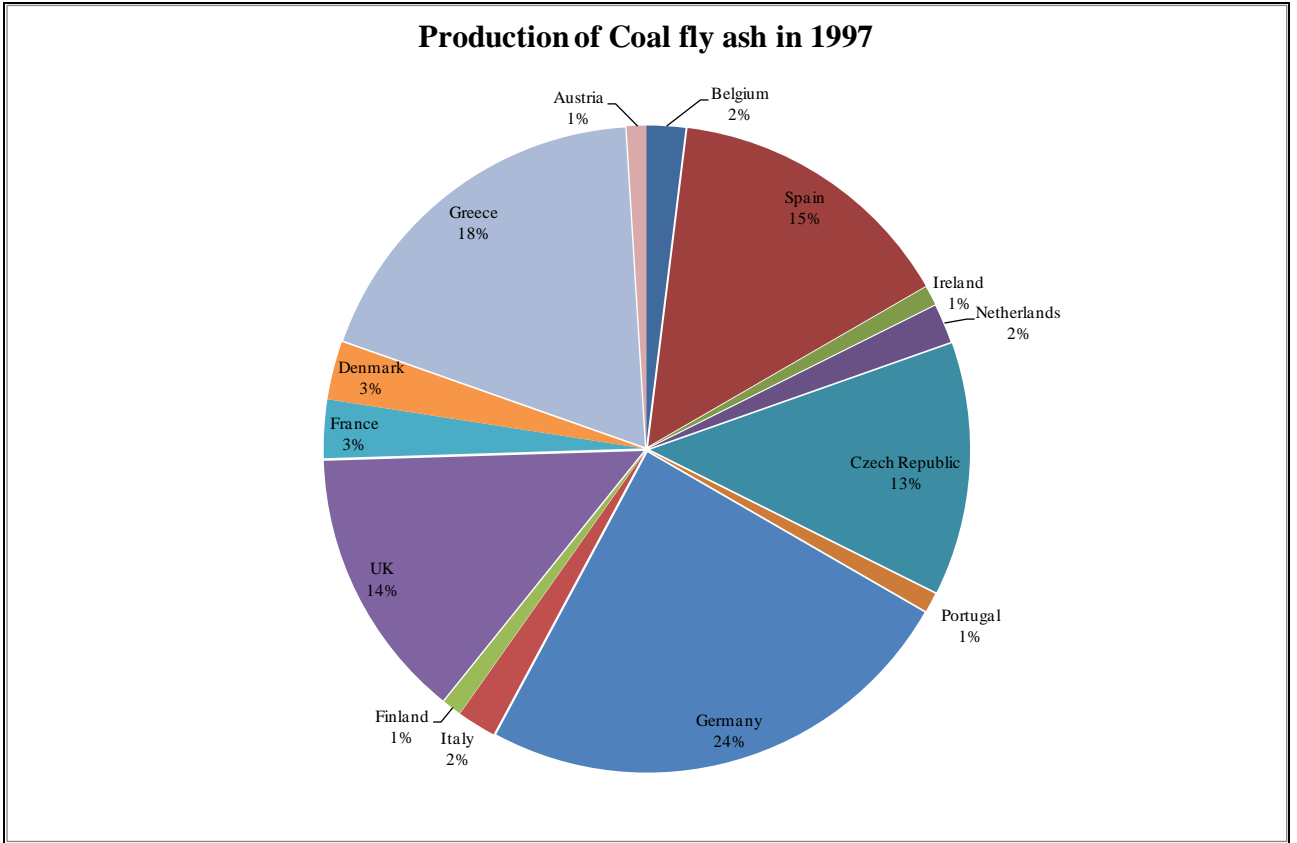


Figure 1. Production of coal fly ash in 1997 (source: ECOBA).

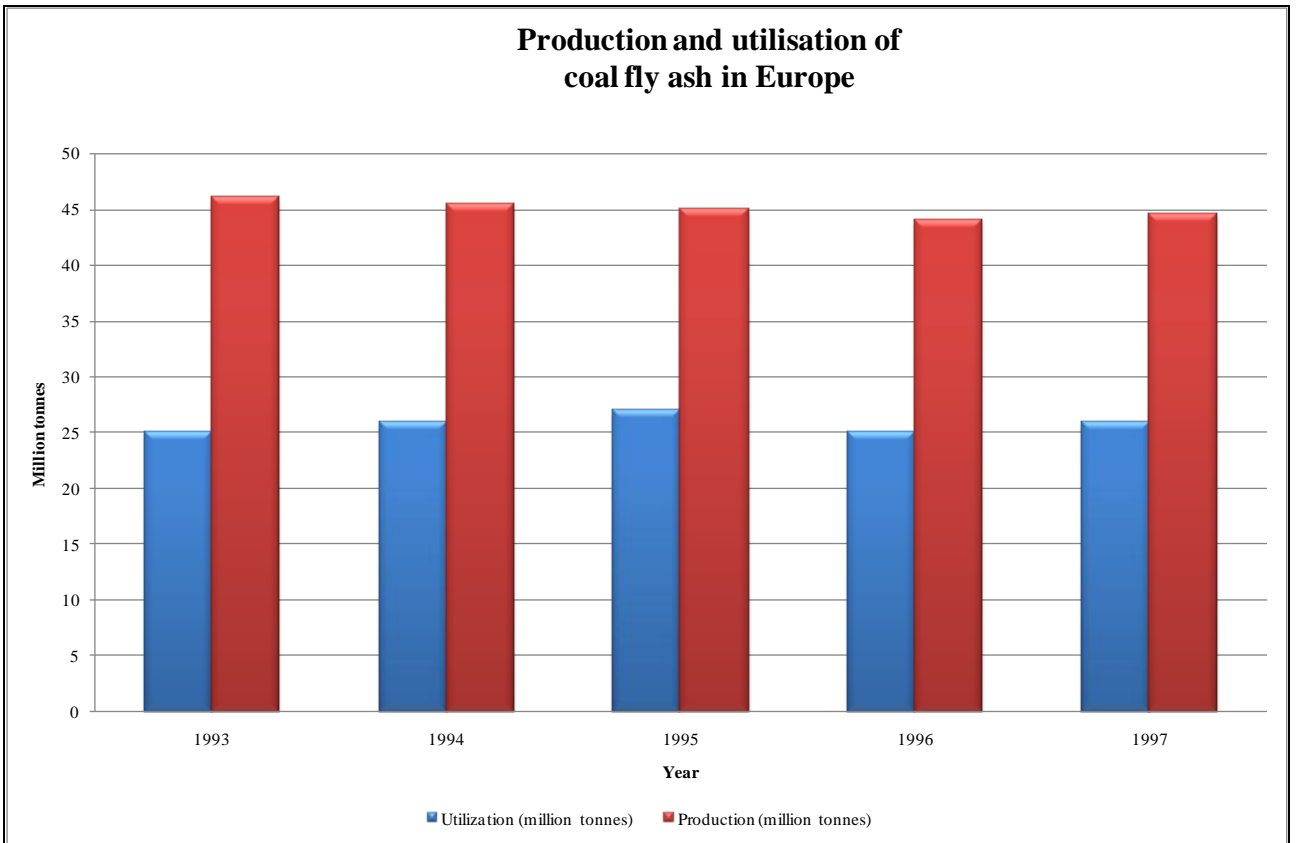


Figure 2. Production and utilization of coal fly ash in Europe (source ECOBA)

2.6.1 Utilisation

Within the countries given in Figure 1, the average utilisation rate of fly ash in 1997 was 58% and in some individual countries, the utilization rate was as high as 100%.

The following information was obtained from “Fly Ash from Coal Fired Power Plants October 1999” p3. The overall utilization of fly ash has increased in the last few years. It is being used more and more in high quality areas, such as the production of concrete and cement (1993: 20%, 1997: 28%) where it is used as a substitute for natural resources. Fly ash is also utilised in a wide range of applications in road construction and in the building industry (*Figure 4*). The use of fly ash as building material allows energy savings and the reduction of CO₂ emissions as one tonne of fly ash replacing cement saves one tonne of CO₂. Coal fly ash can also be processed into a material to be used for landfill cover and isolating lining that has better technical and environmental characteristics than most natural clays. Fly ash is transported within countries and across frontiers mainly for these purposes. Coal fly ash has also been proven to improve the yield from agricultural land and can be used as a pollution control agent, particularly for soil decontamination, sludge and effluent treatment and in hazardous waste stabilisation. Where it is utilised, fly ash often has to meet special requirements requested by its users. In certain applications, fly ash even has to be produced specifically. Therefore, the production system (the power plant) needs to have a supervisory system which collates information on the type of coal that is burnt, the performance of the coal mills, the combustion process, the fly ash collection and precipitation process and, finally, information on a range of fly ash properties. This “Quality Management System” is a necessity in today’s modern power plants. W.S Kyte et al (1999).

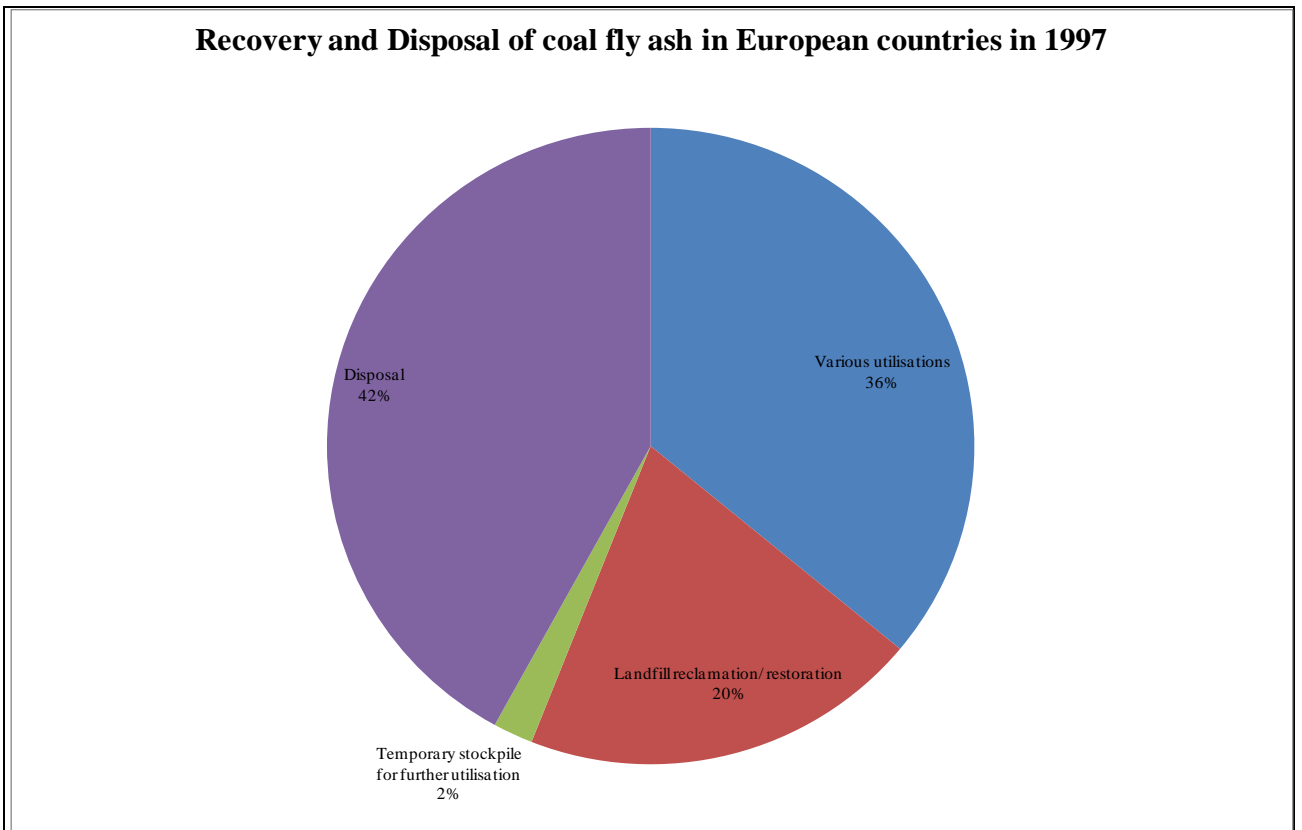


Figure 3. Recovery and Disposal of coal fly ash in European countries (source ECOBA).

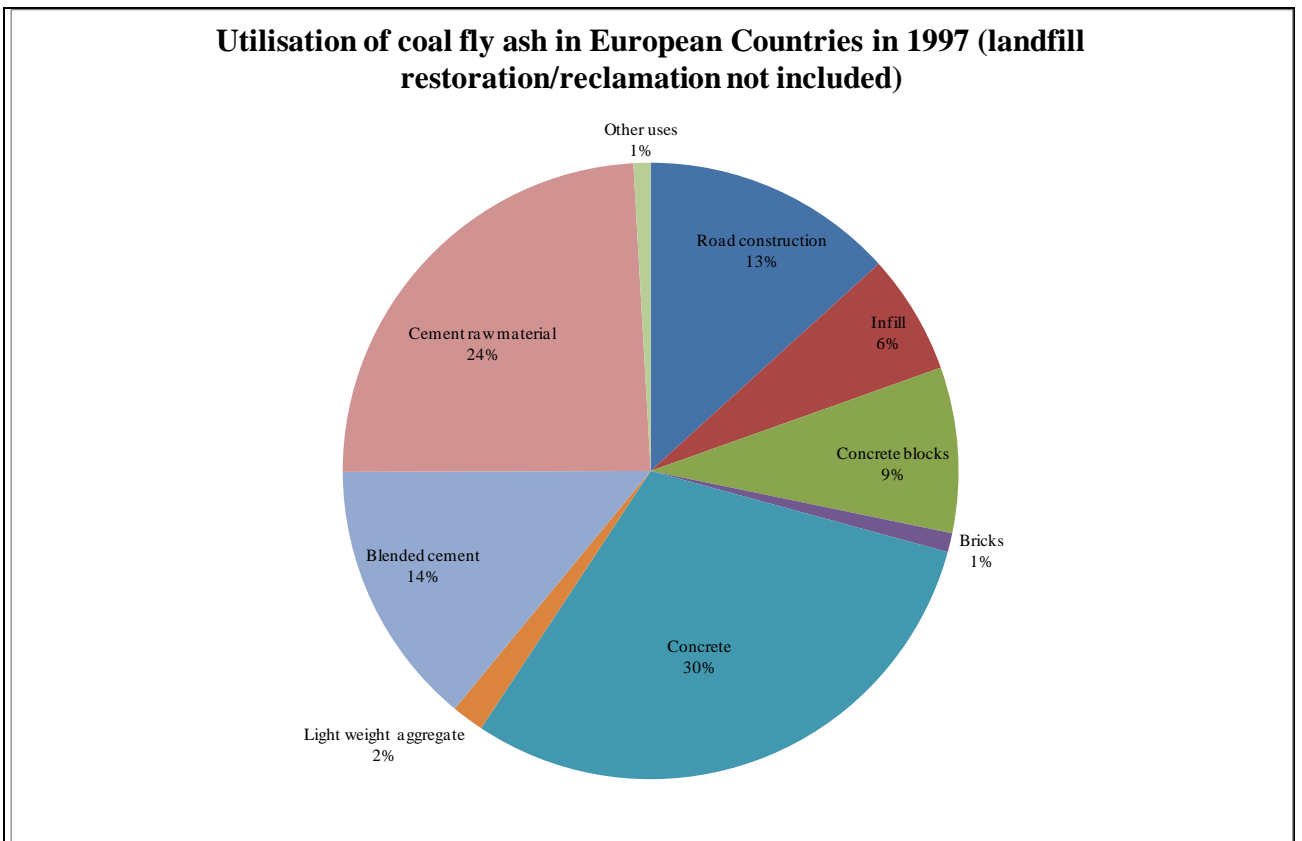


Figure 4. Utilisation of coal fly ash in European Countries in 1997 (source ECOBA).

2.6.2 Transfrontier movements (only for recovery operations)

The following information was obtained from “Fly Ash from Coal Fired Power Plants October 1999” p4. A proportion of the fly ash produced in some countries is exported for recovery operations. In the main, these movements are to neighbouring countries. The fly ash involved is valued as a commercial product of high quality within the European building material market. Where it is destined for specific uses, it has to meet quality standards that are set out in documents such as the European (CEN) Standard EN450 “Fly Ash for Concrete”. For the fly ash producers, users and for the trade associations involved, transboundary marketing is a very important economic issue. The following examples show the significance of transfrontier movements of fly ash for utilisation. In 1998, France exported about 200,000 tonnes of coal fly ash (less than 10% of the French annual production). Most of this went to Germany, Switzerland and Belgium. In the Netherlands, between 40 and 50% (between 400,000 and 500,000 tonnes) of the national production of coal fly ash leaves the country for recovery operations. In Germany, trade relations exist with other member countries of the European Union, including Austria, Belgium, Denmark, France and the Netherlands, and others, such as the Czech Republic, Poland and Switzerland. The result is that each year approximately 600,000 tonnes of fly ash are imported and about 400,000 tonnes (less than 5% of the German annual production) are exported. Thus, about 1 million tonnes of fly ash are transported within, into and out of the European Union in respect of the current German market alone. W.S Kyte et al (1999).

2.6.3 Ecotoxicity

Germany:

In Germany, the fly ash from coal-fired power plants is classified as a substance that typically generates no water pollution. To come to such a conclusion, investigations were made into ecotoxicity effects and the tests included a consideration of:

- Toxicity in fish;
- Toxicity in invertebrate aquatic creatures;
- Toxicity in aquatic plants, e.g. algae; and
- Toxicity in micro-organisms, e.g. bacteria.

The eluate from a 1:1 mixture of fly ash and demineralised water was used to perform these tests. From the results, it was concluded that the test solutions had no permanent and no adverse effect on any of the test organisms. W.S Kyte et al (1999).(Fly Ash from Coal Fired Power Plants October 1999 p10).

United Kingdom:

The following facts were gleaned from “Fly Ash from Coal Fired Power Plants October 1999” p11. In the UK, the Environmental Agency is currently assessing the use of Direct Toxicity Assessment (DTA) for monitoring and controlling the discharge of industrial effluents into surface waters. Pre-emptive studies within the Joint Environmental Programme of National Power, PowerGen and Eastern Generation have shown that the water discharged from operating fly ash disposal lagoons needs no, or in the worst case, minimal, dilution in order for it to have no significant toxicological impact on both fresh and saline receiving waters. This conclusion is based on the results from laboratory acute and chronic toxicity testing at three trophic levels (algae, invertebrate - *Daphnia Magna* and *Tisbe Battagliai* - and fish – Rainbow trout and juvenile Turbot) and from the results of “Microtox” testing. Further work has also shown that sediments in the vicinity of ash disposal site discharges have no marked toxicity despite the sites having been operational for many years. W.S Kyte et al (1999).

2.6.4 Environmental Compatibility

The following information was obtained from “Fly Ash from Coal Fired Power Plants, October 1999” p13. Recovery of fly ash disposal sites for amenity use by covering with soil and grassing over is not the only possibility for an environmentally beneficial site recovery option. Pulverised fuel ash is similar in many ways to soil, and extensive research into methods for recovering ash disposal sites for agricultural purposes have been carried out successfully as well. Now people can specify the land management strategies which need to be adopted to ensure efficient exploitation of reclaimed ash sited for agricultural purposes. The behaviour of coal fly ash stored on-site is usually subject to monitoring, either by the analysis of drainage water or by the collection of water samples from observation wells located around the storage sites. From the results of this monitoring, no significant impacts on surface waters or ground waters have been observed. W.S Kyte et al (1999).

2.7 ASH DISPOSAL

In the European countries fly ash is classified as non-hazardous, but according to Troskie K, (2005) ash is described as the product of the coal burning process and has the ability to contaminate the groundwater. A hydrogeological study was performed at Kendal power station by GCS in November 2007 and it was found that fly ash poses a potential threat to groundwater quality and different types of ashing methods have different impacts on the environment.

2.7.1 Ash disposal methods

Ash disposal can take place both above and below ground. There are three methods of disposing of ash that have been considered for the proposed power station namely, above-ground ashing, in-pit ashing and back-ashing. These three options are described below:

- Above-ground ashing – Ash is disposed on an ash dump. The ash dump is rehabilitated over time, using accepted rehabilitation methods;
- In-pit ashing – The ash is dumped directly into open cast voids at the colliery that supplies coal to the power station. Overburden and topsoil are placed on top of the ash; and
- Back-ashing – The overburden at the colliery is returned to the open pit voids prior to the ash. The ash is then covered with soil and rehabilitated.

These different methods have different impacts on the groundwater environment. In order to identify and quantify these impacts the ash first has to be characterised chemically and physically. (Troskie K, 2005)

2.7.1.1 Above-ground ashing

The following section was abbreviated from (GCS ref. NIN.05/469.November 2005). During above-surface disposal the ash is stored in carefully designed and managed ash dumps. The fly ash is used to construct the walls of the dump, while the bottom ash stored in the centre. One of the reasons for using the fly ash as wall material is that the fine-grained material has a relatively low permeability, therefore limiting seepage of contaminated water from the dump through the walls. According to Troskie K, risks to the water environment associated with surface disposal of the ash material can be described as:

- Elevated constituent concentrations: It is evident that it can be expected that calcium and sulphate will be present in elevated concentrations in the material. Other

constituents that could be present in high concentrations are silicon, magnesium, sodium, and potassium. Trace elements that can be present in elevated concentrations include arsenic, boron, calcium, molybdenum, sulphur, selenium, and strontium;

- Chemical changes due to exposure to air: The chemistry of the ash material can be expected to change due to exposure to carbon dioxide in the air. A chemical reaction will occur between calcium oxide and carbon dioxide that will lead to the crystallisation of calcium carbonate (limestone) as described above. Calcium will also react with sulphate that forms due the oxidation of sulphur minerals and gypsum will crystallise. It can be expected that sulphate concentrations will be elevated; and
- Leaching of constituents: Water contained in the ash material during deposition can leach constituents from the ash dump and transport these to the surrounding environment. Additional water that is recharged from rainfall will supplement the interstitial water and contribute to the leaching of elements.

The water that migrates through the dump can either daylight along the edge of the ash dump and enter the surrounding environment as surface water, or migrate vertically to the bottom of the dump and enter the underlying soil from where it can recharge and contaminate the aquifers. The quality of the water seeping from the ash dump can be predicted by performing leach and element enrichment testing. The results of the tests will show which elements can be expected to be present in elevated concentrations in the long term. The element concentration range can also be determined based on the results. The volume of water that will seep from the ash dump in the long term will be affected by the recharge from rainfall. (Troskie K, 2005)

2.7.1.2 Sub-surface ashing

The following section was abbreviated from “GCS ref. NIN.05/469.November 2005”. Two methods of sub-surface disposal are proposed. These are:

- Back-ashing: This refers to dumping ash within the opencast coal mine, after all the usable coal has been excavated. The overburden (that layer of surface material that is removed prior to mining the coal) would be returned to line the excavation before the ash is placed on top of it. The ash would then be stacked, spread, rehabilitated with topsoil and re-vegetated; and
- In-pit ashing: The difference between this method and back ashing is that the ash would be placed directly into the existing excavation and the overburden and topsoil would be placed on top of the ash. Thereafter the dump would be re-vegetated.

Both of these disposal methods can lead to the direct contamination of the surrounding aquifers because the ash material is likely to be below the regional groundwater level once the water levels have recovered in the post operational environment where dewatering and thus drawdown of groundwater levels have stopped.

It is expected that the permeability of the rehabilitated material will be slightly higher than that of the surrounding natural rock matrix. This will cause higher recharge into the rehabilitated area from ponded water.

Because the groundwater flow will be directed away from the pit area, any salts leached from the ash material will migrate away from the immediate pit area, and into the surrounding environment.

Decant can occur in some areas due to either migration along the coal seam contact, or in areas where the rehabilitated elevation is below that of the recovered groundwater level. The decanting water must be collected in evaporation ponds, or piped to the treatment plant for recycling into the system. From the above description of the back-ashing and in-pit ashing methods and contamination migration pathways, it is evident that back-ashing is the preferred method of the two (from a groundwater perspective). During the lining process, the overburden can be compacted, thereby reducing the transmissivity of the material and effectively forming a flow barrier. This will decrease the volume of water that can migrate from the pit area to the surrounding aquifers and contaminate the environment. It will also decrease inflow of water from surrounding aquifers, thereby effectively decreasing decant potential and volumes.(Troskie K, 2005)

2.7.2 Ash and effluents

Ash and effluents, waste products from the power generation process, are typically co-disposed at power stations. Ash has to be disposed in such a manner that the long-term potential of the ash to encapsulate effluents is not compromised, as this could pose a threat to the groundwater.(Troskie K, 2005) The effluents include:

- Cooling water sludge from the lime softening process, which can act as quicksand and is of moderately high salinity, must always be co-disposed with ash;
- Sludge from the clarification process of cooling water is regarded to be similar in hazard potential to cooling water sludge, and thus should also be co-disposed with ash;
- Sludge and sediments collected from dirty drainage grit separation facilities and dams are regarded as high salinity sludge and must be mixed with ash prior to disposal;

- Spent neutralised regeneration effluents, including caustic soda and sulphuric acid regenerants, must always be disposed as semi-homogeneous mixtures with ash; and
- Desalination plant brine, a high salinity effluent, is co-disposed with the ash.

2.7.3 Dry ash disposal

Dry disposal is advantageous in that the contact with water is reduced. Disadvantages, however, include dust and wind erosion as well as stability of the ash pile in the case of surface disposal. (Troskie K, 2005)

In the case of dry ash disposal, ash is partially wetted at the power station before being transported by conveyor belt to the ash disposal dump. Ideally, the ash on the conveyor belt contains about 15% moisture. The arrangement prevents ash from blowing off the conveyor belt. or in the area where it is being disposed of. Disposal occurs by merely tipping the ash at the end of the conveyor belt. No compaction of the ash, other than under its own weight and under the weight of the machinery being used at the top of the ash dump therefore occurs. In addition to the moisture added to the ash within the power station, a watering gun is available in the area where the ash is being tipped to prevent the ash from drying out and creating a dust problem (Hodgson et al.,1998). Figure 5 is an example of dry ash disposal taken at Kendal Power Station.



Figure 5. Conveyor belt ash disposal.

2.7.4 Wet ash disposal

Wet ash disposal sites transport fly ash in suspension with water to the disposal area where it is released on dried ash. Here the water evaporates and the ash is left behind. As soon as the ash has dried, another layer is deposited on top. This effectively prevents the top layer of ash from being subjected to natural wetting and drying cycles, which leads to the formation of the pozzolanic layer. (Troskie K, 2005)

Wet ash disposal has been the preferred disposal methodology in the past. It is only at Kendal Power Station, which is the most recent station to come onto line, where dry ash disposal is currently being done. In the case of wet ash disposal, ash is generally being pumped from the power station to the ash dams in ash-to-water ratios of 1:5 to 1:10 by volume. (Hodgson et al.,1998)

2.8 COMPARISON BETWEEN EUROPEAN COUNTRIES, CHINA AND SOUTH AFRICA'S FLY ASH PROBLEMS

In the report on European countries fly ash "Fly ash from coal fired power plants October 1999" it is seen that +/- 50% of the fly ash was utilised from 1993 to 1997 (*Figure 4*) and in

some of the countries the utilisation was as high as 100%. Fly ash is referred to as “non-hazardous” due to very low or even very no impact on fresh and saline receiving water. The ash produced has to meet certain standards in order to be utilised and European countries have very few problems with pollution from the ash produced from the power stations.

China is mostly dependent on coal-fired power stations and therefore very large quantities of fly ash are being produced every day. Research found that the actions of the wind and rain cause heavy metals to leach or dissolve into water systems. These heavy metals cause water and soil pollution, but most important of all they impact on human health impacts. From a pollution point of view the European countries classify fly ash as non-hazardous, whereas China has greater problems containing the pollution from the ash dumps. Utilisation in China has been emphasized over the past few years but pollution control work has been marginalized in places where pollution control should be a necessity.

The following information was obtained from “Tailings and mine waste” p189. A typical power station in South Africa burns 12 million tonnes of coal per year, and the estimated mass of the resulting for all South African stations is about 21million tonnes a year. Very little of this of this ash is used or is usable industrially and the vast majority of it (+/-95%) must be disposed of on land. Until about 1984, all of Eskom’s ash disposal facilities were dams into which ash was placed hydraulically. (Fourie A.B and Blight G.E, 1999)

According to Fourie and Blight (1999) South Africa’s power stations produce great masses of ash each year and very little of this ash is utilized for other uses (landfill, concrete or bricks.). Due to this very low utilisation rate the ash must be disposed of on land and this method can lead to groundwater contamination. European countries utilisation rates are very high, as presented in *Figure 4*, whereas some counties have a utilisation rate of 100% and South Africa disposes of +/-95% of fly ash produced. These areas in which the ash is disposed of are monitored to observe the groundwater contamination. If there are contamination problems, mitigations are presented to the power stations to prevent further contamination of the groundwater.

European countries have very little or even no problems with fly ash due to very high utilisation rates, therefore South Africa and China will benefit by focusing more on utilisation and reducing the quantities of fly ash deposited on land sites, and this will also reduce the risk of groundwater contamination.

3 BASELINE STUDY CONDUCTED AT KENDAL POWER STATION - PHYSICAL GEOGRAPHY AND DRAINAGE

3.1 INTRODUCTION

Kendal Power Station is located approximately 35 km south-west of Witbank, Mpumalanga Province. The area under investigation is between grid references (28.8527, -26.0230), (29.1935, -26.1927), as shown on 1:50 000 topography map, Figure 7.

3.2 RAINFALL DATA

The Highveld is part of the summer rainfall region of South Africa. The rainfall is generally in the form of thunderstorms with lightning, rain, wind and sometimes hail. Rainfall events are usually localised and can vary over short distances. The area is relatively cool due to its altitude 1700-2300 mamsl. The temperatures in summer can vary between 3.6 °C (minimum) to 34 °C (maximum). Winter frost occurs regularly.

Kendal Power Station is located in the Limpopo-Olifants Drainage region of South Africa. The average precipitation for this region is between 593 and 676 mm. Rainfall is almost exclusively in the form of showers and thunderstorms and falls mainly in the summer months from November to March. The maximum rainfall usually occurs in January. The winter months are usually dry.

Kendal Power Station lies within rainfall zone B2B and B1A.

The average monthly rainfall recorded at weather stations 0477 695 and 0477 762 within rainfall zone B2B is summarised in Table 1 and displayed graphically in Figure 6. Data from the measurements taken during 70 years (1920 - 1989) were obtained. From the data listed in Table 1, it can be seen that the wettest months (on average) are December, January and February, whilst the driest months are June, July and August.

Table 1. Average rainfall recorded at two weather stations within rainfall zone B2B.

Month	Average Rainfall	
	(0477 695)	(0477 762)
Jan	103.3	117.76
Feb	77.45	88.29
Mar	67.36	76.79
Apr	36.11	41.17
May	16.54	18.86
Jun	7.23	8.25
Jul	6.17	7.03
Aug	6.46	7.37
Sep	21.29	24.27
Oct	59.48	67.8
Nov	95.77	109.17
Dec	95.65	109.04

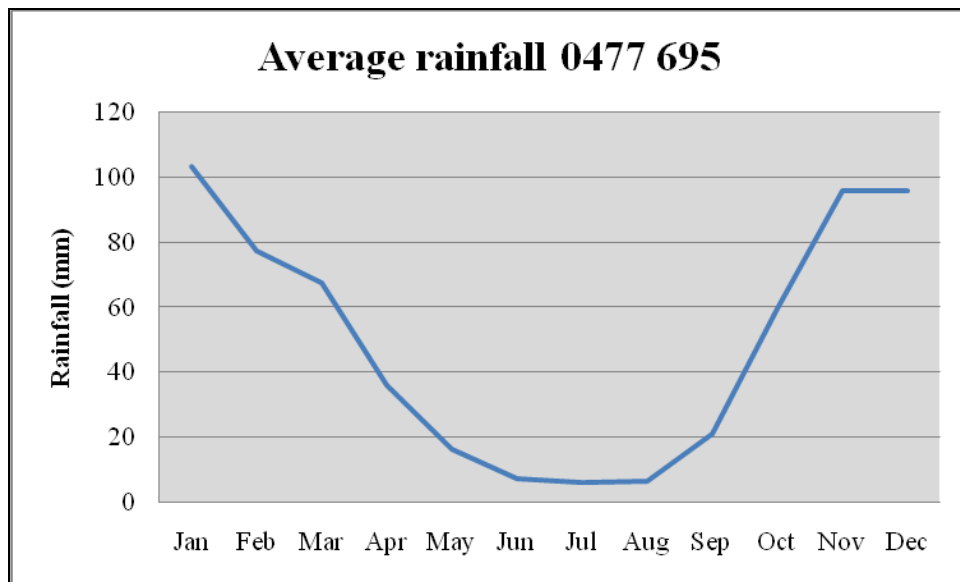


Figure 6. Average rainfall recorded at weather station 0477 695 (Over a period of 70 years).

3.3 SURFACE TOPOGRAPHY AND DRAINAGE

The power station is situated on the Highveld, which consists of open, slightly rolling to very flat surfaces typical of the area. General sloping of the ground tends to be within the 1° to the 5° range. The drainage of the area flows from the east to west and is considered to be part of the Olifants River Catchment area. The facility occurs within drainage region B20F, B20E and B11F. Drainage regions and the surface runoff are indicated in Figure 8.

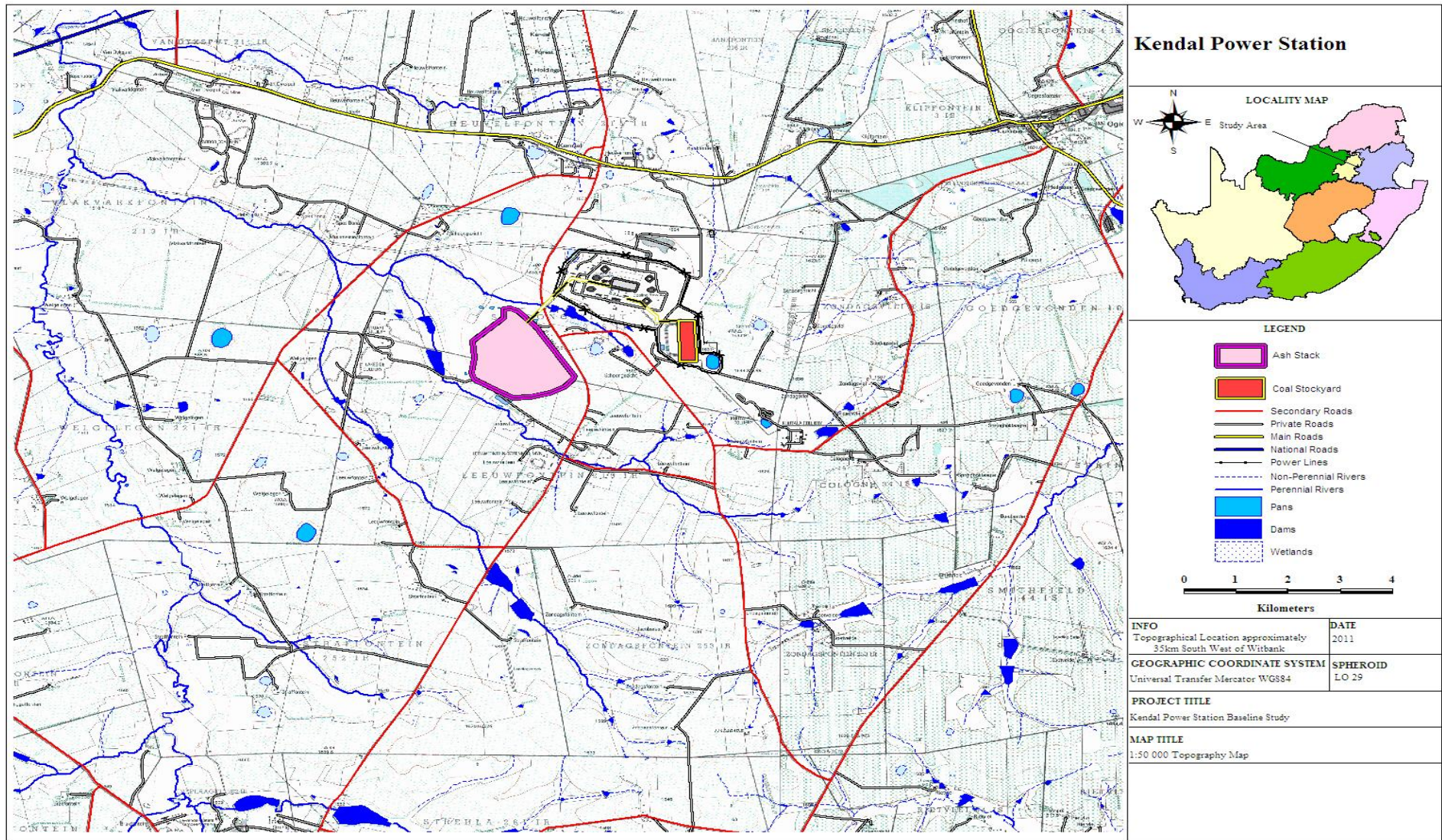


Figure7. 1:50 000 topography map.

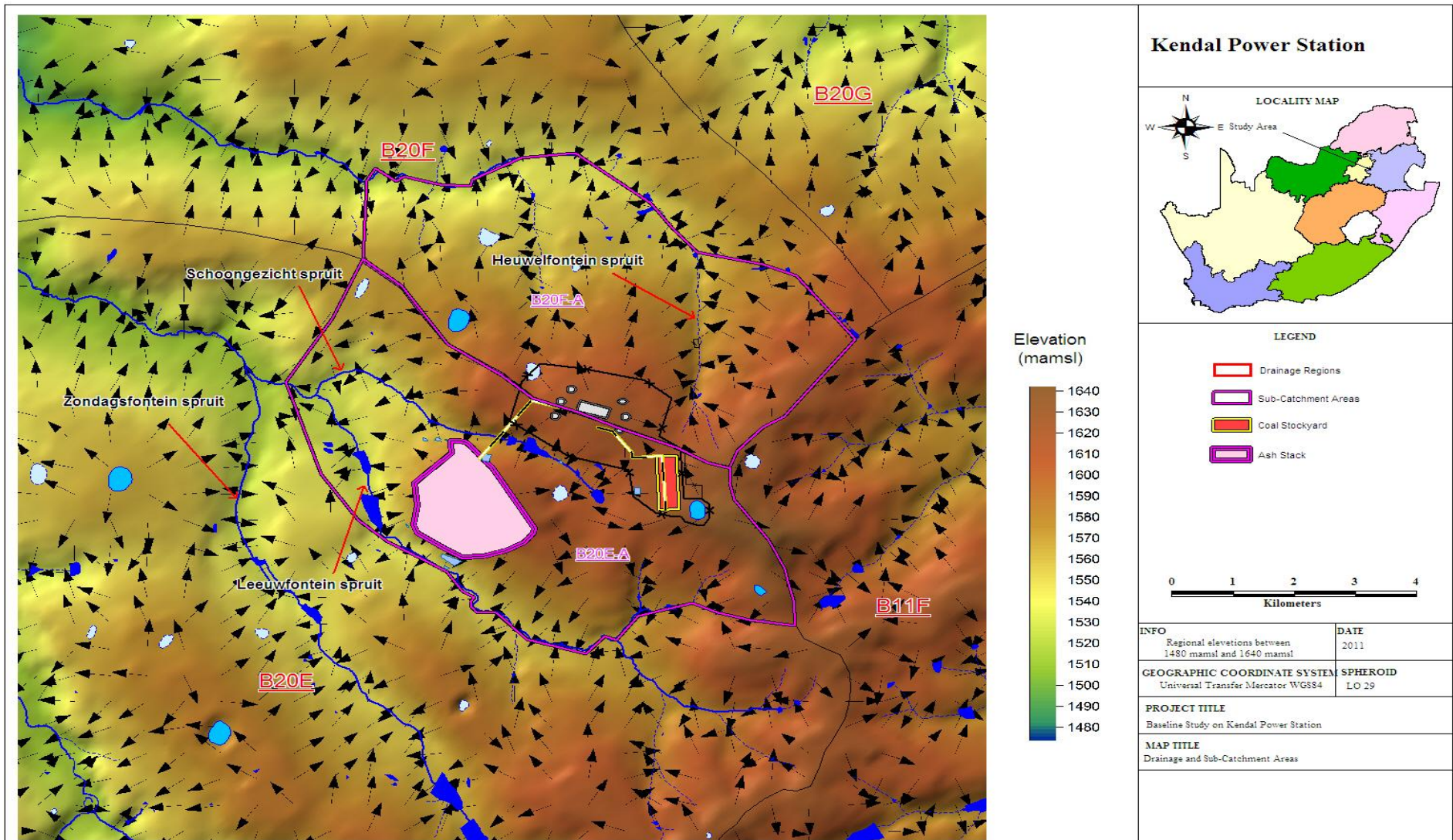


Figure 8. Drainage regions, sub-catchment areas and surface runoff.

3.3.1 Impacts upon receiving waterbodies

The affected watercourses are the perennial, non-perennial streams and pans in the area.

The surface drainage, rivers and streams in the study area run mainly from the east in a westerly direction contributing to the Zondagsfontein spruit, Leeuwfontein spruit, Schoongezicht spruit and Heuvelfontein spruit which flow north-west wards contributing to the Wilge River.

3.3.1.1 Heuvelfontein spruit

Impacts upon the Heuvelfontein spruit would mainly originate from the power station area, which is located to the east and the south of the stream.

3.3.1.2 Schoongezicht spruit

Impacts upon the Schoongezicht spruit would mainly originate from the power station area and the coal stockyard area which is located to the north and east of the stream, as well as from the ashing area which is located to the west of the stream.

3.3.1.3 Leeuwfontein spruit

Impacts upon the Leeuwfontein spruit would mainly originate from the ashing area and the coal stockyard area which is located to the north and north-east of the stream, respectively.

3.3.1.4 Zondagsfontein spruit

Impacts from the Kendal Power Station upon the Zondagsfontein spruit are unlikely.

3.3.2 Sub-catchments

Sub-catchments were identified for the area under investigation to determine the drainage of water across the area. (Refer to Figure7, drainage regions and surface runoff.)

3.3.2.1 Sub-catchment B20F – A

Sub-catchment B20F – A forms part of Drainage region B20F. The local water drainage occurs from the south, across the area in a northern direction and flows into the Heuvelfontein spruit.

3.3.2.2 Sub-Catchment B20E – A

Sub-catchment B20E – A forms part of Drainage region B20E. The local water drainage occurs from the north into the Schoongesight spruit and from the north east into the Leeuwfontein spruit.

3.4 GEOLOGY

Kendal Power Station is located along the northern edge of the Karoo Basin. It is therefore predominantly underlain by Karoo rocks (Figure 9). Geological units belonging to the Bushveld Igneous Complex and Magaliesberg Group, also occur in the general area. The local geological sequence comprise of, soil, clay, shale, siltstone, mudstone and sandstone. The soil horizon is not well developed and comprise of a silty to clayey sand.

Table 2. Table showing local lithological make up with chronological time constraints.

Age	Sequence	Group	Formation	Symbol	Rocktypes (Sedimentary and Volcanic Rocks)	Rocktypes (Intrusive Rocks)
Quaternary				Q	Alluvium sands	
Jurassic				Jd		Dolerite
Permian	Karoo	Ecca	Vryheid	Pv	Sandstone, Mudstone, Shale	
Mokolian				Mle		Granite suite (Bushveld)
Vaalian	Transvaal	Rooiberg	Loskop	Vlo	Agglomerate, Lava	
Vaalian	Transvaal	Rooiberg	Loskop	Vdi		Diabase
Vaalian	Transvaal	Rooiberg	Selons Rivier	Vse	Porphyritic rhyolite with interbedded mudstone and sandstone	

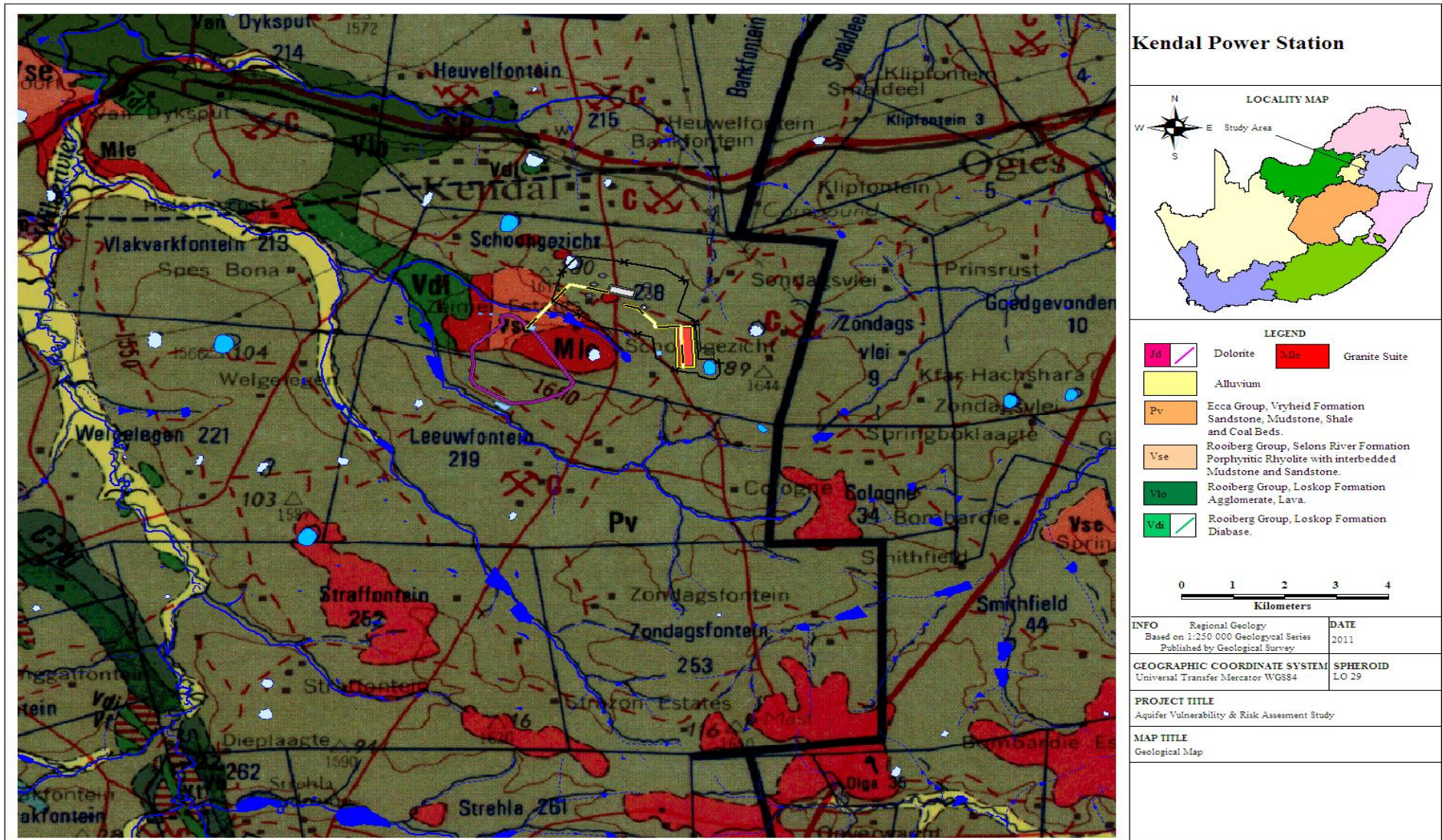


Figure 9. Geology map.

3.5 GEOPHYSICS

3.5.1 Geophysical Investigations

The purpose of the geophysical investigations was to detect and delineate geological features that may be associated with preferential pathways for groundwater migration and contaminant transport. Intrusive magmatic bodies are often associated with baked zones that are usually highly fractured and weathered. Such zones could form preferential pathways along which rapid groundwater flow and contaminant transport can take place. The magnetic method was utilised during the geophysical survey since this method is often very successful in detecting intrusive magmatic bodies such as dolerite/diabase sills or dykes. Magnetic data were recorded on eight traverses at positions that were suitable to the upgraded groundwater monitoring system. The locations of the traverses and the newly drilled boreholes are indicated in Figure 10.

Aerial magnetic data was not utilised to identify the drilling targets or geological structures during the drilling of the new boreholes.

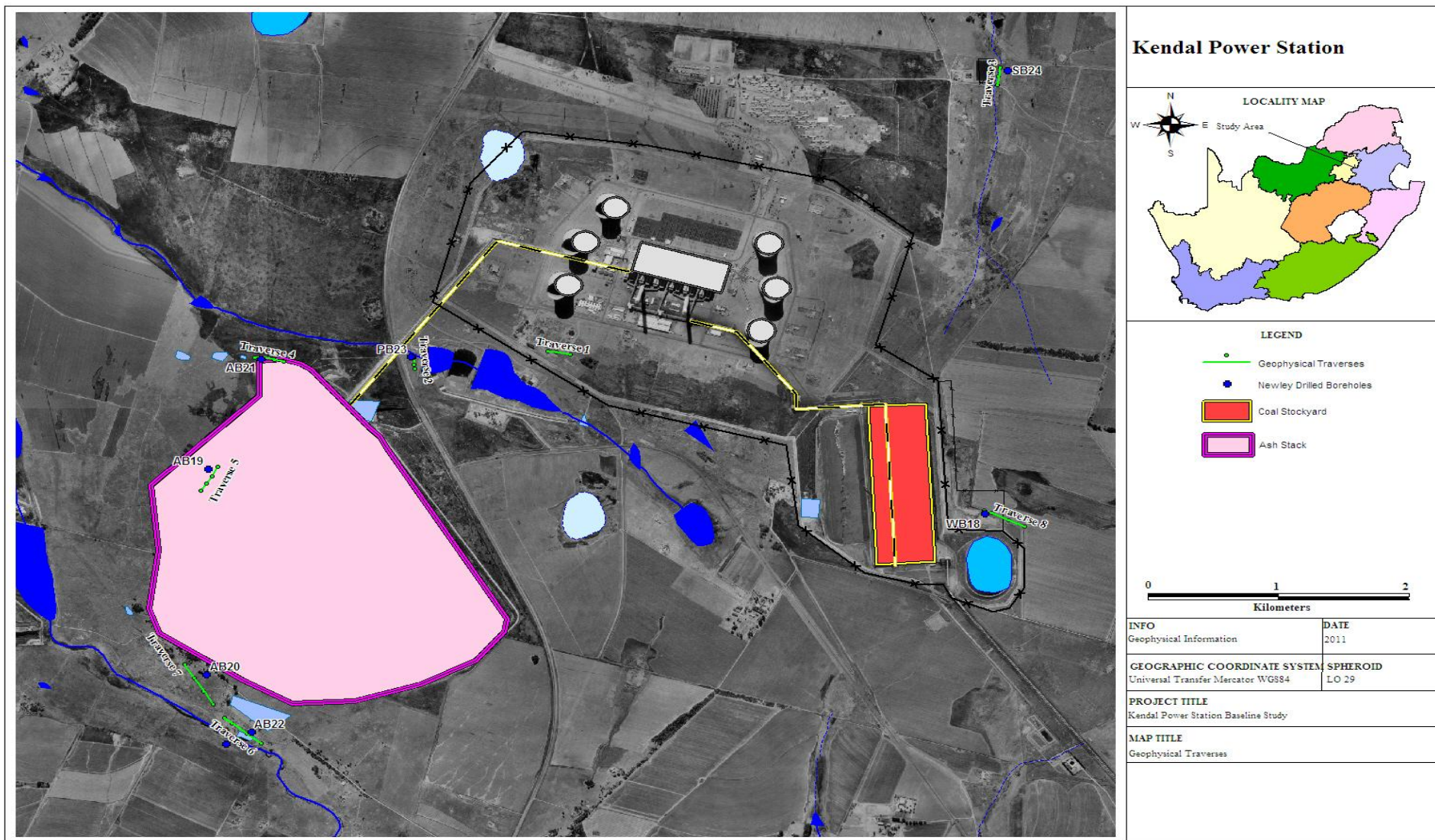


Figure 10. Geophysical traverse and newly drilled boreholes.

3.5.2 Results of magnetometer survey

Traverse 1:

Magnetic data was recorded a 150m long traverse with a west/east strike at a position south of the oil skimmers near the power station. Metallic infrastructure on surface and underground piping led to very noisy magnetic data. After discussions with power station personnel it was decided that no borehole would be drilled downstream from the oil skimmers due to the risk of damaging underground piping or wiring.

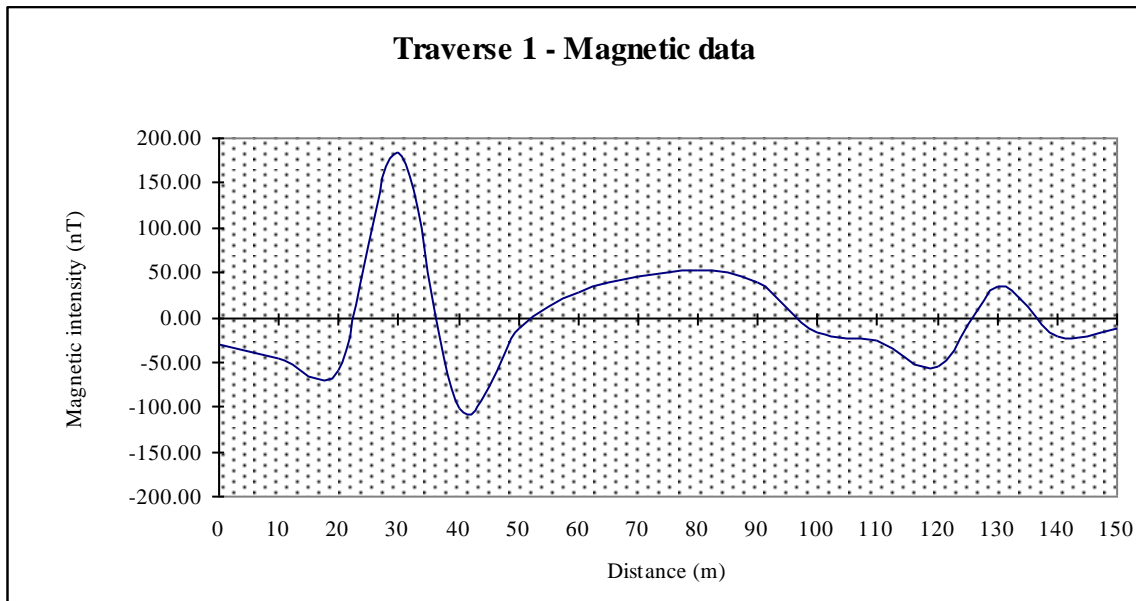


Figure 11. W-E magnetic profile of Traverse 1.

Traverse 2

Magnetic data was recorded at 5 m spacing station spacing on a south/north striking traverse down-gradient from the pollution control dams. A large wavelength magnetic anomaly was observed on the northern part of the traverse. Although one borehole (PB23) was sited and drilled in the vicinity of the anomaly, the placement of the borehole was determined more by the presence of overhead power lines, the need to drill at a position down-gradient from the dams and issues of accessibility for the drilling rig.

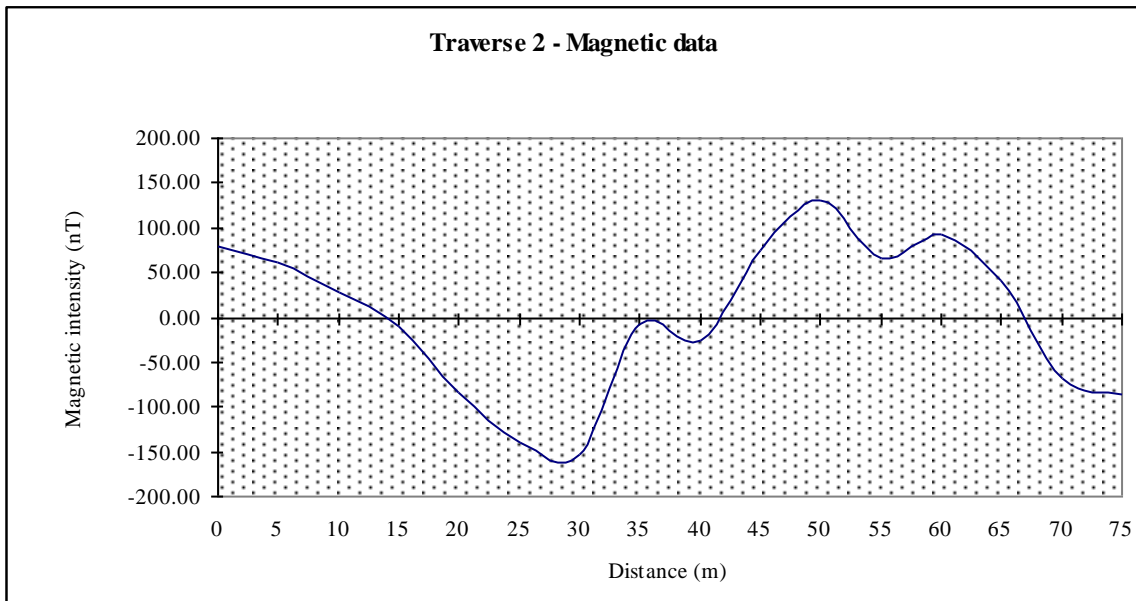


Figure 12. S-N magnetic profile of Traverse 2.

Traverse 3

Geophysical measurements on Traverse 3 were conducted to the east and down-gradient from the sewage plant. Magnetic data was recorded along a south/north striking traverse at a 5 m station spacing. A very small anomaly with amplitude of 27 nT was recorded approximately 90m from the start of the traverse. One borehole (SB24) was drilled at a position along the traverse. The position of drilling was again influenced by external factors such as the presence of a wetland, overhead high voltage power lines and the local topographic gradient.

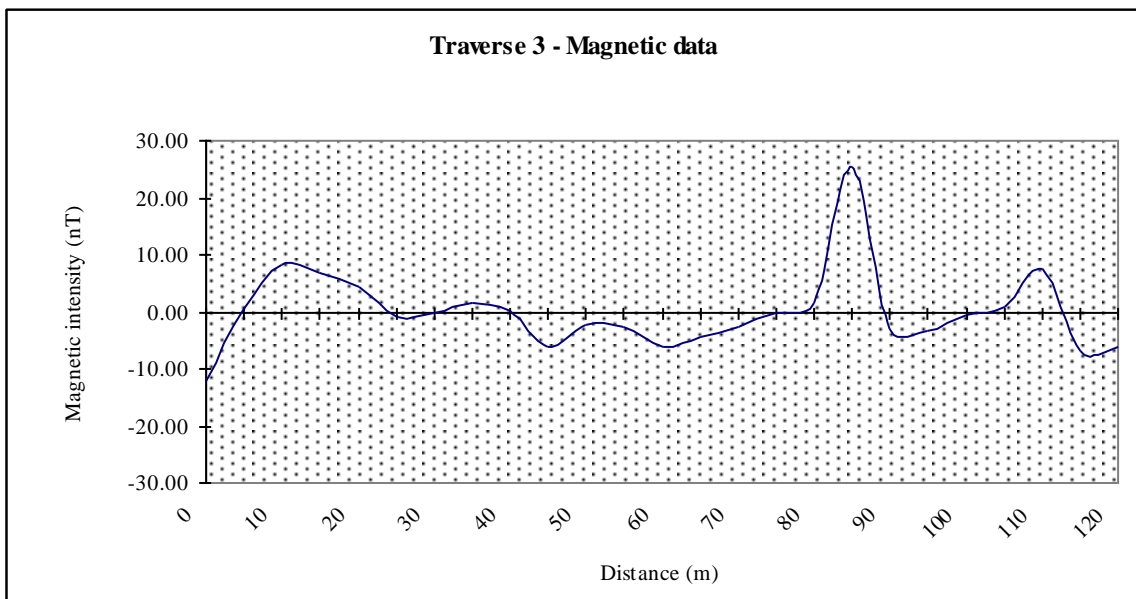


Figure 13. S-N magnetic profile of Traverse 3.

Traverse 4

Traverse 4 was located to the north of the ash stack, downstream from a dry pan and had a west/east strike. Magnetic data on this traverse were recorded at 5 m station spacing. Two prominent magnetic anomalies were recorded, centred at positions 50 and 130m from the start of the traverse. The position of the western anomaly (at 50m) was better suited for a monitoring borehole located downstream from the possible sources of pollution. Borehole AB21 was drilled at a position on the anomaly that also corresponded to a slight linear depression in the local geology. The magnetic anomaly and the observed depression were interpreted to be due to a linear geological feature.

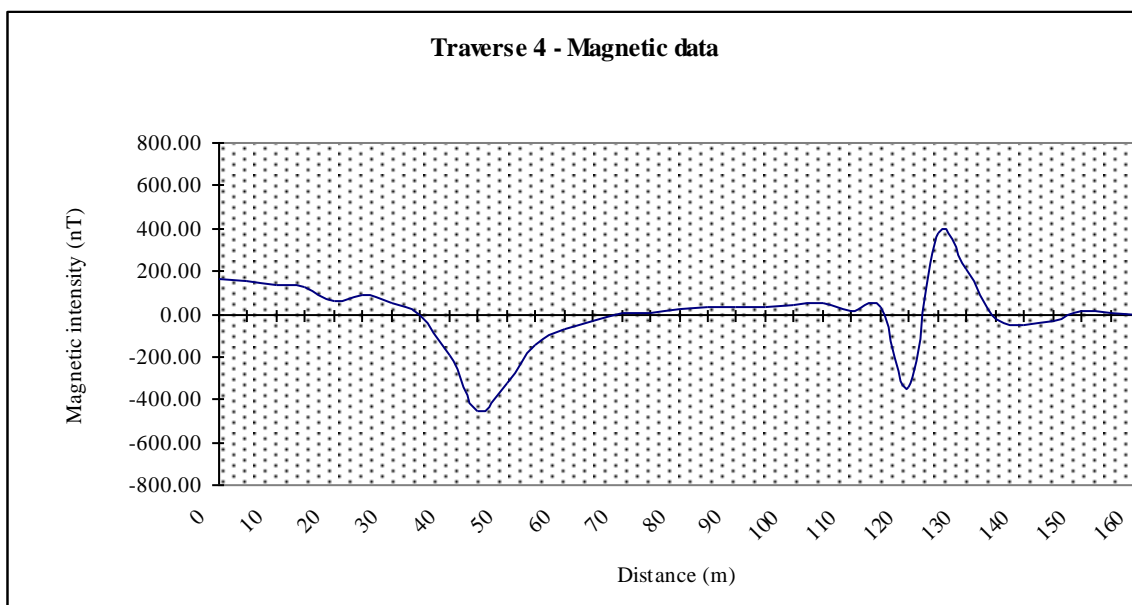


Figure 14. W-E magnetic profile of Traverse 4.

Traverse 5

Magnetic data were recorded along a south-west/north-east striking traverse that ran across a prominent outcrop of granite. A very prominent magnetic anomaly that corresponded with the outcrop was recorded at a position 40m from the start of the traverse. Another large magnetic anomaly was recorded at positions greater than 110m from the start of the traverse. Borehole AB19 was sited and drilled on the north-western flank of the outcrop, on the side of the ash stack.

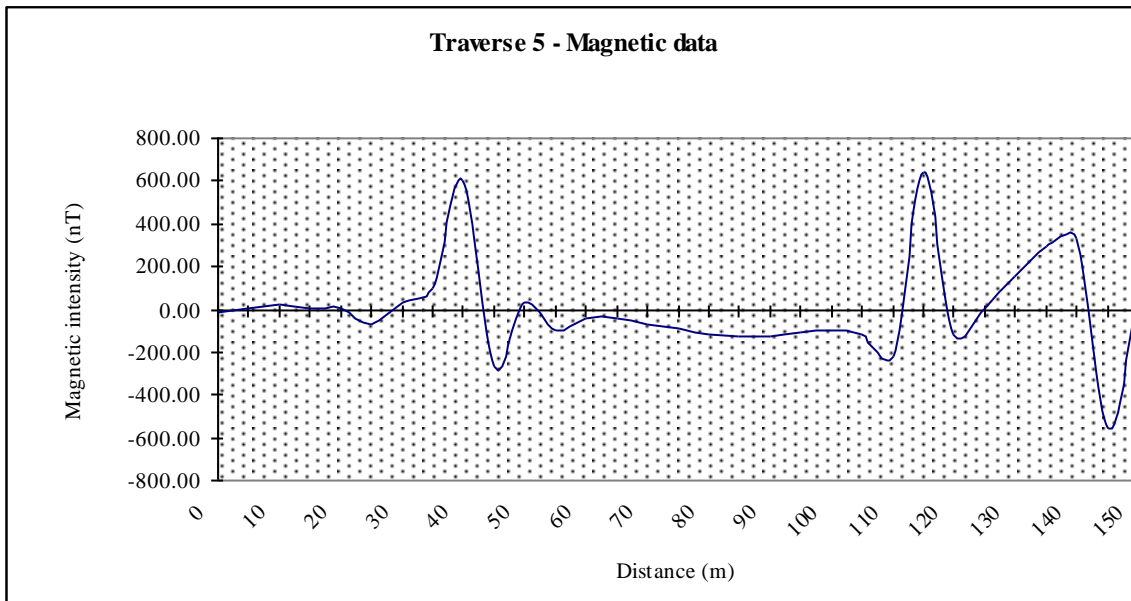


Figure 15. S-N magnetic profile of Traverse 5.

Traverse 6

Magnetic data on Traverse 6 were recorded south-west and down-gradient from the new return water dam being built. No prominent magnetic anomalies were recorded. Borehole AB22 was sited by considering factors such as accessibility and the local topographic gradient.

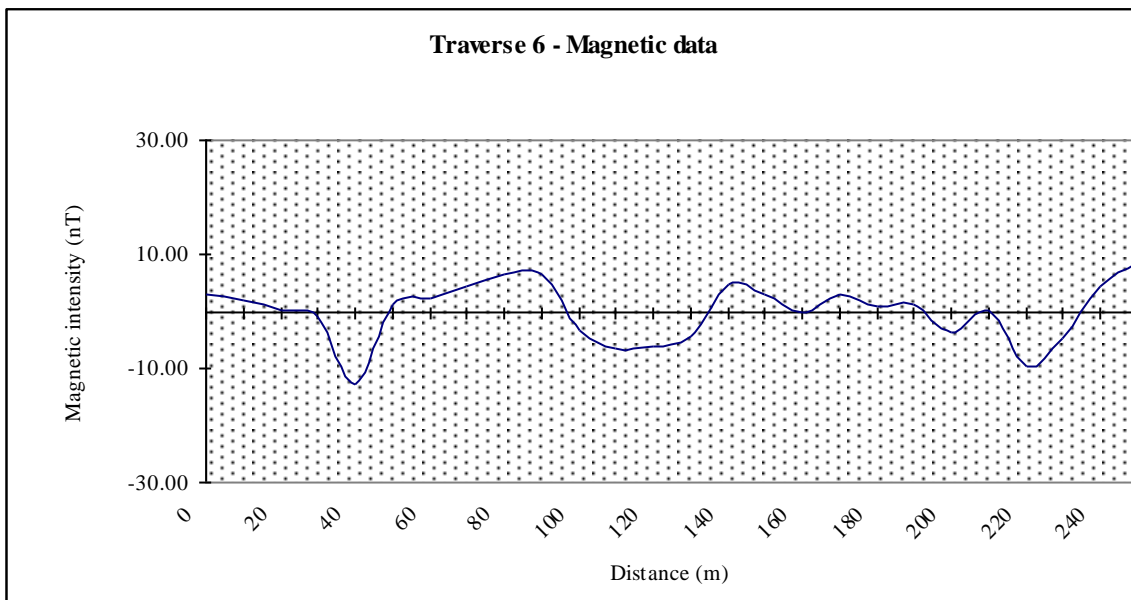


Figure 16. NW-SE magnetic profile of Traverse 6.

Traverse 7

Magnetic data on Traverse 7 were recorded south-west of the ash stack. A broad negative magnetic anomaly near the start of the traverse was seen to coincide with the position of a

local wetland along which water was draining to the south-west. It was thought that the position of the wetland may be geologically controlled. Borehole AB20 was sited to the south of the wetland.

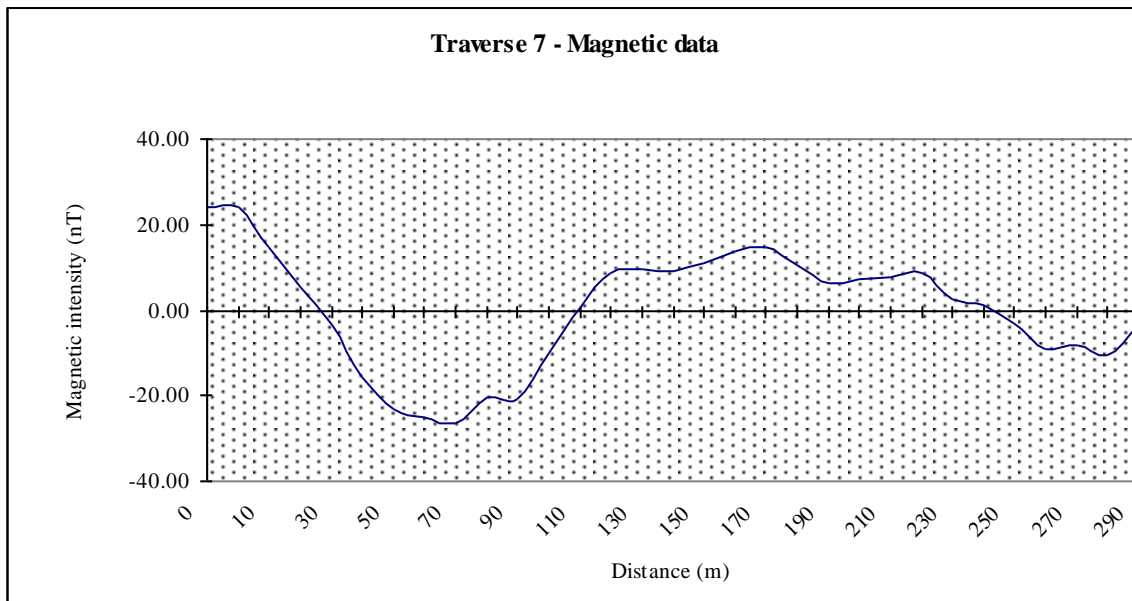


Figure 17. NW-SE magnetic profile of Travers 7.

Traverse 8

Measurements on Traverse 8 were taken to the north-east of the rehabilitated domestic waste site and to the east of the current waste site. No access to the waste site could be obtained as the gates were locked. The geophysical investigation on the outside of the fenced area was performed in an attempt to identify geological structures that cross the waste site area and that may be associated with preferential pathways for groundwater motion. A number of broad magnetic anomalies were recorded along the traverse. Borehole WB18 was sited and drilled at a position to the north and downstream from the current domestic waste site.

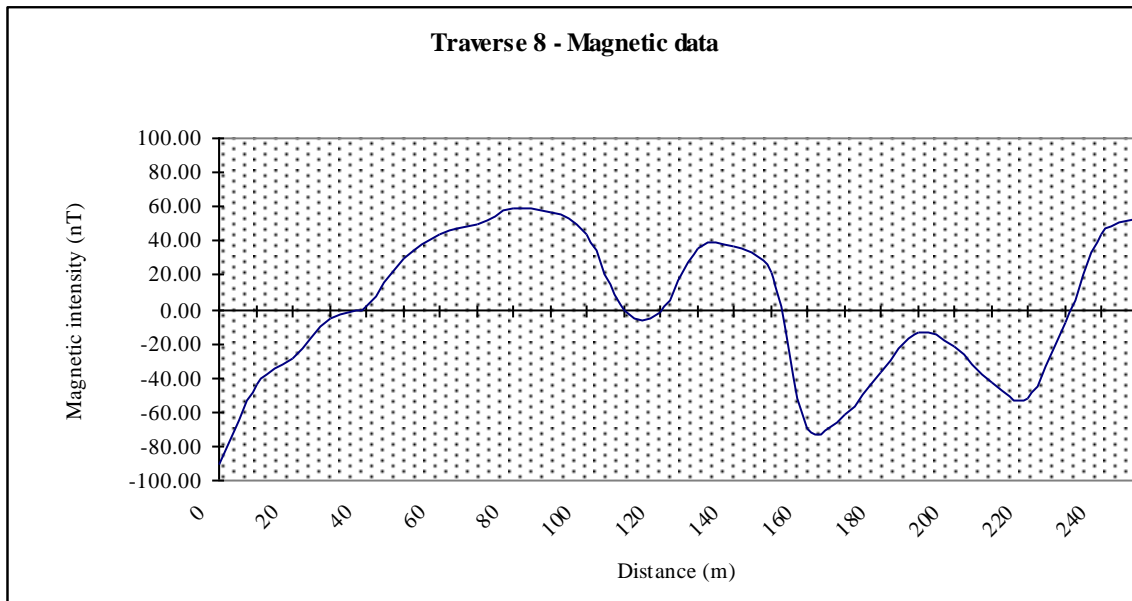


Figure 18. NW-SE magnetic profile of Traverse 8.

3.5.3 Drilling results

The drilling phase at Kendal Power Station occurred for the reason that the monitoring system had to be upgraded due to blockage of existing boreholes. These new boreholes will assure that sampling will be more effective because of more monitoring sites at a pollution source.

The geological borehole logs of the seven boreholes drilled are presented in Appendix A. The rocks encountered during drilling predominantly consisted of sandstones and shales of the Karoo Supergroup. Dolerite, which is an intrusive magmatic rock, was also encountered in boreholes near the ash stack (AB19 and AB21) and near the waste site (WB18). Metamorphic rocks (in the form of slate) were encountered during the drilling of borehole PB21. The presence of metamorphic rocks attests to the fact that high temperatures and pressures were generated at the time of the magmatic intrusions. Coal was also encountered in two boreholes (AB22 and SB24).

These newly drilled boreholes are currently part of the monitoring programme, except for borehole AB19 which is covered with ash due to the extension of the ash stack. The results of the percussion drilling are summarised in Table 3 below.

Table 3. Summary of drilling results.

BH nr.	Description	Coordinates		Rock types	Depth of water strike(s) (m)	Estimated yield (L/s)
		Latitude (°S)	Longitude (°E)			
WB18	North-east of solid waste site	26.1017	28.9848	Sandstone, dolerite	15 & 28	0.50
AB19	West of ash stack	26.1007	28.9437	Dolerite	-	-
AB20	South-west of ash stack	26.1128	28.9436	Claystone, sandstone, shale, coal	9	0.01
AB21	North of ash stack	26.0942	28.9466	Dolerite	11	0.01
AB22	South-west of return water dam	26.1162	28.9461	Sandstone, shale, clay	7	0.01
PB23	West of pollution control dams	26.0941	28.9549	Slate, granite	4	0.10
SB24	East of sewage plant	26.0775	28.9876	Sandstone, shale, coal	2 & 29	0.10

3.5.4 Conclusions

Water was encountered in all the boreholes, except borehole AB19 west of the ash stack. The yields of all the boreholes were low, ranging from 0.01 to 0.5 L/s. No dolerite dykes were intersected during this drilling phase, thus all of the boreholes are low yielding and this reduces the risk of contaminant transport in the groundwater. It would be ideal to drill high yielding boreholes that may be associated with preferential pathways and contaminant transport in order to monitor the water quality at the water strikes.

4 RISK ASSESSMENT

4.1 INTRODUCTION

A risk assessment was performed in order to identify the areas that pose a risk for groundwater contamination and to determine if the identified pollution sources will be capable of contaminating the hydrocensus boreholes in the study area.

Aerial magnetic interpretation was carried out to identify structures that may be associated with preferential pathways and contaminant transport.

Existing water level data were available from the monitoring boreholes at Kendal Power Station, but the water levels of the hydrocensus boreholes were also crucial in order to calculate the gradients from the pollution sources to the hydrocensus boreholes. Therefore Bayesian was utilised to generate water levels for the entire study area to acquire water levels for the hydrocensus boreholes.

Darcy- and seepage velocity were calculated to estimate the distances that the potential contaminants can migrate / travel from the pollution sources.

A hydrocensus study was performed to identify all the surrounding boreholes in the area outside the power station. These boreholes were sampled to gain chemistry data to be utilised as background samples where no contamination of the groundwater caused by the power station has taken place to compare these to the groundwater quality of the boreholes in the vicinity of the power station. Pollution indexes were utilised to indicate whether the groundwater of the power station has been polluted when compared to these background samples. All the additional information regarding these hydrocensus boreholes are presented in Table 4.

Table 4. Hydrocensus borehole information.

Borehole	Coordinate System (WGS 84)		Site Description	Sample Depth (m)	Borehole Depth (m)	Estimated Water Level Elevation (mamsl)	Estimated Elevation (mamsl)	Estimated Water Level (m)	Purpose	Borehole Equipment	Farm Name
	X (metres)	Y (metres)									
FBB26	1963.380	-2889679.58	100m Southeast from road.300m South from mining area. 3.5km Southeast from coal stock yard.		~	1588	1594.29	5.83	~	Wind Pump	Zondagsvlei 9/13
FBB27	423.181	-2886714.72	10m East from house.40m Southeast from tank. In garden of house.2 x 5000L tanks.Takes an hour to fill them up.	Tap	80	1614	1618.52	4.26	Domestic (Drink)	Submersible Pump	Schoongezicht 218/7
FBB28	771.476	-2884196.49	40m Northwest from house.Yield: 8000L/h.	Pumped	~	1593	1598.82	5.83	Domestic (Drink) Irrigation (Garden)	Submersible Pump	Klipfontein 3/32
FBB29	960.572	-2884447.99	5m East from small building.Pumps to same dam as WP242. Yield: 5000L/h.	Pumped	~	1598	1603.49	5.95	Domestic (Drink) Livestock (cattle sheep)	Submersible Pump	Zondagsvlei 9
FBB30	-145.053	-2887750.59	300m Northeast from house.In corn field.5000L tank.	Tap	~	1619	1621.73	2.69	Domestic (Drink)	Submersible Pump	Schoongezicht 218/45
FBB31	-2601.660	-2888877.57	West from house in grass.5000L tank.	Tap	~	1605	1610.71	5.37	Domestic (Drink)	Submersible Pump	Schoongezicht 218/3
FBB32	-2611.670	-2888854.32	Next to house.	25	~	1606	1610.52	4.70	~	None	~
FBB34	-5150.040	-2892085.7	40m North from house.10000L tank.	Tap	~	1583	1588.73	6.12	Domestic (Drink)	Submersible Pump	~
FBB35	-7370.680	-2892764.81	20m North from house.180m Southwest from main gravel road.	Pumped	~	1558	1563.29	5.19	Domestic (Drink)	Hand Pump	~
FBB36	-7637.400	-2893200.37	570m West from bend in main gravel road.260m west from infromal houses next to raod.	Pumped	~	1568	1573.19	5.47	Domestic (Drink)	Hand Pump	~
FBB37	-7609.180	-2891878.62	50m North from house.Under tree.Water usage: 20000L/week.	Tap	18	1548	1553.25	4.89	Domestic (Drink)	Submersible Pump	~
FBB38	-8252.070	-2890496.36	300m Northwest from house.160m North from camp gate, in gras	Tap	60	1538	1542.80	4.64	Domestic (Drink) Brick Factory	Submersible Pump	~
FBB39	-6270.380	-2885161.84	300m Northwest from house.160m North from camp gate, in gras	Tap	~	1560	1565.76	6.19	Domestic (Drink)	Submersible Pump	~

4.2 IDENTIFYING POLLUTION SOURCES

The latest chemistry data available were utilised to identify possible pollution sources. Polluted dams with high SO_4 concentrations were identified as pollution sources as they generate artificial recharge to the groundwater. The water quality tables for these polluted dams are presented in Table 9, the sulphate values are colour-coded green to indicate that the concentrations are elevated. See Table 6 for the classification system utilised to evaluate water quality classes. The ash stack, emergency stack and coal stockyard were also identified as pollution sources as the fly ash contain high SO_4 concentrations. All these identified pollution sources and hydrocensus boreholes are presented in Figure 19.

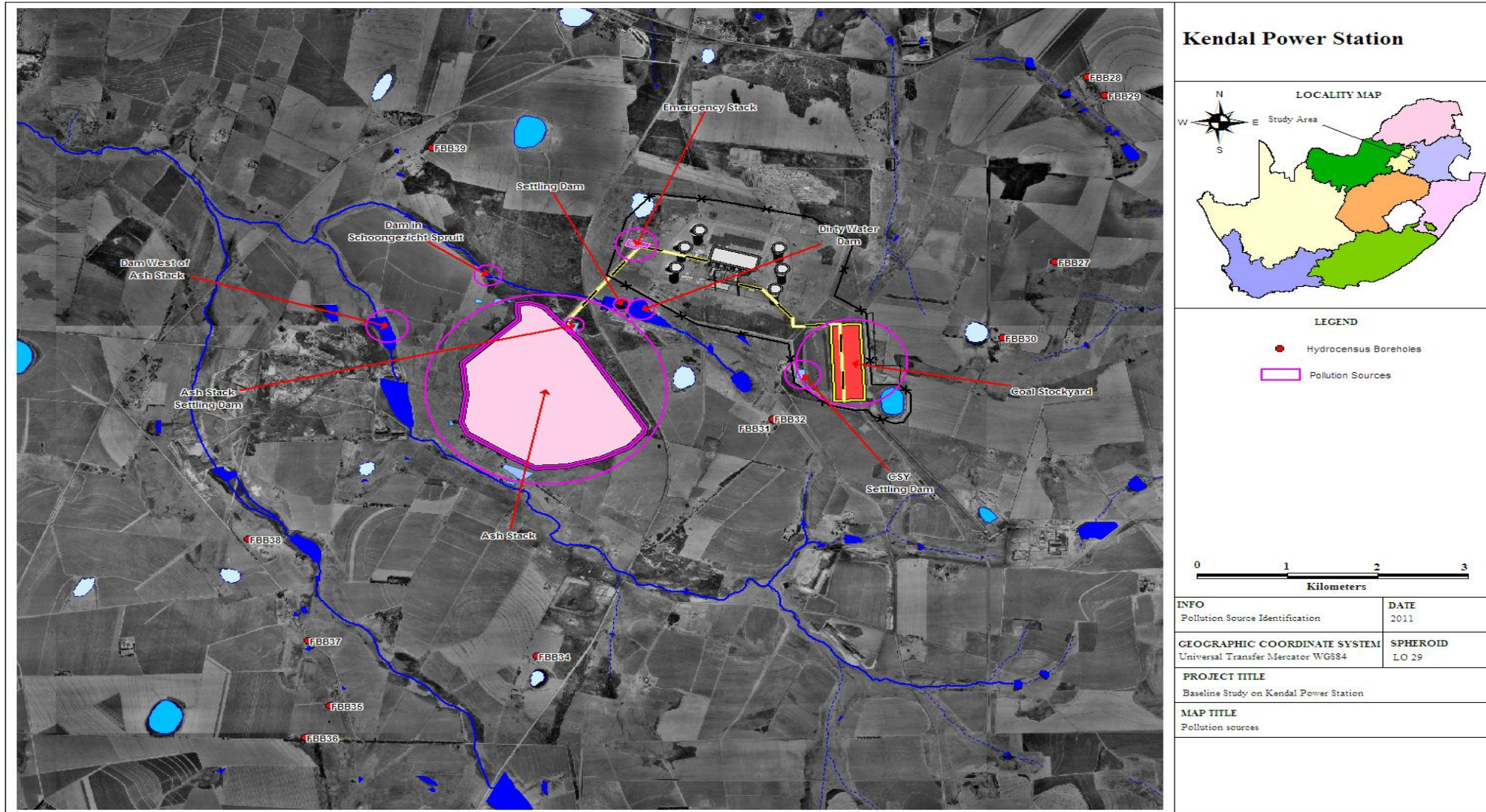


Figure 19. Pollution sources.

4.3 GROUNDWATER QUALITY-INORGANIC PARAMETERS

The results of the chemical analysis of the water samples taken at Kendal Power Station's monitoring boreholes and the hydrocensus boreholes during the latest monitoring phase are listed in Table 7 and Table 8. The water qualities of the monitoring boreholes are also presented a piper diagram for SO₄ concentrations and in time graphs for EC, Na, Ca and Cl parameters. The locations of all of the boreholes are presented in Figure 19. The data is colour-coded according to the SANS 241:2006 physical and chemical requirements (Table 6).

Table 5. Glossary of chemistry abbreviations.

Glossary of chemistry abbreviations	
Abbreviation	Description
pH	Scale measures how acidic or basic a substance is
EC	Electrical Conductivity
Na	Sodium
Ca	Calcium
Mg	Magnesium
K	Potassium
Cl	Chloride
SO ₄	Sulphate
F	Fluoride
NO ₃	Nitrate
Zn	Zink
SANS	South African National Standards for drinking water

Table 6. SANS 241:2006 Edition 6.1.

1	2	3	4	5
Determinand	Unit	Class 1 (Recommended operational limit)	Class 2 (Max. allowable for limited duration)	Class 2 water consumption period, max
Physical and organoleptic requirements				
Colour (aesthetic)	mg/L Pt	< 20	20 - 50	No limit
Conductivity at 25 °C (aesthetic)	mS/m	< 150	150 - 370	7 years
Dissolved solids (aesthetic)	mg/L	<1 000	1000 - 2400	7 years
Odour (aesthetic)	TON	< 5	5.0 - 10	No limit
pH value at 25°C (aesthetic operational)	pH units	5.0 - 9.5	4.0 - 10.0	No limit
Taste (aesthetic)	FTN	< 5	5.0 - 10	No limit
Turbidity (aesthetic/operational/ indirect health)	NTU	< 1	1.0 - 5	No limit
Chemical requirements- macro-determinand				
Ammonia as N (operational)	mg/L	< 1.0	1.0 - 2.0	No limit
Calcium as Ca aesthetic/operational)	mg/L	< 150	150 - 300	7 years
Chloride as Cl ⁻ (aesthetic)	mg/L	< 200	200 - 600	7 years
Fluoride as F ⁻ (health)	mg/L	< 1.0	1.0 - 1.5	1 year
Magnesium as Mg (aesthetic/health)	mg/L	< 70	70 - 100	7 years
(Nitrate and nitrite) as N (health)	mg/L	< 10	10.0 - 20	7 years
Potassium as K (operational/health)	mg/L	< 50	50 - 100	7 years
Sodium as Na (aesthetic/health)	mg/L	< 200	200 - 400	7 years
Sulfate as SO ₄ (health)	mg/L	< 400	400 - 600	1 year
Zinc as Zn (aesthetic/health)	mg/L	< 5.0	5.0 - 10	1 year

Table 7. Water quality tables of monitoring boreholes.

Site No	pH	EC mS/m	Na mg/L	Ca mg/L	Mg mg/L	K mg/L	Cl mg/L	SO ₄ mg/L	F mg/L	NO ₂ -N mg/L	NO ₃ -N mg/L	Zn mg/L
AB07	7.04	11	9.07	10.20	2.60	2.80	3.0	3	0.20	0.10	0.10	0.010
AB08	6.94	81	29.06	96.46	29.57	3.74	21.3	332	0.05	0.02	1.40	0.008
AB14	6.86	5	6.10	4.14	1.64	1.69	2.1	2	0.03	0.01	0.13	0.005
AB15	6.58	7	6.60	11.50	2.80	3.10	2.1	1	0.00		0.90	
AB16	7.69	10	13.10	5.44	1.38	3.71	8.0	4	0.20	0.10	0.10	0.010
AB19	7.95	21	20.20	11.00	3.97	3.47	10.0	13	1.74	0.10	0.19	0.020
AB20	7.86	176		48.80	0.00		4.5	6	1.65		0.05	
AB21	7.16	102	41.65	125.19	45.85	3.06	20.6	398	0.05	0.01	0.15	1.104
AB22	7.42	37	16.27	50.91	7.41	4.92	13.9	65	0.08	0.01	0.02	0.006
AB25	6.53	13	9.19	8.26	5.15	3.86	3.9	37	0.12	0.01	0.27	0.037
AB44	6.79	7	4.77	2.45	1.10	1.18	3.2	3	0.05	0.01	0.26	0.009
AB45	6.81	5	5.10	2.40	1.16	1.44	2.2	2	0.02	0.01	1.14	0.053
CB01	6.95	16	9.22	12.90	6.02	3.41	6.0	6	0.35	0.10	0.10	0.010
CB02	6.14	4	5.03	2.70	1.44	1.87	2.0	4	0.20	0.10	3.30	0.010
CB03	6.58	4	4.01	2.77	0.01	2.28	2.0	1	0.30	0.10	1.80	0.030
CB09	6.98	21	7.40	15.30	6.20	11.00	4.1	6	0.30		0.10	
CB13	7.04	13	8.34	4.44	2.39	1.30	6.0	2	0.20	0.10	0.10	0.010
CB17	7.51	29	13.15	31.65	7.36	6.23	15.2					
CB40	7.20	14	7.42	10.48	5.74	3.71	3.3	2	0.03	0.01	9.44	0.055
PB04	7.93	25	25.30	23.40	5.34	0.65	3.0	7	2.54	0.10	0.10	0.010
PB05	6.74	8	10.60	4.85	2.16	2.32	3.0	4	0.20	0.10	0.13	0.030
PB06	8.11	20	39.92	10.20	0.57	0.41	4.0	5	6.15	0.01	0.11	0.006
PB23	8.07	41	48.70	26.10	6.72	3.19	12.0	85	0.99	0.10	0.10	0.010
PB42	6.82	6	8.17	1.97	1.39	3.62	2.1	2	0.03	0.01	0.15	0.147
SB24	7.72	55	38.10	43.20	28.10	1.77	12.0	19	0.26	0.10	0.10	0.010
WB12	7.23	10	7.24	7.08	4.60	3.20	3.0	4	0.20	0.10	0.10	0.010
WB18	6.55	5	7.18	1.96	1.06	0.51	5.5	1	0.02	0.01	0.13	0.046

Table 8. Water quality tables of hydrocensus boreholes.

No	pH	EC mS/m	Na mg/L	Ca mg/L	Mg mg/L	K mg/L	Cl mg/L	SO ₄ mg/L	F mg/L	NO ₂ -N mg/L	NO ₃ -N mg/L
FBB28	7.28	24	18.18	23.26	7.12	4.43	11.2	3	0.58	0.01	0.63
FBB29	6.42		21.53	10.27	6.72	5.05	36.2	2	0.09	0.01	8.44
FBB30	6.61		10.58	3.18	1.82	1.75	2.2	2	0.02	0.01	7.67
FBB31	6.45	6	4.40	2.70	1.44	4.31	2.4	1	0.11	0.01	2.08
FBB32	6.66	7	4.89	4.08	1.59	3.15	2.9	2	0.08	0.01	0.00
FBB33	7.31	99	20.14	116.10	41.85	3.73	60.0	119	0.02	0.01	46.78
FBB34	7.96	26	18.24	21.20	8.25	7.08	3.3	3	0.26	0.01	0.07
FBB35	6.26	11	6.96	5.50	3.64	4.52	13.9	2	0.02	0.01	5.91
FBB36	7.70	21	15.17	19.58	7.36	4.47	2.2	1	0.10	0.01	0.00
FBB37	7.04	14	10.59	10.73	4.19	3.12	2.1	1	0.12	0.01	0.16
FBB38	7.91	64	134.88	10.46	1.83	2.02	11.6	134	9.61	0.01	0.00
FBB39	6.13	21	13.54	11.44	8.02	5.24	22.6	17	0.05	0.01	11.62

Table 9. Water quality tables of polluted dams.

No	pH	EC mS/m	Na mg/L	Ca mg/L	Mg mg/L	K mg/L	Cl mg/L	SO ₄ mg/L	F mg/L	NO ₂ -N mg/L	NO ₃ -N mg/L	Zn mg/L
AP10 Ash Stack Settling Dam	11.4	149	175.00	113.39	0.16	9.74	29.8	364	0.95	1.19	1.18	0.006
AP11 Dam West of Ash Stack	7.79	91	123.00	60.46	12.32	6.57	23.4	419	0.74	0.04	0.18	0.005
PP02 Dirty Water Dam	8.30	97	174.00	31.42	7.65	7.30	27.4	326	0.83	2.07	0.87	0.007
PP03 Settling Dam	7.54	91	52.43	32.33	9.62	7.15	25.8	315	0.10	0.45	1.07	0.007
PP05 Dam in Schoongezicht spruit	7.67	97	27.06	88.71	64.11	7.94	11.3	428	0.54	0.01	0.23	0.008
CP08 CSY Settling dam	7.06	114	13.01	222.90	33.55	4.52	3.1	624	1.74	0.01	0.10	0.008

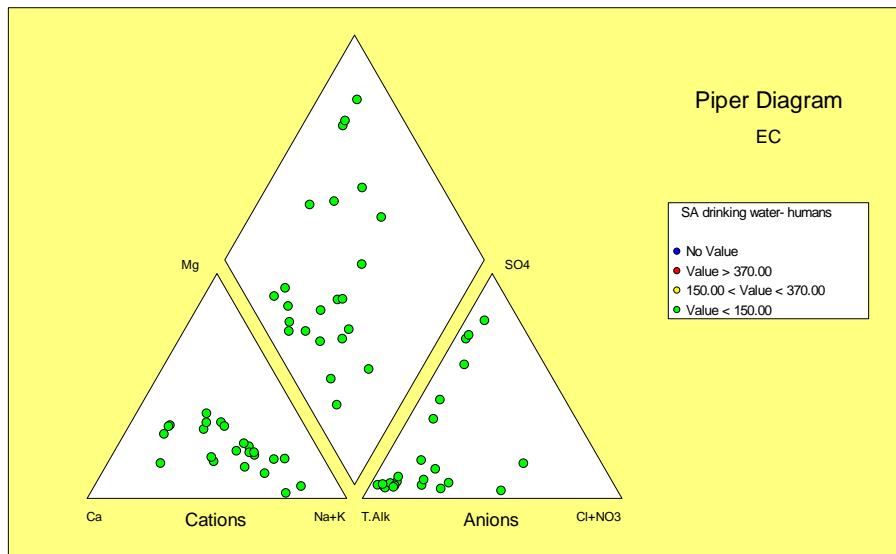


Figure 20. SO_4 concentrations of monitoring boreholes.

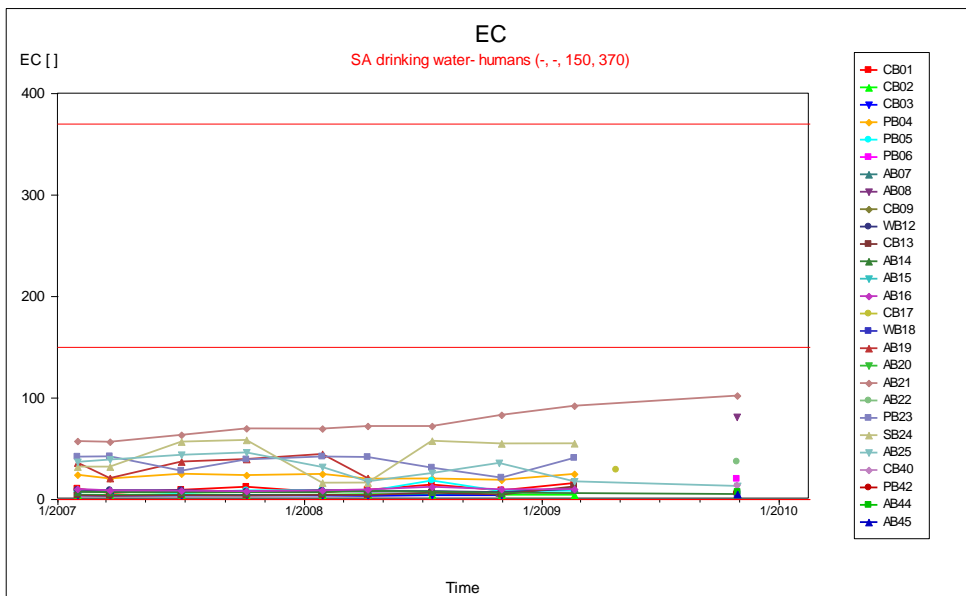


Figure 21. EC concentrations of monitoring boreholes.

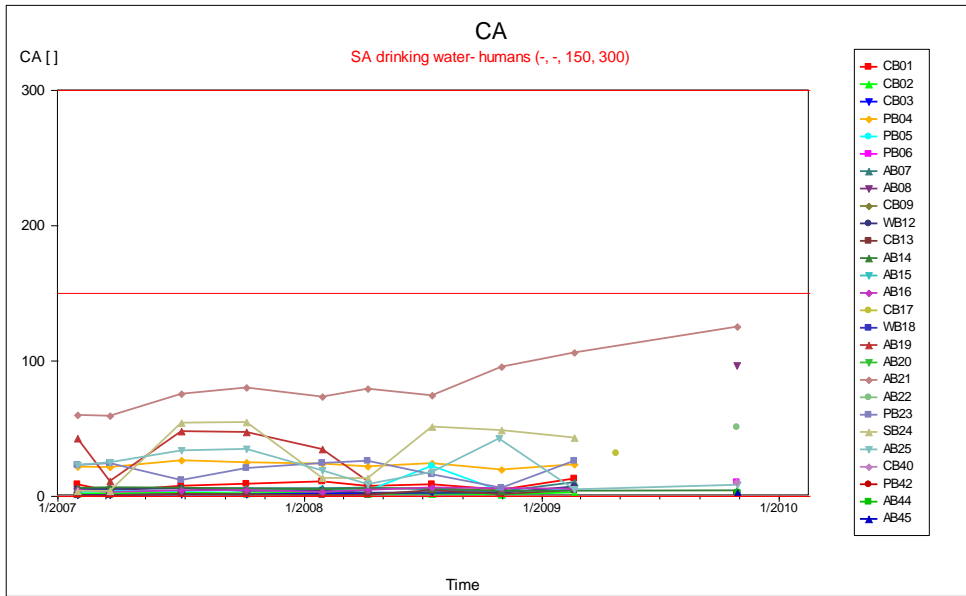


Figure 22. Ca concentrations for monitoring boreholes.

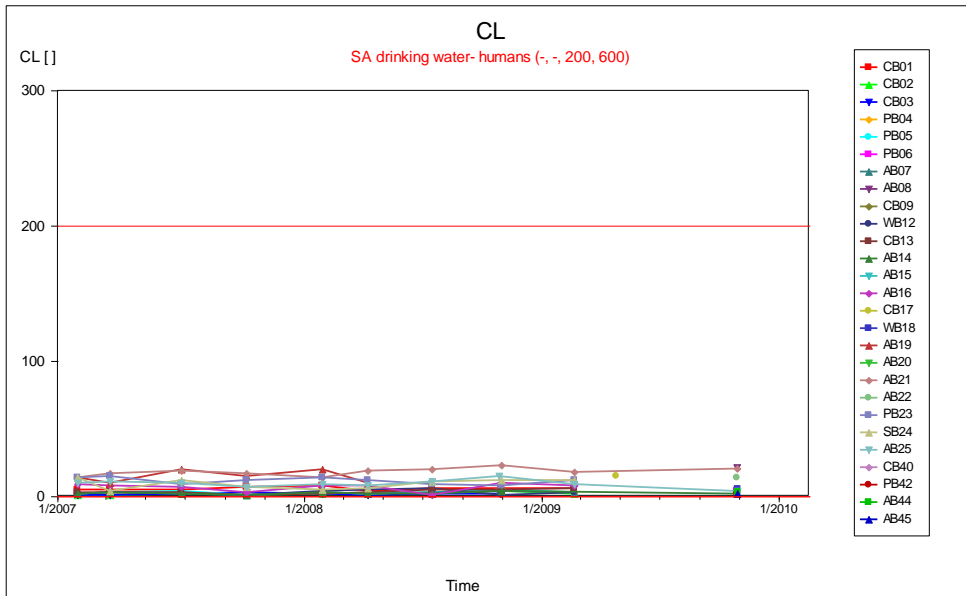


Figure 23. Cl concentrations for monitoring boreholes.

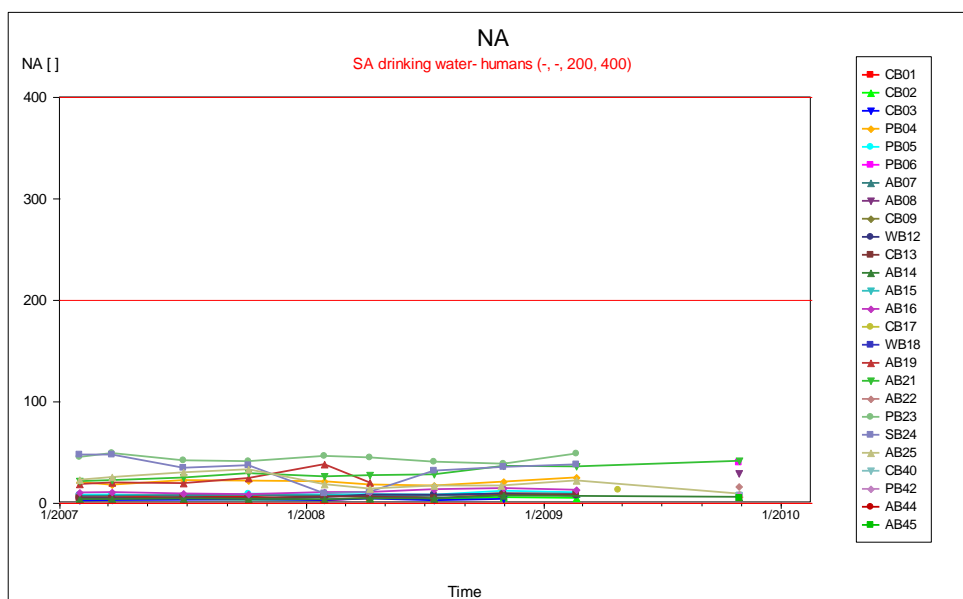


Figure 24. Na concentrations for monitoring boreholes.

4.3.1 Discussion of groundwater qualities

Monitoring boreholes

The piper diagram and time graphs indicate that the boreholes' water qualities are acceptable for parameters Ec, Na, Ca Cl and SO₄. Elevated sulphate concentrations are found at boreholes AB08 and AB21 but are not indicated yellow on the paper diagram as the concentrations are below 400 mg/l. These boreholes are located close to the ash stack and the elevated sulphate concentrations can be due to seepage from the ash stack to the groundwater.

According to Table 7, boreholes AB19, AB20, PB04 and PB06 contain high fluoride concentrations. These high concentrations can be attributed to the dolerite and granites present in the borehole logs in Appendix G.

Hydrocensus boreholes

Borehole FBB38 is classified as Class 2 water quality due to a high fluoride concentration. This high fluoride concentration is mainly due to the geology in the area, but no geological log information is available for any of the hydrocensus boreholes. Elevated nitrate concentrations are found at boreholes FBB33 and FBB39. Nitrate contamination originates mainly from agricultural operations including farm runoff and livestock, so this high

concentration is not as a result of the power station operations. According to the additional parameters included in Table 8, it is clear that the current risk for human health is very low.

4.3.2 Pollution index tables

The pollution index tables were calculated according to (Fourie 2004)

According to the groundwater dictionary, pollution is the introduction into the environment of any substance by the action of man, which is or results in significant harmful effects to man or the environment. Therefore the Pollution Index Tables are used to obtain a first estimate of the probability that pollutants are impacting on the groundwater at Kendal Power Station. For groundwater sites the Pollution Index (PI) for a specific indicator element is calculated by relating the current concentration to the concentrations recorded at a number of uncontaminated background sites, and by assuming that the indicator element concentrations of the background samples follow a normal distribution. The PI for each indicator element under consideration is calculated by taking the difference between the current concentration and the average concentration obtained for the background samples. This difference is then divided by the standard deviation of the background samples, as explained in Eq.1:

$$(PI)_{indicator\ element\ A} = \frac{(Current\ conc. - Geomean\ of\ background\ conc.)_{indicator\ element\ A}}{(St.\ dev.\ of\ background\ conc)_{indicator\ element\ A}} \quad (Eq.1)$$

To interpret the PI's of the groundwater sites, the following should be noted:

Negative PI's imply that the current indicator element concentration is lower than the average background concentration and that pollutant impacts are therefore not visible.

PI's greater than 0.5 imply that the current sample concentration is more than half a standard deviation larger than the average concentration measured at the background sampling sites.

PI's greater than unity imply that the current sample concentration is more than one standard deviation larger than the average concentration measured at the background sampling sites.

PI's greater than two imply that the current sample concentration is more than two standard deviations larger than the average concentration measured at the background sampling sites.

The average parameter values of the background samples and the standard deviations calculated for these sites are listed in Table 10. These values are used to obtain the pollution indexes of the various sites. The monitoring boreholes indicator elements are presented in Table 11 which indicates the current concentrations of the water quality of these boreholes.

The pollution index results are presented in Table 12 which indicates the probability that pollutants are impacting the groundwater at Kendal Power Station. The locations of the hydrocensus and monitoring boreholes are presented in Figure 25.

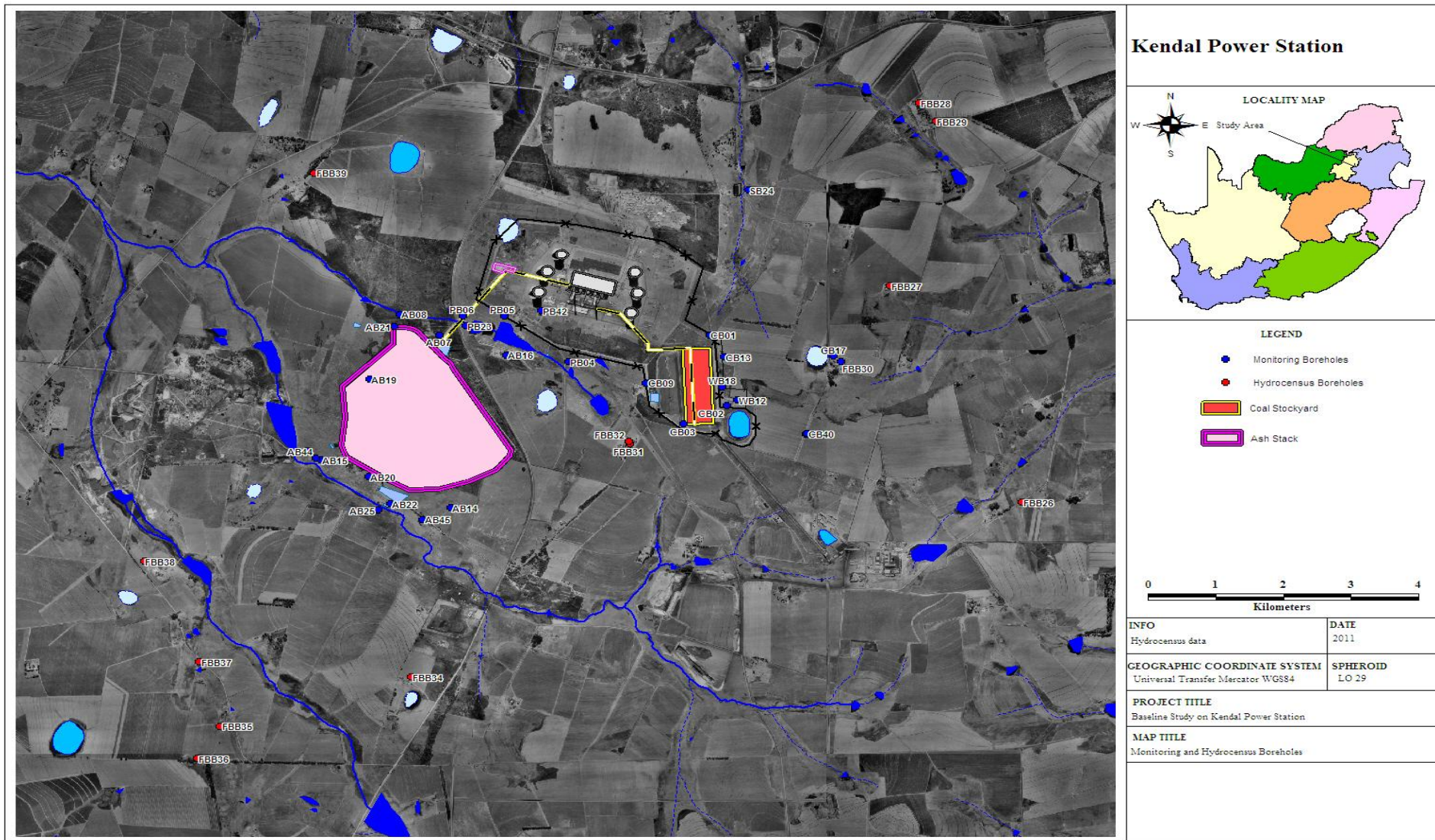


Figure 25. Hydrocensus and monitoring boreholes.

Table 10. Average parameter values.

Background groundwater	EC (mS/m)	Na (mg/L)	Ca (mg/L)	Cl (mg/L)	SO4 (mg/L)
FBB27	21	16	16	4	2
FBB28	24	18	23	11	3
FBB29	~	22	10	36	2
FBB30	~	11	3	2	2
FBB31	6	4	3	2	1
FBB32	7	5	4	3	2
FBB34	26	18	21	3	3
FBB35	11	7	6	14	2
FBB36	21	15	20	2	1
FBB37	14	11	11	2	1
FBB38	64	135	10	12	134
FBB39	21	14	11	23	17
Geomean	17	14	9	6	3
StDev	17	36	7	11	38

4.3.3 Indicator elements

The indicator elements are presented in Table 11 and are the current concentration of the monitoring boreholes sampled used to calculate the pollution indexes listed in Table 12.

These elements are utilised as it is most likely to give a clear indication if pollution sources are influencing the groundwater quality.

Table 11. Current concentration of indicator elements.

Current concentrations of the indicator elements					
All Boreholes					
Sites	Parameters values				
	EC (mS/m)	Na (mg/L)	Ca (mg/L)	Cl (mg/L)	SO ₄ (mg/L)
Ashing Area					
AB07	10.7	9.1	10.2	3.0	2.8
AB08	81.0	29.1	96.5	21.3	332.0
AB14	5.0	6.1	4.1	2.1	1.7
AB15	7.5	6.6	11.5	2.1	0.5
AB16	9.9	13.1	5.4	8.0	4.5
AB19	20.7	20.2	11.0	10.0	13.4
AB20	176.1	~	48.8	4.5	6.2
AB21	102.0	41.7	125.2	20.6	398.0
AB22	37.0	16.3	50.9	13.9	65.0
AB25	13.0	9.2	8.3	3.9	36.9
AB44	7.0	4.8	2.5	3.2	3.0
AB45	5.0	5.1	2.4	2.2	1.5
Coal Sockyard Area					
CB01	15.9	9.2	12.9	6.0	5.9
CB02	4.4	5.0	2.7	2.0	3.9
CB03	3.9	4.0	2.8	2.0	1.2
CB09	20.6	7.4	15.3	4.1	6.1
CB13	12.5	8.3	4.4	6.0	2.3
CB17	29.0	13.2	31.7	15.2	~
CB40	14.0	7.4	10.5	3.3	2.2
WB12	10.1	7.2	7.1	3.0	3.6
WB18	5.0	7.2	2.0	5.5	1.1
Power Station Area					
PB04	24.9	25.3	23.4	3.0	7.4
PB05	8.4	10.6	4.9	3.0	4.4
PB06	20.0	39.9	10.2	4.0	4.9
PB23	40.8	48.7	26.1	12.0	85.4
PB42	6.0	8.2	2.0	2.1	1.6
SB24	55.1	38.1	43.2	12.0	19.2

4.3.4 Pollution index results

Table 12. Pollution index results.

Groundwater					
Sites	Pollution Index				
	EC (mS/m)	Na (mg/L)	Ca (mg/L)	Cl (mg/L)	SO ₄ (mg/L)
Ashing Area					
AB07	-0.34	-0.15	-0.04	-0.23	-0.03
AB08	2.16	0.43	2.86	0.83	7.04
AB14	-0.54	-0.24	-0.24	-0.28	-0.05
AB15	-0.45	-0.23	0.01	-0.28	-0.08
AB16	-0.37	-0.04	-0.20	0.06	0.01
AB19	0.02	0.17	-0.01	0.18	0.20
AB20	5.54	-0.42	1.26	-0.14	0.05
AB21	2.91	0.80	3.82	0.79	8.46
AB22	0.59	0.06	1.33	0.40	1.31
AB25	-0.26	-0.15	-0.10	-0.18	0.71
AB44	-0.47	-0.28	-0.30	-0.22	-0.02
AB45	-0.54	-0.27	-0.30	-0.27	-0.06
Coal Stockyard Area					
CB01	-0.16	-0.15	0.06	-0.06	0.04
CB13	-0.28	-0.17	-0.23	-0.06	-0.04
CB17	0.31	-0.03	0.68	0.48	-0.09
CB40	-0.22	-0.20	-0.03	-0.21	-0.04
WB12	-0.36	-0.21	-0.14	-0.23	-0.01
WB18	-0.54	-0.21	-0.31	-0.09	-0.06
Power Station Area					
PB04	0.16	0.32	0.41	-0.23	0.07
PB05	-0.42	-0.11	-0.22	-0.23	0.01
PB06	-0.01	0.75	-0.04	-0.17	0.02
PB23	0.73	1.01	0.50	0.29	1.75
PB42	-0.51	-0.18	-0.31	-0.28	-0.05
SB24	1.24	0.70	1.07	0.29	0.32

PI > 0.5 - Possibility of pollutant impacts
 PI > 1.0 - High probability of pollutant impacts
 PI > 2.0 - Very high probability of pollutant impacts

4.3.5 Monitoring boreholes exceeding average concentrations of hydrocensus boreholes.

When comparing the current concentrations of the monitoring boreholes to the average concentrations of the hydrocensus boreholes for EC, Ca, Na Cl and SO₄ can be is observed which monitoring boreholes have a higher concentration than the average for the hydrocensus boreholes. This will give estimation if the water quality of the monitoring boreholes is being influenced by the power station if it exceeds the average water quality significantly. These boreholes exceeding the average values are indicated for each parameter in Figure 26 to Figure 30.

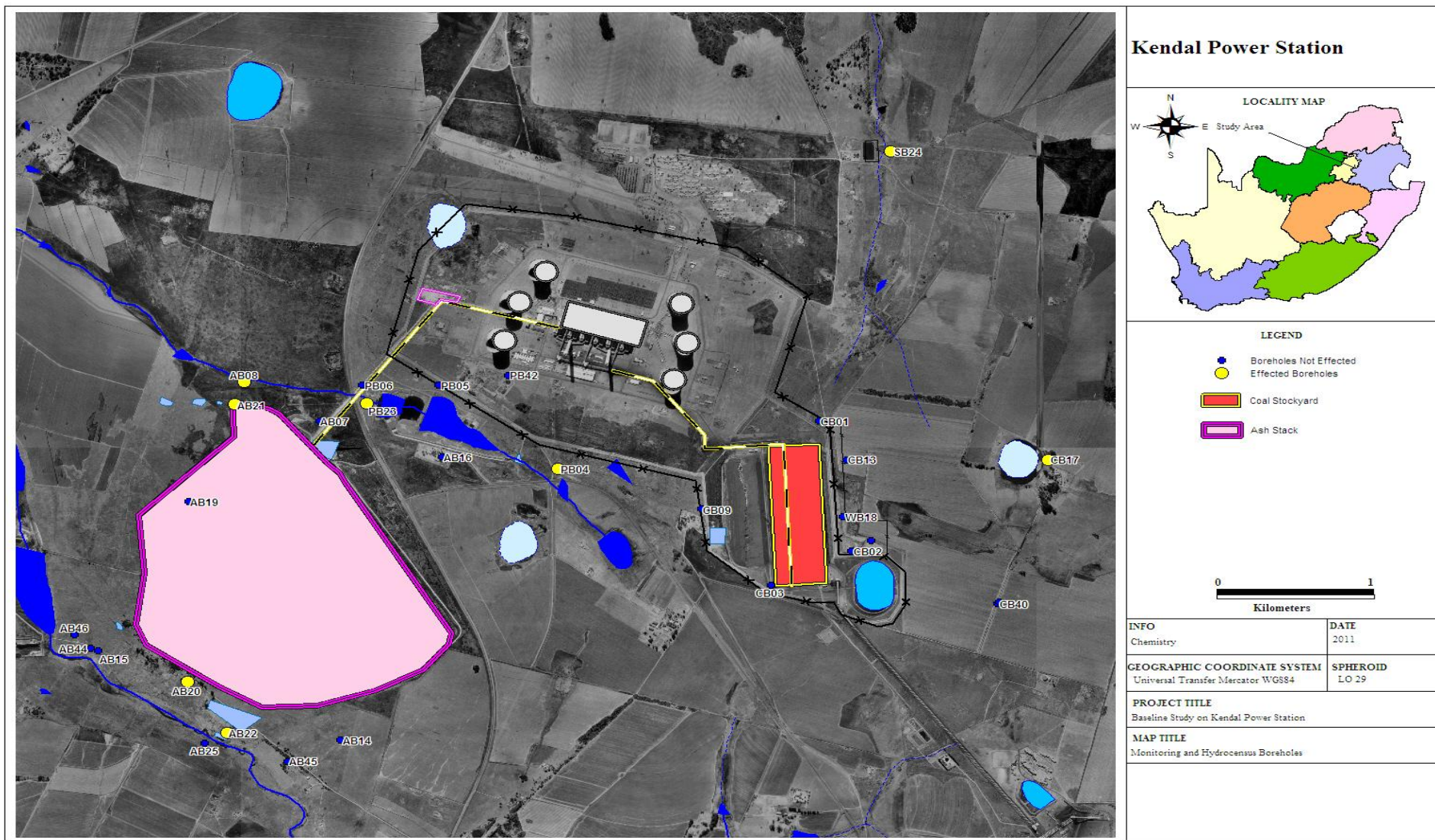


Figure 26. Boreholes exceeding average Ca concentrations of hydrocensus boreholes.

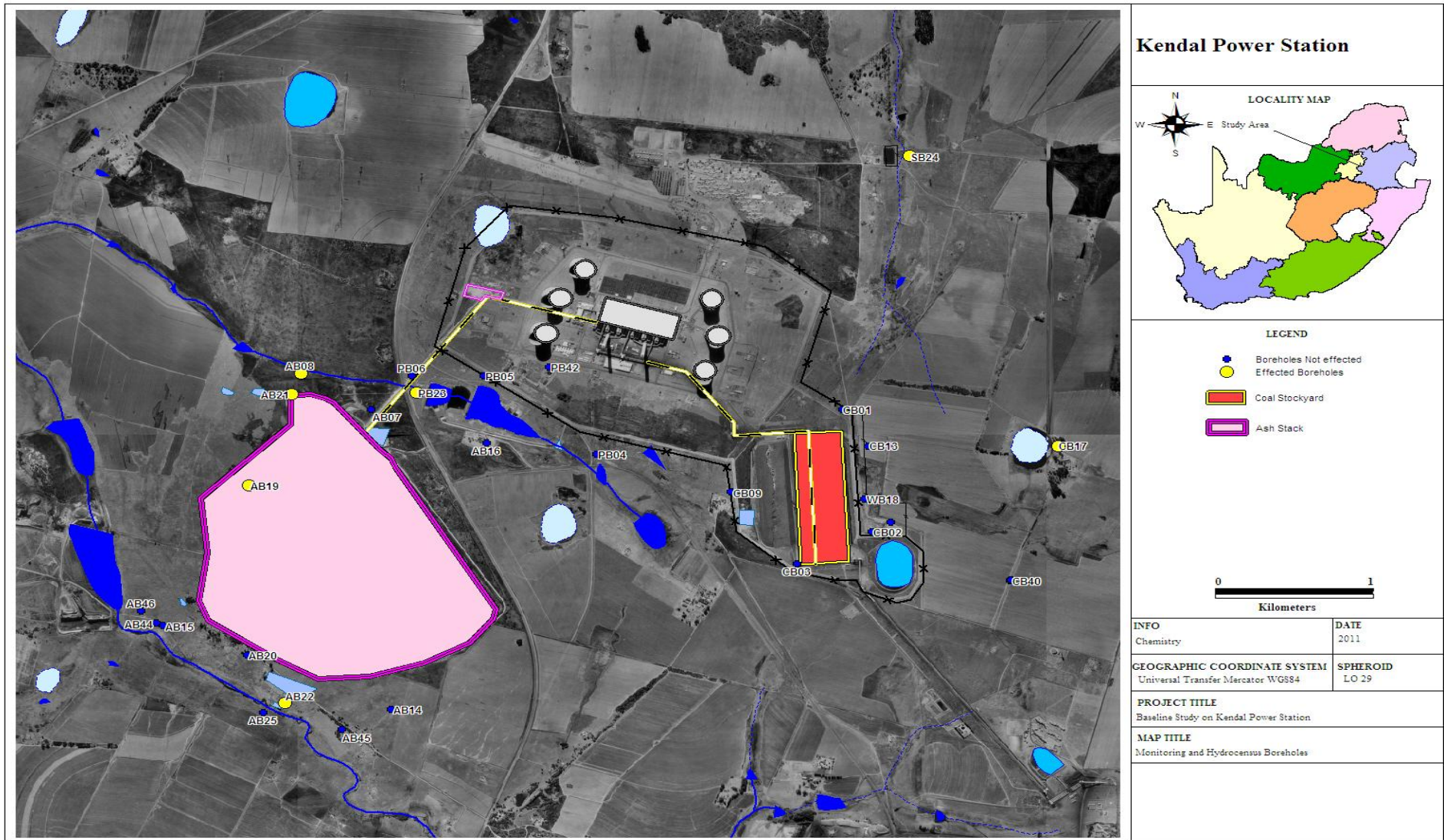


Figure 27. Boreholes exceeding average Cl concentrations of hydrocensus boreholes.

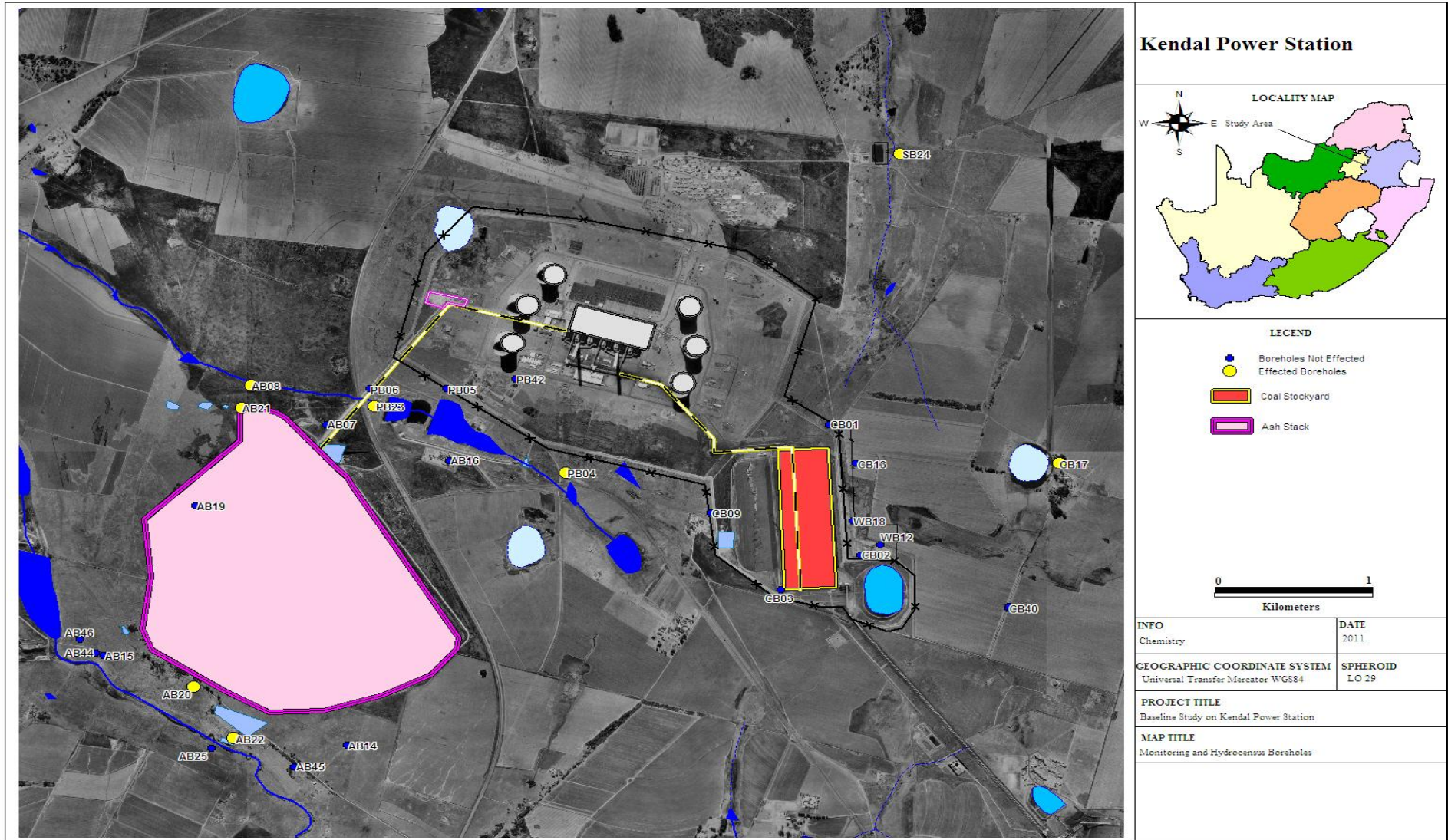


Figure 28. Boreholes exceeding average electrical conductivity of hydrocensus boreholes.



Figure 29. Boreholes exceeding average Na concentrations of hydrocensus boreholes.



Figure 30. Boreholes exceeding average SO₄ concentrations of hydrocensus boreholes.

4.3.6 Conclusions

According to the results of the pollution index, 8 of the 27 boreholes in the study area have a possibility of pollutant impact. It is evident that the boreholes in the vicinity of the ashing area have a higher probability of pollutant impact than the boreholes in the vicinity of the power station and coal stockyard Areas.

It is evident that 9 of the 27 boreholes exceed the average water quality of the hydrocensus boreholes. Boreholes AB08, AB20, AB21, AB22, CB17, PB04, PB06, PB23 and SB24 exceed the average water quality and are also indicated in the pollution index for a possibility of having a pollutant impact, whereas borehole PB04 is not indicated as having a possible pollutant impact in the pollution index. This is because that the water quality of PB04 is not elevated as much as necessary over the average hydrocensus water quality to indicate a possible impact by the power station.

It is clear that boreholes AB08, AB20, AB21 and AB22 in the ashing area exceed the water quality of the hydrocensus boreholes and are indicated as a high to a very high probability of pollutant impact. These boreholes are also located close to the ash stack, therefore the water quality is likely to be impacted by seepage from the ash stack.

Only borehole CB17 indicates a possibility of pollutant impact and exceeds the average water quality concentration of the hydrocensus boreholes in the vicinity of the coal stockyard area.

4.4 AERIAL MAGNETIC INTERPRETATION

Aerial magnetic interpretation was performed to identify structures that may be associated with preferential pathways and contaminant transport. No clear images of dolerite dykes could be detected close to the pollution sources, as the aerial magnetic intensity is low.

Cultivated land areas around the power station make the interpretation of the orthophoto map more difficult as the top soil is disturbed. It is recommended that more consideration must be given to identifying preferential pathways as these areas have a very high hydraulic conductivity and if pollutants reach these areas, the pollution will be transported greater distances than in seepage and will pose a greater risk for groundwater contamination. Figure 25 indicates the aerial magnetic map of Kendal Power Station.

It was found that there are no dolerite dykes at the geophysical traverses completed during the drilling of the new boreholes. In order to identify any structures at the pollution sources, the traverses must be conducted around the pollution sources to assure that there are no preferential pathways that can support contaminant transport.

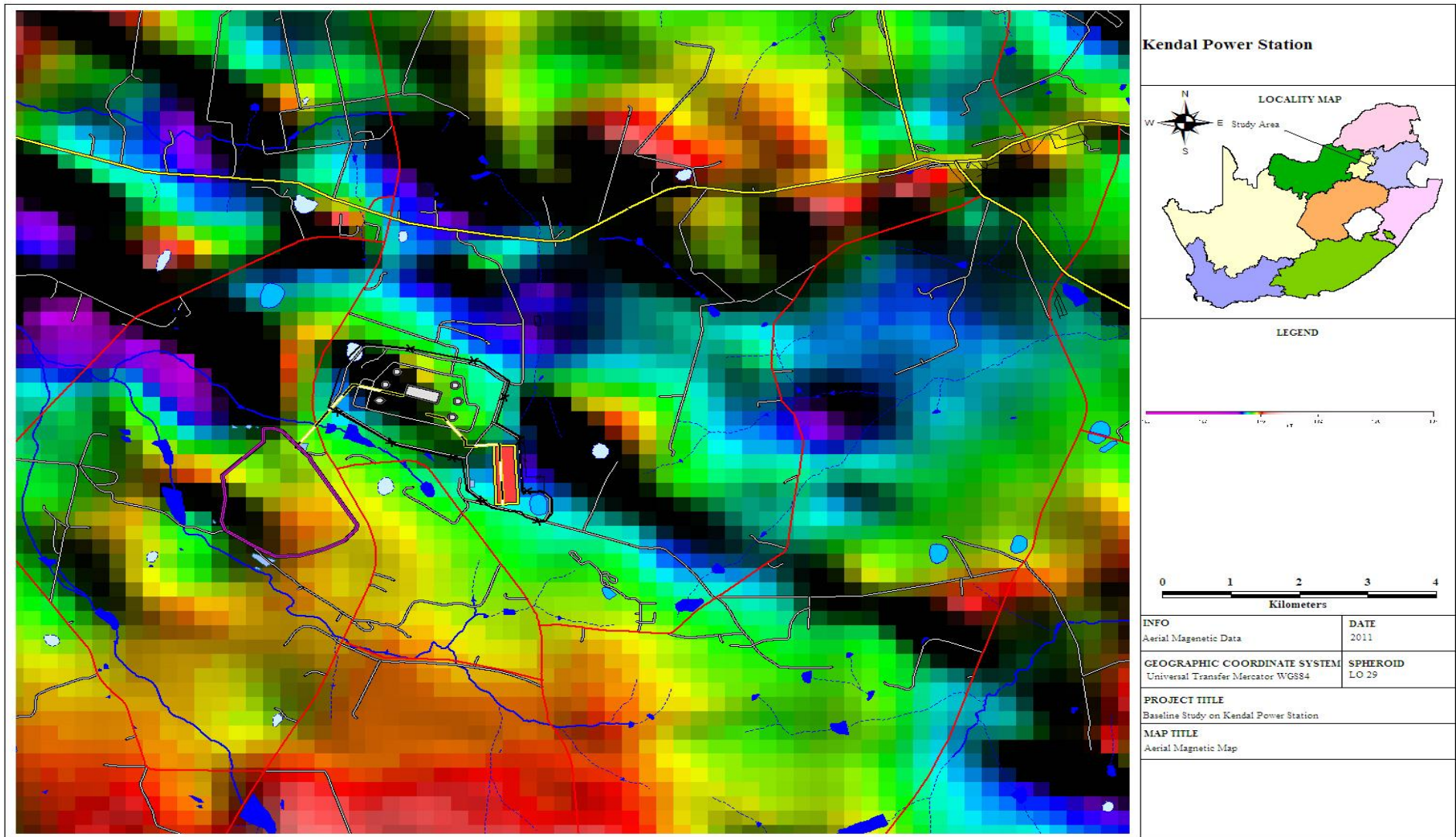


Figure 31. Aerial magnetic map.

4.5 GENERATING WATER LEVELS

Water level data were available for the monitoring boreholes at the Kendal Power Station, but only one of the hydrocensus boreholes had a water level measurement due to equipment (submersible pump, hand pump or wind pump) installed at the farmer's boreholes. The existing water level data were utilised to generate water levels for the entire study area. Bayesian was utilised to generate the water levels for the study area and to calculate the water levels for the hydrocensus boreholes (Table 13). These water levels are essential in calculating the water level gradient from the pollution sources to the hydrocensus boreholes in order to determine whether the contamination can migrate from the pollution sources to the hydrocensus boreholes.

Table 13. Calculated hydrocensus boreholes water levels.

Number	Longitude(oE)	Latitude (oS)	Water Level Elevation	Topo Elevations	Water level
FBB26	29.01963	-26.11594	1588.5	1594.29	5.8
FBB27	29.00423	-26.08918	1614.3	1618.52	4.3
FBB28	29.00771	-26.06645	1593.0	1598.82	5.8
FBB29	29.009596	-26.068721	1597.5	1603.49	5.9
FBB30	28.99855	-26.09853	1619.0	1621.73	2.7
FBB31	28.97399	-26.1087	1605.3	1610.71	5.4
FBB32	28.97389	-26.10849	1606.0	1610.52	4.7
FBB34	28.9485	-26.13765	1582.6	1588.73	6.1
FBB35	28.92629	-26.14377	1558.1	1563.29	5.2
FBB36	28.92362	-26.1477	1567.7	1573.19	5.5
FBB37	28.92391	-26.13577	1548.4	1553.25	4.9
FBB38	28.91749	-26.12329	1538.2	1542.80	4.6
FBB39	28.93733	-26.07515	1559.6	1565.76	6.2

In order to use the Bayesian method, correlation between the topography and groundwater levels are indicated in Figure 32.

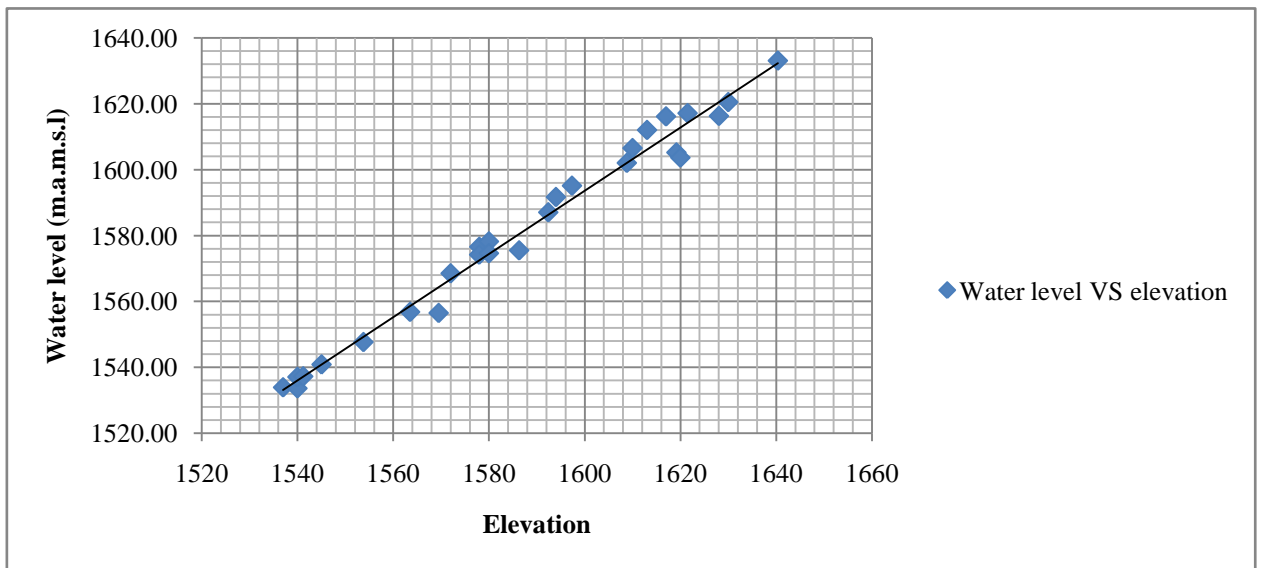


Figure 32. Correlation between topography and groundwater level.

Surfer was used to generate the map (Figure 33) indicating the groundwater flow.

Surfer software is a full-function 3D visualization, contouring and surface modeling package. Surfer is used extensively for terrain modeling, landscape visualization, surface analysis, contour mapping, 3D surface mapping, gridding, volumetrics, and much more. The interpolation engine transforms your scattered XYZ data into publication-quality maps.

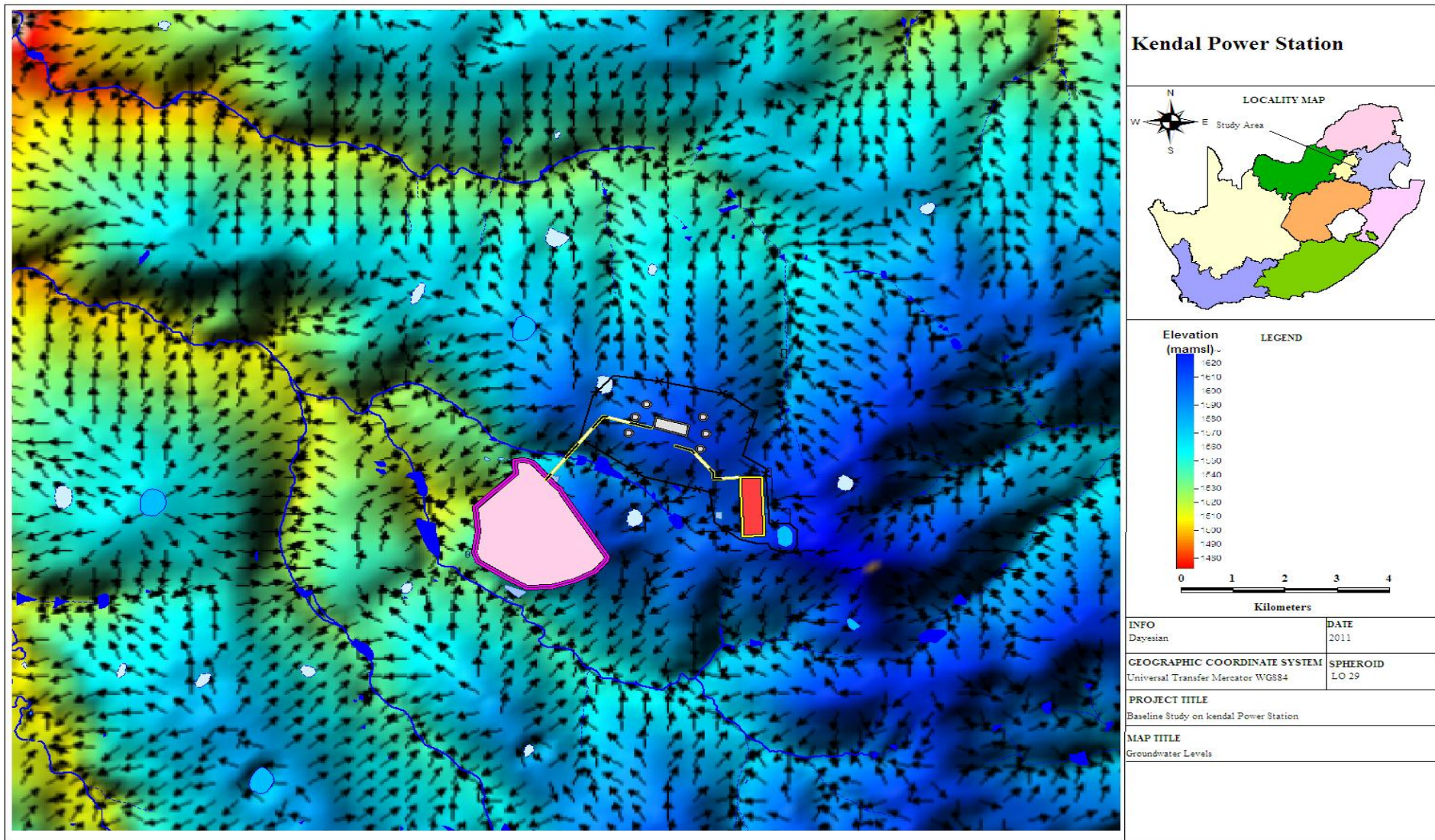


Figure 33. Groundwater flow.

4.6 CALCULATING POLLUTION MIGRATION DISTANCES

The water levels acquired in Table 13 are utilised to calculate the gradient from the different pollution sources to the hydrocensus boreholes. The groundwater levels of the pollution sources were also acquired by using bayesian and are presented in Table 14. The pollution sources are numbered from source P_A to P_I. The coordinates used in Table 14 are obtained from the middle of the pollution source.

Table 14. Calculated pollution source water levels.

Souce Nr	Pollution Source	Coordinate System (WGS84)				Water level
		Long	Lat	X (meters)	Y (meters)	
P_A	CSY	28.98248	-26.10165	-1753.00	-2888096.25	1607.3
P_B	Ash Stack	28.94955	-26.104918	-5046.25	-2888459.25	1576.8
P_C	Emergency Stack	28.95928	-26.087154	-4074.25	-2886491.25	1601.7
P_D	CSY Settling Dam	28.97715	-26.103084	-2286.25	-2888255.25	1605.5
P_E	Dam in Schoongezicht spruit	28.94334	-26.090925	-5668	-2886909	1537.5
P_F	Dirty Water dam	28.95982	-26.095122	-4020.25	-2887374	1581.1
P_G	Dam West of Ash Atack	28.93250	-26.097135	-6752.5	-2887597.5	1511.8
P_H	Ash Stack Settling dam	28.95267	-26.097007	-4734.25	-2887582.5	1583.6
P_I	Settling Dam	28.95767	-26.09452	-4234.75	-2887307.25	1579.4

Maps were created for each pollution source to indicate the shortest distances from the pollution sources to the hydrocensus boreholes and are used to calculate the gradients, the calculations are presented in Table 15. It is assumed that the contamination can flow directly from the pollution source to the hydrocensus boreholes without any variation in the water level except for the calculated gradients in order to create a worst case scenario.

Figure 34 indicates the distances from the coal stockyard to each of the background boreholes in the study area. Maps indicating the distances from the additional pollution sources to the hydrocensus boreholes are indicated in Appendix B.

4.6.1 Calculated gradients

To determine the gradient, the differences in water level (m) were divided by the distance from the pollution source to the hydrocensus boreholes. These gradients are utilised to calculate the Darcy and seepage velocity. Some of the gradients are negative, because the water levels of the boreholes are higher than the water levels at the pollution sources. These seepage velocities are not calculated because there are no threats for that pollution source to affect the hydrocensus boreholes.

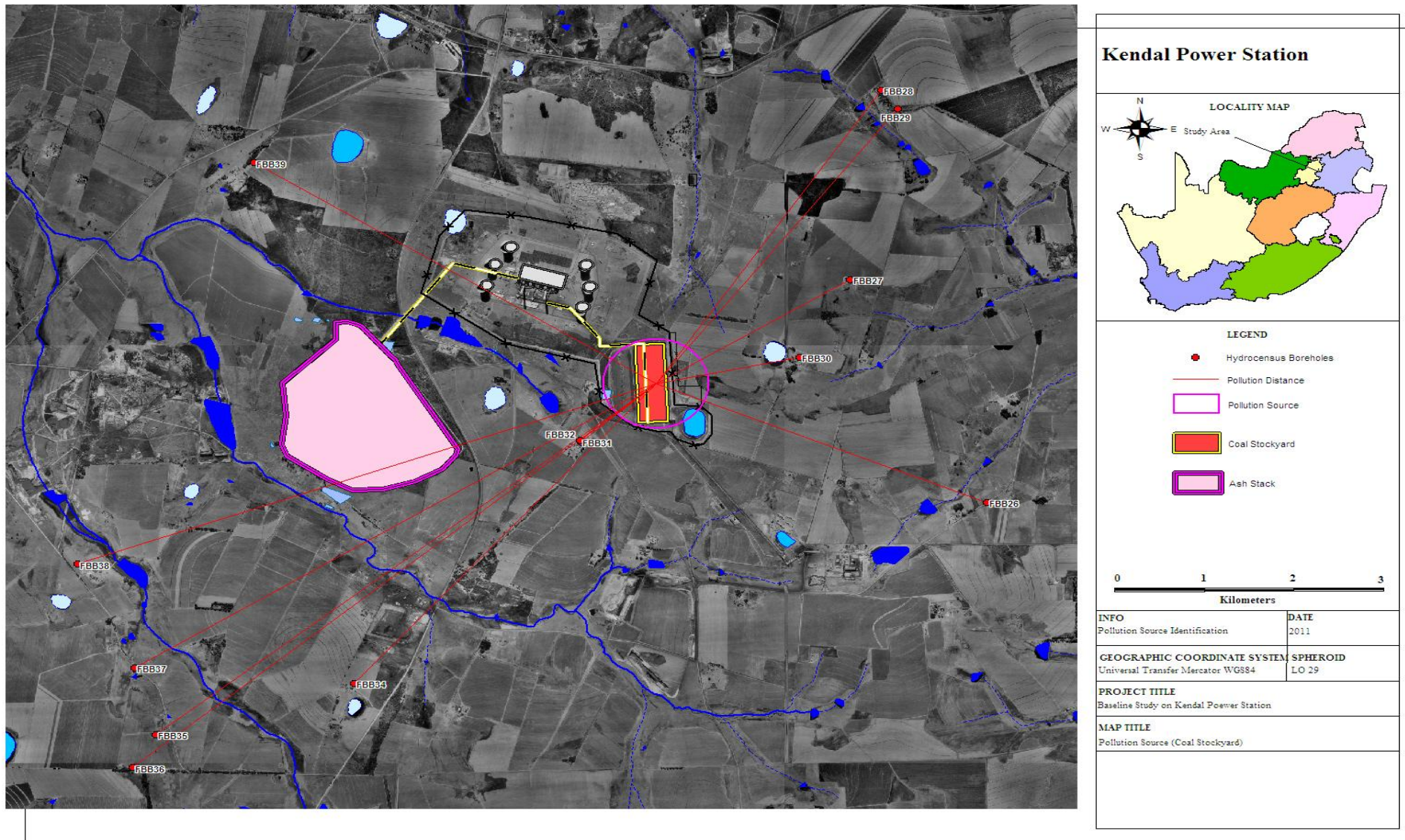


Figure 34. Pollution distances (coal stockyard.)

Table 15. Calculated gradients.

Pollution Source	Distance form Pollution Source to Borehole (m)										
	BH WI	P_A CSY	P_B Ash Stack	P_C Emergency Stack	P_D CSY Settling Dam	P_E Dam in Schoongezicht spruit	P_F Dirty Water dam	P_G Dam West of Ash Atack	P_H Ash Stack Settling dam	P_I Settling Dam	
Pollutin Sorce WI		1607	1577	1602	1605	1537	1581	1512	1584	1579	
FBB26	1588	4040	7115	6828	4482	8119	6412	8961	7018	6637	
FBB27	1614	2578	5741	4503	3117	6094	4492	7230	5230	4695	
FBB28	1593	4646	7212	5362	5082	6987	5750	8257	6464	5894	
FBB29	1598	4547	7223	5434	5004	7071	5777	8331	6500	5930	
FBB30	1619	1645	4952	4126	2200	5587	3893	6609	4592	4114	
FBB31	1605	1154	2480	2804	698	3644	2067	4344	2495	2266	
FBB32	1606	1145	2466	2779	682	3623	2043	4327	2474	2242	
FBB34	1583	5240	3628	5697	4783	5203	4845	4766	4522	4865	
FBB35	1558	7304	4893	7087	6796	6098	6347	5204	5814	6294	
FBB36	1568	7790	5403	7597	7286	6592	6858	5672	6324	6805	
FBB37	1548	6971	4273	6444	6439	5335	5760	4366	5169	5682	
FBB38	1538	6928	3798	5787	6373	4421	5259	3264	4568	5129	
FBB39	1560	5387	3517	2567	5044	1848	3155	2483	2867	2957	
		Water level Difference [Pollution WI - Borehole WI] (m)									
FBB26	1588	19	-12	13	17	-51	-7	-77	-5	-9	
FBB27	1614	-7	-38	-13	-9	-77	-33	-102	-31	-35	
FBB28	1593	14	-16	9	12	-56	-12	-81	-9	-14	
FBB29	1598	10	-21	4	8	-60	-16	-86	-14	-18	
FBB30	1619	-12	-42	-17	-14	-82	-38	-107	-35	-40	
FBB31	1605	2	-29	-4	0	-68	-24	-94	-22	-26	
FBB32	1606	1	-29	-4	-1	-69	-25	-94	-22	-27	
FBB34	1583	25	-6	19	23	-45	-1	-71	1	-3	
FBB35	1558	49	19	44	47	-21	23	-46	25	21	
FBB36	1568	40	9	34	38	-30	13	-56	16	12	
FBB37	1548	59	28	53	57	-11	33	-37	35	31	
FBB38	1538	69	39	63	67	-1	43	-26	45	41	
FBB39	1560	48	17	42	46	-22	22	-48	24	20	
		Gradient (i)									
FBB26	1588	0.005	-0.002	0.002	0.004	-0.006	-0.001	-0.009	-0.001	-0.001	
FBB27	1614	-0.003	-0.007	-0.003	-0.003	-0.013	-0.007	-0.014	-0.006	-0.007	
FBB28	1593	0.003	-0.002	0.002	0.002	-0.008	-0.002	-0.010	-0.001	-0.002	
FBB29	1598	0.002	-0.003	0.001	0.002	-0.008	-0.003	-0.010	-0.002	-0.003	
FBB30	1619	-0.007	-0.009	-0.004	-0.006	-0.015	-0.010	-0.016	-0.008	-0.010	
FBB31	1605	0.002	-0.012	-0.001	0.000	-0.019	-0.012	-0.022	-0.009	-0.011	
FBB32	1606	0.001	-0.012	-0.002	-0.001	-0.019	-0.012	-0.022	-0.009	-0.012	
FBB34	1583	0.005	-0.002	0.003	0.005	-0.009	0.000	-0.015	0.000	-0.001	
FBB35	1558	0.007	0.004	0.006	0.007	-0.003	0.004	-0.009	0.004	0.003	
FBB36	1568	0.005	0.002	0.004	0.005	-0.005	0.002	-0.010	0.003	0.002	
FBB37	1548	0.008	0.007	0.008	0.009	-0.002	0.006	-0.008	0.007	0.005	
FBB38	1538	0.010	0.010	0.011	0.011	0.000	0.008	-0.008	0.010	0.008	
FBB39	1560	0.009	0.005	0.016	0.009	-0.012	0.007	-0.019	0.008	0.007	

Table 16. Distances between hydrocens boreholes and pollution sources and additional information.

Borehole	Coordinate System (WGS 84)		Site Description	Distance from Pollution A (m)	Distance from Pollution B (m)	Distance from Pollution C (m)	Distance from Pollution D (m)	Distance from Pollution F (m)	Distance from Pollution H (m)	Distance from Pollution I (m)	Sample Depth (m)	Borehole Depth (m)	Estimated Water Level Elevation (mamsl)	Estimated Elevation (mamsl)	Estimated Water Level (m)	Purpose	Borehole Equipment	Farm Name
	X (metres)	Y (metres)																
FBB26	1963.380	-2889679.58	100m Southeast from road.300m South from mining area. 3.5km Southeast from coal stock yard.	4040	7115	6828	4482	6412	7018	6637		~	1588	1594.29	5.83	~	Wind Pump	Zondagsvlei 9/13
FBB27	423.181	-2886714.72	10m East from house.40m Southeast from tank. In garden of house.2 x 5000L tanks.Takes an hour to fill them up.	2578	5741	4503	3117	4492	5230	4695	Tap	80	1614	1618.52	4.26	Domestic (Drink)	Submersible Pump	Schoongezicht 218/7
FBB28	771.476	-2884196.49	40m Northwest from house.Yield: 8000L/h.	4646	7212	5362	5082	5750	6464	5894	Pumped	~	1593	1598.82	5.83	Domestic (Drink) Irrigation (Garden)	Submersible Pump	Klipfontein 3/32
FBB29	960.572	-2884447.99	5m East from small building.Pumps to same dam as WP242. Yield: 5000L/h.	4547	7223	5434	5004	5777	6500	5930	Pumped	~	1598	1603.49	5.95	Domestic (Drink) Livestock (cattle sheep)	Submersible Pump	Zondagsvlei 9
FBB30	-145.053	-2887750.59	300m Northeast from house.In corn field.5000L tank.	1645	4952	4126	2200	3893	4592	4114	Tap	~	1619	1621.73	2.69	Domestic (Drink)	Submersible Pump	Schoongezicht 218/45
FBB31	-2601.660	-2888877.57	West from house in grass.5000L tank.	1154	2480	2804	698	2067	2495	2266	Tap	~	1605	1610.71	5.37	Domestic (Drink)	Submersible Pump	Schoongezicht 218/3
FBB32	-2611.670	-2888854.32	Next to house.	1145	2466	2779	682	2043	2474	2242	25	~	1606	1610.52	4.70	~	None	~
FBB34	-5150.040	-2892085.7	40m North from house.10000L tank.	5240	3628	5697	4783	4845	4522	4865	Tap	~	1583	1588.73	6.12	Domestic (Drink)	Submersible Pump	~
FBB35	-7370.680	-2892764.81	20m North from house.180m Southwest from main gravel road.	7304	4893	7087	6796	6347	5814	6294	Pumped	~	1558	1563.29	5.19	Domestic (Drink)	Hand Pump	~
FBB36	-7637.400	-2893200.37	570m West from bend in main gravel road.260m west from infromal houses next to raod.	7790	5403	7597	7286	6858	6324	6805	Pumped	~	1568	1573.19	5.47	Domestic (Drink)	Hand Pump	~
FBB37	-7609.180	-2891878.62	50m North from house.Under tree.Water usage: 20000L/week.	6971	4273	6444	6439	5760	5169	5682	Tap	18	1548	1553.25	4.89	Domestic (Drink)	Submersible Pump	~
FBB38	-8252.070	-2890496.36	300m Northwest from house.160m North from camp gate, in gras	6928	3798	5787	6373	5259	4568	5129	Tap	60	1538	1542.80	4.64	Domestic (Drink) Brick Factory	Submersible Pump	~
FBB39	-6270.380	-2885161.84	300m Northwest from house.160m North from camp gate, in gras	5387	3517	2567	5044	3155	2867	2957	Tap	~	1560	1565.76	6.19	Domestic (Drink)	Submersible Pump	~

4.6.2 Slug test method

The slug test method is one of a number of different methods that are used to evaluate the permeability (or hydraulic conductivity) of the borehole. The procedure involves either adding or removing a measured quantity of water from a borehole rapidly, followed by making a rapid series of water-level measurements to assess the rate of water-level recovery (either rising-head or falling-head). These evaluations have advantages and disadvantages when compared with other methods.

Advantages of the slug test method:

- Relatively low cost;
- Requires little time to conduct and
- Involves removal of little or no water from the aquifer.

4.6.3 Calculation of hydraulic conductivity

A number of methods have been developed to calculate hydraulic conductivity (or permeability) from slug test data. Hydraulic conductivity is defined as the volume of water that will move through a unit time under a unit hydraulic gradient through a unit area angle to the direction of flow. Hydraulic conductivity is usually measured in unit distance and unit time, for instance, meters per day (m/d).

The Bouwer and Rice Method (1976) is usually used to obtain hydraulic conductivity from raw slug test data. This method was originally published in an article entitled "Slug Test Procedure to Evaluate Hydraulic Conductivity of an Aquifer Applicable to Fully or Partially Penetrating boreholes in Unconfined Aquifers".

The Bouwer and Rice (1976) method was applied to the data recorded in boreholes. AB07, AB08, AB14, AB16, AB21, AB22, AB25, AB44, AB45, CB13,, CB40, PB04, PB05, PB06, PB23, PB42, SB24, WB18. The Bouwer and Rice equation reads:

$$K = \frac{r^2 \ln(R_e / r_w)}{2d} \frac{1}{t} \ln \frac{h_0}{h_t}$$

Where:

r_e = radius of the unscreened part of the borehole where the head is rising.

r_w = horizontal distance from the borehole centre to the undisturbed aquifer.

R_c = radial distance over which the difference in head is dissipated in the flow system of the aquifer.

d = length of the borehole screen or open section of the borehole.

h_0 = head in the borehole at time = 0.

h_t = head in the borehole at time = t.

The estimated K-value of Bouwer and Rice is dependent on the thickness open to flow.

4.6.4 Slug test results

Summarised in Table 17 are the results of the slug tests performed at Kendal Power Station. These results indicate an upper and a lower range for the hydraulic conductivities of these

boreholes. The average hydraulic conductivity indicates the upper range and the geometric mean indicates the lower range in order to compare these results, as the pollution migration was calculated from all the pollution sources to the hydrocensus boreholes. The interpretation of the slug test data from borehole AB16 is presented in Figure 35 and the additional slug tests are presented in Appendix C.

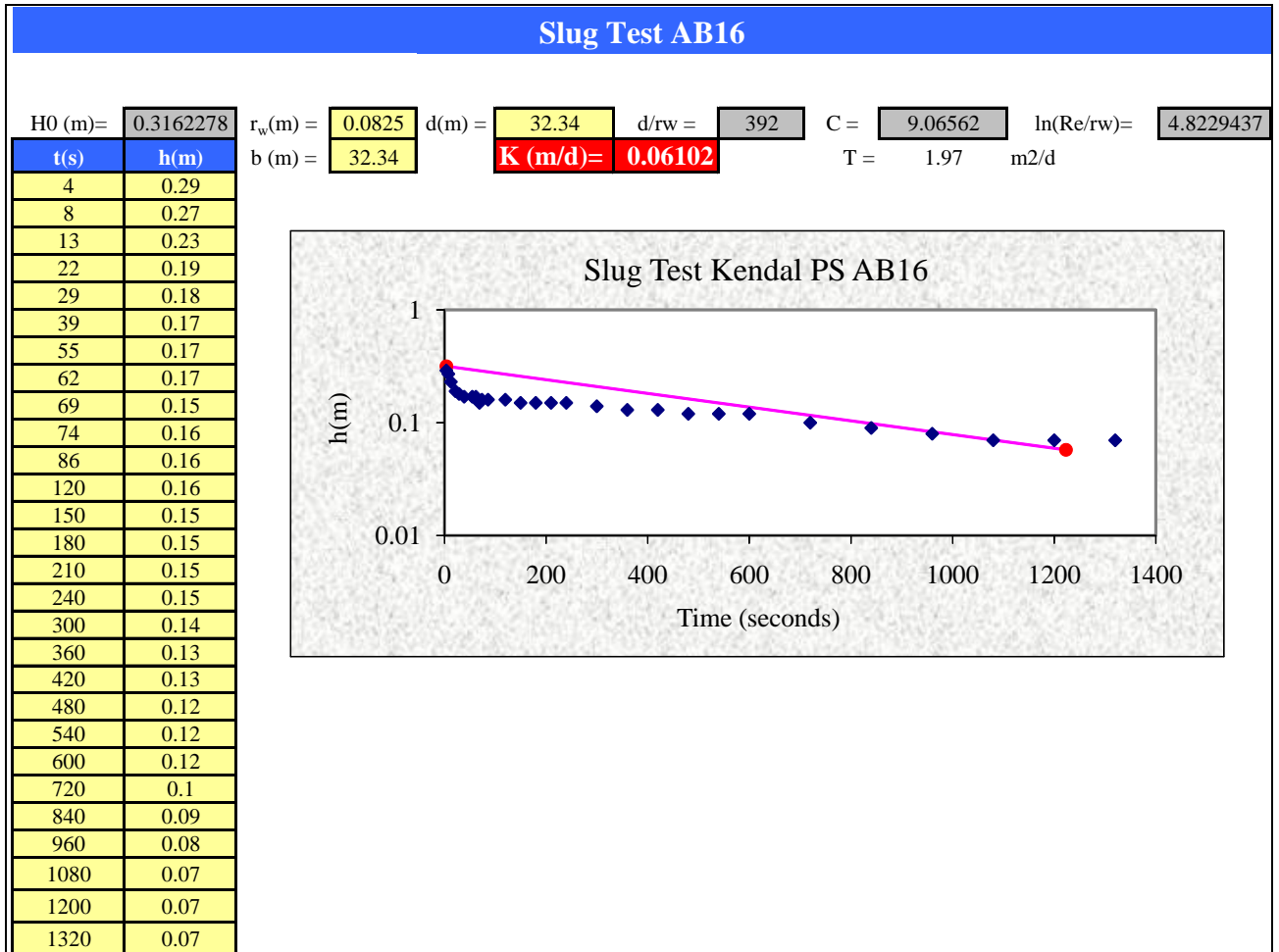


Figure 35. Slug test data analysed by means of the Bower and Rice method (borehole AB16).

Table 17. Slug test results.

Borehole	Hydraulic Conductivity (K)	Hydraulic Conductivity (K)
AB16	0.060	0.060
AB07	0.007	0.007
AB08	0.226	0.226
AB14	0.038	0.038
AB21	0.240	0.240
AB22	0.012	0.012
AB25	0.012	0.012
AB44	1.280	1.280
AB45	0.017	0.017
CB13	0.020	0.020
CB40	0.076	0.076
PB04	0.028	0.028
PB05	0.053	0.053
PB06	0.045	0.045
PB23	0.060	0.060
PB42	0.311	0.311
SB24	0.015	0.015
WB18	0.014	0.014
	0.14	0.05
	Upper Range (Average)	Lower Range (Geometric mean)

According to Muller, J. (1994), the effective porosity is of major importance with respect to the ground water seepage velocity. These porosities were used by Muller for a geohydrological evaluation at Kendal Power Station.

Table 18. Effective porosity table. (Source: Muller, J. 1994).

Rocktype	Effective Porosity
Shale	1% -10%
Sandstone	5% - 15%
Fractured dolerite	5% - 15%

The borehole logs from Kendal Power Station indicate that the study area comprises a great deal of sandstones and shales in the study area. Therefore assuming the effective porosity of the study area to be 2% the seepage velocities for a worst case scenario was calculated.

The hydraulic conductivity [K (m²/d)] and transmissivity [T (m²/d)] were calculated by means of slug tests. The Darcy flux [V_s (m/d)] and seepage velocities [V_s (m/d)] of potential contaminants using equations 1 and 2. These calculations and the pollution migration distances (coal stockyard to hydrocensus boreholes) are presented in Table 19 and Table 20.

The calculations and pollution migration distances between the additional pollution sources and boreholes are indicated in Appendix D.

Equation 1: $V = Ki$

where;

V = Darcy Velocity or Flux

K = Hydraulic Conductivity

i = Hydraulic Gradient

Equation 2: $V_s = \frac{V}{n_e}$

where;

V_s = Seepage Velocity

V = Darcy Velocity or Flux

n_e = Effective Porosity

Table 19. Darcy and seepage velocity calculation; coal stockyard to hydrocensus boreholes.

Borehole	Coordinate System (WGS84)			Water Level Elevation (mamsl)	Pollution Source Head (mamsl)	Piezometric Head difference (metres)	Gradient (i)	Hydraulic Conductivity [Lower Range, Average] (K)	Hydraulic Conductivity [Upper Range, Geomean] (K)	Darcy Velocity, q_n [Lower Range] (m/d)	Darcy Velocity, q_n [Upper Range] (m/d)	Effective Porosity (n_e)	Seepage Velocity, v_n [Lower Range] (m/d)	Seepage Velocity, v_n [Upper Range] (m/d)
	X (metres)	Y (metres)	Pollution Source (Coal Stockyard) X & Y Coordinates											
FBB26	1963.38	-2889679.58	-1753 -2888096.25	1588.46	1607.28	18.82	0.0047	0.050	0.143	0.00023	0.00066	0.02	0.01164	0.03323
FBB27	423.181	-2886714.72	-1753 -2888096.25	1614.26	1607.28	-6.98	-0.0027	Above Gradient	Above Gradient	Above Gradient	Above Gradient	Above Gradient	Above Gradient	Above Gradient
FBB28	771.476	-2884196.49	-1753 -2888096.25	1592.99	1607.28	14.29	0.0031	0.050	0.143	0.00015	0.00044	0.02	0.00769	0.02194
FBB29	960.572	-2884447.99	-1753 -2888096.25	1597.54	1607.28	9.74	0.0021	0.050	0.143	0.00011	0.00031	0.02	0.00535	0.01528
FBB30	-145.053	-2887750.59	-1753 -2888096.25	1619.03	1607.28	-11.75	-0.0071	Above Gradient	Above Gradient	Above Gradient	Above Gradient	Above Gradient	Above Gradient	Above Gradient
FBB31	-2601.66	-2888877.57	-1753 -2888096.25	1605.34	1607.28	1.94	0.0017	0.050	0.143	0.00008	0.00024	0.02	0.00420	0.01200
FBB32	-2611.67	-2888854.32	-1753 -2888096.25	1606.02	1607.28	1.26	0.0011	0.050	0.143	0.00005	0.00016	0.02	0.00275	0.00785
FBB34	-5150.04	-2892085.7	-1753 -2888096.25	1582.61	1607.28	24.67	0.0047	0.050	0.143	0.00024	0.00067	0.02	0.01176	0.03358
FBB35	-7370.68	-2892764.81	-1753 -2888096.25	1558.11	1607.28	49.17	0.0067	0.050	0.143	0.00034	0.00096	0.02	0.01682	0.04802
FBB36	-7637.4	-2893200.37	-1753 -2888096.25	1567.72	1607.28	39.56	0.0051	0.050	0.143	0.00025	0.00072	0.02	0.01269	0.03622
FBB37	-7609.18	-2891878.62	-1753 -2888096.25	1548.36	1607.28	58.92	0.0085	0.050	0.143	0.00042	0.00121	0.02	0.02111	0.06028
FBB38	-8252.07	-2890496.36	-1753 -2888096.25	1538.16	1607.28	69.12	0.0100	0.050	0.143	0.00050	0.00142	0.02	0.02492	0.07116
FBB39	-6270.38	-2885161.84	-1753 -2888096.25	1559.57	1607.28	47.71	0.0089	0.050	0.143	0.00044	0.00126	0.02	0.02213	0.06317

Table 20. Pollution migration distance; coal stockyard to hydrocensus boreholes.

Borehole	Estimated Pollution Migration [Lower Range, 1 Year Period] (m)	Estimated Pollution Migration [Upper Range, 1 Year Period] (m)	Estimated Pollution Migration [Lower Range, 5 Year Period] (m)	Estimated Pollution Migration [Upper Range, 5 Year Period] (m)	Estimated Pollution Migration [Lower Range, 10 Year Period] (m)	Estimated Pollution Migration [Upper Range, 10 Year Period] (m)
FBB26	4.25	12.13	21.24	60.64	42.48	121.28
FBB27	Above Gradient	Above Gradient				
FBB28	2.81	8.01	14.03	40.04	28.05	80.09
FBB29	1.95	5.58	9.77	27.88	19.53	55.77
FBB30	Above Gradient	Above Gradient				
FBB31	1.53	4.38	7.67	21.91	15.34	43.81
FBB32	1.00	2.86	5.02	14.32	10.03	28.65
FBB34	4.29	12.26	21.46	61.28	42.93	122.57
FBB35	6.14	17.53	30.69	87.63	61.38	175.26
FBB36	4.63	13.22	23.15	66.11	46.31	132.22
FBB37	7.71	22.00	38.53	110.02	77.07	220.04
FBB38	9.10	25.97	45.49	129.87	90.97	259.74
FBB39	8.08	23.06	40.38	115.29	80.76	230.58

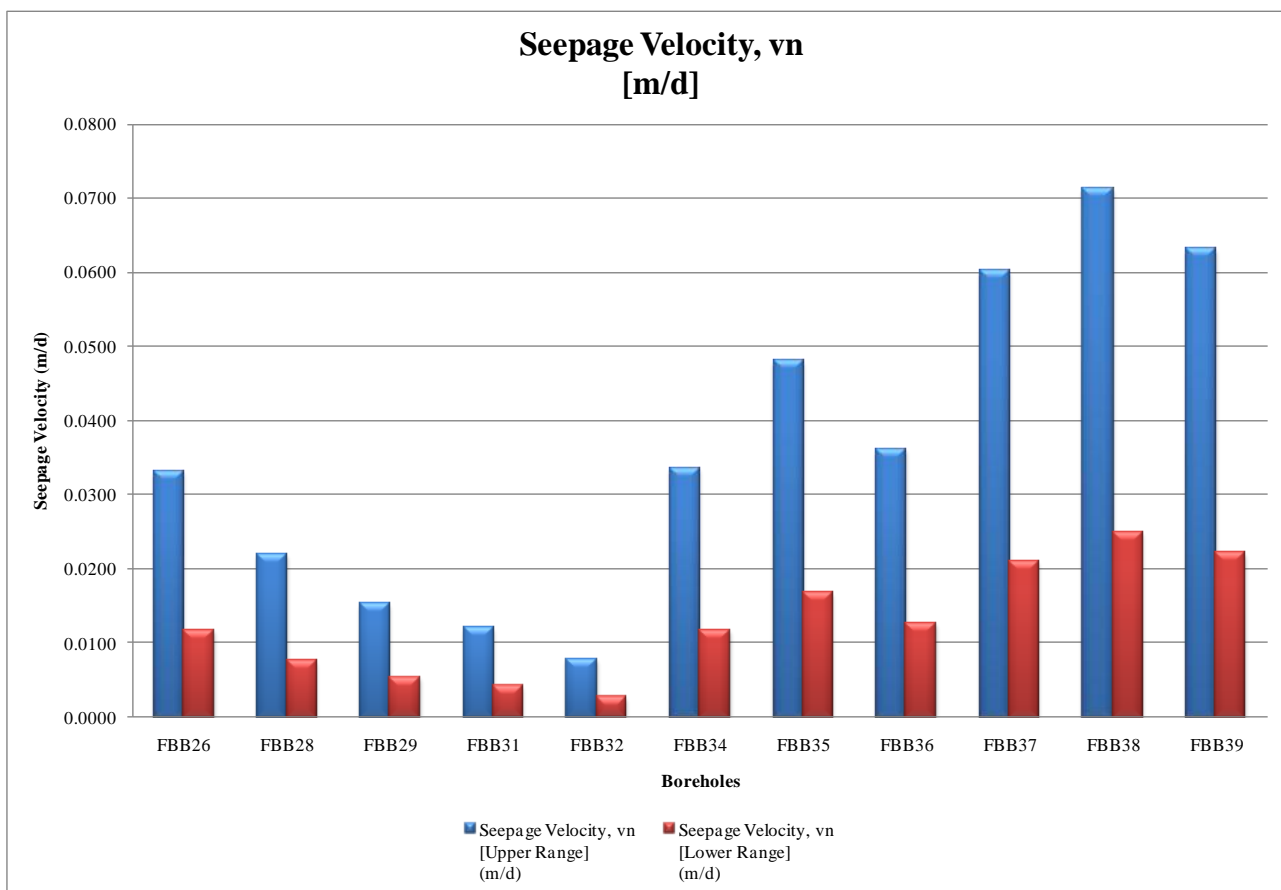


Figure 36. Seepage velocity, coal stockyard to hydrocensus boreholes

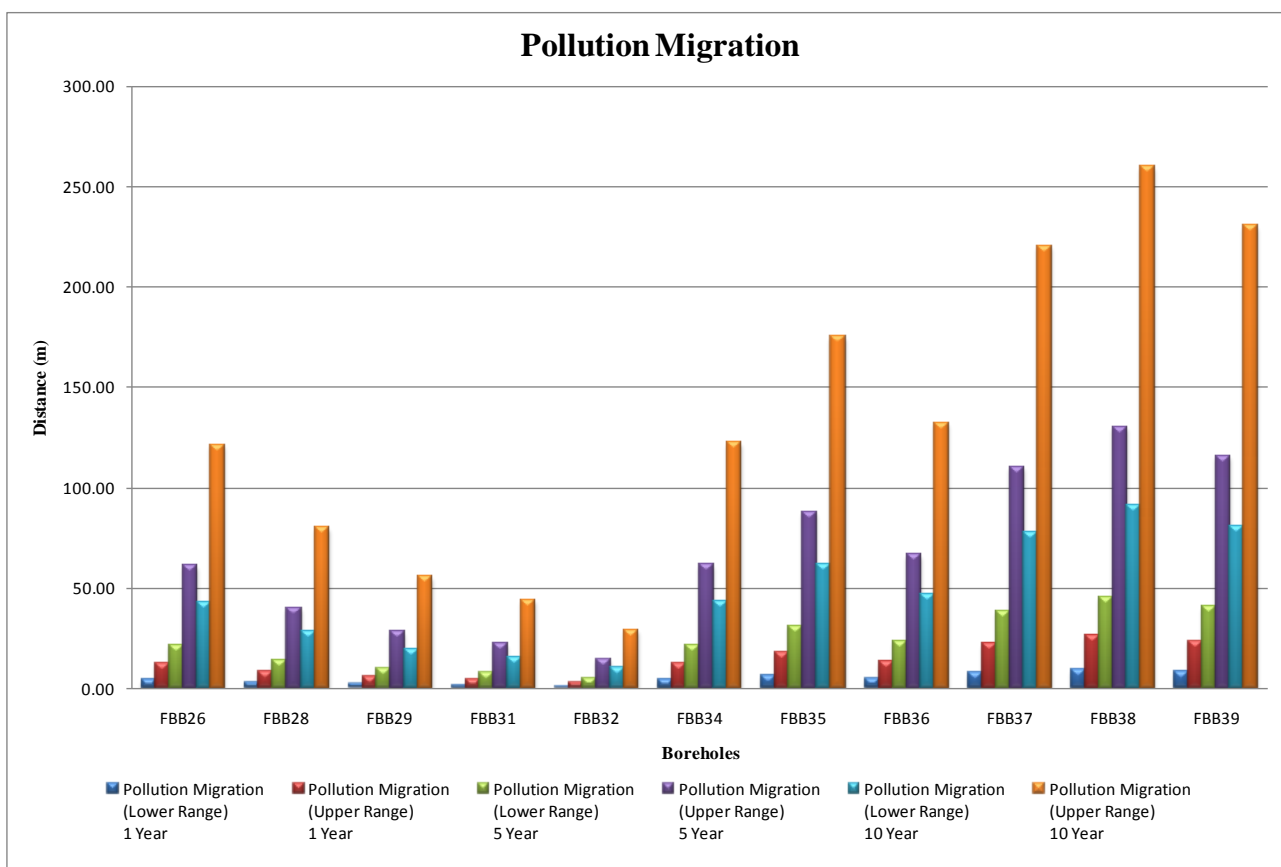


Figure 37. Pollution migration distances; bar chart.

4.6.5 Conclusions

Figure 37 presents the distances the pollution will travel assuming the effective porosity (n_e) is 0.02. The lower and upper range of the hydraulic conductivity were both utilised to calculate the distances of the pollution migration to observe the difference of the distances between the lower and upper ranges. These calculations and bar charts for all of the additional pollution sources are provided in Appendix C.

It is evident that borehole FBB38 has the greatest gradient, therefore the pollution migration from the coal stockyard to FBB38 will be the furthest. The lower and upper ranges create a great difference at borehole FBB38, especially over a 10 year time period.

The effects of the lower and upper ranges have a large influence on the pollution migration, the greater the gradient is. This is evident when comparing boreholes FBB38 ($i=0.10$) and FBB32 ($i=0.0011$). The difference between upper and lower ranges in distance over 10 years at borehole FBB38 is 337.22m and at FBB32 it is 39.22m and this is clearly indicated in Figure 38.

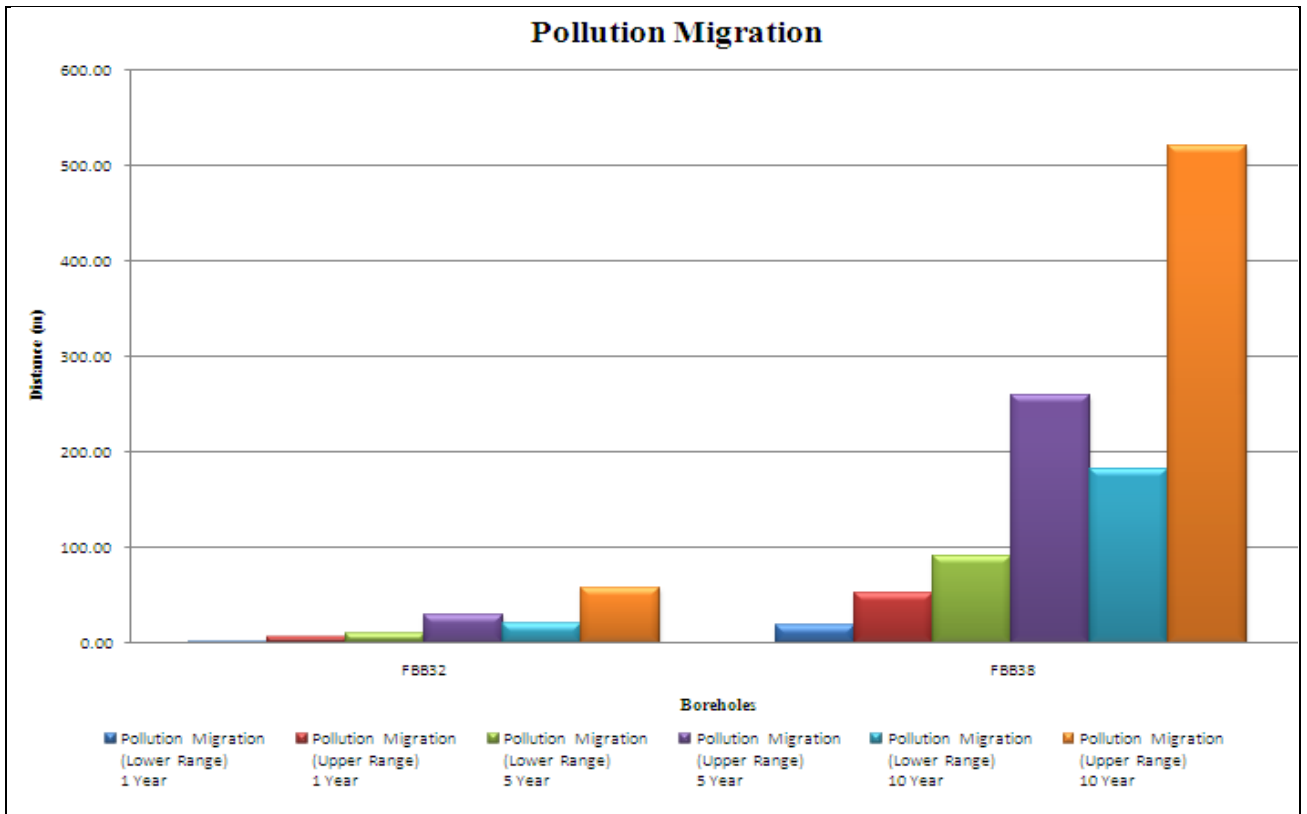


Figure 38. Pollution migration when comparing hydrocensus boreholes FBB32 and FBB38.

It is concluded that there is a larger risk for a pollution source to reach a certain destination the greater the difference in water levels or the greater the gradient if the effective porosity and hydraulic conductivities stay constant.

The distances the contamination migrated and the distances from the pollution sources to the hydrocensus boreholes was utilised to indicate the sum of years it will take for the contamination to reach the boreholes. These calculations are indicated in Table 21 and Table 22.

Table 21. Distances to hydrocensus boreholes and distances travelled over 10 years.

Hydrocensus Boreholes	Distance from coal stockyard to hydrocensus borehole	Calculated distance travelled (10 years)	Distance from ash stack to hydrocensus borehole	Calculated distance travelled (10 years)	Distance from emergency stack to hydrocensus borehole	Calculated distance travelled (10 years)	Distance from coal stockyard settling dam to hydrocensus borehole	Calculated distance travelled (10 years)	Distance from dirty water dam to hydrocensus borehole	Calculated distance travelled (10 years)	Distance from ash stack settling dam to hydrocensus borehole	Calculated distance travelled (10 years)	Distance from settling dam to hydrocensus borehole	Calculated distance travelled (10 years)
FBB26	4040	121	7115	Above Gradient	6828	50	4482	99	6412	Above Gradient	7018	Above Gradient	6637	Above Gradient
FBB27	2578	Above Gradient	5741	Above Gradient	4503	Above Gradient	3117	Above Gradient	4492	Above Gradient	5230	Above Gradient	4695	Above Gradient
FBB28	4646	80	7212	Above Gradient	5362	42	5082	64	5750	Above Gradient	6464	Above Gradient	5894	Above Gradient
FBB29	4547	56	7223	Above Gradient	5434	20	5004	41	5777	Above Gradient	6500	Above Gradient	5930	Above Gradient
FBB30	1645	Above Gradient	4952	Above Gradient	4126	Above Gradient	2200	Above Gradient	3893	Above Gradient	4592	Above Gradient	4114	Above Gradient
FBB31	1154	44	2480	Above Gradient	2804	Above Gradient	698	5	2067	Above Gradient	2495	Above Gradient	2266	Above Gradient
FBB32	1145	29	2466	Above Gradient	2779	Above Gradient	682	Above Gradient	2043	Above Gradient	2474	Above Gradient	2242	Above Gradient
FBB34	5240	123	3628	Above Gradient	5697	87	4783	124	4845	Above Gradient	4522	6	4865	6
FBB35	7304	175	4893	99	7087	160	6796	181	6347	94	5814	114	6294	114
FBB36	7790	132	5403	44	7597	116	7286	135	6858	51	6324	65	6805	65
FBB37	6971	220	4273	173	6444	215	6439	231	5760	148	5169	177	5682	177
FBB38	6928	260	3798	265	5787	286	6373	275	5259	213	4568	259	5129	259
FBB39	5387	231	3517	127	2567	427	5044	237	3155	178	2867	218	2957	218

Table 22. Years for contamination to reach down gradient hydrocensus boreholes.

Hydrocensus Boreholes	Years to reach borehole from Coal stockyard	Years to reach borehole from Ash Stack	Years to reach borehole from Emergency stack	Years to reach borehole from Coal stockyard settling dam	Years to reach borehole from Dirty water dam	Years to reach borehole from Ash stack settling dam	Years to reach borehole from Settling dam
FBB26	333	~	1358	453	~	~	~
FBB27	~	~	~	~	~	~	~
FBB28	580	~	1275	794	~	~	~
FBB29	815	~	2758	1211	~	~	~
FBB30	~	~	~	~	~	~	~
FBB31	263	~	~	1329	~	~	~
FBB32	400	~	~	~	~	~	~
FBB34	428	~	655	384	~	8191	8813
FBB35	417	493	443	375	672	510	552
FBB36	589	1240	653	540	1348	969	1043
FBB37	317	247	299	279	389	291	320
FBB38	267	144	203	232	247	176	198
FBB39	234	276	60	213	177	132	136

A worst case scenario was created by utilising 2% effective porosity and the upper range of the hydraulic conductivity, as the results indicate that the majority of the boreholes will become affected after 100 years. These calculations only indicate the number of years it will take for the contamination to travel the various distances from the pollution sources to the hydrocensus boreholes.

Therefore, by utilising a worst case scenario and assuming that the contamination can flow directly from the pollution source to the hydrocensus boreholes without any variation in the water level, it is concluded that, even for the worst case scenario, the pollutant has very little risk of reaching the hydrocensus boreholes, and dilution of the pollutant was not included, which can also decrease the risk of the pollution source influencing the water quality of the hydrocensus boreholes.

It was found that the water levels between all of the pollution sources and the hydrocensus boreholes fluctuate when the water level contour map is taken into consideration. The hydrocensus boreholes are behind a water divide which is caused by topography highs or streams (Figure 39) which indicate that the pollution will not flow constantly down gradient to the hydrocensus boreholes. Therefore there is no risk of any of the pollution sources reaching the hydrocensus boreholes.

The water quality table (Table 8) of the hydrocensus boreholes also indicates that there are no effects of groundwater pollution from the power station activities.

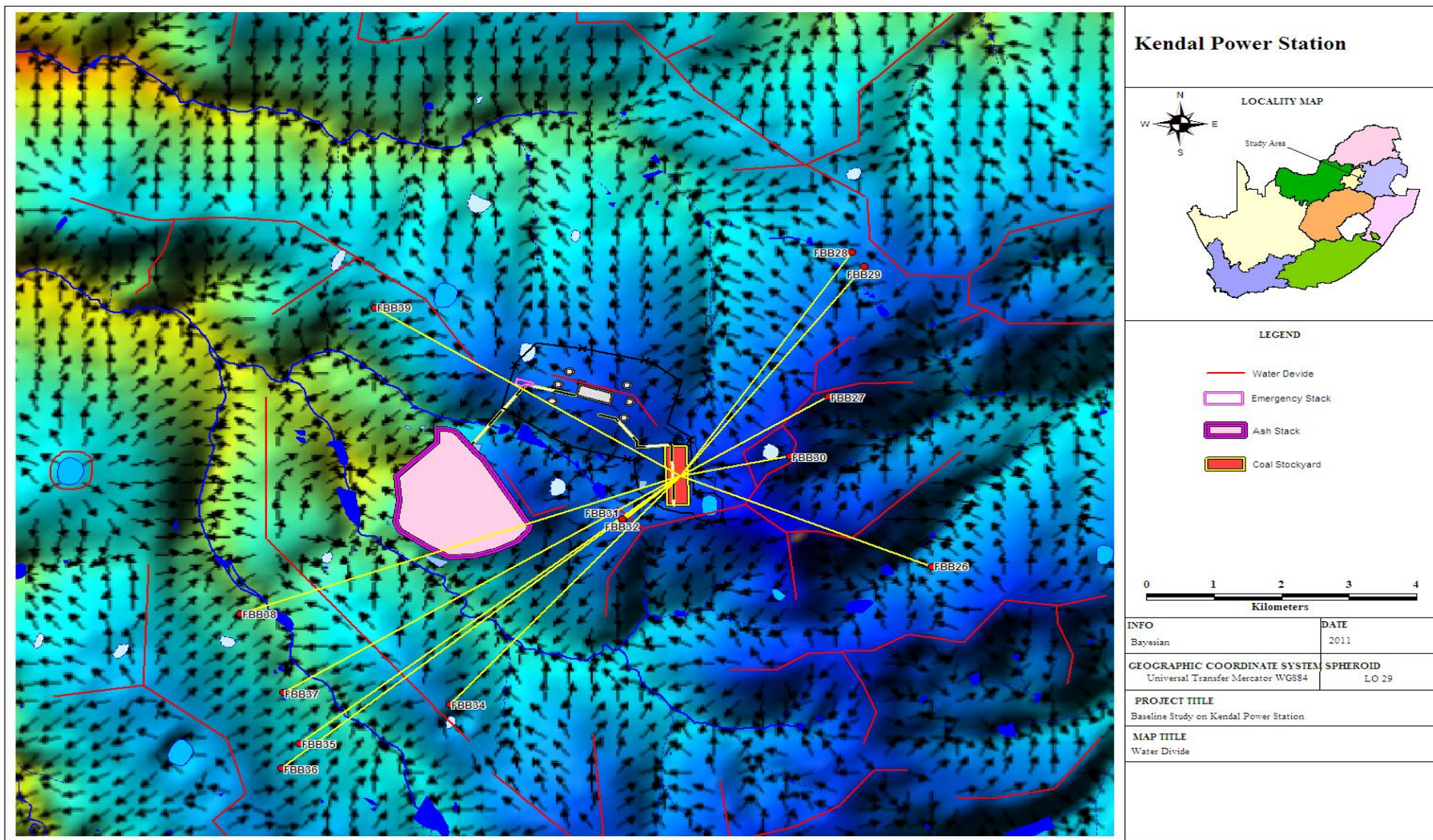


Figure 39. Water divide influencing pollution migration.

4.7 COMPARING METHODS TO EVALUATE RISK ASSESSMENT

Utilising all the collected data from the study area the pollution migration was calculated over 10 years and could therefore quantify the risk for the pollution source reaching the hydrocensus boreholes. The Ogata Banks method was compared to the seepage velocity calculations to observe if the methods agree if there is a risk for the pollution to reach the hydrocensus boreholes, assuming the pollution flow in a straight line.

4.7.1 Ogata Banks

Ogata & Banks (1961) developed an analytical solution to the 1D advection-dispersion equation. This method uses this analytical solution to determine the concentration of a contaminant down-gradient from a constant source, at a given distance, and time.

Seepage velocity was utilised to calculate the pollution migration distances as discussed in chapter 4, but using this method there was no concentrations for the pollution sources included in the formula. Utilising Ogata Banks, concentrations of the pollution sources was included in the programme and could therefore calculate the concentration of the pollution source if it reaches the hydrocensus boreholes. The sulphate concentrations used for the polluted dams are presented in Table 9. A worst case was created for the coal stockyard, ash stack and the emergency stack by utilising a concentration of 2000 mg/l. An example for one of the calculated concentrations is presented in Figure 40, all of the results for Ogata banks are presented in Table 23. Boreholes indicating no results are up gradient from the pollution source. Calculations for the additional boreholes are presented in Appendix F.

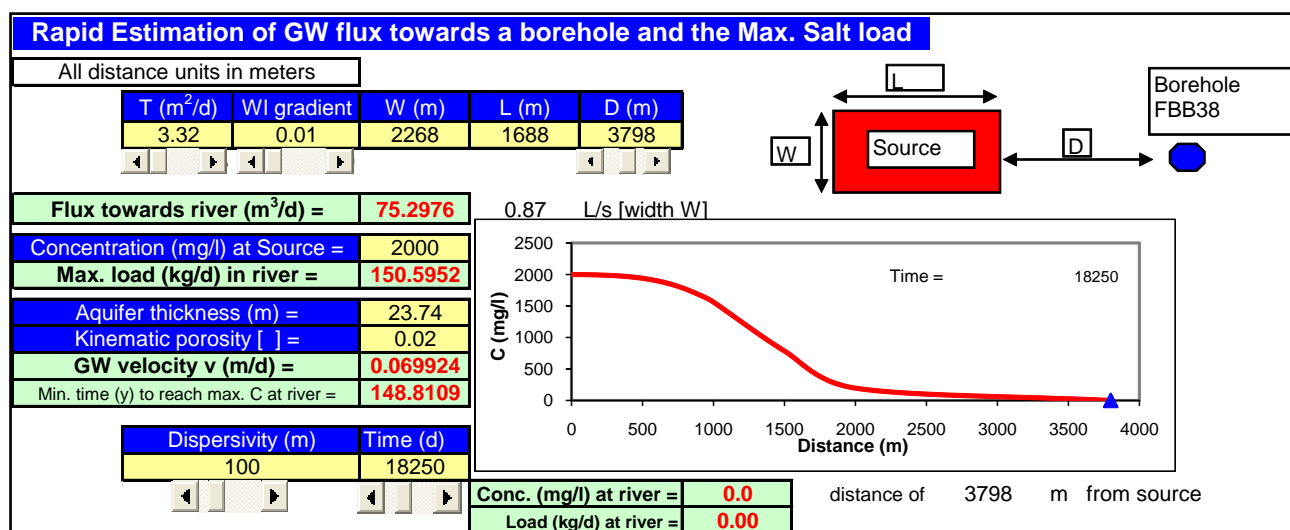


Figure 40. Rapid estimation of groundwater flux towards borehole FBB38.

Table 23. Ogata Banks results.

Hydrocensus boreholes	Pollution sources													
	Coal stockyard		Ash stack		Emergency stack		Coal Stockyard Settling dam		Dirty water dam		Ash stack settling dam		Settling dam	
	Conc. (mg/l) at borehole	Load (kg/d) at borehole	Conc. (mg/l) at borehole	Load (kg/d) at borehole	Conc. (mg/l) at borehole	Load (kg/d) at borehole	Conc. (mg/l) at borehole	Load (kg/d) at borehole	Conc. (mg/l) at borehole	Load (kg/d) at borehole	Conc. (mg/l) at borehole	Load (kg/d) at borehole	Conc. (mg/l) at borehole	Load (kg/d) at borehole
FBB26	0	0	~	~					~	~	~	~	~	~
FBB27	~	~	~	~	~	~	~	~	~	~	~	~	~	~
FBB28	0	0	~	~	0	0	0	0	~	~	~	~	~	~
FBB29	~	~	~	~	0	0	0	0	~	~	~	~	~	~
FBB30	0	0	~	~	~	~	~	~	~	~	~	~	~	~
FBB31	0	0	~	~	~	~	0	0	~	~	~	~	~	~
FBB32	0	0	~	~	~	~	~	~	~	~	~	~	~	~
FBB34	0	0	~	~	0	0	0	0	~	~	0	0	0	0
FBB35	0	0	0	0	0	0	0	0	0	0	0	0	0	0
FBB36	0	0	0	0	0	0	0	0	0	0	0	0	0	0
FBB37	0	0	0	0	0	0	0	0	0	0	0	0	0	0
FBB38	0	0	0	0	0	0	0	0	0	0	0	0	0	0
FBB39	0	0	0	0	488.6	6.23	0	0	0	0	0	0	0	0

It is apparent that all of the pollution sources have no risk of reaching the hydrocensus boreholes (except for borehole FBB39) over a time period of 50 years according to Ogata Banks. This is mainly due to the great distances between the hydrocensus boreholes and the pollution sources.

The seepage calculations indicate that borehole FBB39 will be the first hydrocensus borehole to be effected and Ogata Banks calculated FBB39 as the only borehole that will be affected within 50 years. Assuming the pollution will flow in a straight line and creating a worst case scenario both methods indicate that there is a risk for borehole FBB39 that can be affected from pollution flowing from the emergency stack. It should however be kept in mind that the groundwater flow (Figure 33) indicate that the pollution will not flow in a straight line to FBB39 and that the borehole is located behind a water divide, resulting in a minimal risk.

4.8 BACKTRACKING

Pathlines commonly represent the boundaries of the catchment of a pumping well and was estimated utilising visual modflow. This is a one layer model, assuming the wells are pumped at 3m³/d (domestic use) for 100 years to compare with the risk assessment to estimate whether the hydrocensus boreholes will subtract water from the pollution source areas. For this model, an effective porosity of 2% was assumed, and a hydraulic conductivity of 0.14m/d was utilised.

According to the model, after a 100 years of pumping at 3m³/d, the hydrocensus boreholes will not extract water from the pollution sources, and it can be positively concluded that comparing seepage velocity calculations, Ogata Banks and backtracking, that there is no risk for the hydrocensus boreholes to be contaminated.

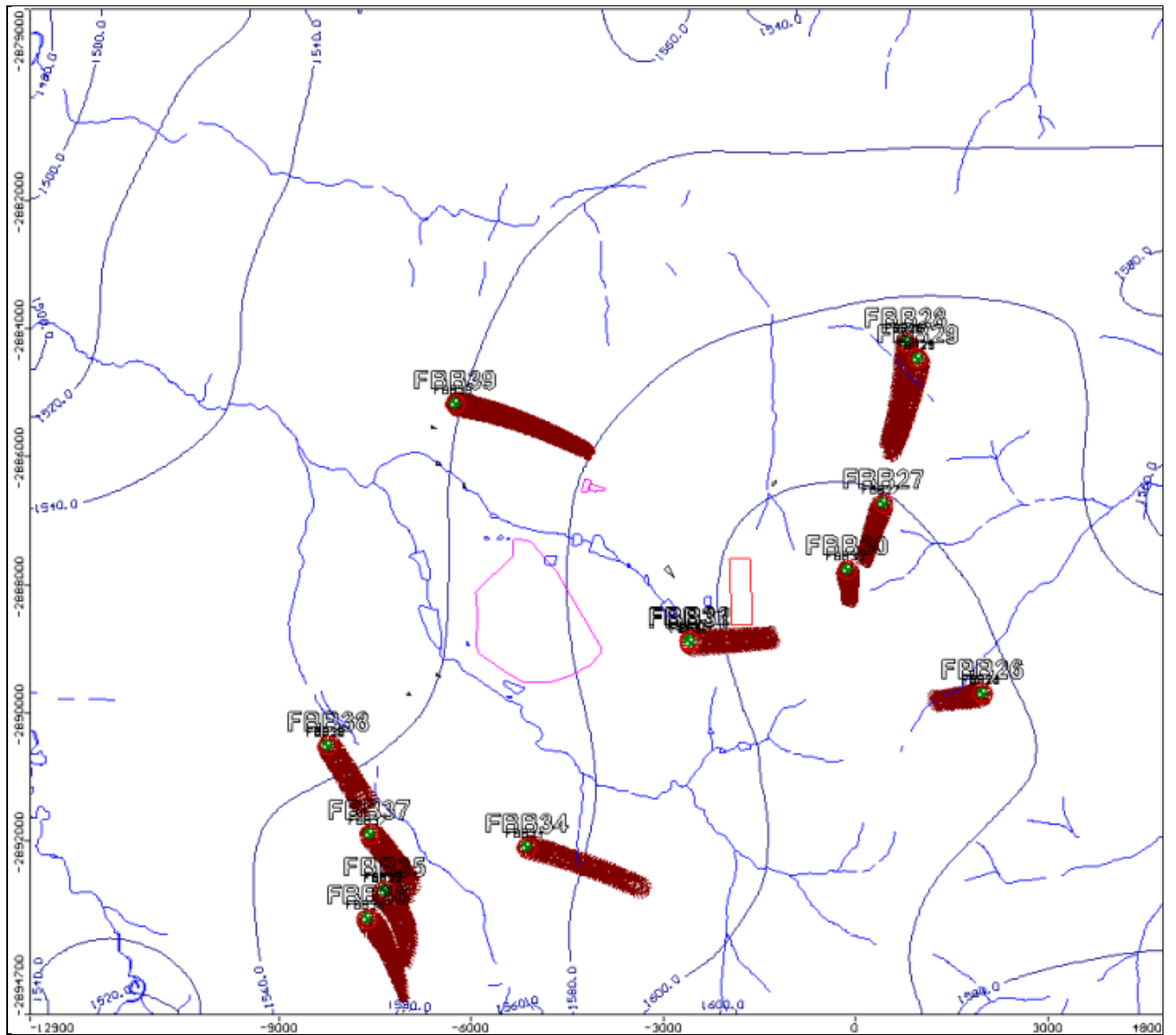


Figure 41. Backtracking.

4.9 EFFECTS OF KENDAL POWER STATION ON LEEUWFontein AND SCHOONGEZICHT SPRUIT

4.9.1 Leeuwfontein Spruit

As explained on page 31 section 3.3.1, the impacts upon the Leeuwfontein spruit would mainly originate from the ashing area and the coal stockyard Area which are located to the north and north east of the stream respectively. The chemistry data from the hydrocensus study and monitoring events were utilised in order to identify whether the ash stack has an impact on the water quality of the Leeuwfontein spruit. Sampling site R01 indicates a drastic increase of sulphate concentration, as it was found that this site is located next to a coal mine indicated in Figure 42. Figure 43 indicates that the sulphate concentrations of the hydrocensus and monitoring sites upstream from the ash stack are low sulphate concentration.



Figure 42. Coal mine next to sampling site R01.

Site AP11 downstream from R01 also indicates a high sulphate concentration, but it is almost half of that at R01. Thus it cannot be defined to what extent the ash stack is polluting the Leeuwfontein spruit (if it has an influence on the surface water quality) due to the high concentrations at R01.

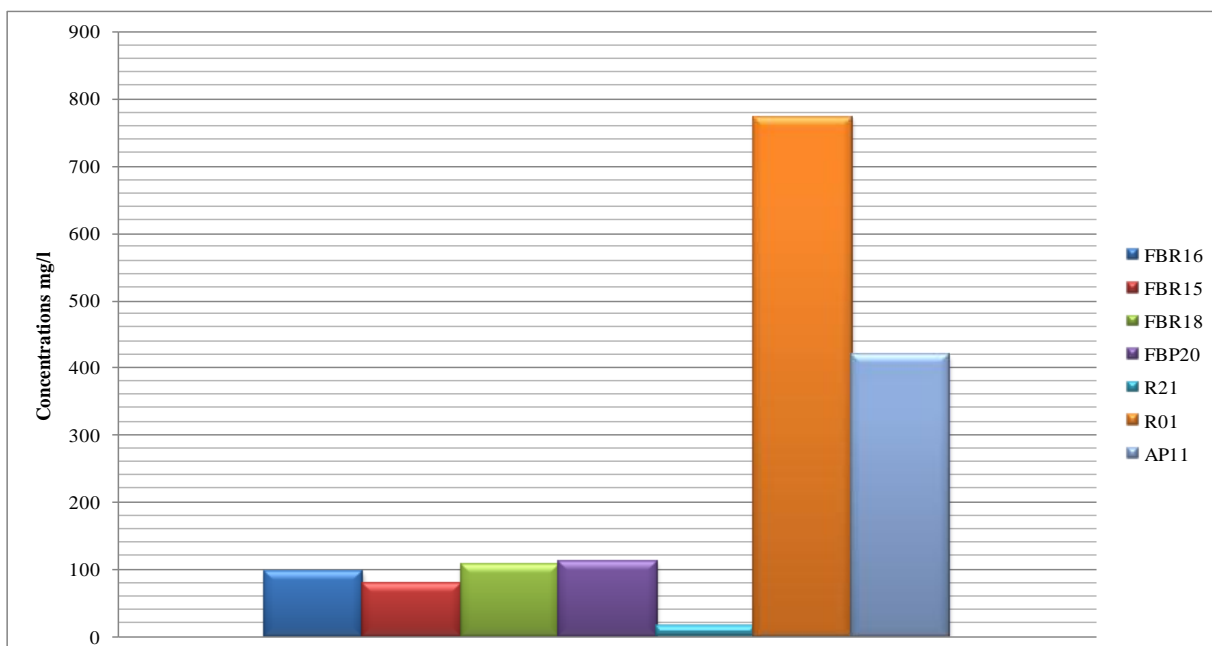


Figure 43. Sulphate concentrations at monitoring sites in Leeuwfontein spruit.

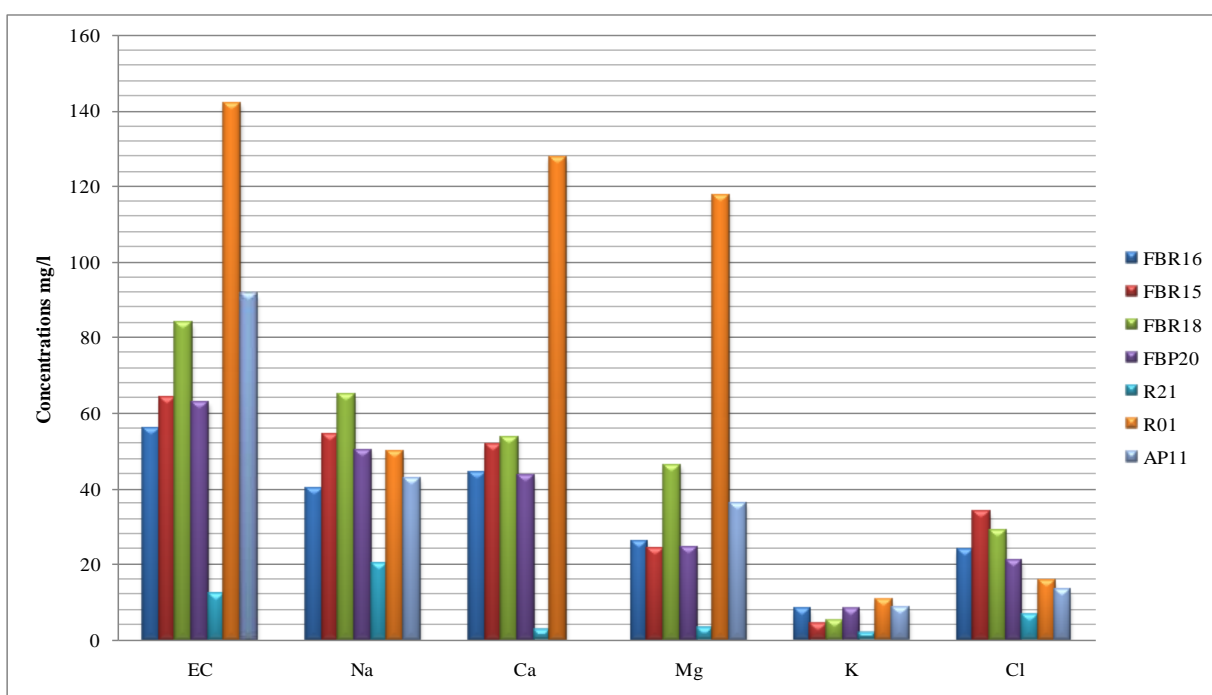


Figure 44. Additional concentrations at monitoring sites in Leeuwfontein spruit.

4.9.2 Schoongezicht Spruit

As explained on page 31 section 3.3.1, impacts upon the Schoongezicht spruit would mainly originate from the power station area and the coal stockyard area which are located to the north and east of the stream, as well as from the ashing area which is located to the west of the stream.

Sites PP02 and PP03 indicate high sulphate concentrations, but these dams are being used to hold dirty water that is recycled for the power station. This dirty water is not released into the stream and is not supposed to affect the water quality of the Schoongezicht spruit downstream, except if a spill occurs. Figure 45 illustrates the arrangement of dirty and clean water dams to create a stream diversion.

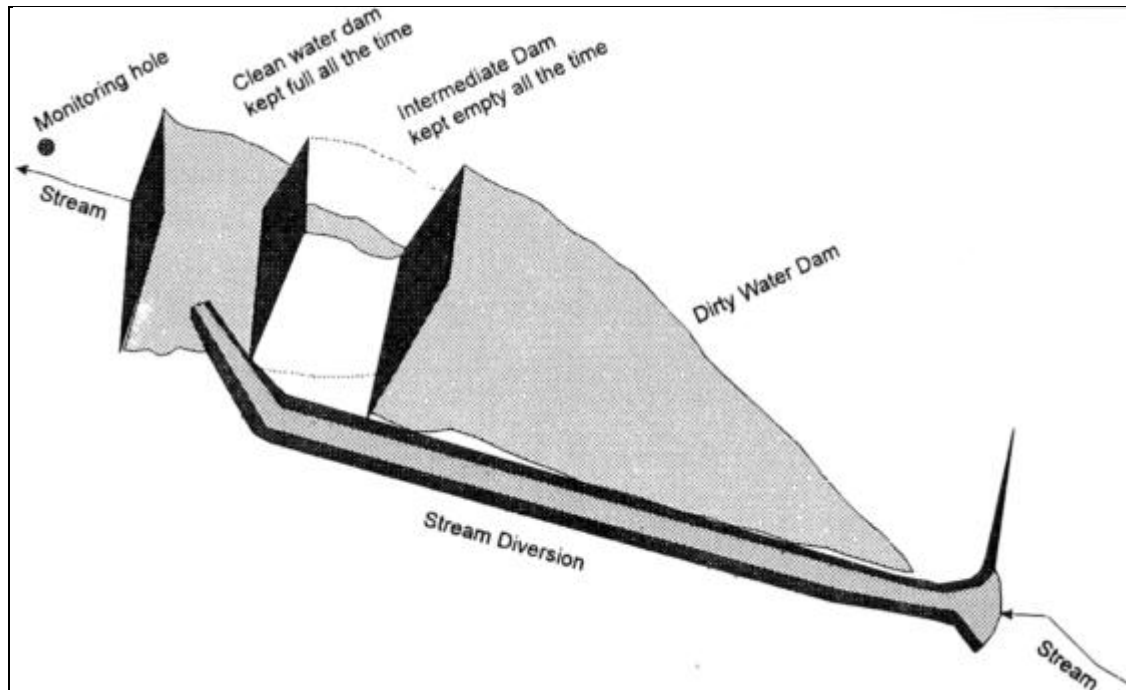


Figure 45. Arrangement of dirty and clean water dams at Kendal Power Station (source FDI Hodgson et al., 1998)

Monitoring pan PP05 indicates a high sulphate concentration in Figure 48, however the historical data indicate that the sulphate concentrations of this site are mostly of an acceptable value and are comparable to site R03 (upstream sample of PP05) in Figure 46. It is evident that the sulphate concentration of site PP05 (Figure 46) drastically increased in 1992, 2001 and 2009 during the last sampling event. The Schoongezicht spruit is located close to the ash stack and is also likely to be influenced by surface runoff during heavy rainfalls. Rainfall data for Secunda was obtained from Weather SA as it is the closest town to Kendal Power Station with sufficient rainfall data. When comparing the rainfall data (Figure 47) and the sulphate concentrations (Figure 46) it is found that the sulphate concentrations do not increase drastically as the rainfall increases during heavy rainfall seasons.

Thus the drastic increase in sulphate concentrations cannot be attributed to surface runoff from the ash stack to the spruit during heavy rainfall seasons. These sudden increased values can be attributed to the dirty water dams that could have flooded and affected the water quality of pan PP05. These intense increased values are not recognised at site R03 because, if a

spill occurred, the pollution would have exceeded the sampling point in the river before routine monitoring.

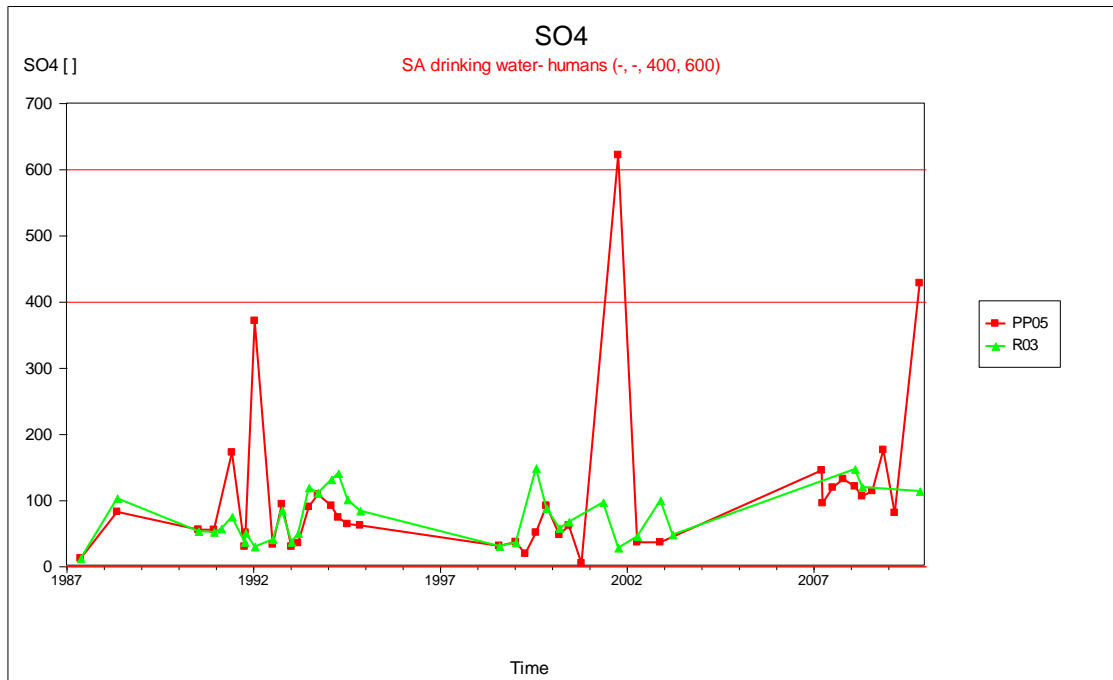


Figure 46. Sites R03 and PP05 sulphate concentrations.

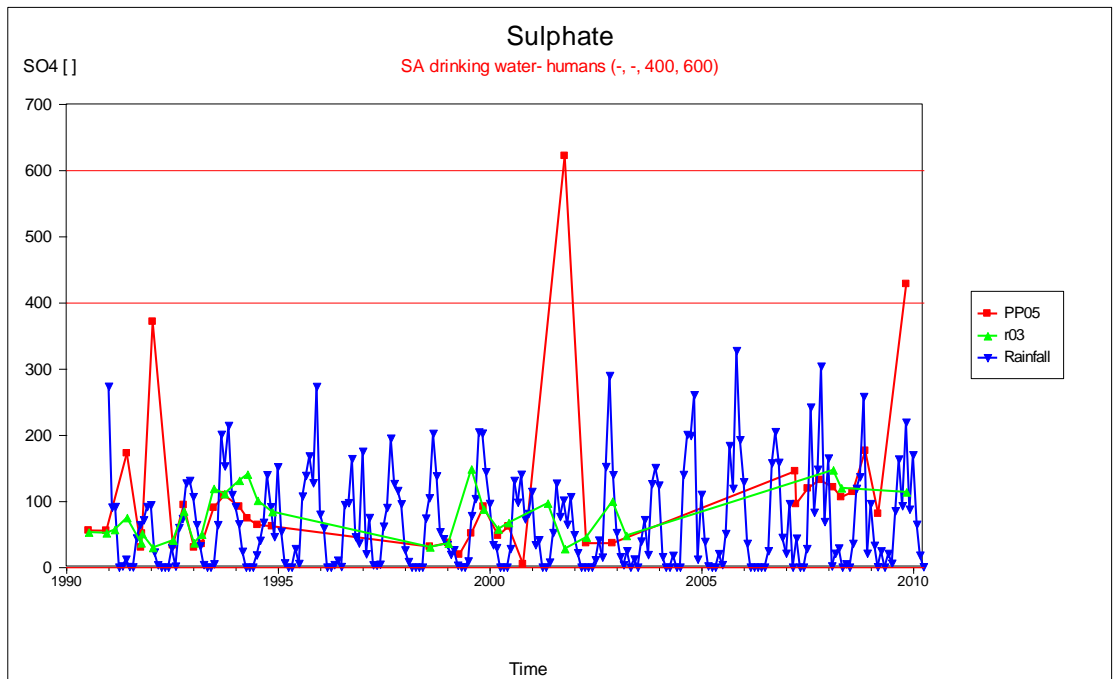


Figure 47. 1991 to 2010 rainfall.

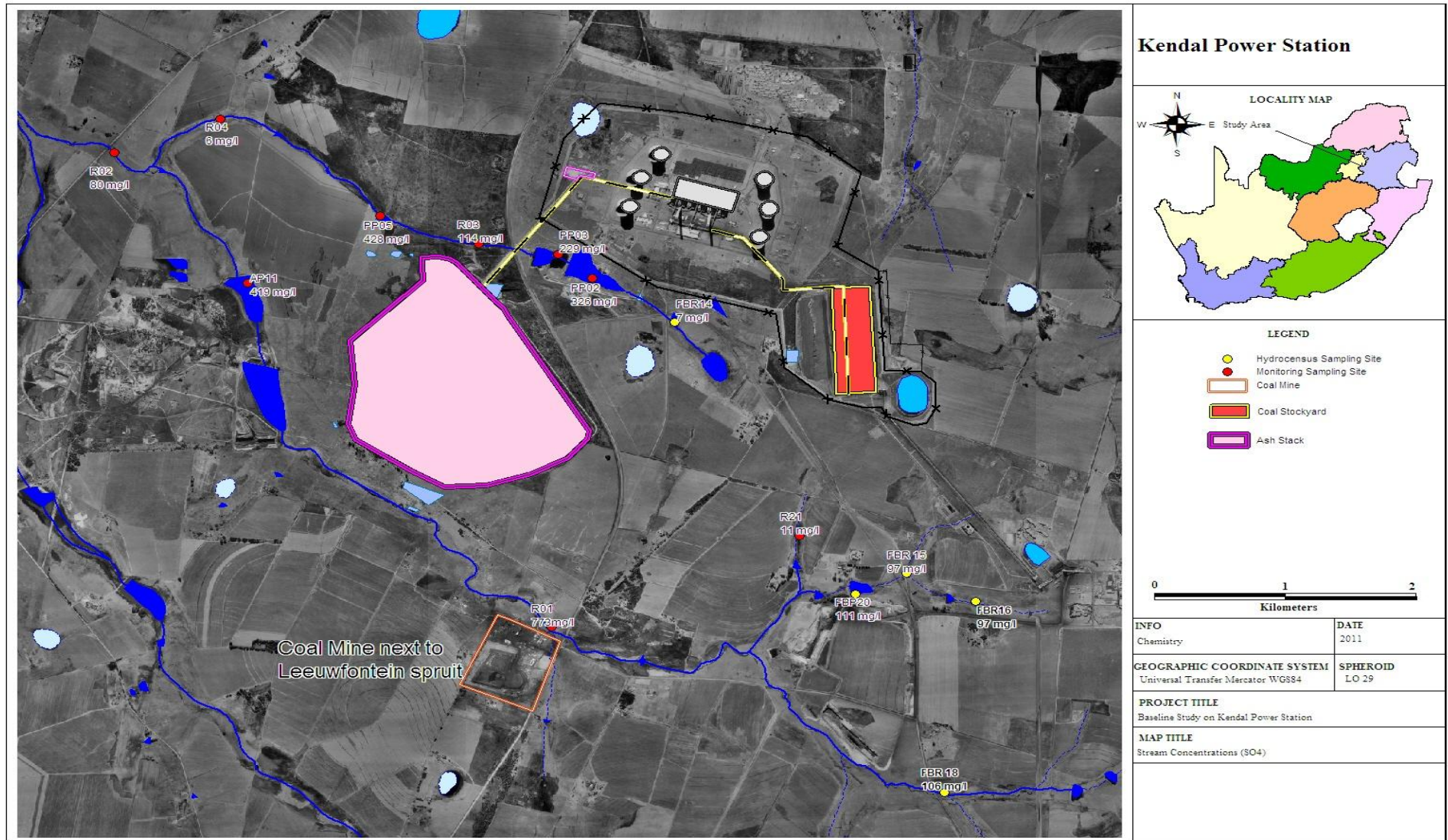


Figure 48. Sulphate concentrations at Leeuwfontein and Schoongezicht spruit.

4.9.3 Stiff diagrams

The stiff diagrams are utilised to give a graphical presentation of the chemical analysis and to display the major ion composios of the water samples at different sites in the Schoongezicht spruit. Conclusions can be drawn from these diagrams to state whether the water quality diluted or increased downstream and to determine whether the dirty water dams are releasing water into the Schoongezicht spruit.

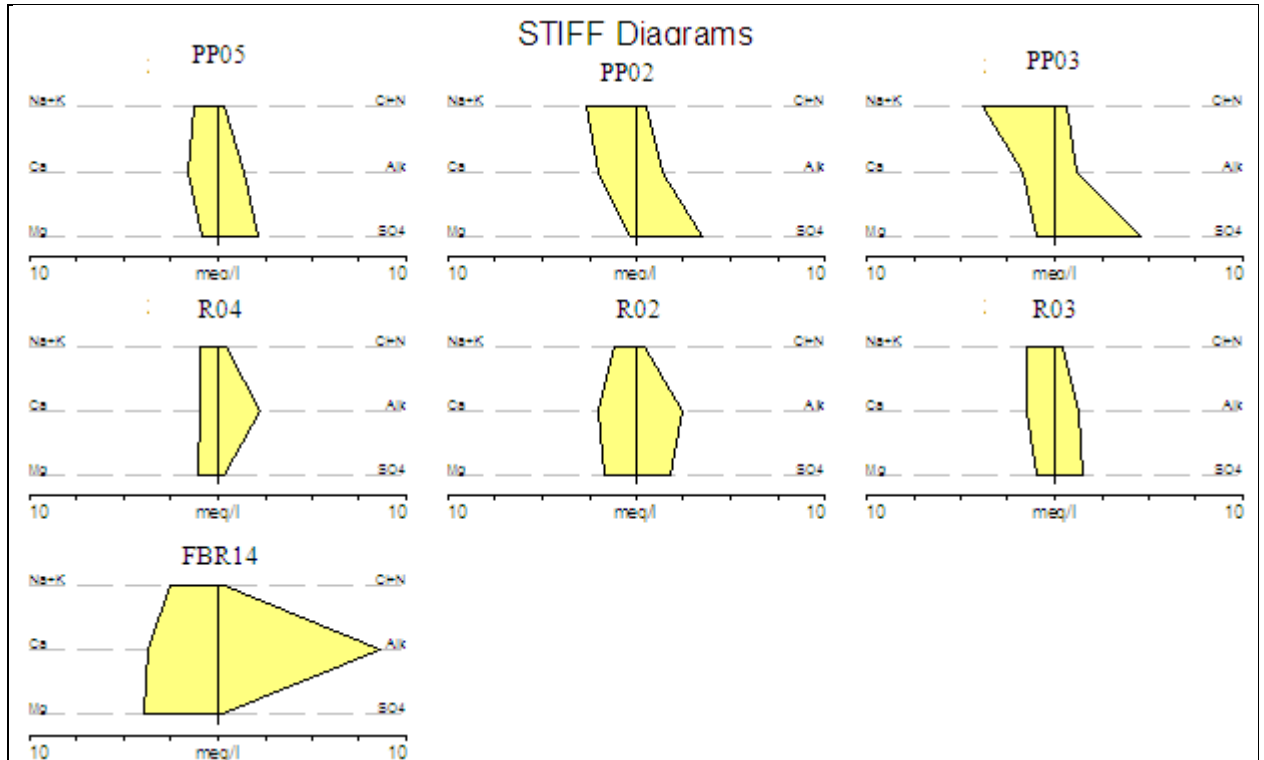


Figure 49. Current concentrations (2009).

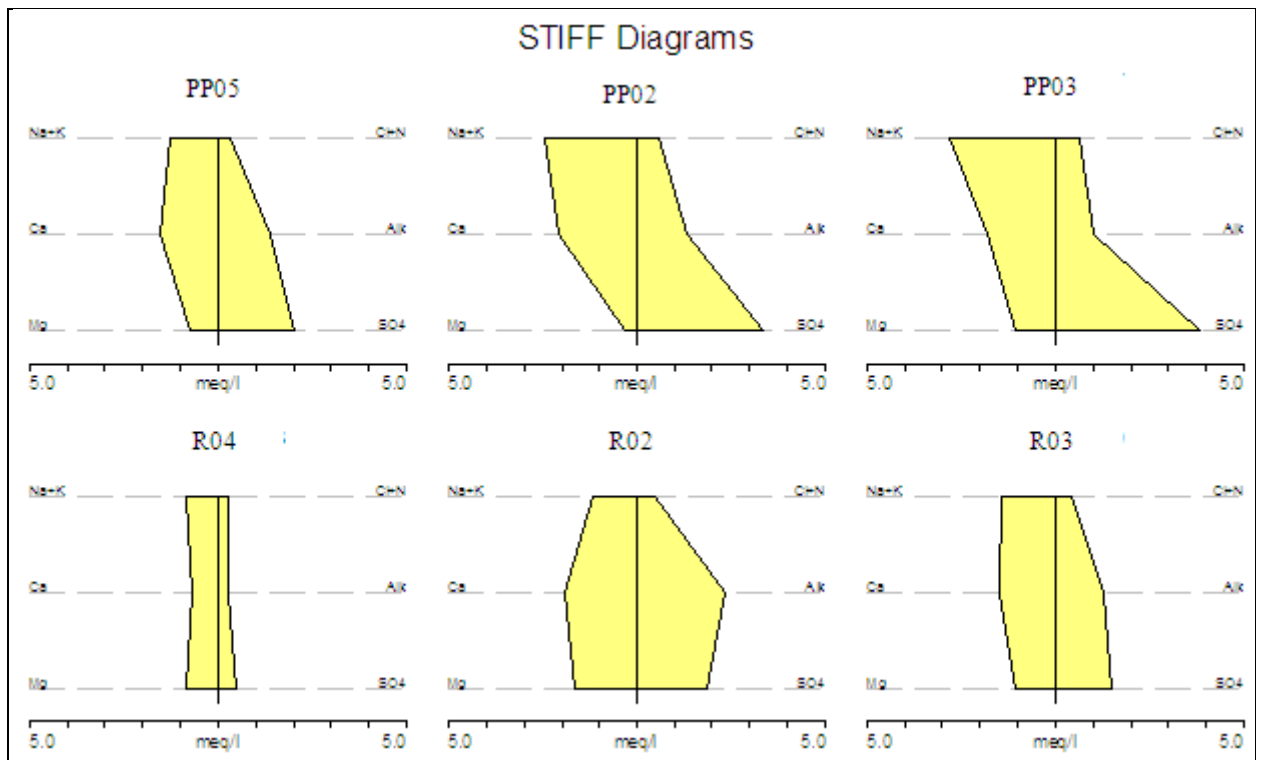


Figure 50. January 2008 concentrations.

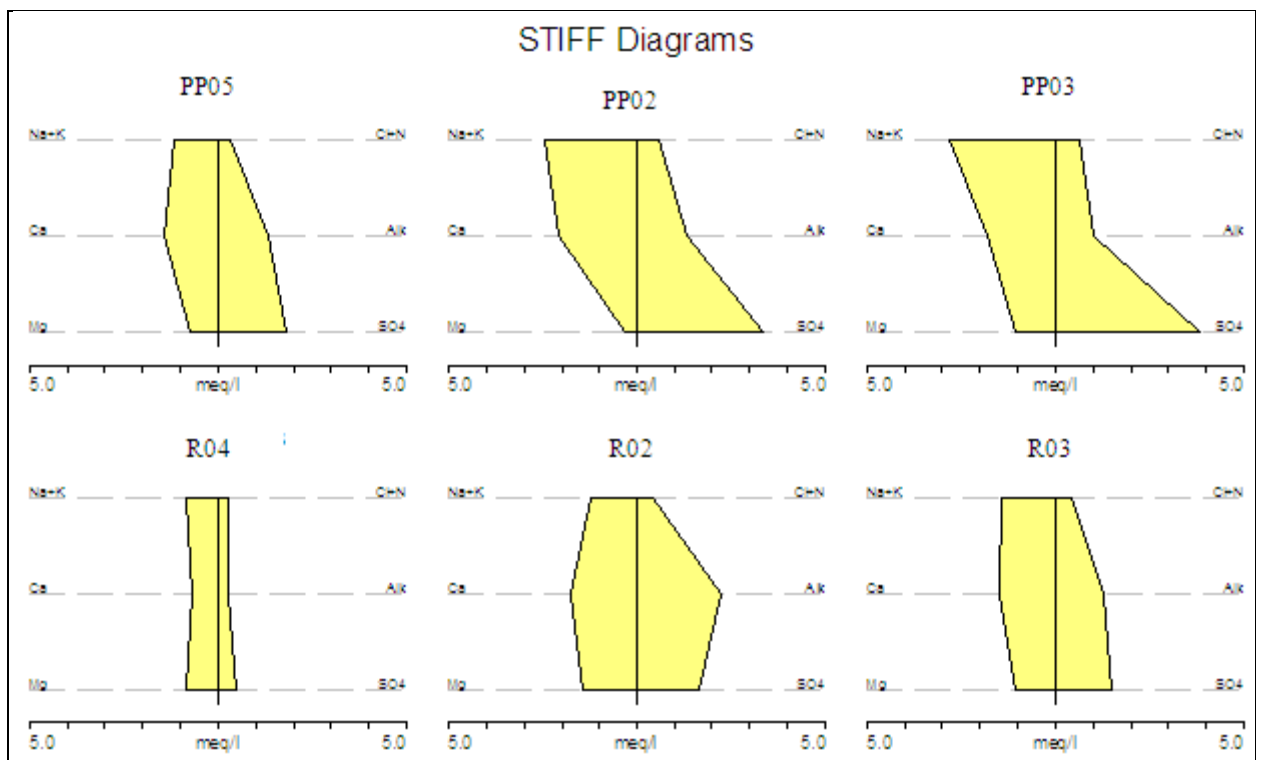


Figure 51. July 2003 concentrations.

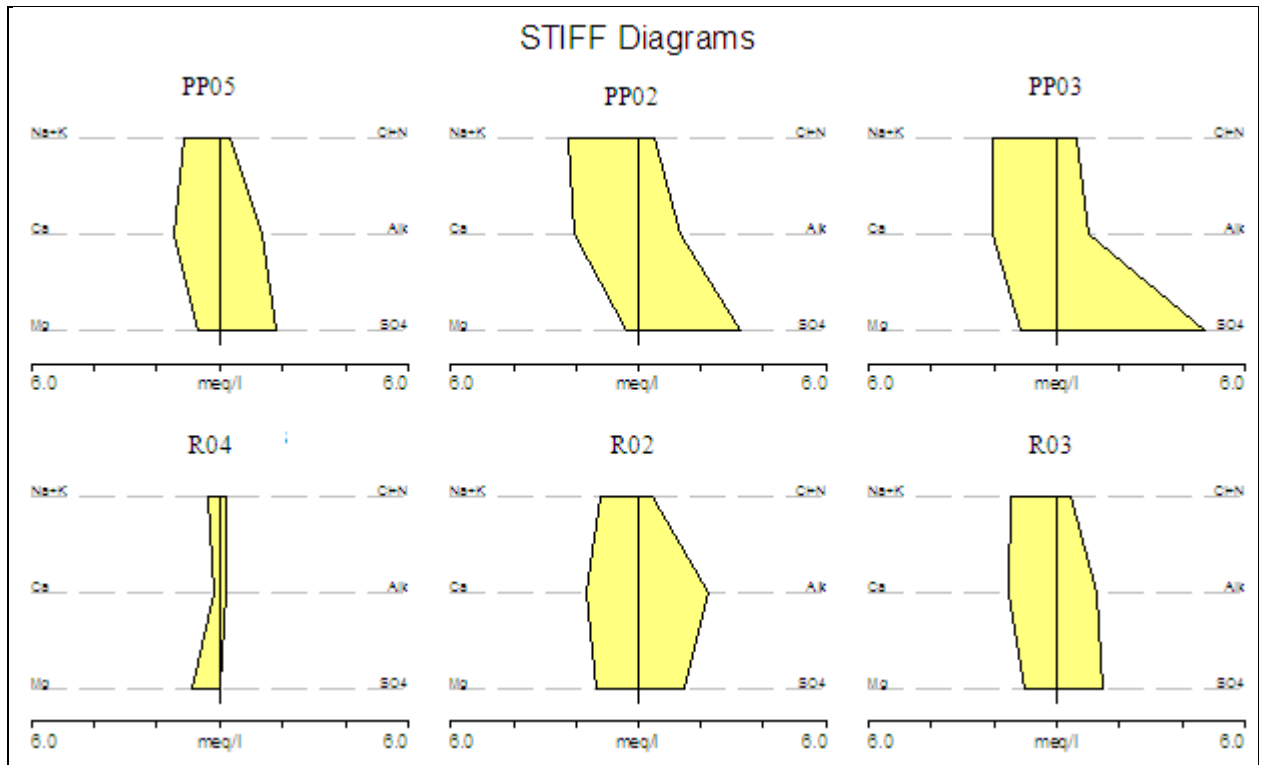


Figure 52. November 2002 concentrations.

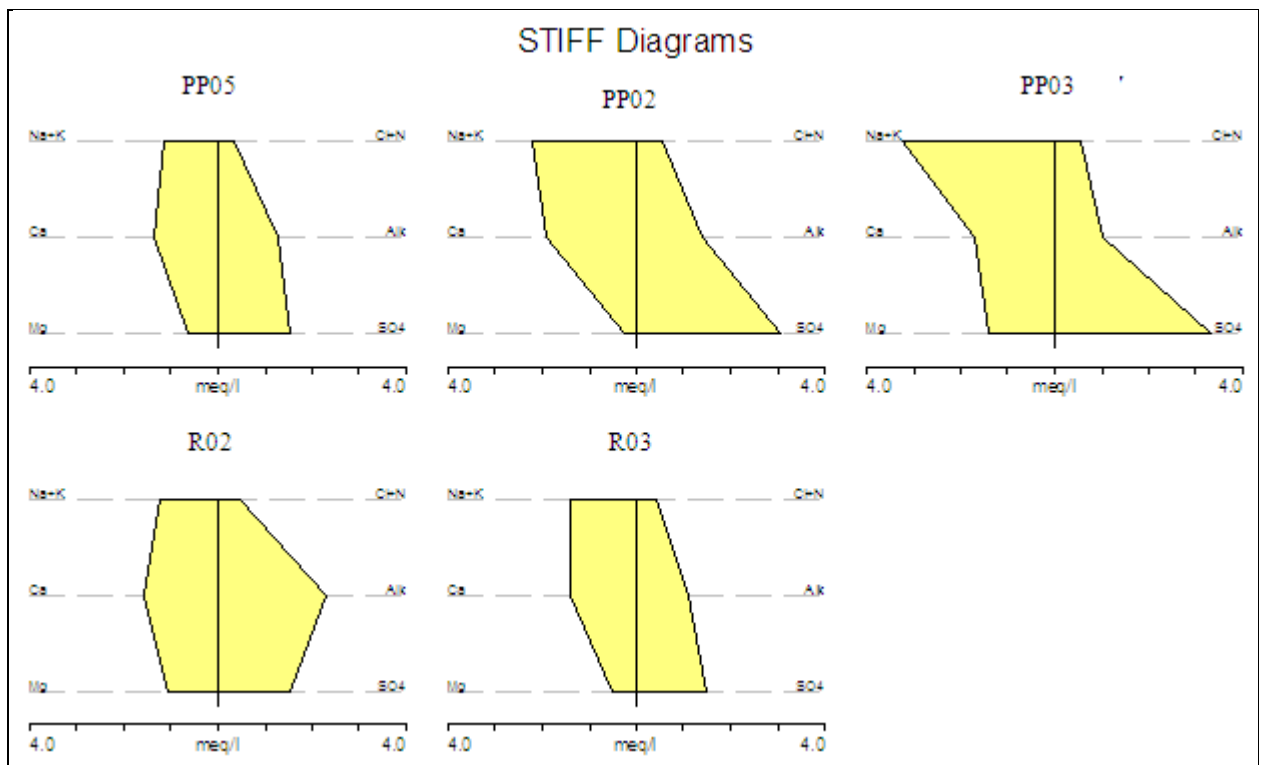


Figure 53. July 2000 concentrations.

4.9.4 Conclusions

It can be concluded that the mining taking place next to the Leeuwfontein spruit has an effect on the surface water quality at R01 as illustrated in Figure 43 and Figure 44. The effect the ash stack has on the Leeuwfontein is not apparent due to the poor water quality of the spruit before it passes the ash stack.

When the stiff diagrams are taken into consideration, it is evident that at sites R03 and PP05 the major ion compositions are relatively the same as for the dirty water dams PP02 and PP03. This is an indication that the stream diversion is working as presented in Figure 45, to indicate that the dirty water dams do not influence the water qualities downstream.

Site R04 indicates clean water further downstream from PP05 as dilution occurs and no further impacts are made on the Schoongezicht spruit, but R02 indicates an increase in the major ion composition. This increase is due to the influence of the Leeuwfontein spruit as site R02 is beyond where the Leeuwfontein and Schoongezicht spruit come together.

Monitoring at sites PP05 and R03 in the Schoongezicht spruit indicates mostly acceptable sulphate concentrations from 1987 to 2009, as illustrated in Figure 46, but these sulphate concentrations exceed the sulphate concentrations of hydrocensus site FBR14 and downstream site R04. It is concluded that the Schoongezicht spruit can be affected by means of the dirty water dams if a spill occurs, but the water quality of these monitoring sites is of an acceptable value which indicates that the ash stack has minimal impact on the surface water quality of the Schoongezicht spruit.

4.10 GROUNDWATER POLLUTION MIGRATION FROM ASH STACK TO LEEUWFontein AND SCHOONGEZICHT SPRUIT.

A risk assessment study was done in order to evaluate whether the ash stack will have an effect on the groundwater at the Leeuwfontein and Schoongezicht spruit. A numerical model from (Staats, 2009) indicates the current pollution plume (2010) which will expand to these streams, as indicated in Figure 54. This current pollution plume displays 22 years of operating and indicates that the groundwater pollution has reached the Schoongezicht spruit and is close to the Leeuwfontein spruit.

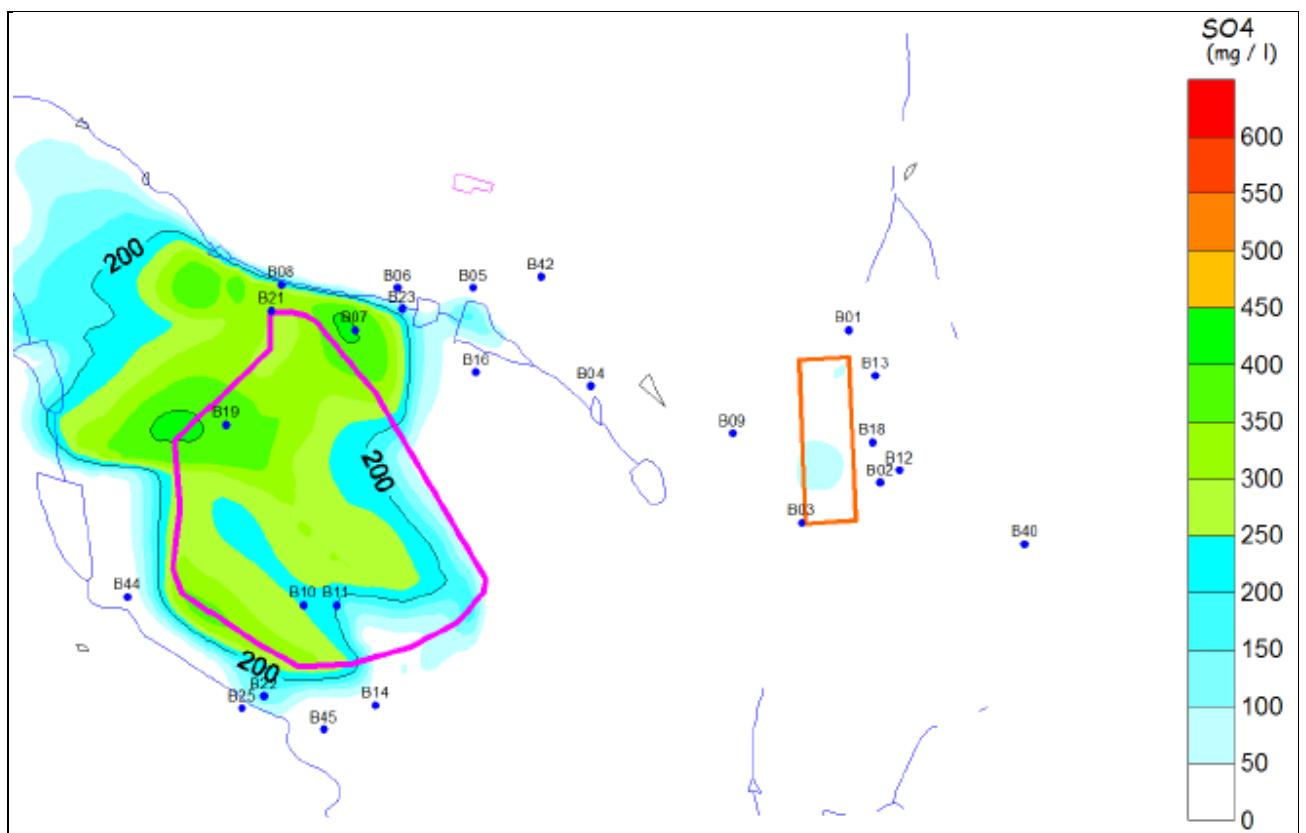


Figure 54. 2010 Simulated SO₄ pollution plume contours. (Source: Groundwater plume investigations 2009)

4.10.1 Seepage Velocity calculations

An average gradient was calculated between the ash stack and the streams at different areas, to calculate the groundwater pollution migration from the ash stack to the Leeuwfontein and Schoongezicht spruit by means of Darcy flow and seepage velocity. The lines utilised to calculate the gradients are displayed in Figure 55 and the calculations are presented in Table 24 and Table 25.

A 2% effective porosity was not used in this case, to avoid results indicating a worst case scenario, thus a 10% (Table 18) was assumed and the geometric mean of the hydraulic conductivity was utilised (Table 17) to calculate the Darcy flow and seepage velocities.

Table 24. Gradient calculations.

Stream Name	Point at stream	Groundwater elevation at stream	Groundwater elevation of ash stack	Water level difference	Distance from ash stack to stream	Gradient	Average gradient
Leeuwfontein Spruit	L1	1539.3	1553.4	14.2	337	0.042	0.031
	L2	1538.3	1550.8	12.4	348	0.036	
	L3	1533.1	1541.6	8.5	355	0.024	
	L4	1533.8	1541.8	8.0	372	0.022	
	L5	1525.9	1541.8	15.9	524	0.030	
Schoongezicht Spruit	S6	1566.7	1569.0	2.3	271	0.008	0.049
	S7	1559.6	1569.0	9.4	173	0.054	
	S8	1550.4	1569.0	18.6	222	0.084	

Table 25. Seepage velocity calculations.

Point at stream	Distance from ash stack to stream	Gradient	Hydraulic Conductivity [Upper Range, Geomean] (K)	Darcy Velocity, qn [Upper Range] (m/d)	Effective Porosity (ne)	Seepage Velocity, vn [Upper Range] (m/d)	Years to reach stream from ash stack
L1	337	0.031	0.143	0.004	0.1	0.044	21.1
L2	348	0.031	0.143	0.004	0.1	0.044	21.7
L3	355	0.031	0.143	0.004	0.1	0.044	22.2
L4	372	0.031	0.143	0.004	0.1	0.044	23.2
L5	524	0.031	0.143	0.004	0.1	0.044	32.7
S6	271	0.049	0.143	0.007	0.1	0.070	10.7
S7	173	0.049	0.143	0.007	0.1	0.070	6.8
S8	222	0.049	0.143	0.007	0.1	0.070	8.8

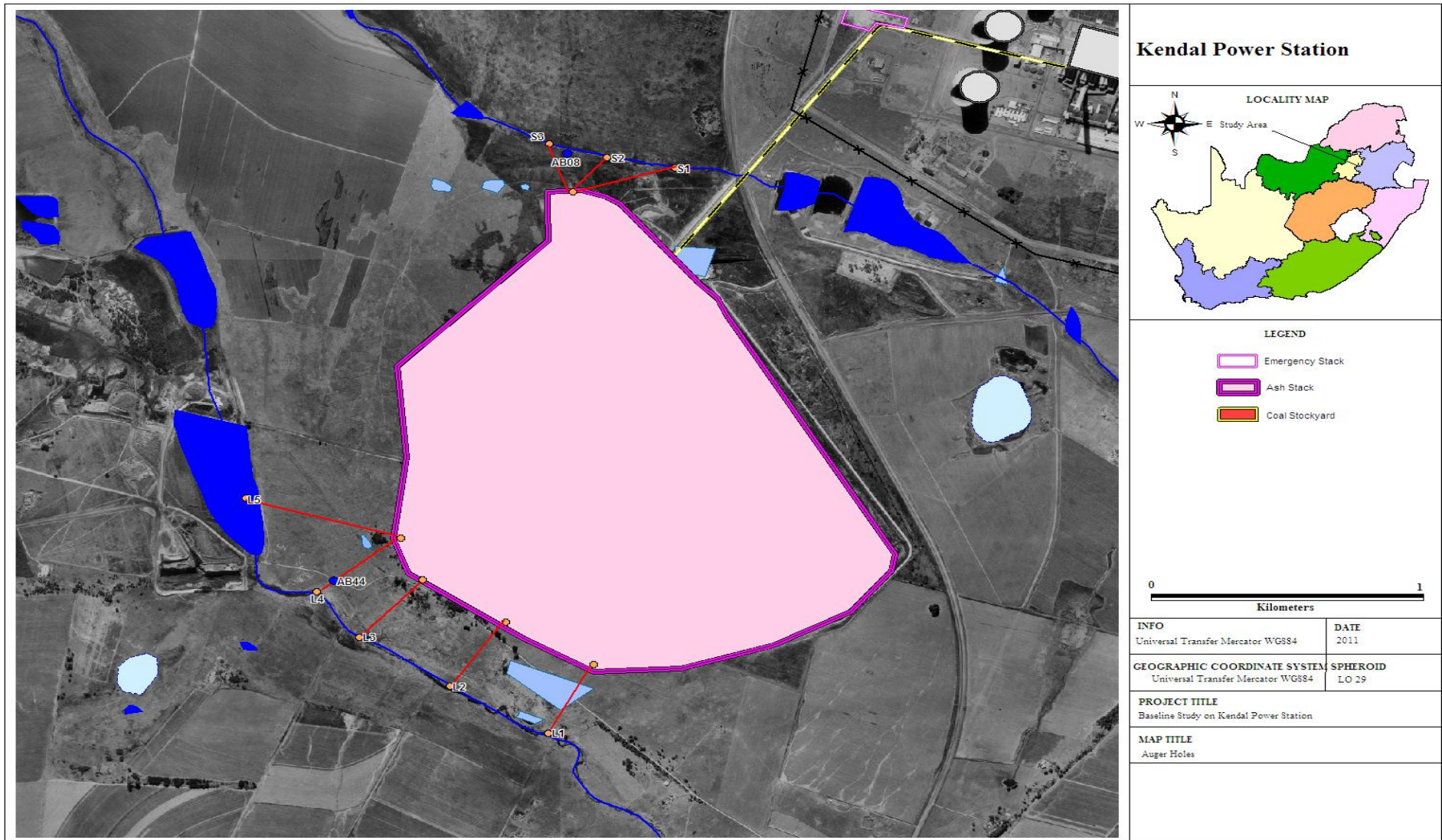


Figure 55. Gradient lines from ash stack to Schoongezicht and Leeuwfontein spruit.

4.10.2 Conclusions

When comparing the numerical model and the seepage velocity calculations, it was found that the model and the calculations indicate that the groundwater at the Schoongezicht spruit will be influenced from the ash stack.

The groundwater quality of borehole AB08 (located next to the Schoongezicht spruit) exceeds the average qualities for parameters EC, Na, Ca, Cl and SO₄. The pollution index results (Table 12) indicate a high to a very high probability of contaminant impacts, indicating that seepage from the ash stack may have occurred. It should, however, be kept in mind that the groundwater quality of borehole AB08 is acceptable (Table 6).

It was also found that the model indicates that the groundwater at the Leeuwfontein spruit will not be influenced after 22 years of operation, whereas the calculations indicate that the pollution plume will reach the groundwater through gradients L1, L2, L3 and L4 within 21 to 32 years. These results are slightly over-estimated as the groundwater quality of borehole AB44 (Table 7) indicates that the water quality has not been affected and the pollution index tables (Table 12) also indicate no probability of contaminant impacts.

The model indicates that borehole B22 will be influenced after 22 years of operation, but this is due to concentrations introduced to the pan located next to the borehole and not the ash stack.

5 AQUIFER VULNERABILITY

5.1 INTRODUCTION

The objective of defining and mapping aquifer vulnerability is to help planners to protect groundwater as an essential economic resource and to act as a foundation for the designation of protection zones. The concept of aquifer vulnerability derives from the assumption that the physical environment may provide some degree of protection of groundwater against human impacts, especially with regard to pollutants entering the subsurface. Aquifer vulnerability thus combines the hydraulic inaccessibility of the saturated zone to the penetration of pollutants, with the attenuation capacity of the strata overlying the saturated zone (Foster, 1998).

The vulnerability of the underground water source is related to the distance that the contaminant must flow to reach the water table, and the ease with which it can flow through the soil and rock layers above the water table. An assessment of the soil and rock types and the distance to the water table may be obtained from an area hydrogeological report prepared after site inspection. (Groundwater protocol version 2, 2003)

Table 26. *Vulnerability of groundwater aquifer due to hydrogeological conditions (Groundwater protocol version 2, 2003).*

Vulnerability Class	Measurements	Definition
Extreme (usually highly fractured rock and/or high ground water table)	High risk and short distance (< 2m) to water table	Vulnerable to most pollutants with relatively rapid impact from most contamination disposed of at or close to the surface
High (usually gravely or fractured rock, and/or high water table)	High risk and medium distance (2-5m) to water table	Vulnerable to many pollutants except those highly absorbed, filtered and/or readily transformed
Medium (usually fine sand, deep loam soils with semi-solid rock and average water table (>10m))	Low risk and medium to long distances to water table	Vulnerable to inorganic pollutants but with negligible risk of organic or microbiological contaminants
Low (usually clay or loam soils with semi-solid rock and deep water table (>20m))	Minimal and low risk, and long to very long distance to water table	Only vulnerable to the most persistent pollutants in the very long term
Negligible (usually dense clay and/or solid impervious rock with deep water table)	Minimal risk with confining layers	Confining beds present with no significant infiltration from surface areas above aquifer

 Site Criteria Bracket

5.2 UNSATURATED ZONE CHARACTERISTICS

To classify the unsaturated zone, 12 auger holes were drilled on the 18th of November 2010. The locations of these holes are presented in Figure 59. Only one soil sample was taken from the auger holes if they comprised a homogenous soil profile. If the hole comprised more than one soil horizon, samples were taken from the different horizons. These samples were analysed by means of sieve analysis for the determination of soil hydraulic parameters.

The unsaturated zone of the study area is comprised mostly of clayey sand topsoil at the auger holes which were drilled. The matrix's comprised mostly of sandstones and shales observed from the borehole logs of previously drilled boreholes. The average water level of all of the boreholes in the study area is 7.56 meters and they are utilised as the depth of the unsaturated zone. The shallow groundwater table makes the aquifer more vulnerable to contamination from surface activities such as the coal stockyard, ash stack and the emergency ash stack. The results of the permeabilities calculated for auger hole PD02 by means of sieve analyses are presented in Figure 57 and Figure 58. The permeability results of the additional drilled auger holes are indicated in Appendix E.

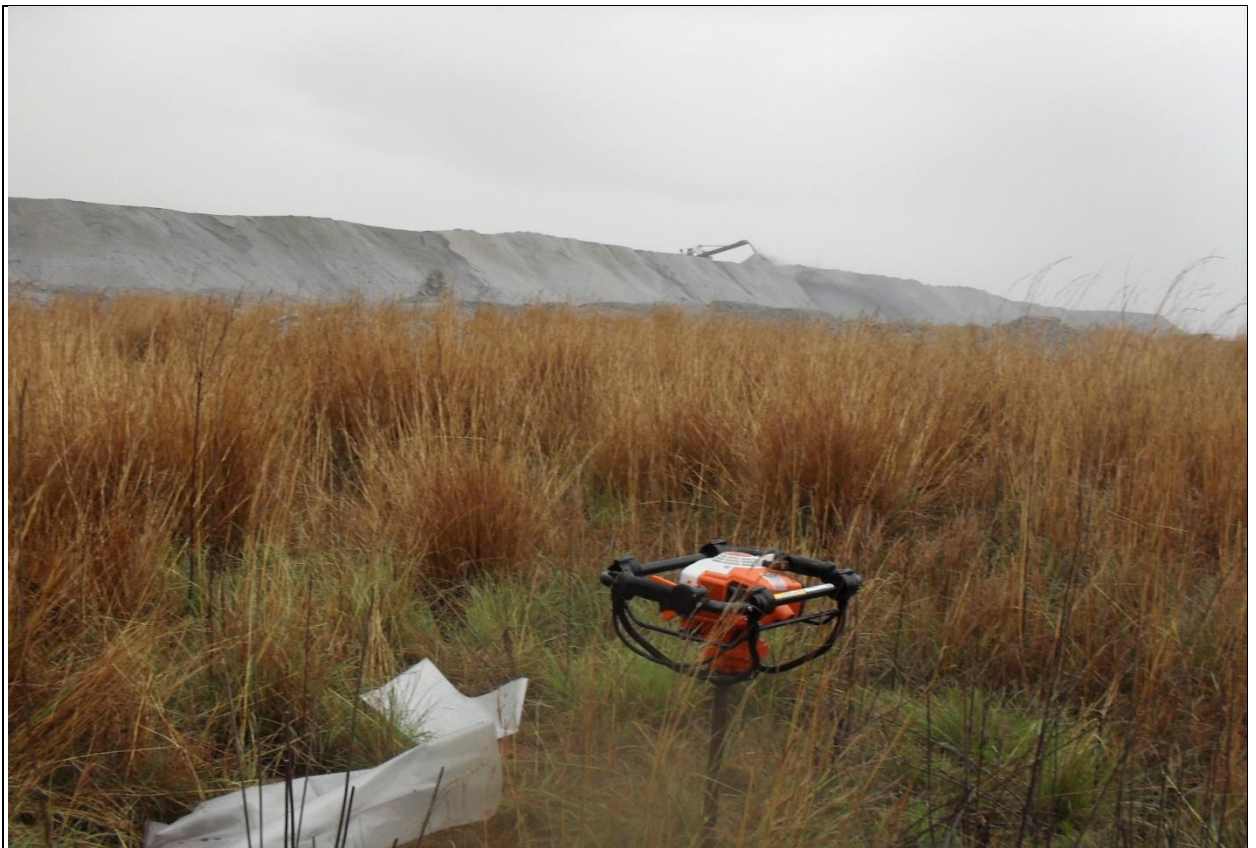


Figure 56. Auger hole AD09 drilled at ash stack.

DETERMINATION OF SOIL HYDRAULIC PARAMETERS

Date: 18-Jan-10
Sample no.: PD02 - A
Material Depth: (0 - 1 m)
Classification: Brown Clayey Sand

Grain size d (mm)	Sieve anal. (%)	Hydraulic Conductivity		
		Shephard (1989) Calculated	(m/day)	(m/s)
53	100		16.3687	1.89E-04
38	78			
27	76			
19	75			
13	73			
5	65			
2	54			
0	48			
0	30			
0	4			
0.66	Ave. GS 50%			

<u>Rawls & Brakensiek (1985)</u>		
Calculated	(m/day)	(m/s)
	0.0968	1.12E-06

<u>Brooks & Corey Parameters</u>		
Porosity	30%	Est.
Residual water saturation	0.9048	
Air entry head	0.8013	
Pore size distr.	0.4322	

	Clay	Silt	Sand	Gravel
Grain Size (mm)	< 0.002	< 0.06	< 2	< 60
% Passing	3.6	28.9	54.3	100
% Fraction	3.6	25.3	25.4	45.7

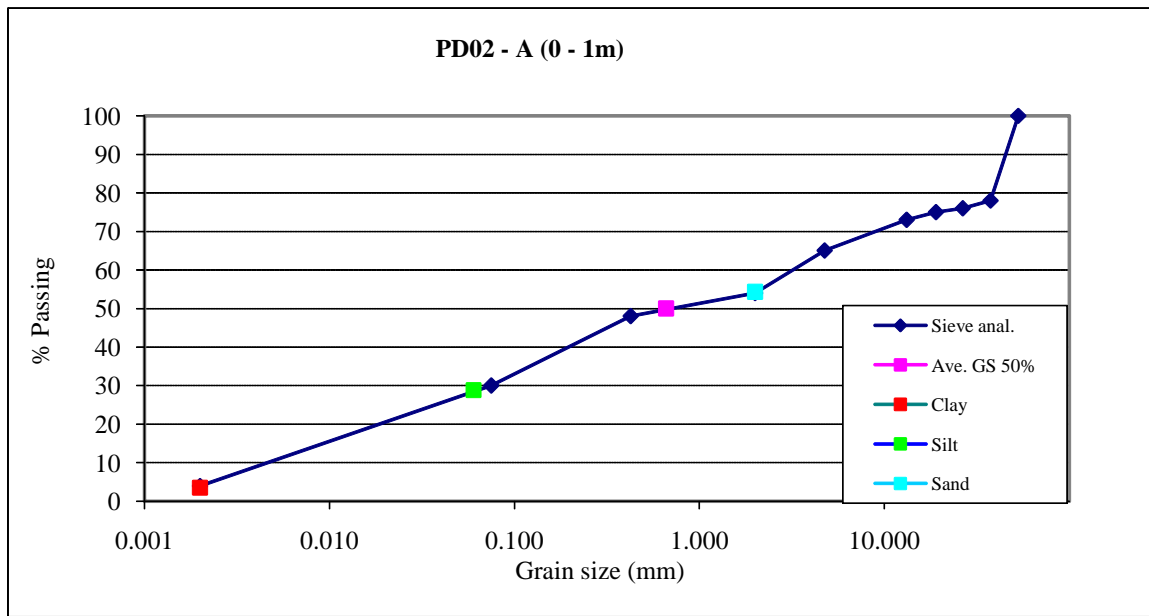


Figure 57. Sieve permeability and SOPROP calculations for PD02-A.

DETERMINATION OF SOIL HYDRAULIC PARAMETERS

Date: 18-Jan-10
Sample no.: PD02 - B
Material Depth: (1 - 1.5 m)
Classification: Light Brown Clayey Sand

Grain size d (mm)	Sieve anal. (%)	Hydraulic Conductivity		
		Shephard (1989) Calculated	(m/day)	(m/s)
26.5	100		1.8579	2.15E-05
19.00	99			
13.20	97			
4.760	86	Rawls & Brakensiek (1985) Calculated	(m/day)	(m/s)
2.000	77		0.1642	1.90E-06
0.425	65	Brooks & Corey Parameters		
0.075	40	Porosity	30%	Est.
0.002	9	Residual water saturation	0.1798	
0.15	Ave. GS 50%	Air entry head	0.6438	
		Pore size distr.	0.4308	

	Clay	Silt	Sand	Gravel
Grain Size (mm)	< 0.002	< 0.06	< 2	< 60
% Passing	10	37.1	77.2	100
% Fraction	10	27.1	40.1	22.8

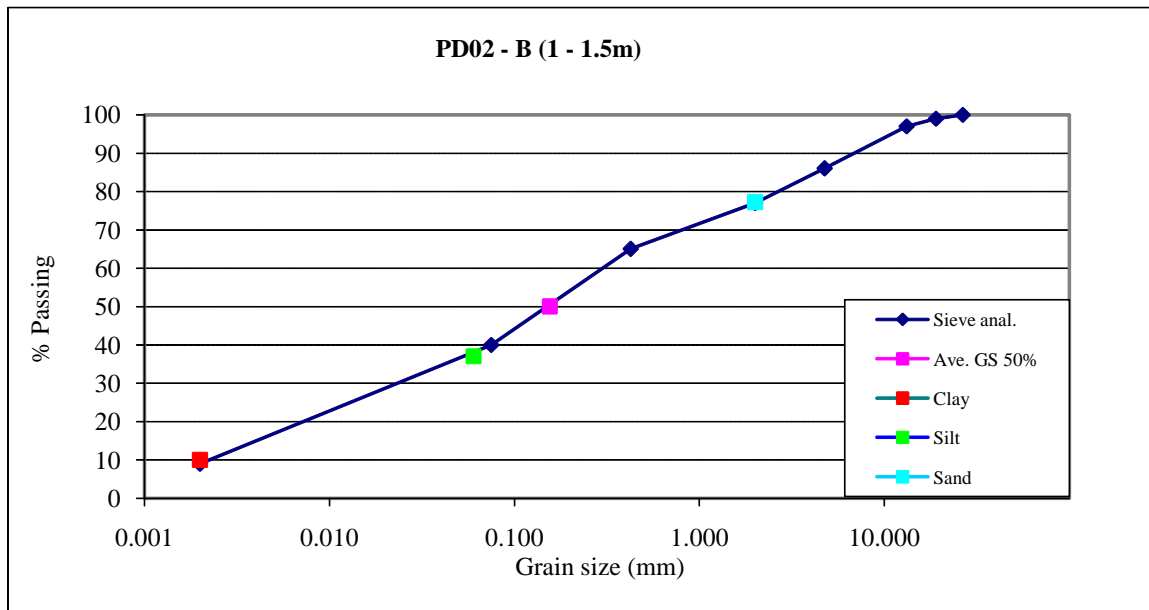


Figure 58. Sieve permeability and SOPROP calculations for PD02-B.

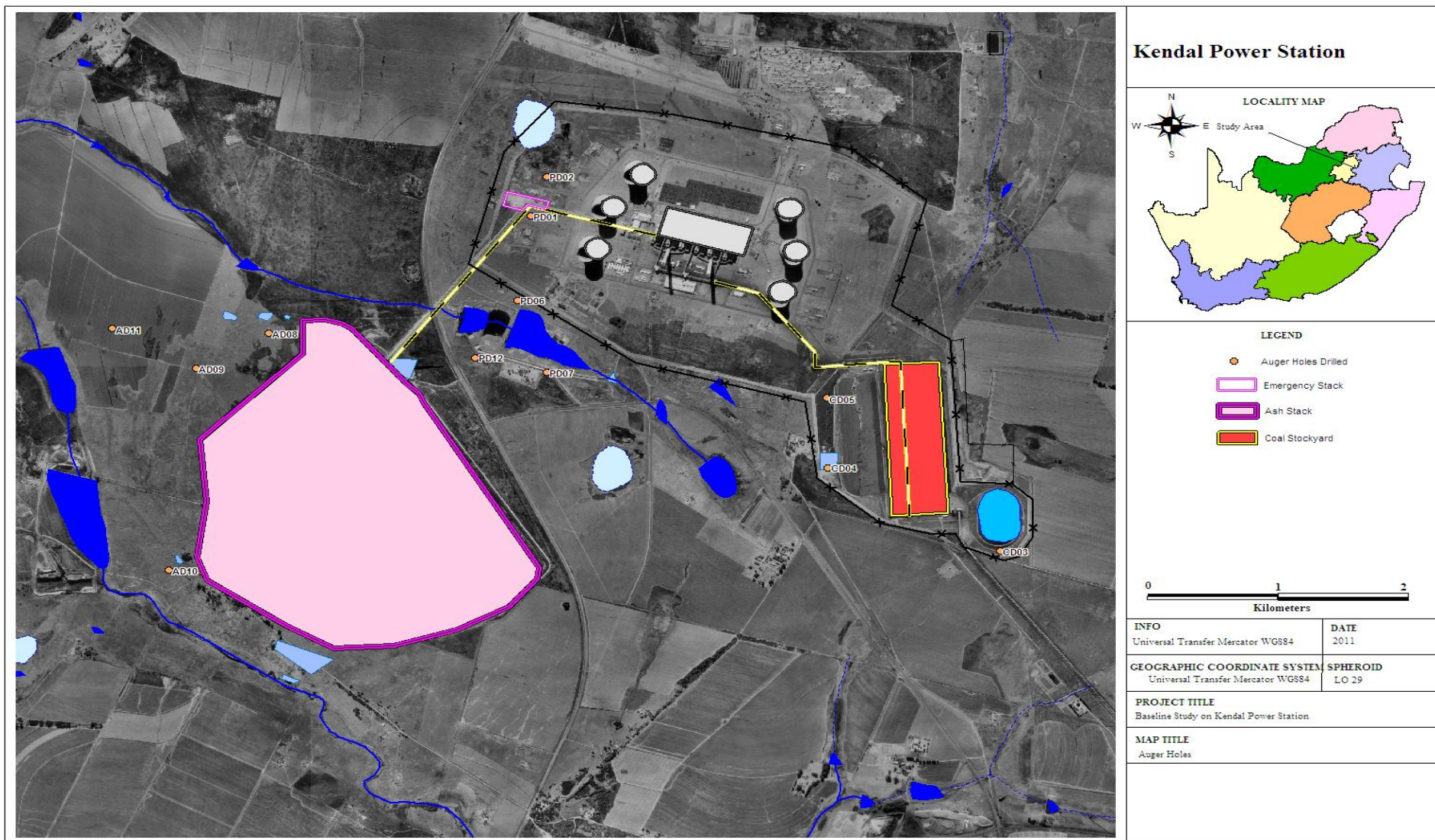


Figure 59. Auger holes drilled for sieve analysis.

5.2.1 Soil hydraulic parameters results

The hydraulic conductivity for all of the soil samples was calculated by means of Shephard (1989). An average and geometric means are presented in Table 27. The geometric mean was used for aquifer vulnerability classification due to large differences of hydraulic conductivity at various samples.

Table 27. Average and geometric mean of hydraulic conductivity at soil samples.

Auger Hole	Hydraulic Conductivity (K) Shephard (1989)	Hydraulic Conductivity (K) Shephard (1989)
PD01	85.904	85.904
PD02 - A	16.369	16.369
PD02 - B	1.858	1.858
CD03 - A	0.637	0.637
CD03 - B	1.107	1.107
CD04	0.840	0.840
CD05 - A	0.840	0.840
CD05 - B	0.518	0.518
PD06 - A	6.668	6.668
PD06 - B	10.448	10.448
PD07 - A	12.417	12.417
PB07 - B	2.286	2.286
AD08	0.518	0.518
AD09	75.338	75.338
AD10	18.156	18.156
AD11	4.721	4.721
PD12	0.680	0.680
	14.08	3.61
	(Average)	(Geometric mean)

5.3 VULNERABILITY OF GROUNDWATER AQUIFER DUE TO HYDROGEOLOGICAL CONDITIONS

The vulnerability of the underground water is related to the distance the contaminant must flow from the topsoil to the water table. The assessment of the soil parameters is discussed above and is used to classify the vulnerability of the groundwater aquifer. The soil depth was obtained by determining how deep the auger holes could have been drilled over the study area before entering the rock medium, which comprises an average of 1.4 meters of the total depth

(7.56m) of the unsaturated zone. Data over the entire study area of Kendal Power Station was utilised to classify the aquifer vulnerability and are listed in Table 28.

Table 28. Vulnerability of groundwater aquifer due to hydrogeological conditions.

Vulnerability Class	Measurements	Definition
Extreme (usually highly fractured rock and/or high ground water table)	High risk (table 1) and short distance (< 2m) to water table	Vulnerable to most pollutants with relatively rapid impact from most contamination disposed of at or close to the surface
High (usually gravely or fractured rock, and/or high water table)	High risk (table 1) and medium distance (2-5m) to water table	Vulnerable to many pollutants except those highly absorbed, filtered and/or readily transformed
Medium (usually fine sand, deep loam soils with semi-solid rock and average water table (>10m))	Low risk (table 1) and medium to long distances to water table	Vulnerable to inorganic pollutants but with negligible risk of organic or microbiological contaminants
Low (usually clay or loam soils with semi-solid rock and deep water table (>20m))	Minimal and low risk (table 1), and long to very long distance to water table	Only vulnerable to the most persistent pollutants in the very long term
Negligible (usually dense clay and/or solid impervious rock with deep water table)	Minimal risk (table 1) with confining layers	Confining beds present with no significant infiltration from surface areas above aquifer

 Site Criteria Bracket

The vulnerability of Kendal Power Station is high. The aquifer is vulnerable to many pollutants except to those highly absorbed, filtered and/or readily transformed. The aquifer has a high vulnerability due to a thin, permeable unsaturated zone and a very high seepage velocity flowing from the topsoil to the water table. The soil also comprises only 1.4 meters of the unsaturated zone which decreases the chance for attenuation to occur.

5.4 CLASSIFYING AQUIFER VULNERABILITY WITHIN DIFFERENT AREAS RELATIVE TO THE SATURATED ZONE

Classifying the aquifer vulnerability of the groundwater was identified by using the data over the entire study area of Kendal Power Station. By using the same data but only within different areas, it can be quantified whether certain areas are more vulnerable to pollution impacts than former areas. These areas will be separated as follows: The ash stack, coal stockyard and the power station area. The data (water levels, hydraulic conductivity of matrix, soil hydraulic parameters and geological logs) will be acquired from the boreholes and auger holes to quantify the aquifer vulnerability within these certain areas.

5.4.1 Coal Stockyard Area

Table 29 and Table 30 indicate all the data from the coal stockyard which will be taken in consideration to quantify how vulnerable the aquifer is. The borehole logs used to classify the saturated and unsaturated zones are presented in Appendix G. Figure 60 indicates all the boreholes and auger holes in the vicinity of the coal stockyard area that will be utilised for interpretation.

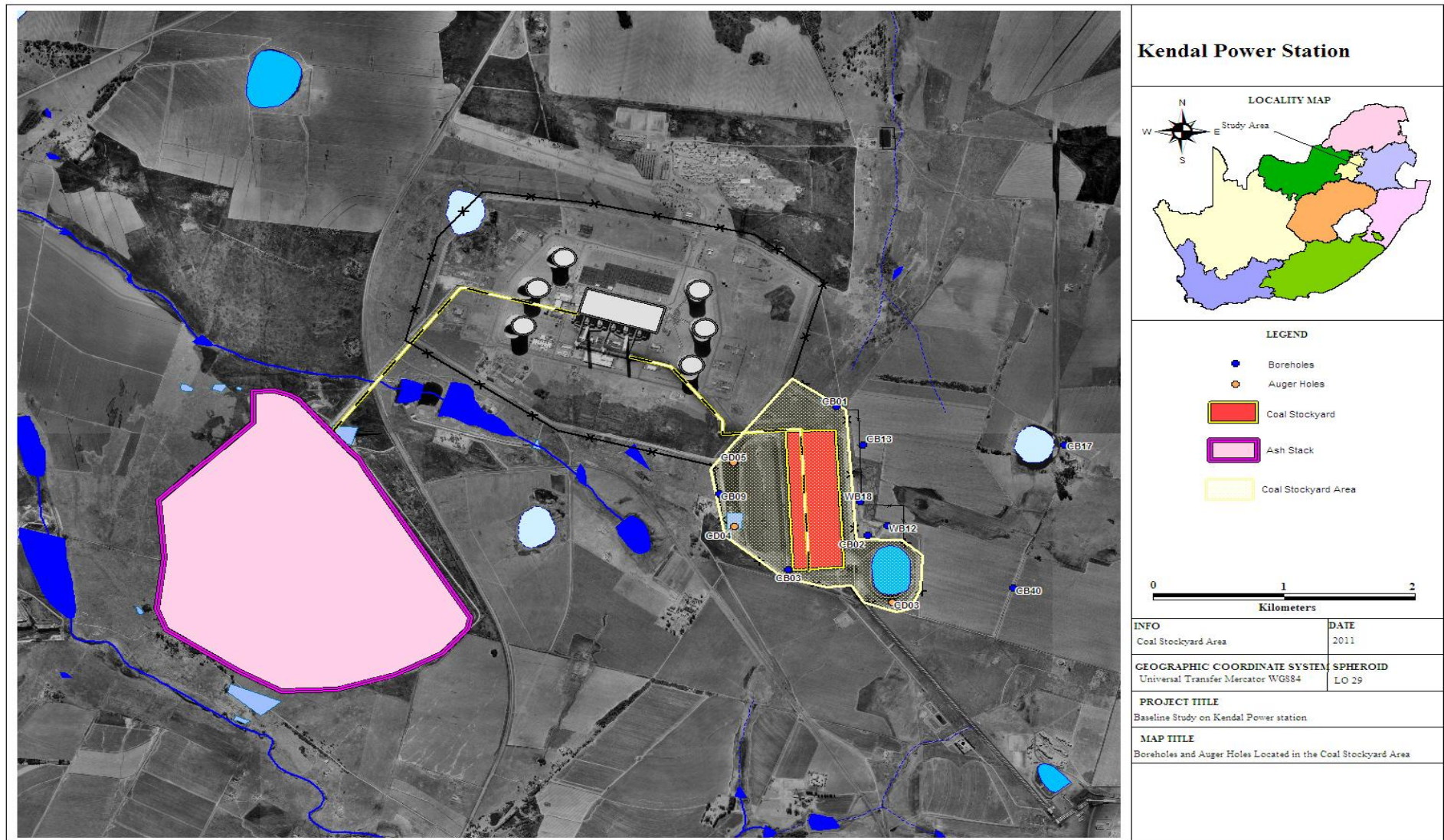


Figure 60. Boreholes and auger holes in the coal stockyard area.

Table 29. Coal stockyard borehole data.

Borehole	Water Level (m)	Matrix Hydraulic conductivity	Unsaturated zone	Saturated Zone
CB01	1.3	~	Yellow brown clay	Shale, hard massive dolerite
CB02	12.04	~	Yellow brown clay	Deep clay, shale, sandstone
CB03	14.4	~	Yellow brown clay	Sandstone, granite
CB09	3.7	~	~	~
CB13	4.53	0.020	Sand, weathered clay	Sandstone, mudstone, dolerite
CB17	1.1	~	~	~
CB40	7.58	0.076	~	~
WB12	9.81	~	Yellow brown clay	Clay, shale, sandstone
WB18	16.56	0.014	Light brown clay	Sandstone, dolerite

Table 30. Coal stockyard auger hole data.

Auger hole	Soil hydraulic conductivity Shepard (1989)
CD03 - A	0.637
CD03 - B	1.1067
CD04	0.840
CD05 - A	0.8395
CD05 - B	0.518

Various boreholes have a deep water level which indicates a slightly deeper unsaturated zone than over the entire study area. The unsaturated zone consists mainly of yellowish-brown clay and the boreholes with a deep water level consist of clay which will allow attenuation to occur when pollution sources filtrate through the clay to the water table. The saturated zone consists of shale, sandstone, mudstone, dolerite and granite. The sandstones and shales are weathered at some of the boreholes, which can allow easier flow through the matrix, although the hydraulic conductivity of the matrix is very low, as indicated in Table 29. Boreholes CB01, CB13 and WB18 consist of hard fresh dolerites, and borehole CB03 consists of granites which will slow down the flow of pollutants into the deeper aquifer.

The soil hydraulic parameters in Table 30 indicate that all of the soil samples have a lower hydraulic conductivity than to the soil samples at the power station and ash stack area.

The pollution index results (Table 12) indicate that there is no probability of contaminant impacts for the boreholes in the coal stockyard area, which also gives a indication that the coal stockpile has little effect on the groundwater qualities in this area.

Table 31. Vulnerability of groundwater aquifer at coal stockyard.

Vulnerability Class	Measurements	Definition
Extreme (usually highly fractured rock and/or high ground water table)	High risk (table 1) and short distance (< 2m) to water table	Vulnerable to most pollutants with relatively rapid impact from most contamination disposed of at or close to the surface
High (usually gravely or fractured rock, and/or high water table)	High risk (table 1) and medium distance (2-5m) to water table	Vulnerable to many pollutants except those highly absorbed, filtered and/or readily transformed
Medium (usually fine sand, deep loam soils with semi-solid rock and average water table (>10m))	Low risk (table 1) and medium to long distances to water table	Vulnerable to inorganic pollutants but with negligible risk of organic or microbiological contaminants
Low (usually clay or loam soils with semi-solid rock and deep water table (>20m))	Minimal and low risk (table 1), and long to very long distance to water table	Only vulnerable to the most persistent pollutants in the very long term
Negligible (usually dense clay and/or solid impervious rock with deep water table)	Minimal risk (table 1) with confining layers	Confining beds present with no significant infiltration from surface areas above aquifer

 Site Criteria Bracket

The vulnerability of the coal stockyard is medium. As it is Vulnerable to inorganic pollutants with a negligible risk of organic or microbiological contaminants. The aquifer has a medium vulnerability due to a medium to long distance to water table, deep clays with a low hydraulic conductivity for attenuation to occur, and solid hard rock in the deep aquifer.

5.4.2 Ash stack

Table 29 and Table 30 indicate all the data from the ash stack which will be taken in consideration to quantify how vulnerable the aquifer is. The borehole logs utilised to classify the saturated and unsaturated zones are presented in Appendix G. Figure 61 indicates all of the boreholes and auger holes in the vicinity of the ash stack area that will be utilised for interpretation.

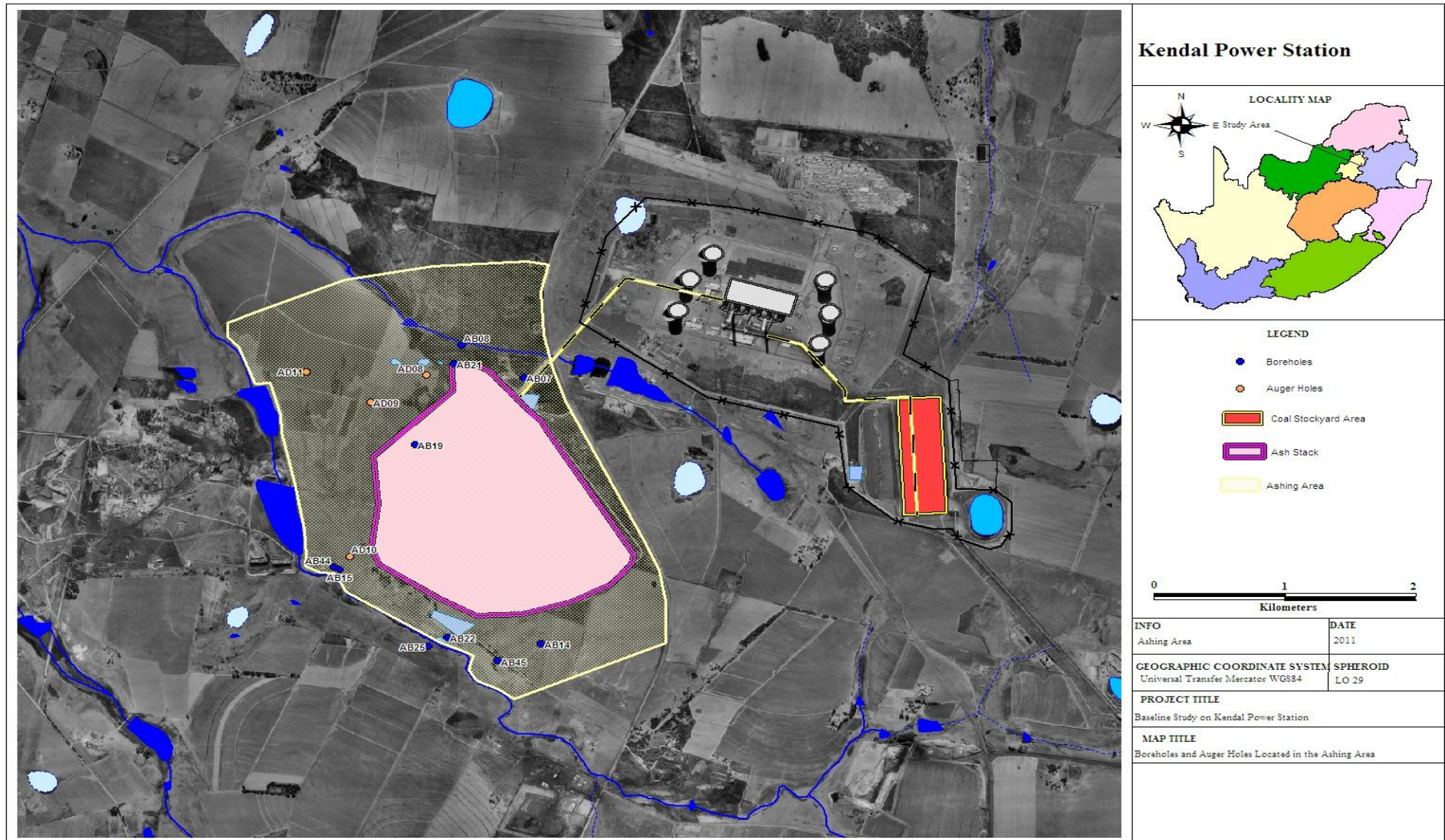


Figure 61. Boreholes and auger holes located in the ashing area.

Table 32. Ash stack borehole data.

Borehole	Water Level (m)	Matrix Hydraulic conductivity	Unsaturated zone	Saturated Zone
AB07	11.24	0.007	Brown clayey	Weatehred, baked clay
AB08	6.95	0.226	Yellowish soil	Weathered Shale, granite
AB14	13.13	0.038	Sand, mudstone, weatehred rhyolite	Fgractured rhyolite, fractured diabase, sandstone
AB15	3.37	~	Sand, clay	Sandstone, diabase, rhyolite
AB16	2.5	0.06	~	~
AB19	35.51	~	Weathered dolerite	Hard fresh dolerite
AB21	6.62	0.24	Red clay	Weathered, hard massive dolerite
AB22	3.47	0.012	Clay	Sandstone, shale, coal
AB25	5.2	0.012	~	~
AB44	3.96	1.28	~	~
AB45	6.5	0.017	~	~

Table 33. Ash stack auger hole data.

Auger hole	Soil hydraulic conductivity Shepard (1989)
AD08	0.518
AD09	75.338
AD10	18.156
AD11	4.721

Only boreholes AB07, AB14 and AB19 have a deep water level, indicating that the unsaturated zone is not very deep over the entire area of the ash stack. The unsaturated zone does not consist of deep soil profiles according to the borehole logs presented in Appendix G therefore attenuation cannot occur as efficiently as in the deep soil profiles in the coal stockyard area. In the saturated zone, the sandstones and shales are weathered at some of the boreholes, which can allow easier flow through the matrix, although the hydraulic conductivity of the matrix is very low as indicated in Table 32. Boreholes AB19 and AB21 consist of hard, fresh and massive dolerites which will slow down the flow of pollutants into the deeper aquifer in the vicinity of boreholes AB19 and AB21.

The soil hydraulic parameters in Table 33 indicate a very high hydraulic conductivity of the soil samples taken in the vicinity at the ash stack which increases the risk of the water flowing through the soil to the water table.

Table 34. Vulnerability of groundwater aquifer at ash stack.

Vulnerability Class	Measurements	Definition
Extreme (usually highly fractured rock and/or high ground water table)	High risk (table 1) and short distance (< 2m) to water table	Vulnerable to most pollutants with relatively rapid impact from most contamination disposed of at or close to the surface
High (usually gravely or fractured rock, and/or high water table)	High risk (table 1) and medium distance (2-5m) to water table	Vulnerable to many pollutants except those highly absorbed, filtered and/or readily transformed
Medium (usually fine sand, deep loam soils with semi-solid rock and average water table (>10m))	Low risk (table 1) and medium to long distances to water table	Vulnerable to inorganic pollutants but with negligible risk of organic or microbiological contaminants
Low (usually clay or loam soils with semi-solid rock and deep water table (>20m))	Minimal and low risk (table 1), and long to very long distance to water table	Only vulnerable to the most persistent pollutants in the very long term
Negligible (usually dense clay and/or solid impervious rock with deep water table)	Minimal risk (table 1) with confining layers	Confining beds present with no significant infiltration from surface areas above aquifer

 Site Criteria Bracket

The vulnerability of the ash stack is high. The aquifer is vulnerable to many pollutants except to those highly absorbed, filtered and/or readily transformed. The aquifer has a high vulnerability due to a thin soil profile with a high hydraulic conductivity, minimising the attenuation before the pollutants reach the water table. The matrix consists of a low hydraulic conductivity although the saturated zones include fractured and weathered rock.

5.4.3 Power station

Table 35 and Table 36 indicate all the data from the power station which will be taken into consideration to quantify how vulnerable the aquifer is. The borehole logs used to classify the saturated and unsaturated zones are presented in Appendix G. Figure 62 indicates all the boreholes and auger holes in the vicinity of the power station area that will be utilised for data interpretation.

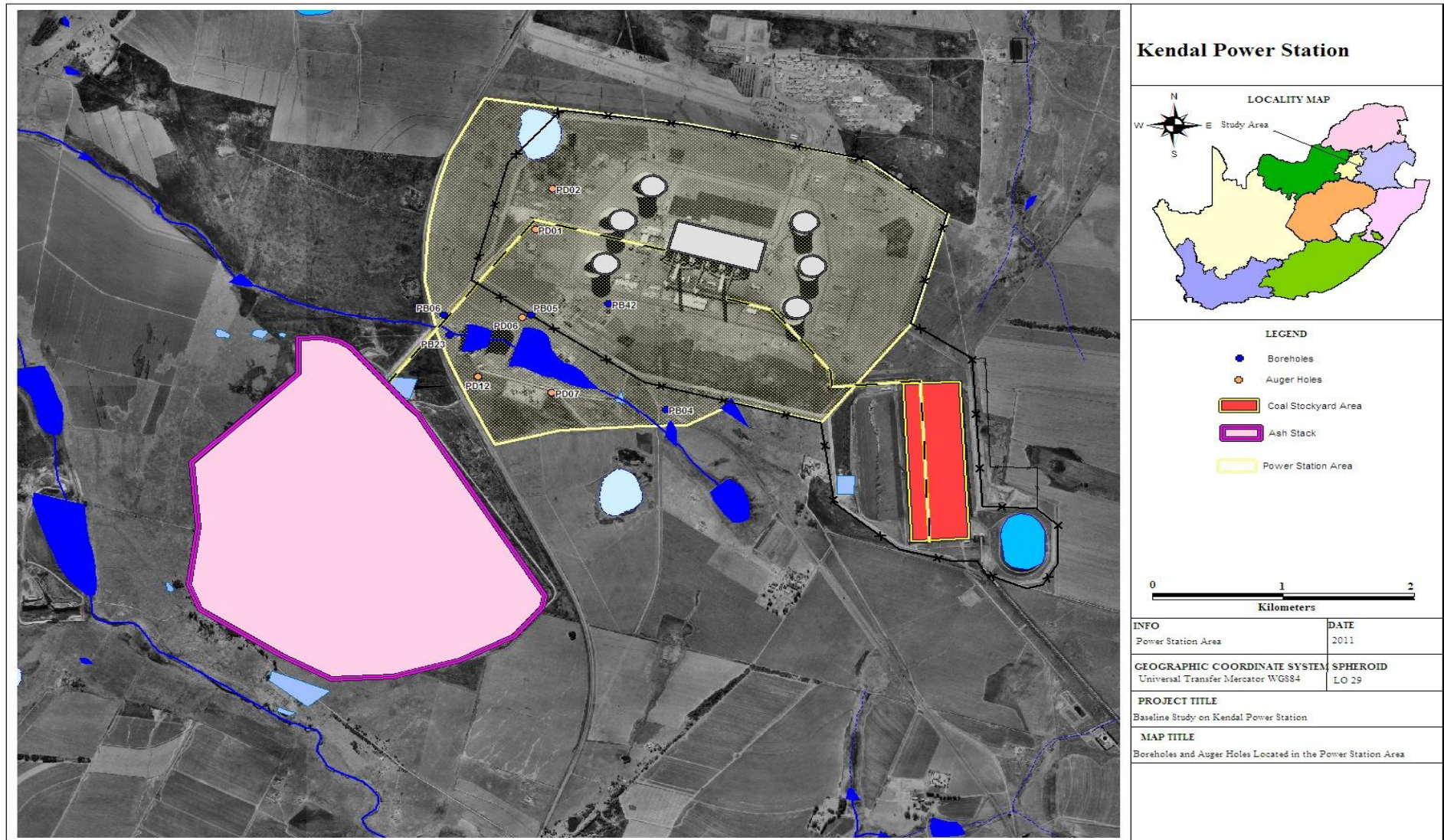


Figure 62. Boreholes and auger holes located in the power station area.

Table 35. Power station borehole data.

Borehole	Water Level (m)	Matrix Hydraulic conductivity	Unsaturated zone	Saturated Zone
PB04	2.38	0.028	Gravel, soil	Fractured and massive rhyolite
PB05	5.62	0.053	Soil	Weathered shale, tilite
PB06	4.04	0.045	Gravel	Baked shale, granite
PB23	2.34	0.060	~	~
PB42	6.86	0.311	~	~

Table 36. Power station auger hole data.

Auger hole	Soil hydraulic conductivity Shepard (1989)
PD01	85.904
PD02 - A	16.369
PD02 - B	1.858
PD06 - A	6.668
PD06 - B	10.448
PD07 - A	12.417
PB07 - B	2.286
PD12	0.680

There are no boreholes in the vicinity of the power station which consist of a deep water level, indicating a shallow unsaturated zone. The unsaturated zone consists of soil and gravel with no clay according to the borehole logs in Appendix G. Therefore attenuation cannot occur as efficiently as in the deep soil profiles in the coal stockyard area. The saturated zone consists of fractured and massive rhyolite, weathered and baked shale and tilite, which can allow easier flow through the matrix, although the hydraulic conductivity of the matrix is very low, as indicated in Table 35.

The soil hydraulic parameters in Table 36 indicate a very high hydraulic conductivity of the soil samples taken in the vicinity at the power station which increases the risk of water flowing through the soil and gravel to the water table.

Table 37. Vulnerability of groundwater aquifer at power station.

Vulnerability Class	Measurements	Definition
Extreme (usually highly fractured rock and/or high ground water table)	High risk (table 1) and short distance (< 2m) to water table	Vulnerable to most pollutants with relatively rapid impact from most contamination disposed of at or close to the surface
High (usually gravely or fractured rock, and/or high water table)	High risk (table 1) and medium distance (2-5m) to water table	Vulnerable to many pollutants except those highly absorbed, filtered and/or readily transformed
Medium (usually fine sand, deep loam soils with semi-solid rock and average water table (>10m))	Low risk (table 1) and medium to long distances to water table	Vulnerable to inorganic pollutants but with negligible risk of organic or microbiological contaminants
Low (usually clay or loam soils with semi-solid rock and deep water table (>20m))	Minimal and low risk (table 1), and long to very long distance to water table	Only vulnerable to the most persistent pollutants in the very long term
Negligible (usually dense clay and/or solid impervious rock with deep water table)	Minimal risk (table 1) with confining layers	Confining beds present with no significant infiltration from surface areas above aquifer

 Site Criteria Bracket

The vulnerability of the power station is high. The aquifer is vulnerable to many pollutants except to those highly absorbed, filtered and/or readily transformed. The aquifer has a high vulnerability due to a thin soil profile containing gravel with a high hydraulic conductivity, minimising the attenuation before the pollutants reach the water table. The water table has a medium distance (2-5 m) from the surface and the matrix consists of a low hydraulic conductivity, although the saturated zones include fractured and weathered rock.

6 CONCLUSIONS

Classifying the aquifer vulnerability of the groundwater was identified by using the data over the entire study area of Kendal Power Station. By using the same data, but only within different areas, it can be quantified whether certain areas are more vulnerable to pollution impacts than former areas.

By means of applying the data from the geological logs from different areas, it was found that the soil profiles over the entire study are deeper than the estimated 1.4 meters of the auger holes drilled, but the coal stockyard area comprises a deeper soil profile than the profiles in the ashing- and power station areas. The water levels were slightly deeper and the hydraulic conductivity of the soil samples was lower than that of the soil samples taken from the ashing- and power station area, thus illustrating that attenuation will occur more effectively throughout the thick soil profiles with low hydraulic conductivities in the vicinity of the coal stockyard.

The vulnerability of the coal stockyard was classified as medium, while the ashing area and power station area was classified as high. The aquifer vulnerability of the entire study was high, but when taking areas separately into consideration, there were some differences between these areas and the coal stockyard was identified as medium aquifer vulnerability due to various factors. The pollution indexes (Table 12) indicate that the groundwater in the vicinity of the power station and ashing area has a possible to a very high possibility of pollutant impacts. Only borehole CB17 indicates a possibility of pollutant impact in the coal stockyard area, in agreement with the aquifer vulnerability classification within different areas.

Therefore it is also important to identify certain smaller areas for vulnerability assessment due to the variation that may occur in water levels, soil properties and the geology in different areas.

Calculating the pollution migration with seepage velocity gave a good indication of how far the contamination can migrate within the aquifer from the pollution sources to the hydrocensus boreholes. It indicated that there is no risk of the contamination reaching the hydrocensus boreholes even when a worst case scenario was initiated. One of the major factors indicating that there is no risk of the contamination reaching the hydrocensus

boreholes is the fact that these boreholes are located behind a water divide from the pollution sources when the water level contours (Figure 39) were taken into consideration.

It was also assessed whether the ash stack has an influence on the water quality of the Schoongezicht and Leeuwfontein spruit and concluded that high rainfall events are not likely to influence the water quality of the Schoongezicht spruit via surface runoff.

6.1 RECOMMENDATIONS

At first it is of absolute importance to evaluate the groundwater qualities of the monitoring boreholes in the study area. A hydrocensus study has to be conducted to identify other groundwater users in the study area and evaluate the groundwater qualities of these “unpolluted” boreholes. The water qualities of these hydrocensus boreholes could be compared with the monitoring borehole to evaluate if and to what extent the monitoring boreholes are polluted. SANS 241 2006 Edition 6.1 can also be used to indicate if the water qualities of the monitoring boreholes are affected.

If it is found that the pollution sources e.g. coal stockyard or the ash stack, have an effect on the groundwater qualities, it is possible that these pollutants can migrate further to down gradient users. It should also be stated the use of this water, as high volumes of groundwater can be used for drinking water. A risk assessment must thus be done to identify the risk for the users of the polluted groundwater. Seepage velocity calculations and Ogata Banks can be utilised to calculate if the pollutant can reach these down gradient users within a given period. These calculations do not have to be calculated for a worst case scenario, but it is advisable, as then the risk influencing the users is not underestimated.

Backtracking can also be used from the hydrocensus boreholes to identify the catchment area if these boreholes are pumped. This will also give a good estimate whether or not water will be extracted from within the pollution source areas over a given period, indicating the volatility these boreholes have to risk of being affected.

The risk assessment should include if the pollution sources can influence any nearby streams or rivers through surface water runoff during heavy rainfall events, as this water is also being used downstream by farmers and communities. This can be done by monitoring the water qualities upstream, (before influence of pollutant) during, and downstream of the pollutants. This will indicate whether the water qualities are being affected by means of the pollutant or not.

For aquifer vulnerability, it is crucial to identify the types of soil and the geology of the unsaturated zone, as these properties will indicate the ease that the pollutant can flow from the surface to the groundwater. If the unsaturated zone consists of deep clay profiles and a matrix with a very low hydraulic conductivity, the vulnerability of the aquifer will be low. If the unsaturated zone consists of sandy soil profiles and a matrix with a high hydraulic conductivity, the aquifer vulnerability will be high. It is thus important to evaluate the unsaturated zone and the depth thereof to calculate the aquifer vulnerability.

It is more proficient to study the aquifer vulnerability of smaller areas, as the properties and the depth of the unsaturated zone can differ within larger areas. Utilising sieve analysis, it can give a good estimation of the hydraulic conductivities of the soil profiles, but it is recommended that sieve analysis must not only be done for the soil profiles collected by means of auger hole drilling. Samples of the geology in the unsaturated zone should also be tested with sieve analysis to calculate the hydraulic conductivity of the geology in the unsaturated zone. These samples can be collected by means of percussion drilling within the study area.

It is recommended to commence an aquifer vulnerability study before an area can be identified, as a possible area for dumping or storing of waste that can affect the groundwater. If dirty water dams should be built in an area with high aquifer vulnerability, the dams must be lined to prevent dirty water from leaching to the groundwater. It is recommended to rather prevent the groundwater from being polluted in an area with high aquifer vulnerability, than rehabilitating the polluted groundwater resources.

7 REFERENCES

- AILUN, Y., KANG, R., XINGMIN, Z., XU, H., HANHUA, Z., MIAOHAN, S., HONGYUAN, T and FEI, L (2010). The True Cost of Coal-An Investigation into Coal Ash in China.
- DUNNE, T., and LEOPOLD, L.B., (1987). Water Environmental Planning, San Francisco, W.H. Freeman and Co.
- ECOBA, By-products of coal-fired power stations, Production and utilisation in ECOBA Member Countries,. 1992-1996.
- FOSTER, S.S.D. (1998). Groundwater Recharge and Pollution Vulnerability of British Aquifers: a Critical review. In: ROBINS, N.S. (Ed.), Groundwater Pollution, Aquifer Recharge and Vulnerability. Geological Society, London, Special Publications, vol. 130, pp. 7–22.
- FOURIE, A.B. and BLIGHT, G.E (1999). Tailings and mine waste p 189.
- FOURIE, F (2004). RVN 329.9/565. Matla routine monitoring phase 35 p35.
- HAYNES, R.J (2009). Journal of environmental management. p 45.
- HODGSON, FDI.and KRANTZ RM. (1998). Groundwater Quality Deterioration in the Olifants River Catchment above the Loskop Dam with Specialized Investigation in the Witbank Dam Sub-Catchment.-WRC Report No.-291/1/98.
- JALA, S., GOYAL D. (2006). Fly Ash as a Soil Ameliorant for Improving Crop Production—a review. Bioresource Technology 97, 1136–1147.
- KYTE, WS., CRAWLEY, D., de, LANNOY, R., JENSEN, SA., KRAUS, F., SRIEGER, S., LAWLOR, G., MADEIRA, G., MIHALY, B., PETERS, F., PLAZA, V., PROKOPEC, L., ROMANO, F., SIMON, O., SIRGADO, P., SOETENS, E., SIOMAKALLIO, H., SZABO, J., VAN DER POEL, M., WAYGOOD, S.and SCOWCROFT, J.F. (1999). Fly Ash from Coal Fired Power Plants, a Non-Hazardous Material.
- LIU, G., ZHANG, H., GAO, L., ZHENG, L., PENG, Z. (2004). Petrological and mineralogical characterizations and chemical composition of coal ashes from power plants in Yanzhou mining district, China. Fuel Processing Technology 85, 1635–1646.

MORENO, N., QUEROL, X., ANDRES, J.M., STANTON, K., TOWLER, M., NUGTEREN, H., et al., 2005. Physico-chemical characteristics of European pulverized coal combustion fly ashes. *Fuel* 84, 1351–1363.

Muller, J. (1994). Geohydrological evaluation for Kendal Power Station solid waste disposal site permit application. ref 10051.

NESS, J., HEELEY, P. (2007). Production and handling of coal combustion products. In: Gurba, L.W., Heidrich, C., Ward, C.R. (Eds.), *Coal Combustion Products Handbook*. Cooperative Research Centre for Coal in Sustainable Development, Brisbane.

ROBINS, N.S., CHILTON, P.J. and COBBING, J.E. (2006). *Adapting Existing Experience with Aquifer Vulnerability and Groundwater Protection for Africa*.

STAATS, S. (2009). RVN 569.3/1056. Groundwater plume investigation hydrological and geohydrological baseline study.

THIRUMALAIIVASAN, D. (2001). *Aquifer Vulnerability Assessment using Analytic Hierarchy Process and GIS for upper Palar Watershed*.

TROSKIE, K. (2005). GCS ref. NIN.05/469.

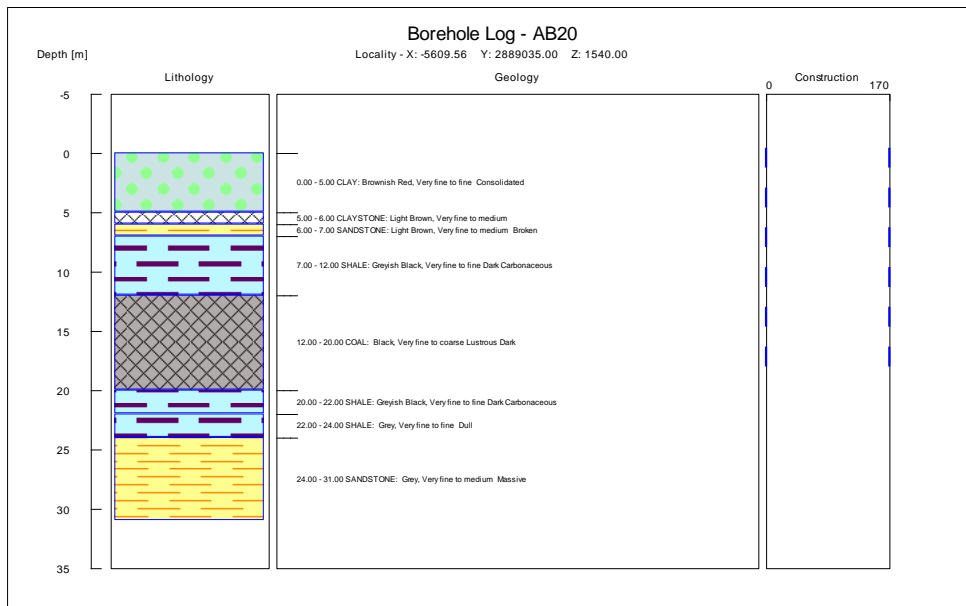
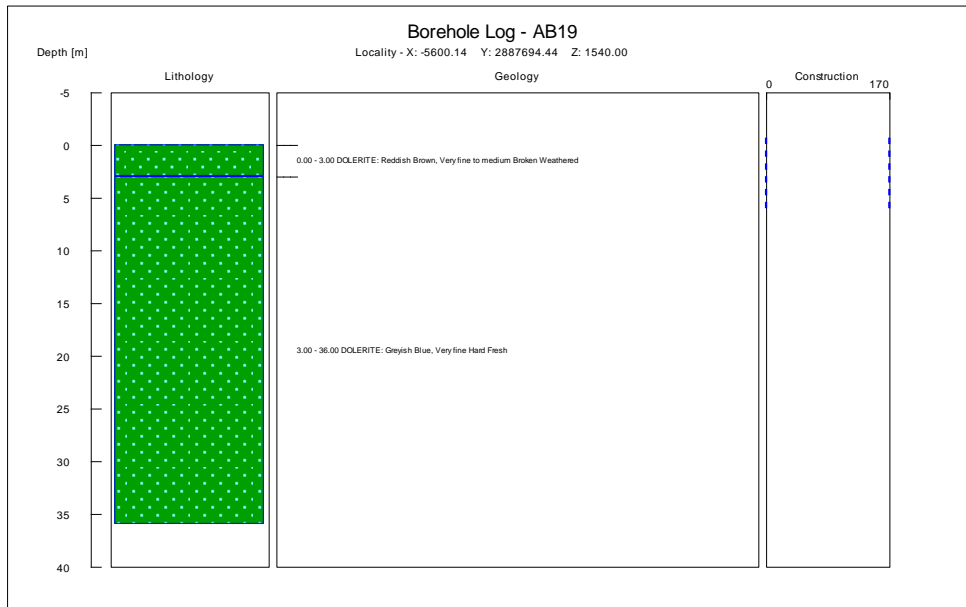
WARD, C.R., FRENCH, D., JANKOWSKI, J., DUBIKOVA, M., LI, Z. and RILEY, K.W. (2009). *International Journal of Coal Geology*.

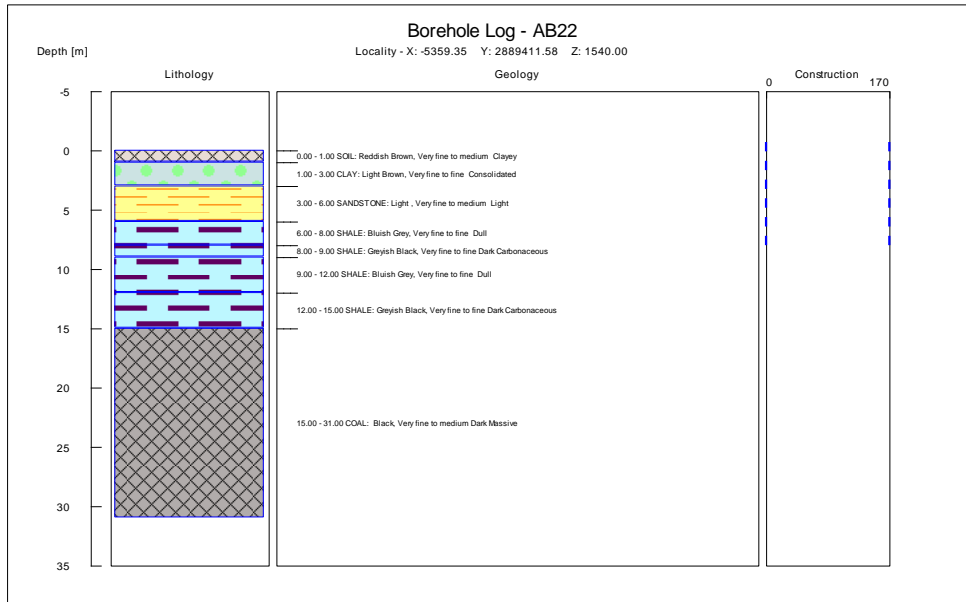
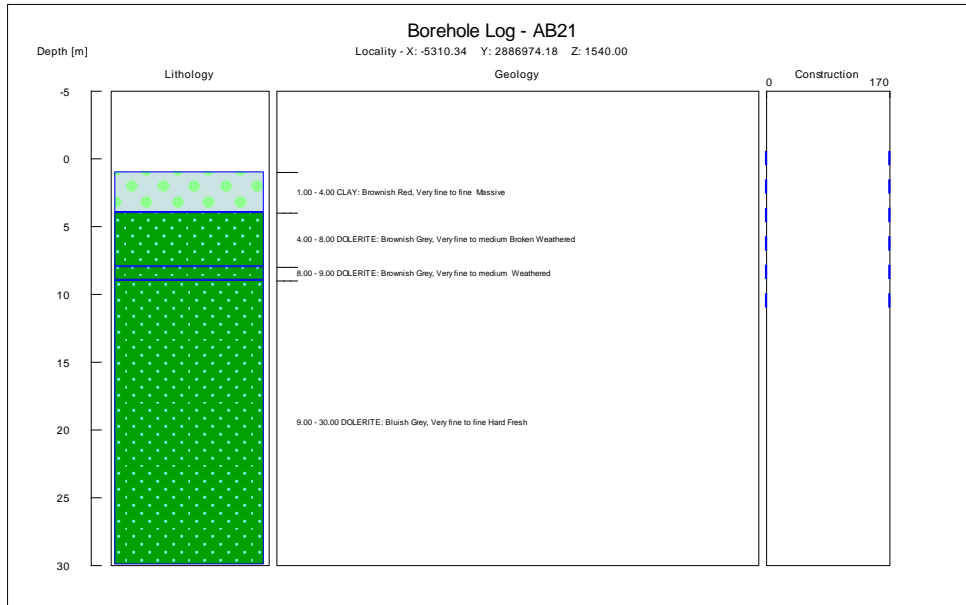
<http://www.sourcewatch.org> (Accessed on November 24th 2010)

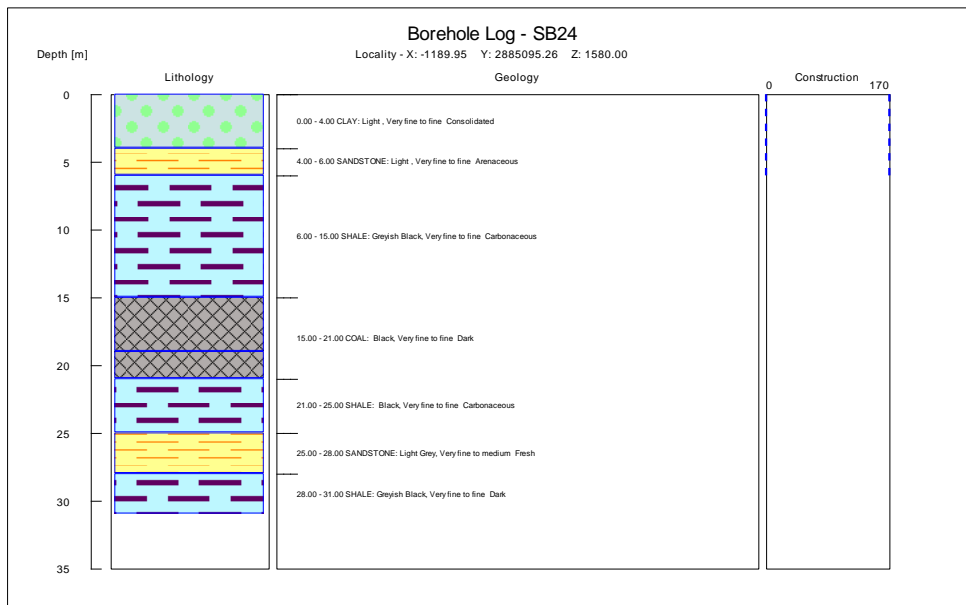
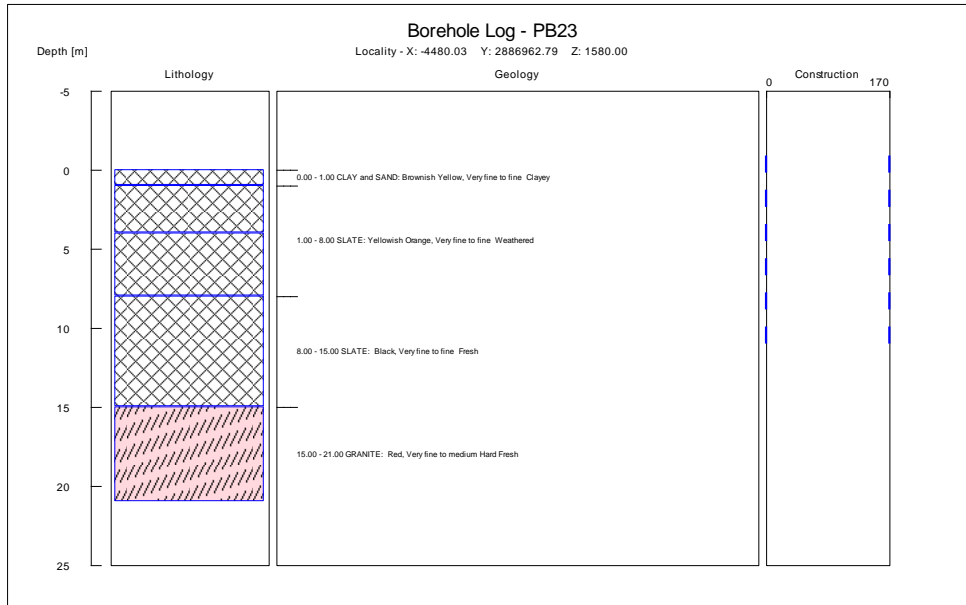
8 APPENDICES

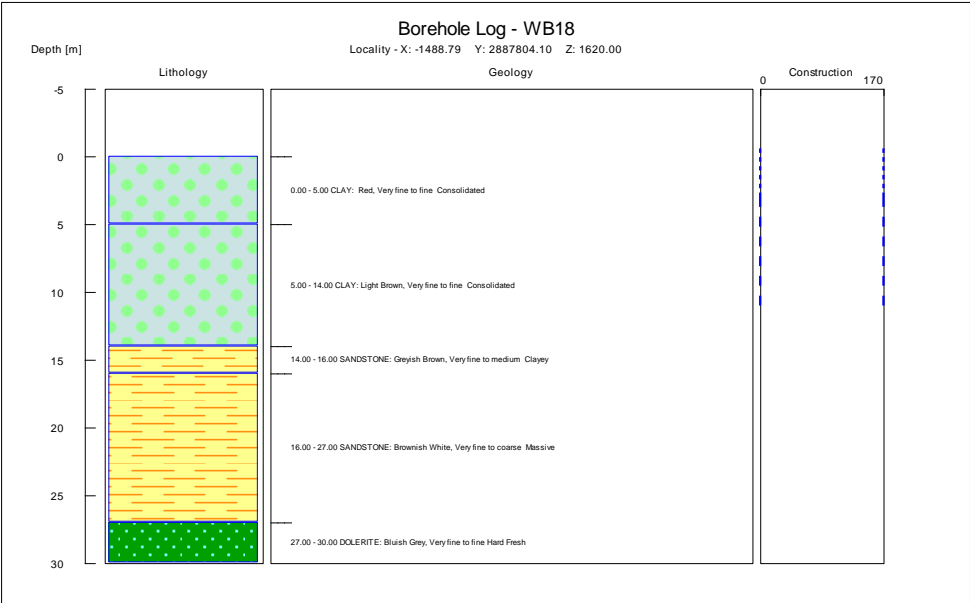
Appendix A to G are supplied on disk.

Appendix A Newly Drilled Boreholes



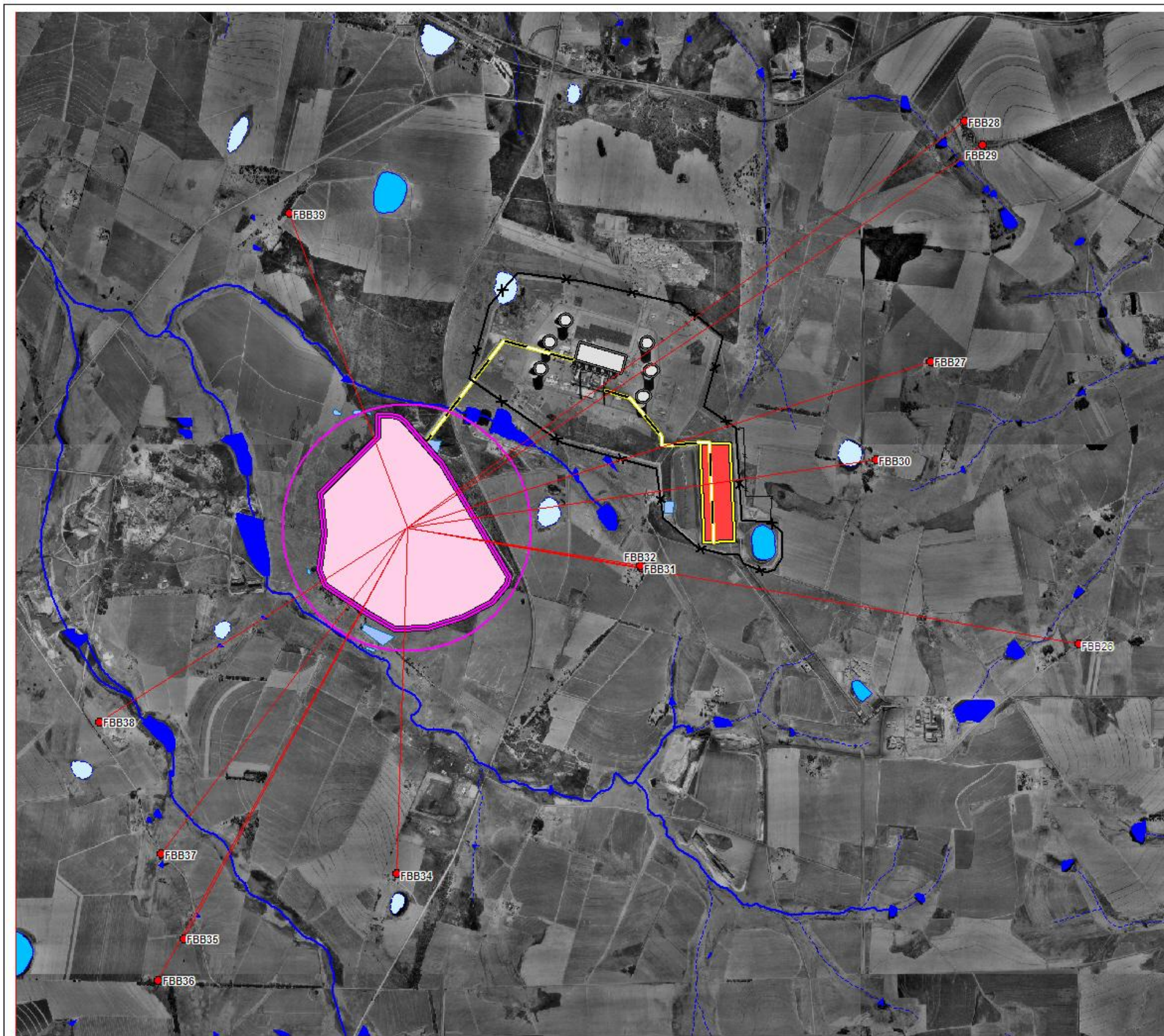




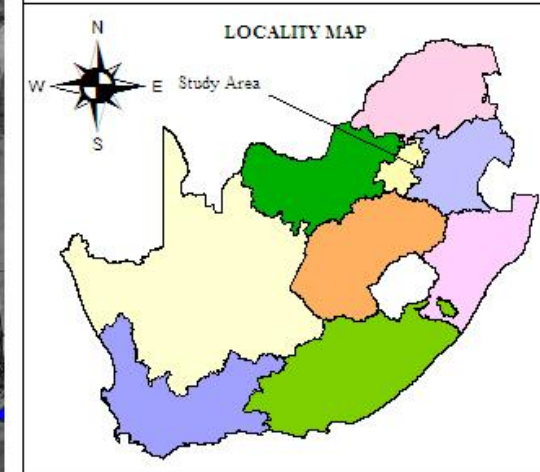


APPENDIX B

Pollution Sources and gradient lines.

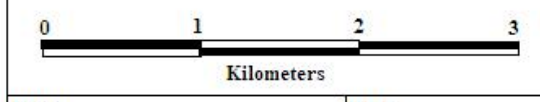


Kendal Power Station

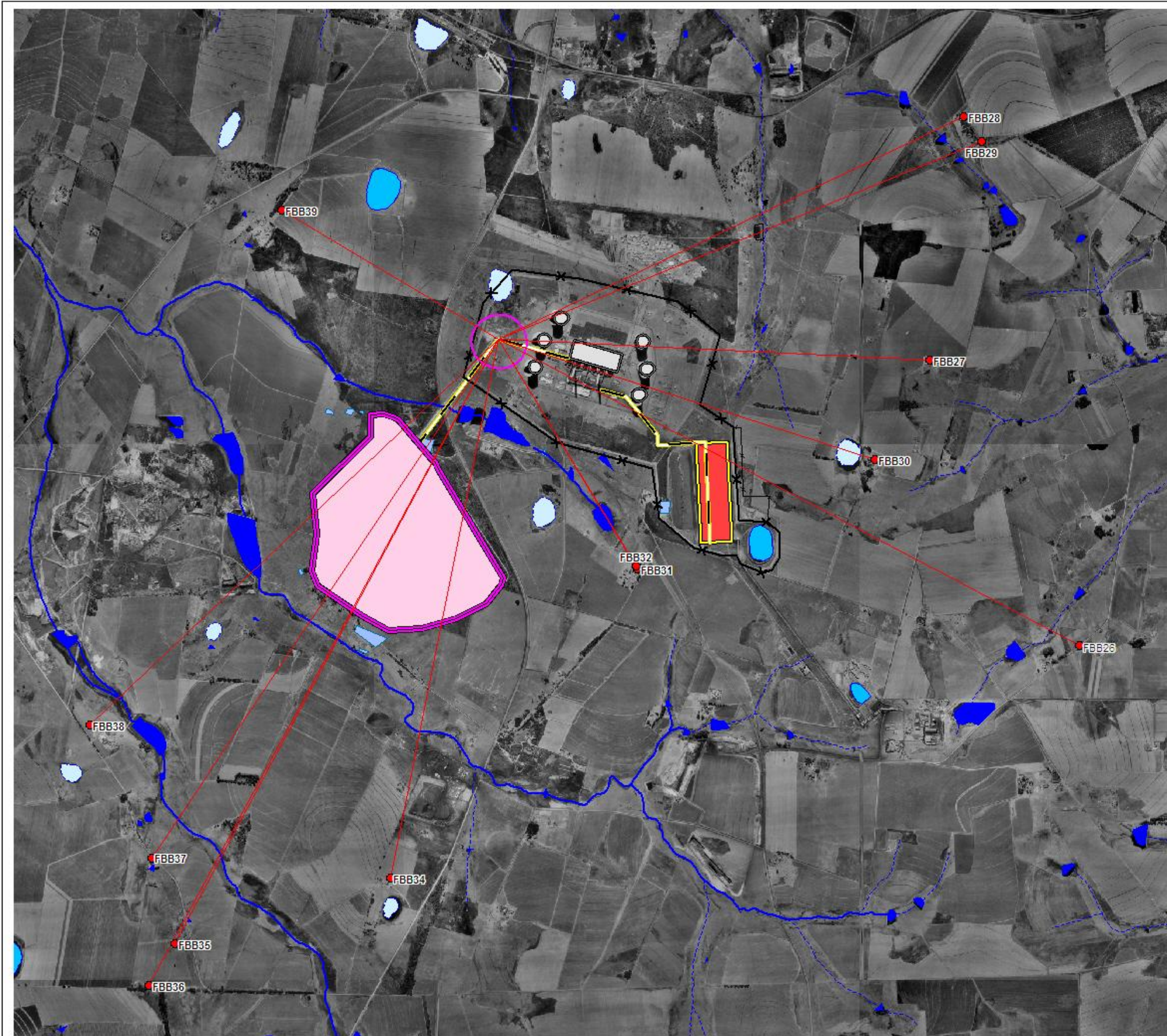


LEGEND

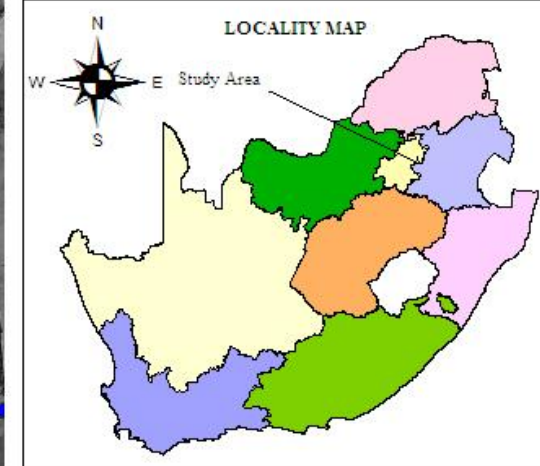
- Hydrocensus Boreholes
- Pollution Source
- Coal Stockyard
- Ash Stack



INFO	
Pollution Source Identification	DATE 2011
GEOGRAPHIC COORDINATE SYSTEM	
Universal Transfer Mercator WGS84	SPHEROID LO 29
PROJECT TITLE	
Baseline Study on Kendal Power Station	
MAP TITLE	
Pollution Source (Ash Stack)	

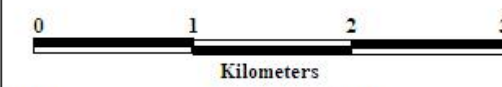


Kendal Power Station

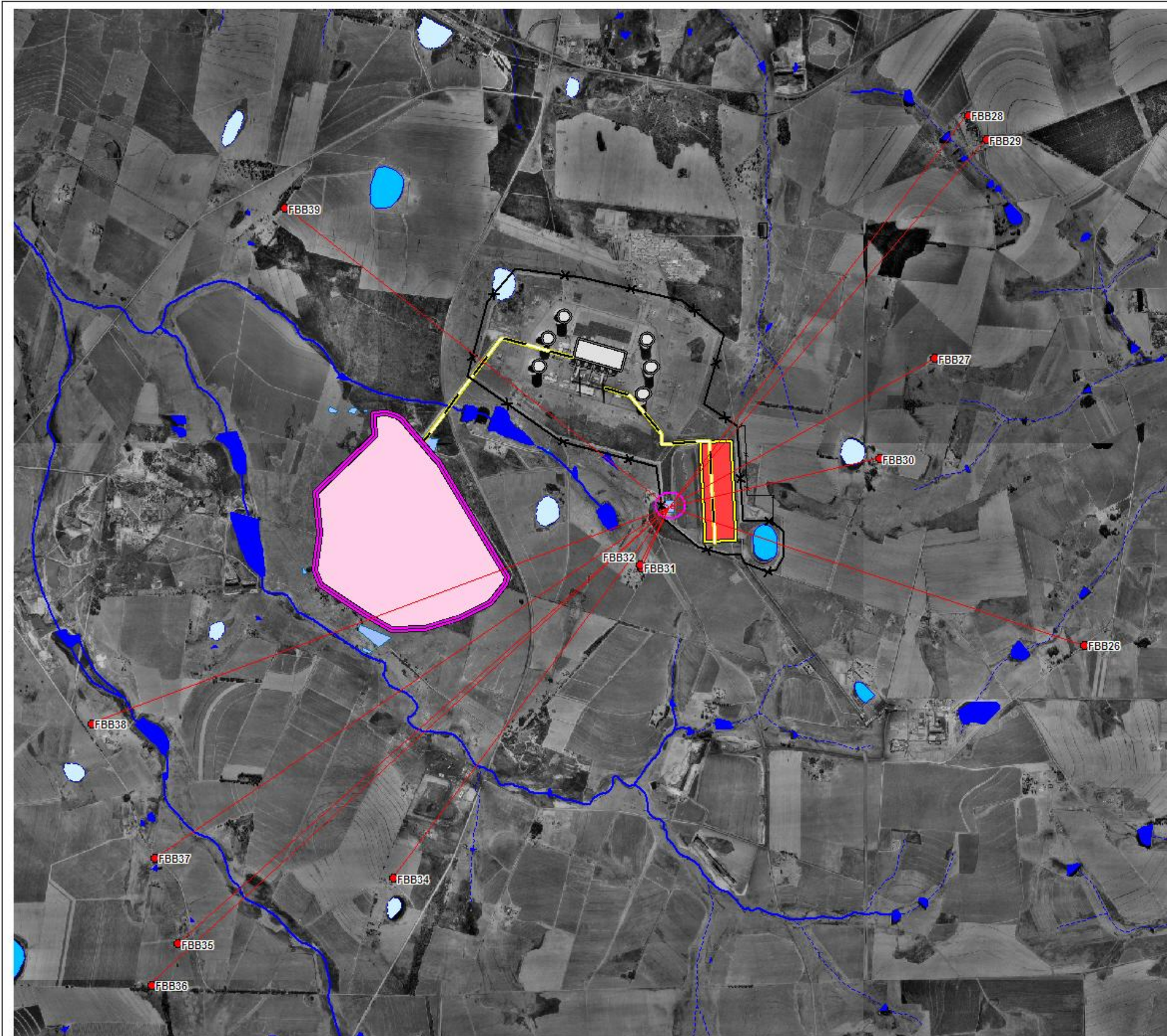


LEGEND

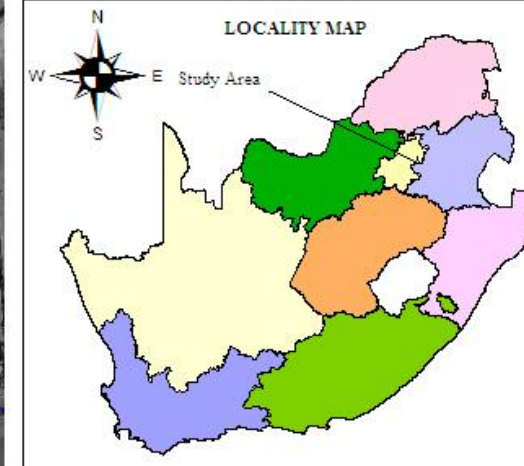
- Hydrocensus Boreholes
- Pollution Distance
- Pollution Source
- Coal Stockyard
- Ash Stack



INFO	DATE
Pollution Source Identification	2011
GEOGRAPHIC COORDINATE SYSTEM	SPHEROID
Universal Transfer Mercator WGS84	LO 29
PROJECT TITLE	
Baseline Study on Kendal Power Station	
MAP TITLE	
Pollution Source (Emergency Stack)	

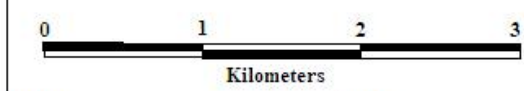


Kendal Power Station



LEGEND

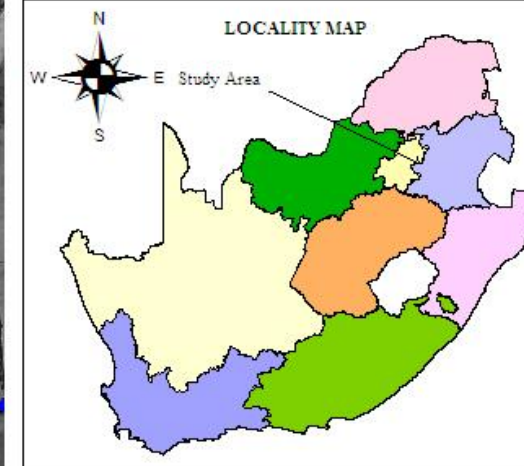
- Hydrocensus Boreholes
- Pollution Distace
- Pollution Source
- Coal Stockyard
- Ash Stack



INFO Pollution Source Identification	DATE 2011
GEOGRAPHIC COORDINATE SYSTEM Universal Transfer Mercator WGS84	SPHEROID LO 29
PROJECT TITLE Baseline Study on Kendal Power Station	
MAP TITLE Pollution Source (Coal Stockyard Settling Dam)	

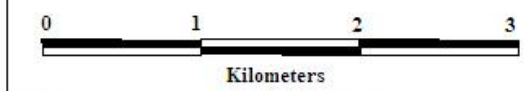


Kendal Power Station



LEGEND

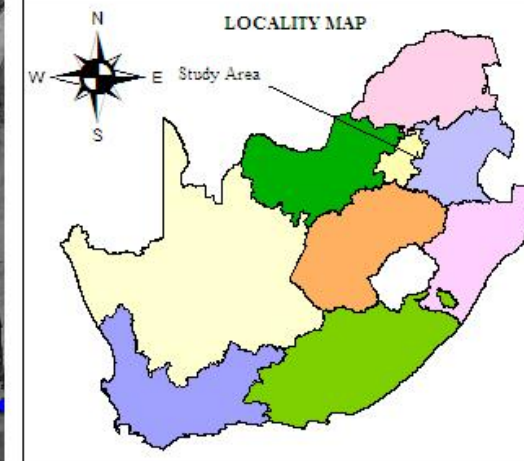
- Hydrocensus Boreholes
- Pollution Distance
- Pollution Source
- Coal Stockyard
- Ash Stack



INFO	DATE
Pollution Source Identification	2011
GEOGRAPHIC COORDINATE SYSTEM	SPHEROID
Universal Transfer Mercator WGS84	LO 29
PROJECT TITLE	
Baseline Study on Kendal Power Station	
MAP TITLE	
Pollution Source (Schoongezicht Spruit)	

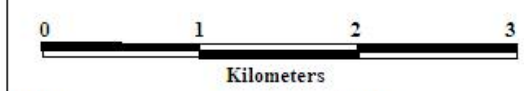


Kendal Power Station

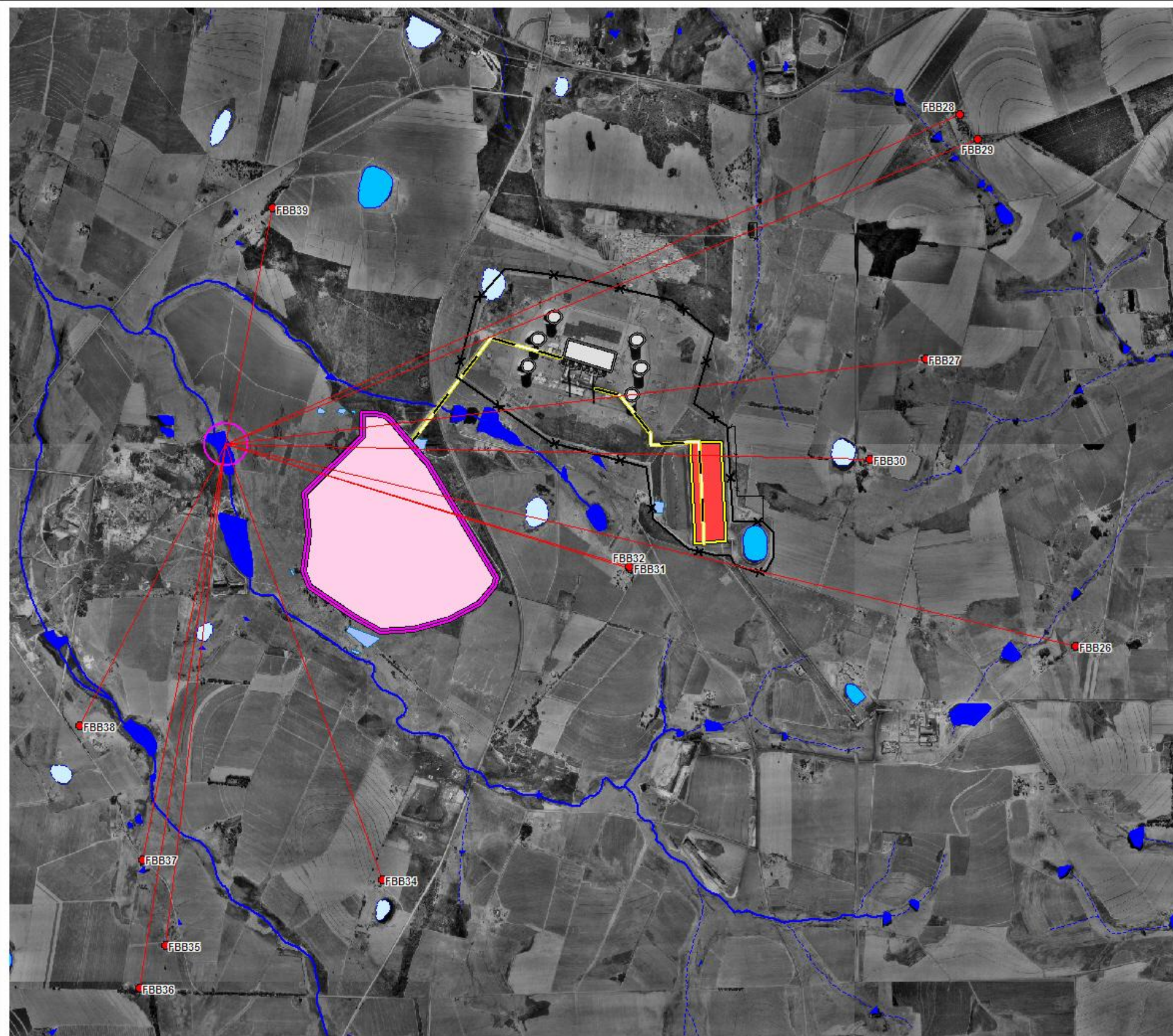


LEGEND

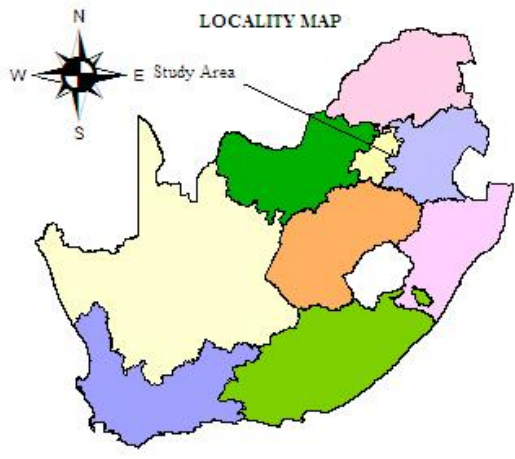
- Hydrocensus Boreholes
- Pollution Distance
- Pollution Source
- Coal Stockyard
- Ash Stack



INFO	DATE
Pollution Source Identification	2011
GEOGRAPHIC COORDINATE SYSTEM	SPHEROID
Universal Transfer Mercator WGS84	LO 29
PROJECT TITLE	
Baseline Study on Kendal Power Station	
MAP TITLE	
Pollution Source (Dirty Water Dam)	

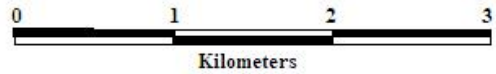


Kendal Power Station

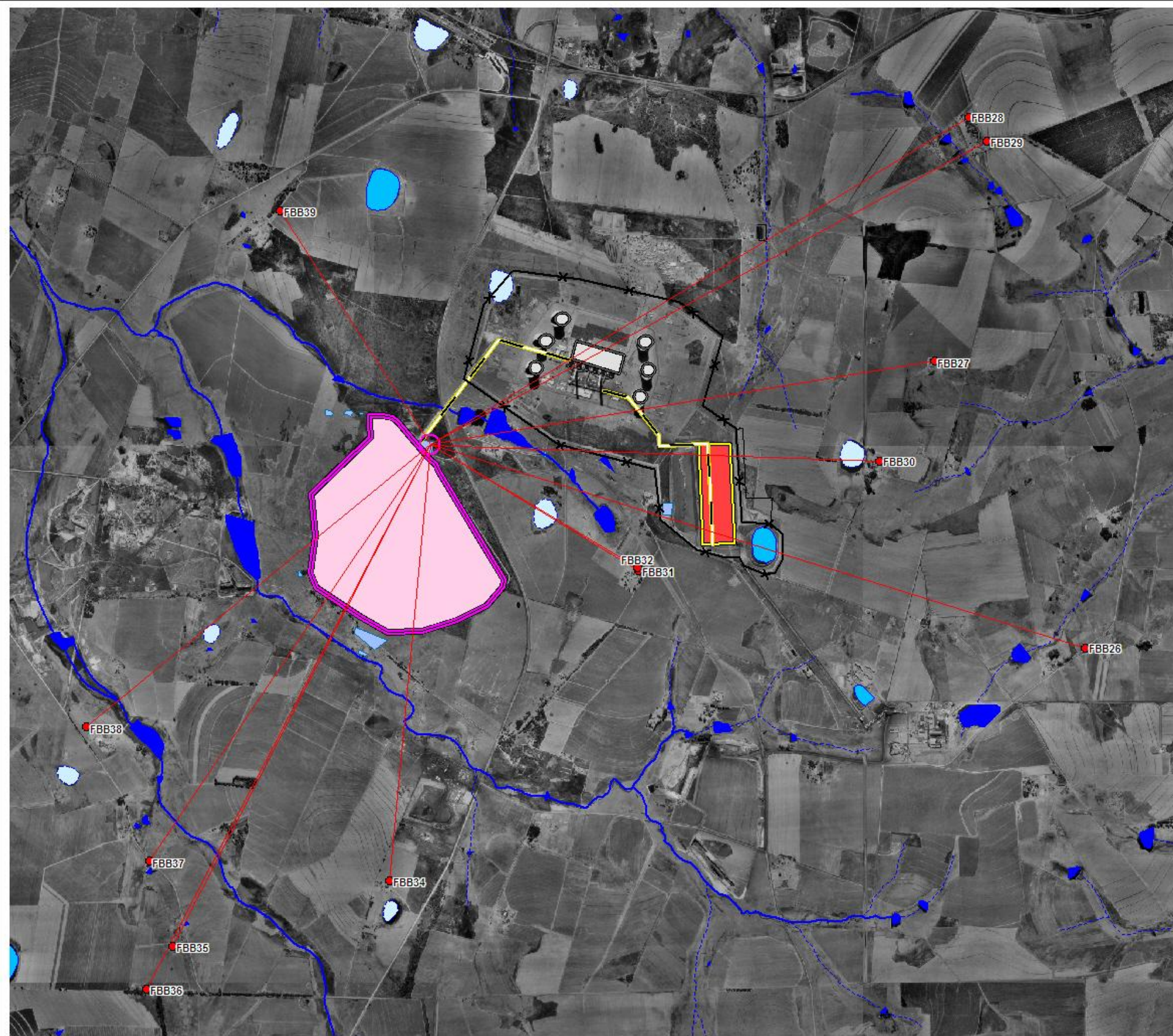


LEGEND

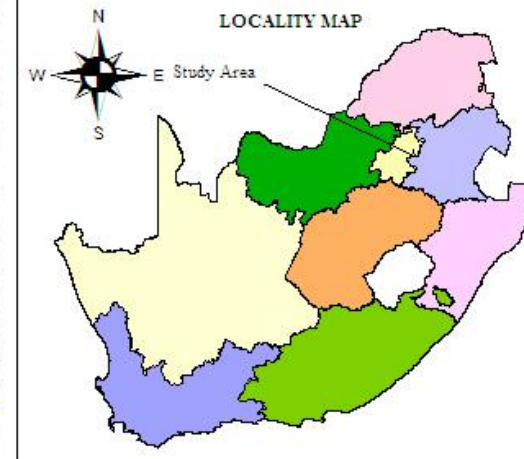
- Hydrocensus Boreholes
- Pollution Distance
- Pollution Source
- Coal Stockyard
- Ash Stack



INFO Pollution Source Identification	DATE 2011
GEOGRAPHIC COORDINATE SYSTEM Universal Transfer Mercator WGS84	SPHEROID LO 29
PROJECT TITLE Baseline Study on Kendal Power Station	
MAP TITLE Dam West of Ash Stack	

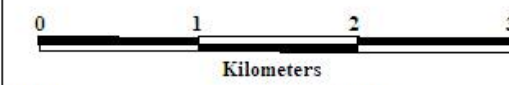


Kendal Power Station

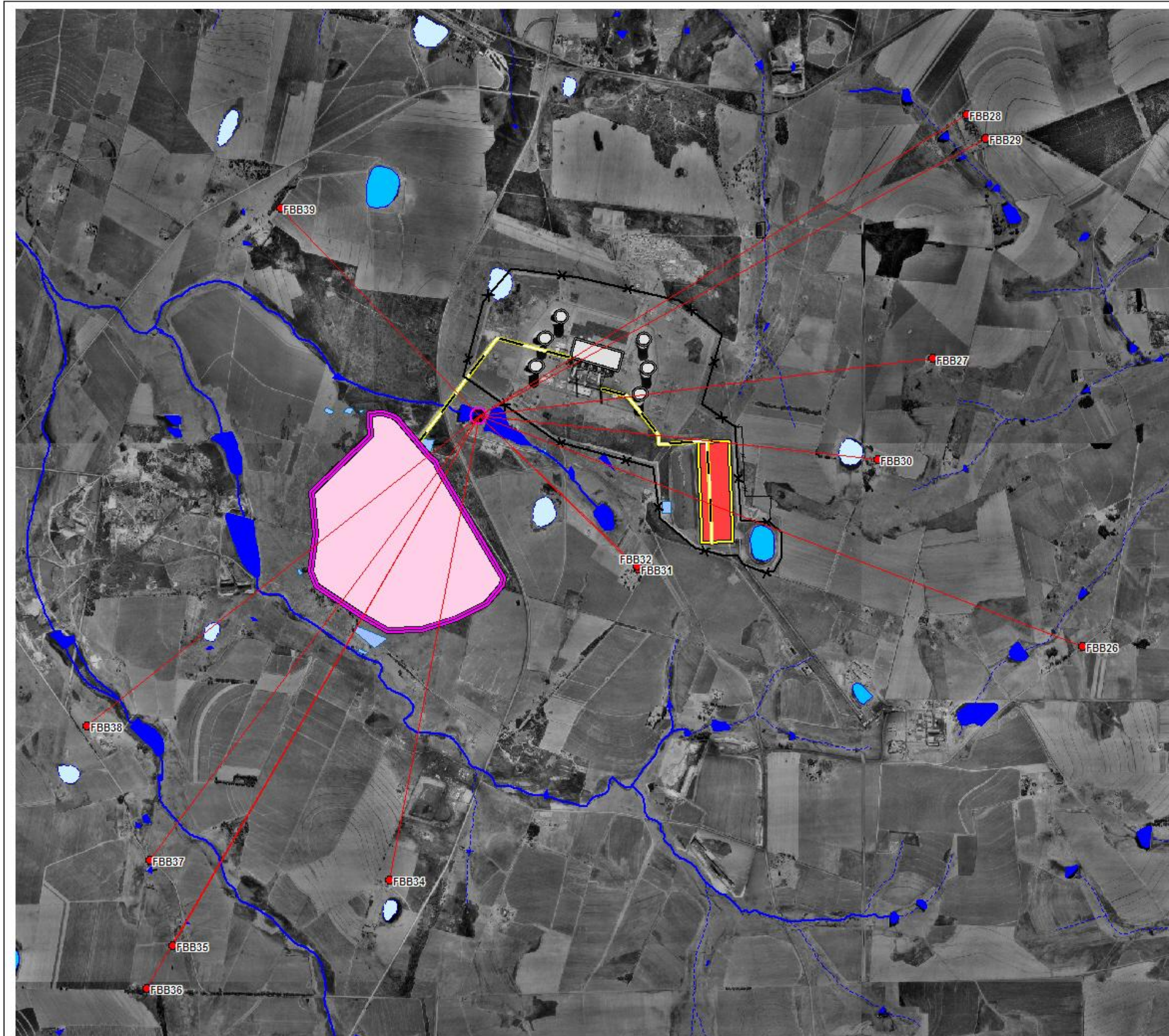


LEGEND

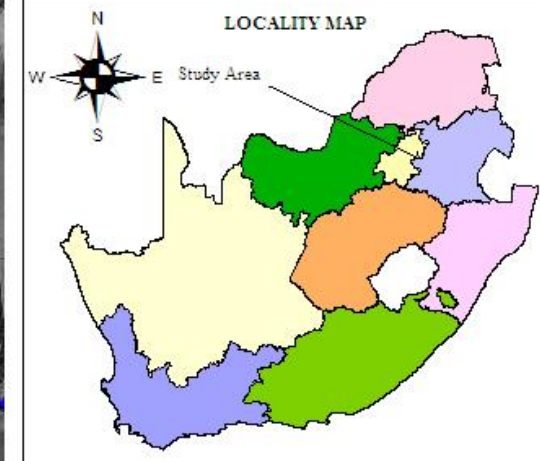
- Hydrocensus Boreholes
- Pollution Distance
- Pollution Source
- Coal Stockyard
- Ash Stack



INFO	DATE
Pollution Source Identification	2011
GEOGRAPHIC COORDINATE SYSTEM	SPHEROID
Universal Transfer Mercator WGS84	LO 29
PROJECT TITLE	
Baseline Study on Kendal Power Station	
MAP TITLE	
Pollution Source (Ash Stack Settling Dam)	



Kendal Power Station



LEGEND

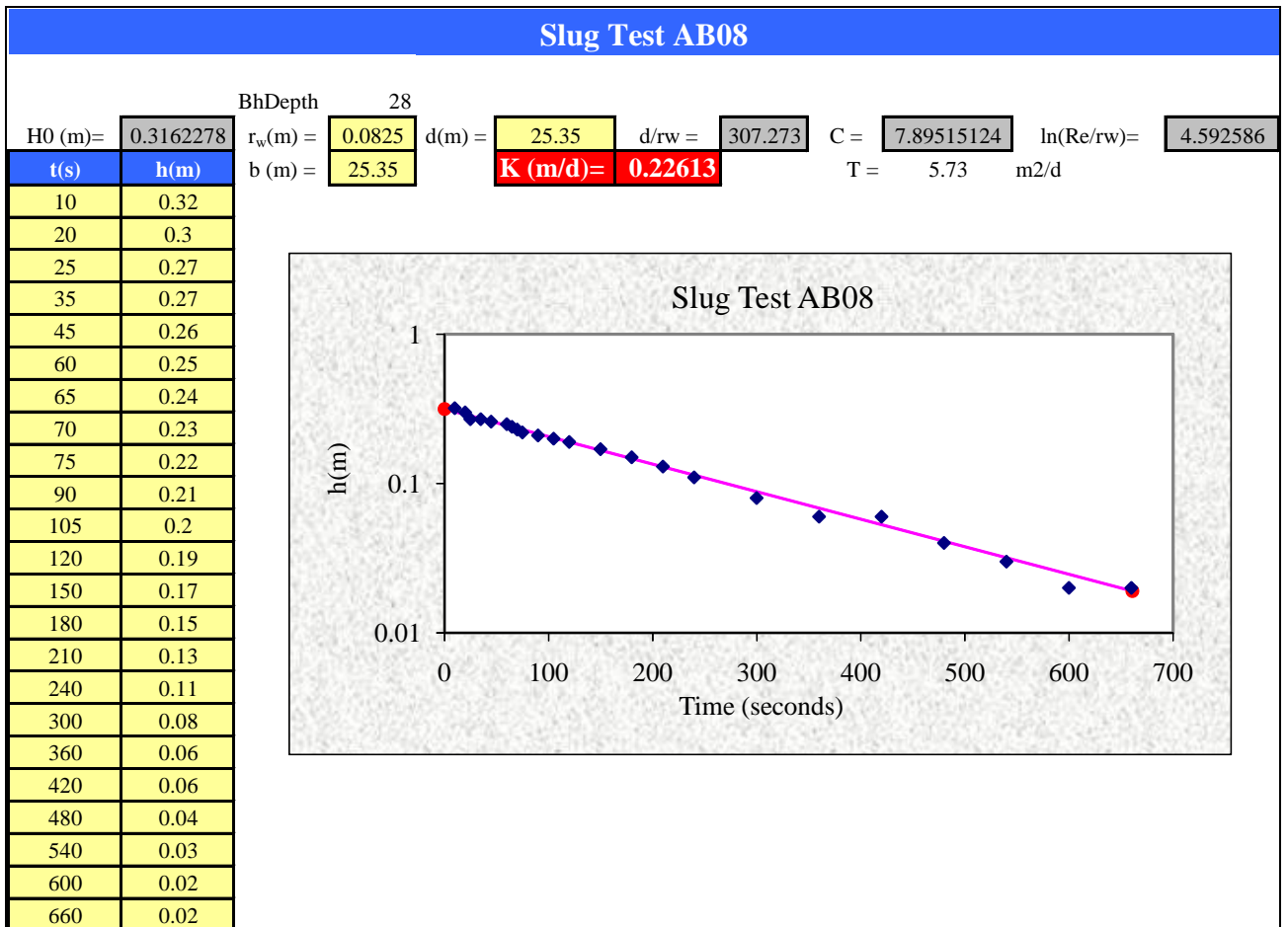
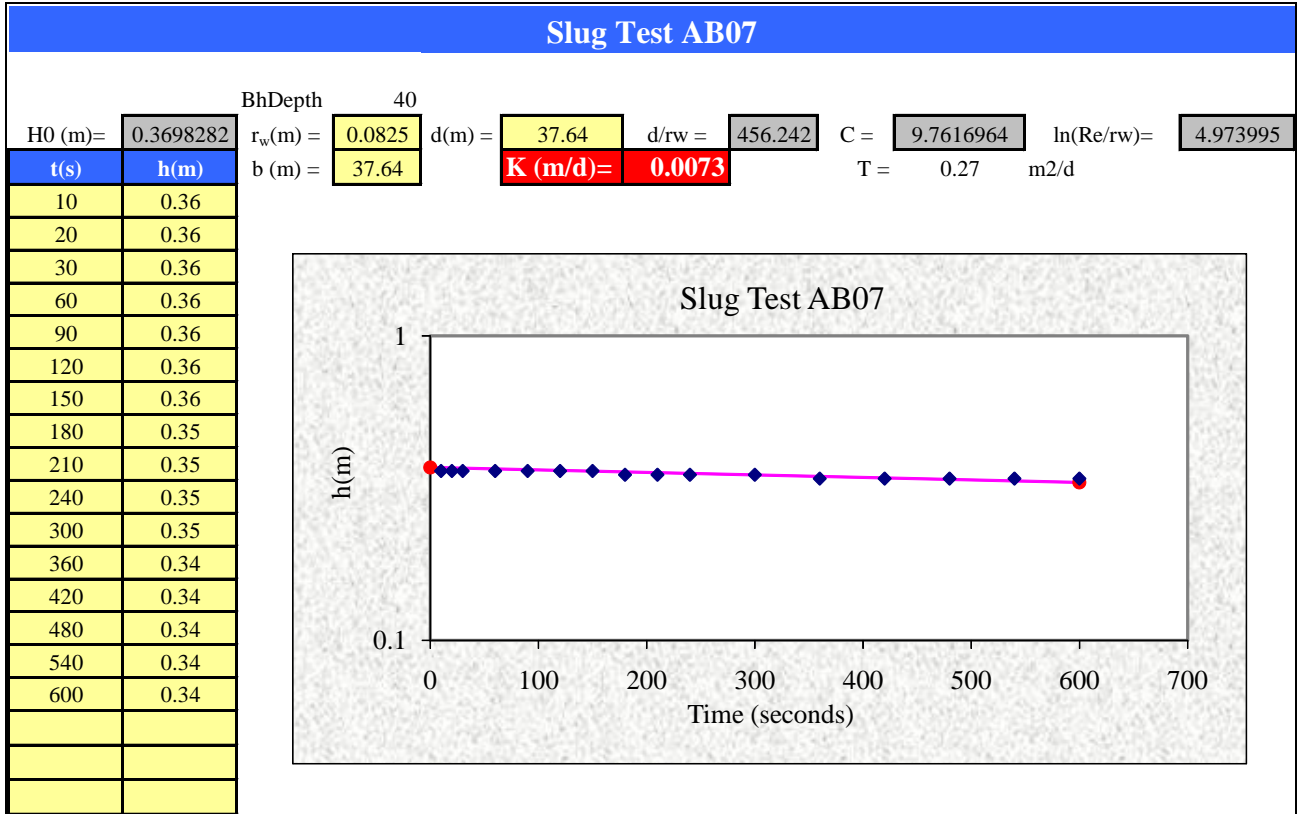
- Hydrocensus Boreholes
- Pollution Distance
- Pollution Source
- Coal Stockyard
- Ash Stack



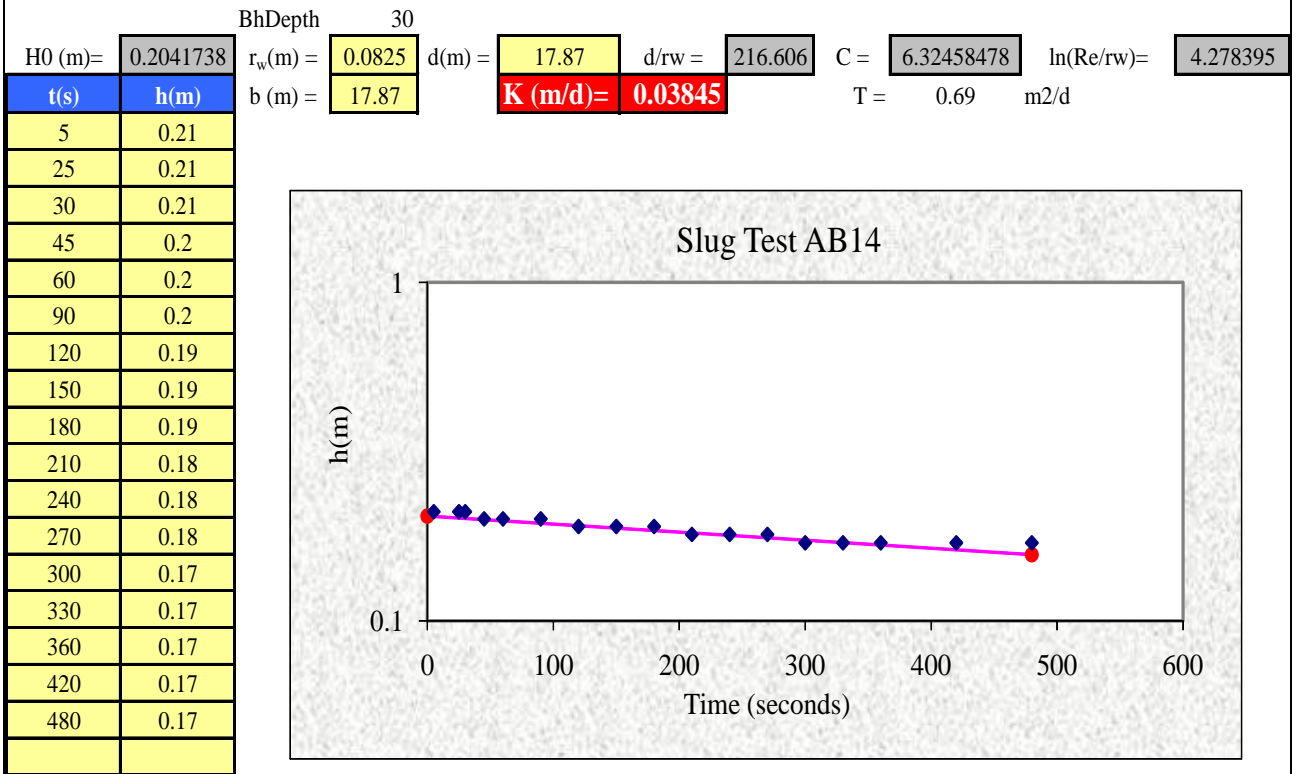
INFO	DATE
Pollution Source Identification	2011
GEOGRAPHIC COORDINATE SYSTEM	SPHEROID
Universal Transfer Mercator WGS84	LO 29
PROJECT TITLE	
Baseline Study on Kendal Power Station	
MAP TITLE	
Pollution Source (Settling Dam)	

APPENDIX C

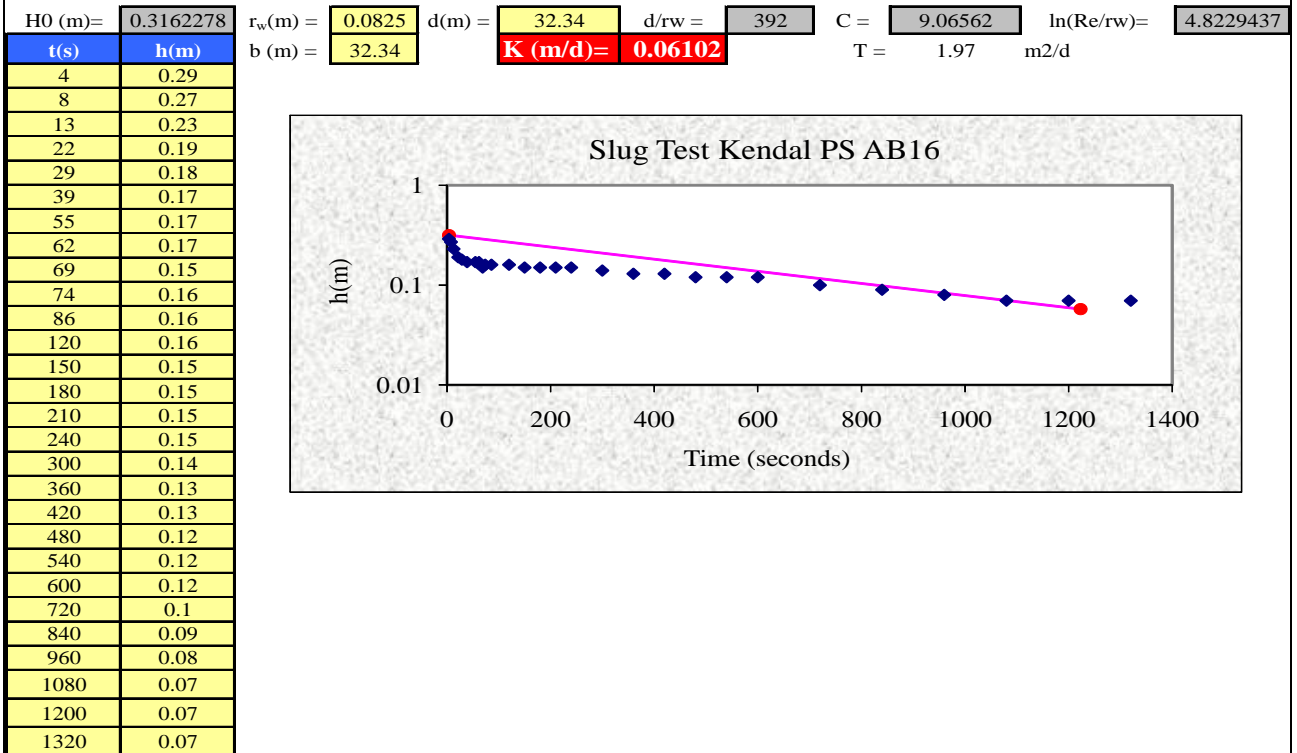
Slug Tests



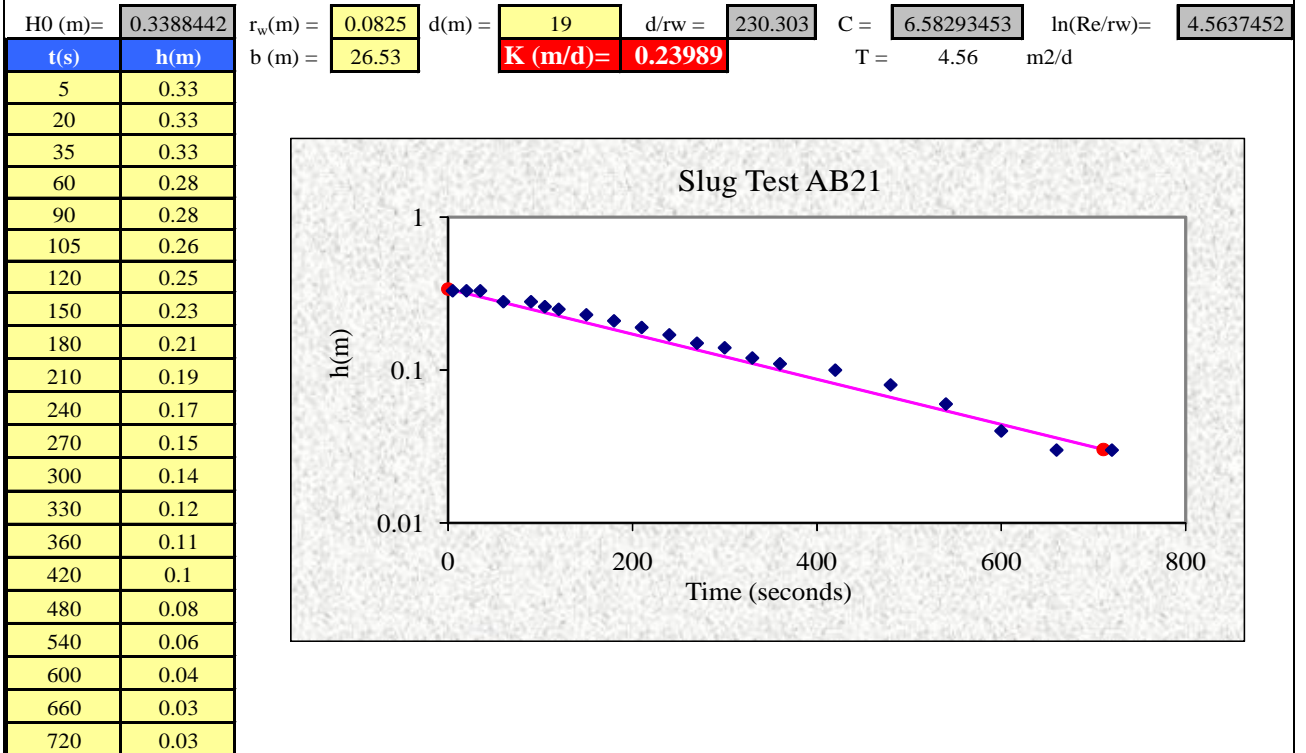
Slug Test AB14



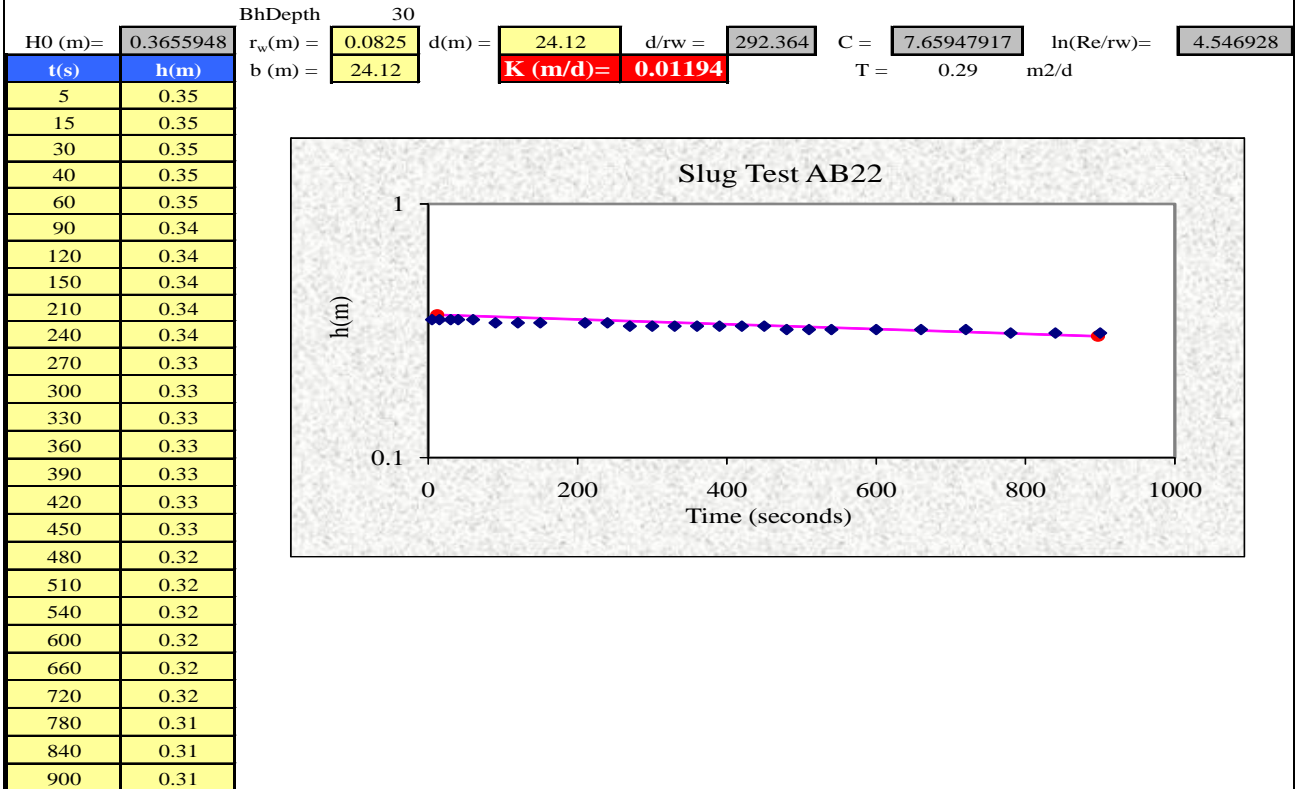
Slug Test Ab16



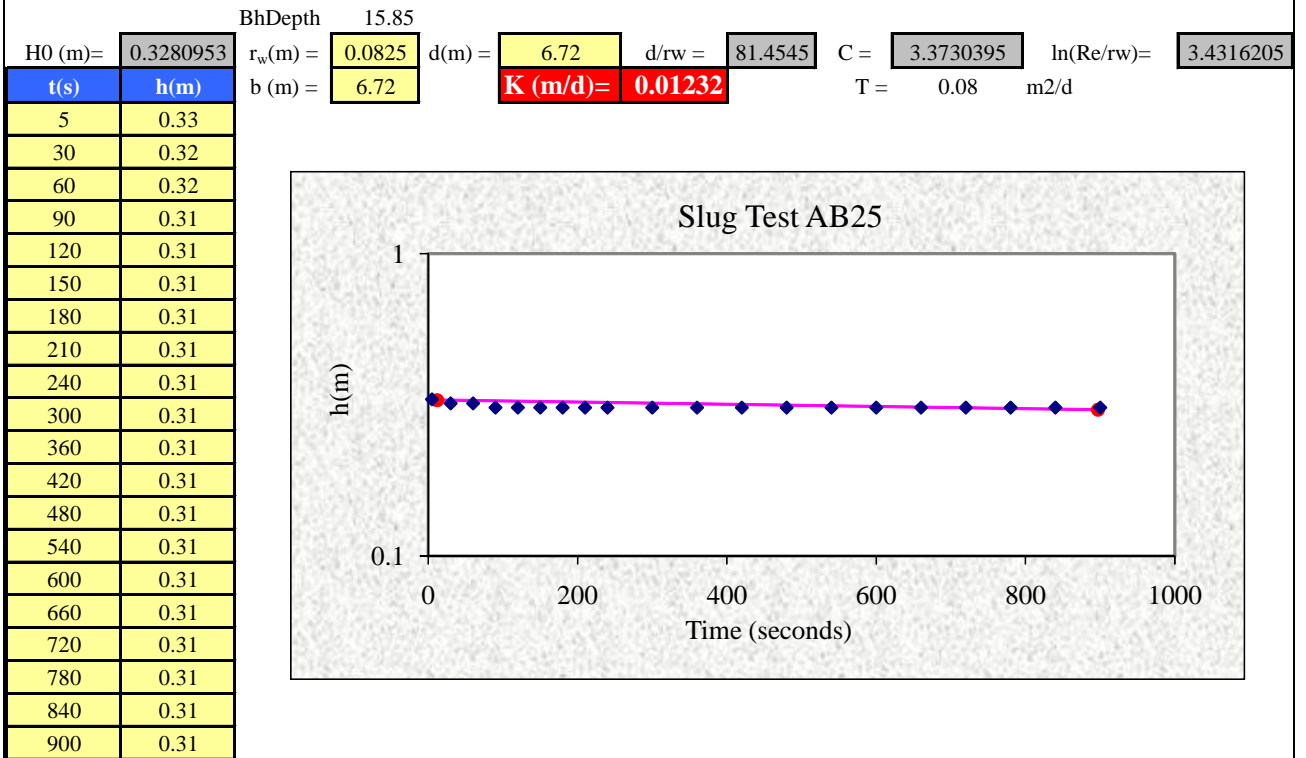
Slug Test AB21



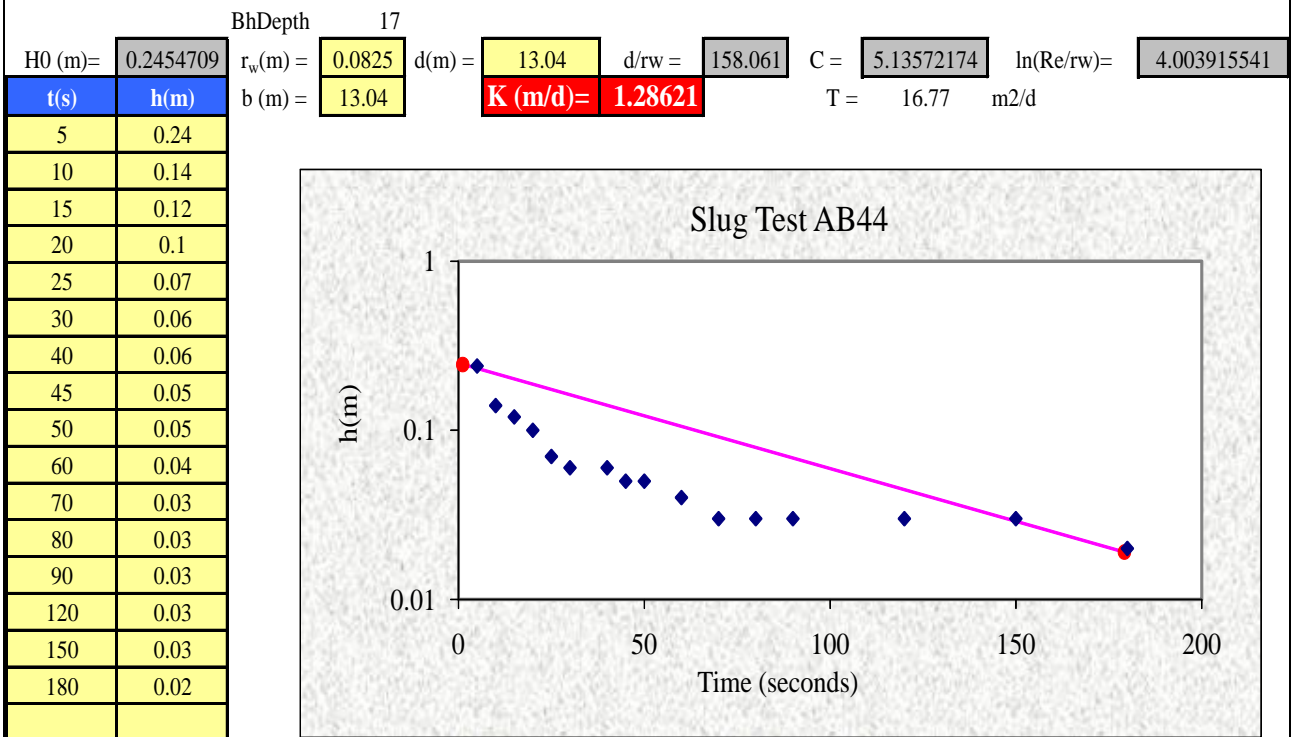
Slug Test AB22



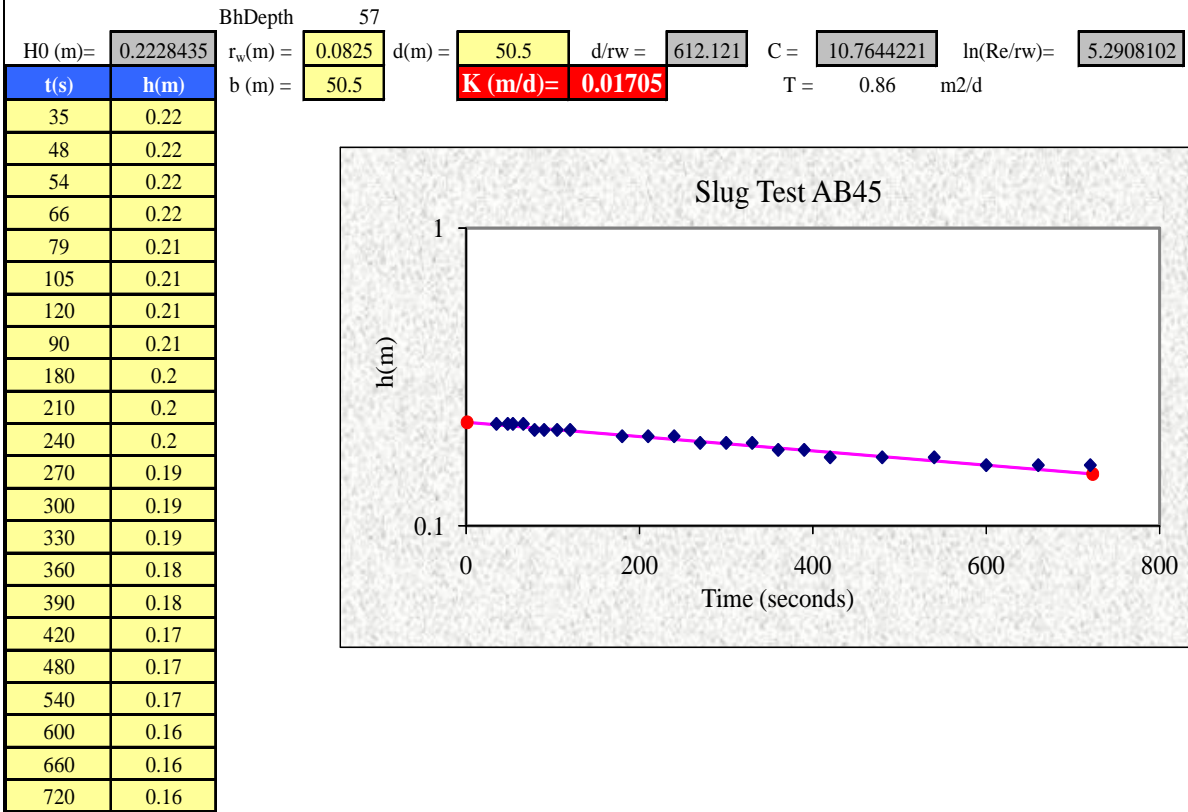
Slug Test AB25



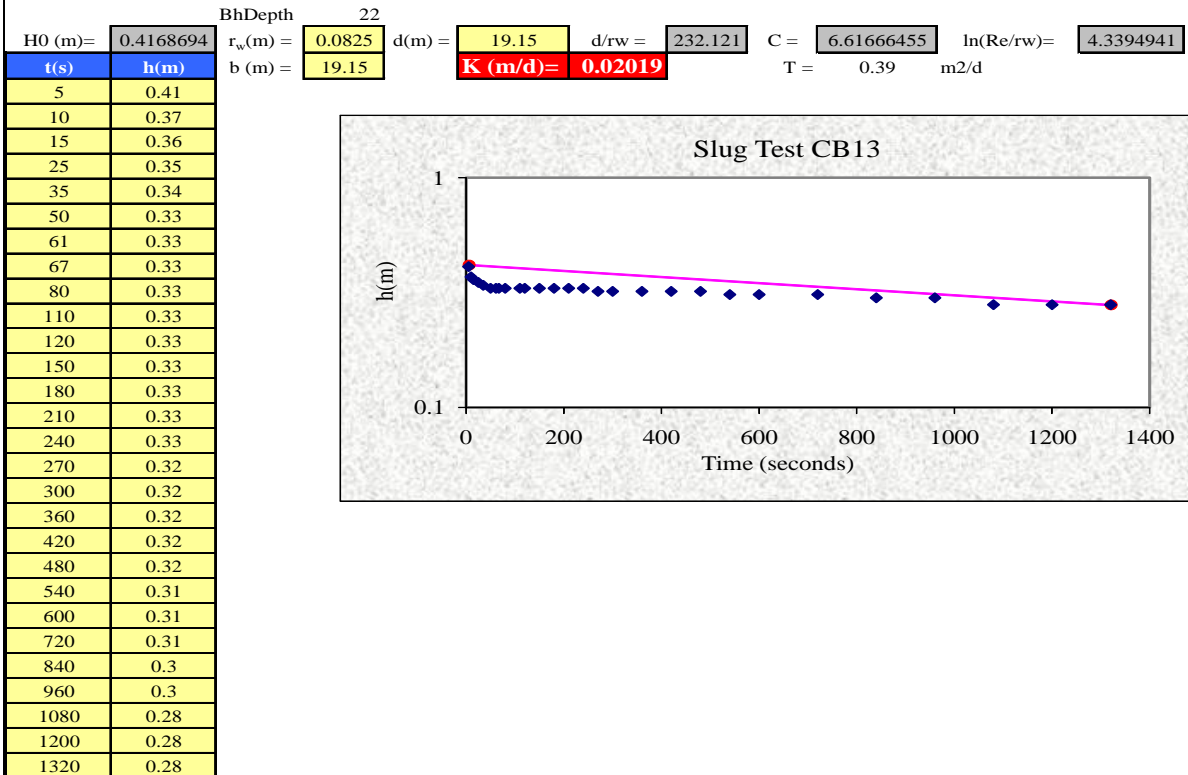
Slug Test AB44



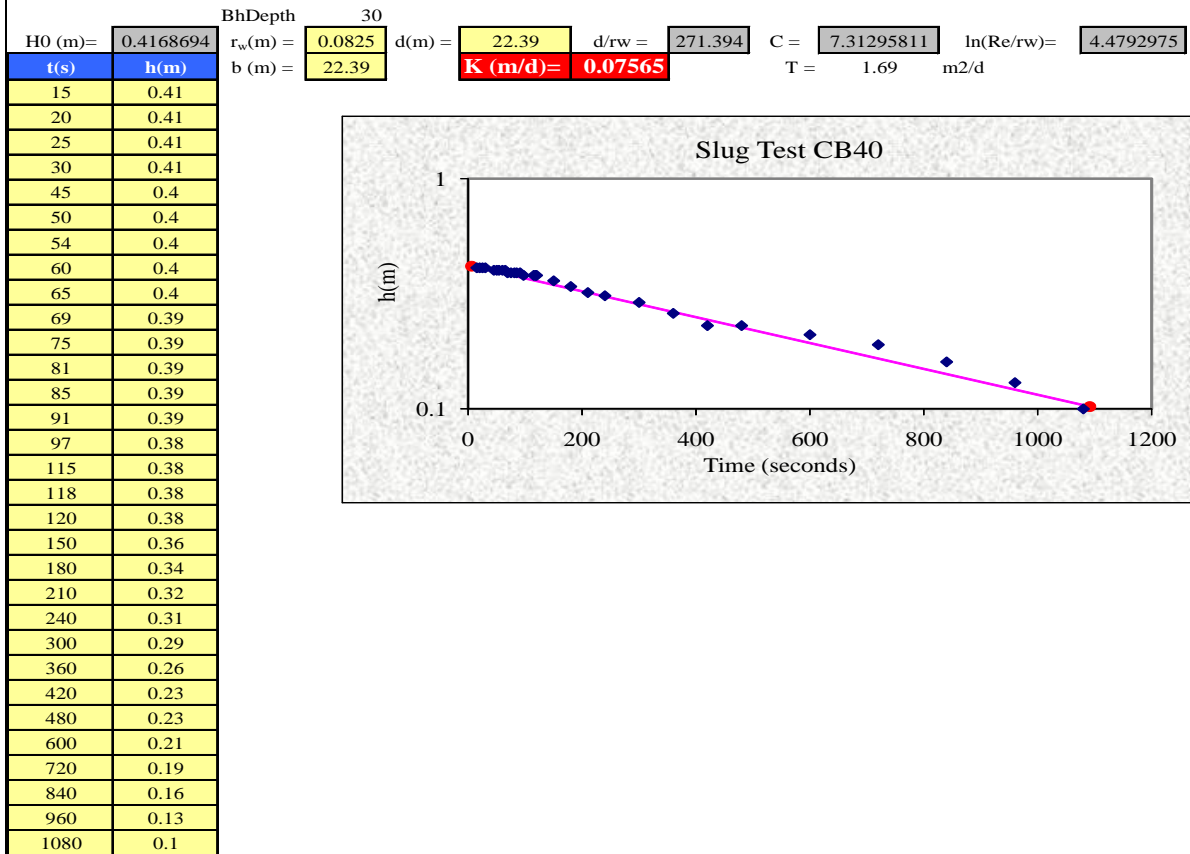
Slug Test AB45



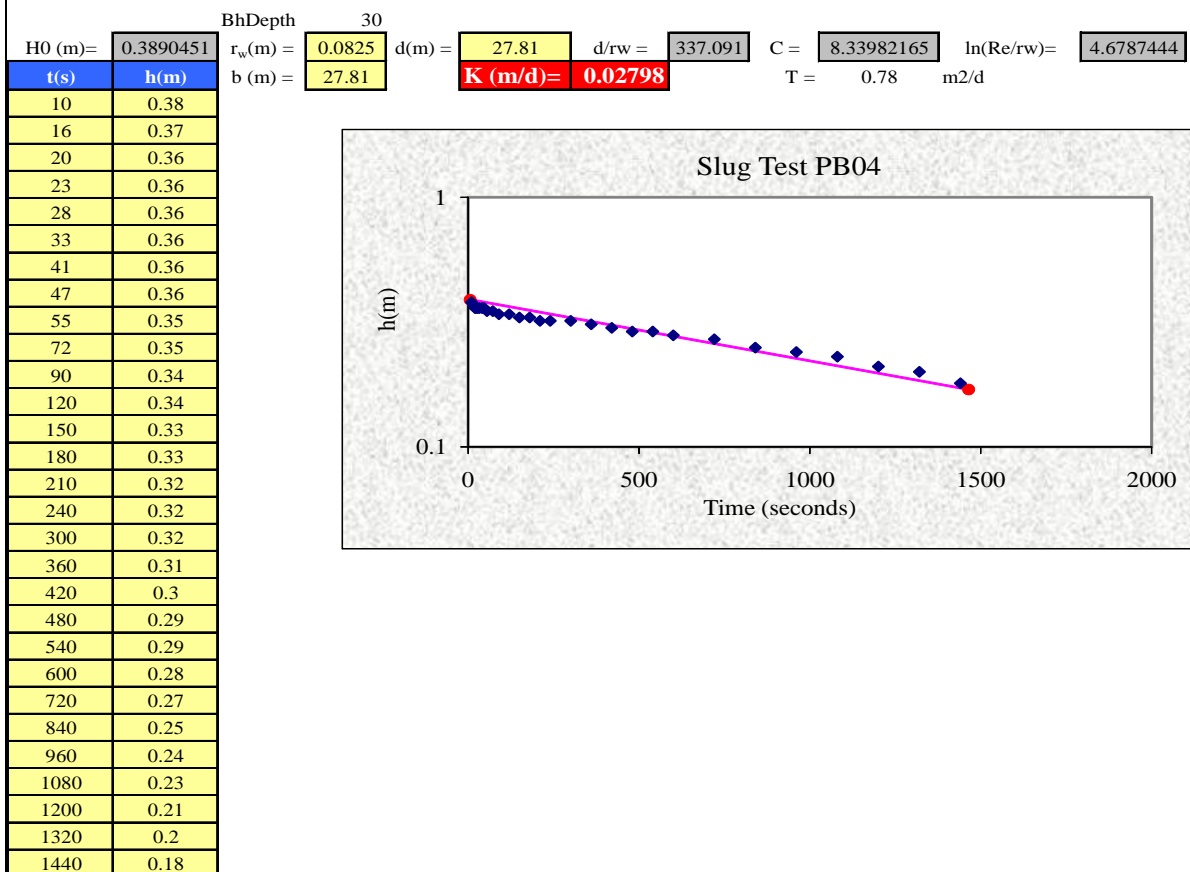
Slug Test CB13



Slug Test CB40



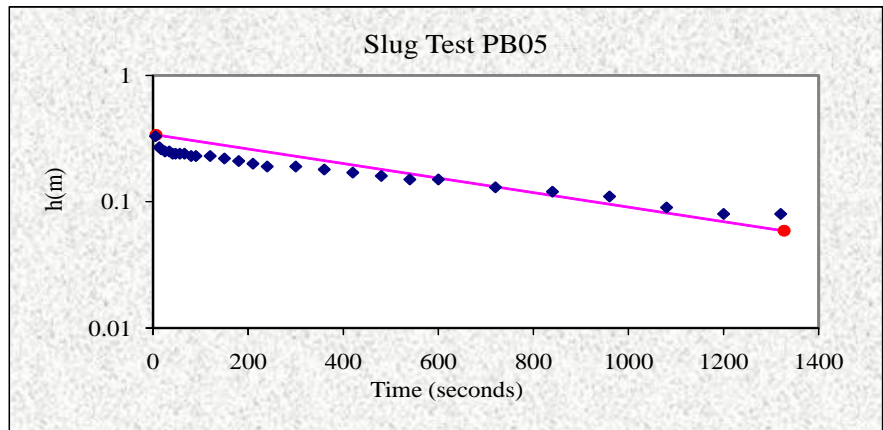
Slug Test PB04



Slug Test PB05

BhDepth = 40
 H0 (m) = 0.3388442 r_w (m) = 0.0825 d (m) = 36.45 d/rw = 441.818 C = 9.61977934 ln(Re/rw) = 4.9414318
 b (m) = 36.45 **K (m/d) = 0.05251** T = 1.91 m²/d

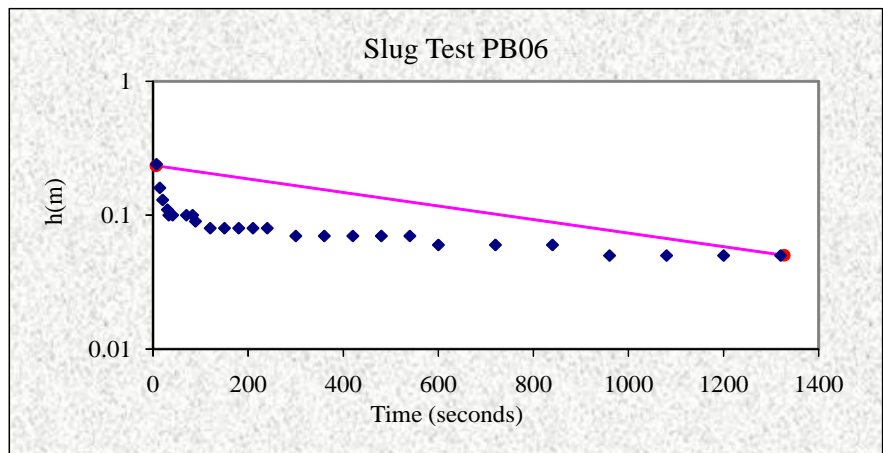
t(s)	h(m)
5	0.33
13	0.27
17	0.26
25	0.25
34	0.25
41	0.24
47	0.24
56	0.24
66	0.24
80	0.23
90	0.23
120	0.23
150	0.22
180	0.21
210	0.2
240	0.19
300	0.19
360	0.18
420	0.17
480	0.16
540	0.15
600	0.15
720	0.13
840	0.12
960	0.11
1080	0.09
1200	0.08
1320	0.08



Slug Test PB06

BhDepth = 40
 H0 (m) = 0.2344229 r_w (m) = 0.0825 d (m) = 37.76 d/rw = 457.697 C = 9.77554544 ln(Re/rw) = 4.9772401
 b (m) = 37.76 **K (m/d) = 0.04501** T = 1.70 m²/d

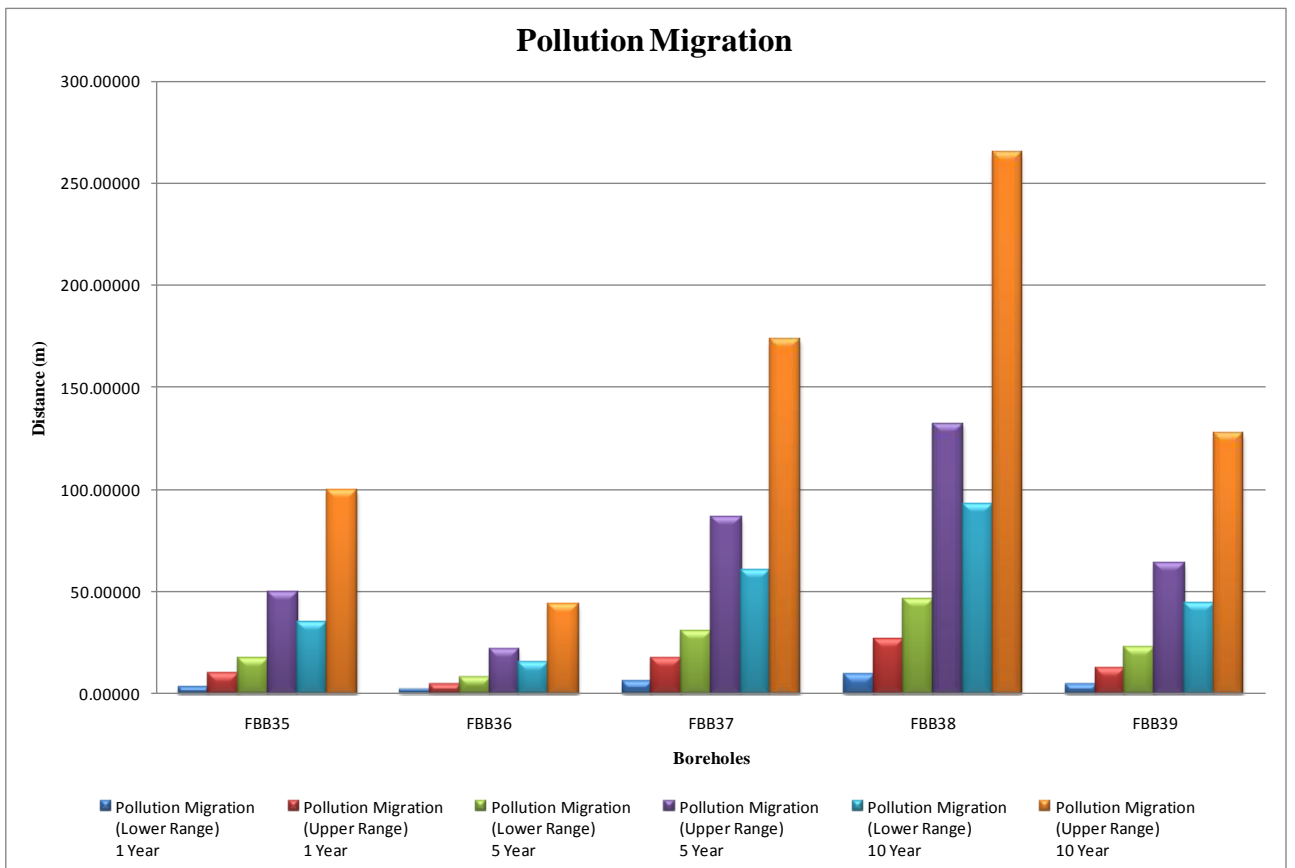
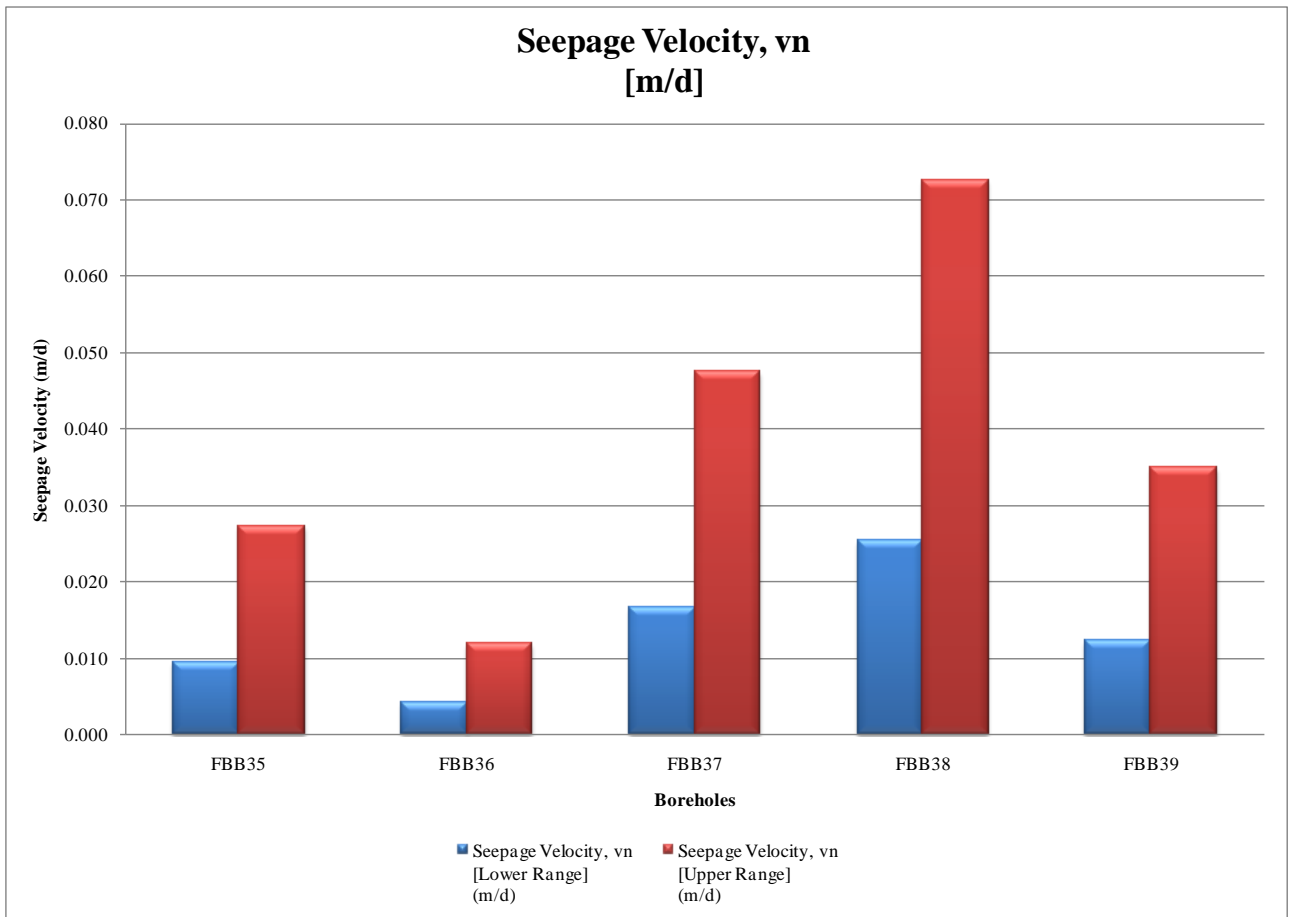
t(s)	h(m)
7	0.24
14	0.16
20	0.13
30	0.11
33	0.1
41	0.1
70	0.1
83	0.1
89	0.09
120	0.08
150	0.08
180	0.08
210	0.08
240	0.08
300	0.07
360	0.07
420	0.07
480	0.07
540	0.07
600	0.06
720	0.06
840	0.06
960	0.05
1080	0.05
1200	0.05
1320	0.05



APPENDIX D
Pollution Source: Ash Stack

Borehole	Coordinate System (WGS84)				Water Level Elevation (mamsl)	Pollution Source Head (mamsl)	Piezometric Head difference (meters)	Gradient (i)	Hydraulic Conductivity [Lower Range, Average] (K)	Hydraulic Conductivity [Upper Range, Geomean] (K)	Darcy Velocity, q_h [Lower Range] (m/d)	Darcy Velocity, q_h [Upper Range] (m/d)	Effective Porosity (n_e)	Seepage Velocity, v_n [Lower Range] (m/d)	Seepage Velocity, v_n [Upper Range] (m/d)
	X (meters)	Y (meters)	Pollution Source (Ash Stack) X & Y Coordinates												
FBB26	1963.38	-2889679.58	-5046.25	-2888459.25	1588.46	1576.76	-11.70	-0.0016	Above Gradient	Above Gradient	Above Gradient	Above Gradient	Above Gradient	Above Gradient	Above Gradient
FBB27	423.181	-2886714.72	-5046.25	-2888459.25	1588.46	1576.76	-37.50	-0.0065	Above Gradient	Above Gradient	Above Gradient	Above Gradient	Above Gradient	Above Gradient	Above Gradient
FBB28	771.476	-2884196.49	-5046.25	-2888459.25	1588.46	1576.76	-16.23	-0.0023	Above Gradient	Above Gradient	Above Gradient	Above Gradient	Above Gradient	Above Gradient	Above Gradient
FBB29	960.572	-2884447.99	-5046.25	-2888459.25	1588.46	1576.76	-20.78	-0.0029	Above Gradient	Above Gradient	Above Gradient	Above Gradient	Above Gradient	Above Gradient	Above Gradient
FBB30	-145.053	-2887750.59	-5046.25	-2888459.25	1588.46	1576.76	-42.28	-0.0085	Above Gradient	Above Gradient	Above Gradient	Above Gradient	Above Gradient	Above Gradient	Above Gradient
FBB31	-2601.66	-2888877.57	-5046.25	-2888459.25	1588.46	1576.76	-28.58	-0.0115	Above Gradient	Above Gradient	Above Gradient	Above Gradient	Above Gradient	Above Gradient	Above Gradient
FBB32	-2611.67	-2888854.32	-5046.25	-2888459.25	1588.46	1576.76	-29.26	-0.0119	Above Gradient	Above Gradient	Above Gradient	Above Gradient	Above Gradient	Above Gradient	Above Gradient
FBB34	-5150.04	-2892085.7	-5046.25	-2888459.25	1588.46	1576.76	-5.85	-0.0016	Above Gradient	Above Gradient	Above Gradient	Above Gradient	Above Gradient	Above Gradient	Above Gradient
FBB35	-7370.68	-2892764.81	-5046.25	-2888459.25	1588.46	1576.76	18.65	0.0038	0.050	0.143	0.00019	0.00054	0.02	0.00952	0.02719
FBB36	-7637.4	-2893200.37	-5046.25	-2888459.25	1588.46	1576.76	9.04	0.0017	0.050	0.143	0.00008	0.00024	0.02	0.00418	0.01194
FBB37	-7609.18	-2891878.62	-5046.25	-2888459.25	1588.46	1576.76	28.40	0.0066	0.050	0.143	0.00033	0.00095	0.02	0.01660	0.04741
FBB38	-8252.07	-2890496.36	-5046.25	-2888459.25	1588.46	1576.76	38.60	0.0102	0.050	0.143	0.00051	0.00145	0.02	0.02539	0.07249
FBB39	-6270.38	-2885161.84	-5046.25	-2888459.25	1588.46	1576.76	17.19	0.0049	0.050	0.143	0.00024	0.00070	0.02	0.01221	0.03486

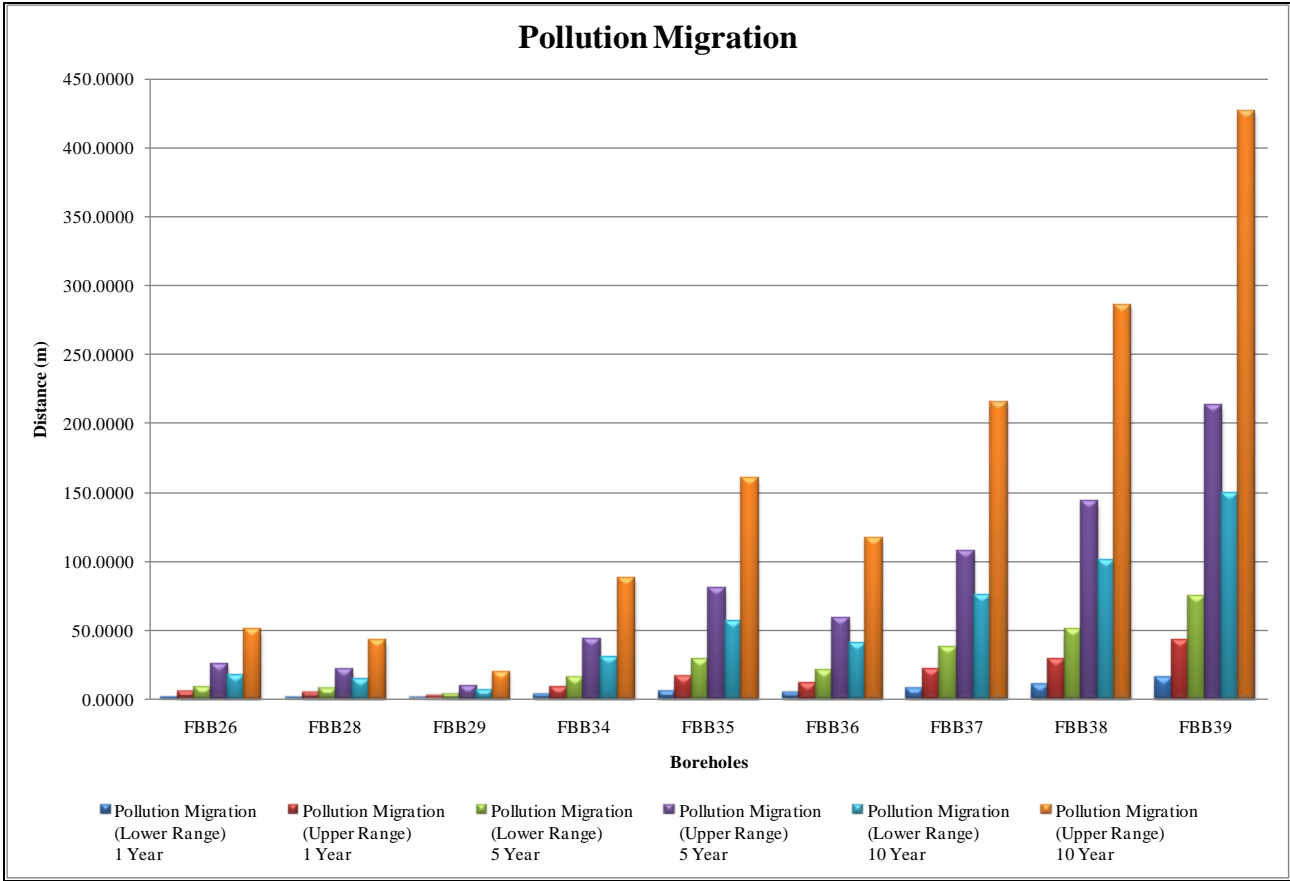
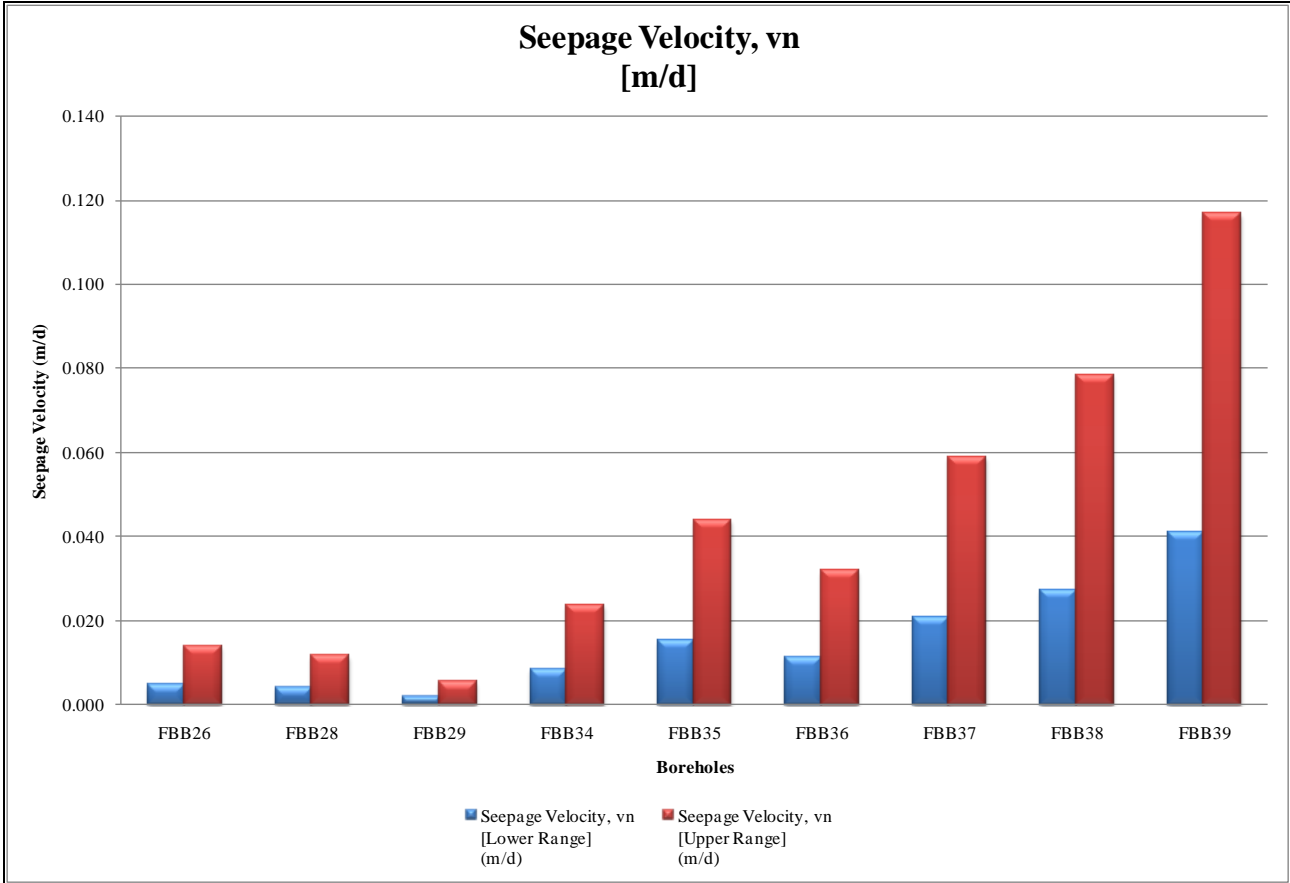
Borehole	Estimated Pollution Migration [Lower Range, 1 Year Period] (m)	Estimated Pollution Migration [Upper Range, 1 Year Period] (m)	Estimated Pollution Migration [Lower Range, 5 Year Period] (m)	Estimated Pollution Migration [Upper Range, 5 Year Period] (m)	Estimated Pollution Migration [Lower Range, 10 Year Period] (m)	Estimated Pollution Migration [Upper Range, 10 Year Period] (m)
FBB26	Above Gradient	Above Gradient				
FBB27	Above Gradient	Above Gradient				
FBB28	Above Gradient	Above Gradient				
FBB29	Above Gradient	Above Gradient				
FBB30	Above Gradient	Above Gradient				
FBB31	Above Gradient	Above Gradient				
FBB32	Above Gradient	Above Gradient				
FBB34	Above Gradient	Above Gradient				
FBB35	3.48	9.92	17.38	49.62	34.76	99.25
FBB36	1.53	4.36	7.63	21.78	15.26	43.57
FBB37	6.06	17.30	30.30	86.52	60.60	173.03
FBB38	9.27	26.46	46.33	132.29	92.67	264.57
FBB39	4.46	12.72	22.28	63.62	44.56	127.23



Pollution Source: Emergency Stack

Borehole	Coordinate System (WGS84)				Water Level Elevation (mamsl)	Pollution Source Head (mamsl)	Piezometric Head difference (metres)	Gradient (i)	Hydraulic Conductivity [Lower Range, Average] (K)	Hydraulic Conductivity [Upper Range, Geomean] (K)	Darcy Velocity, q _n [Lower Range] (m/d)	Darcy Velocity, q _n [Upper Range] (m/d)	Effective Porosity (n _e)	Seepage Velocity, v _n [Lower Range] (m/d)	Seepage Velocity, v _n [Upper Range] (m/d)
	X (metres)	Y (metres)	Pollution Source (Emergency Stack) X & Y Coordinates												
FBB26	1963.38	-2889679.58	-4074.25	-2886491.25	1588.46	1601.65	13.19	0.0019	0.050	0.143	0.00010	0.00028	0.02	0.00483	0.01378
FBB27	423.181	-2886714.72	-4074.25	-2886491.25	1588.46	1601.65	-12.61	-0.0028	Above Gradient	Above Gradient	Above Gradient	Above Gradient	Above Gradient	Above Gradient	Above Gradient
FBB28	771.476	-2884196.49	-4074.25	-2886491.25	1588.46	1601.65	8.66	0.0016	0.050	0.143	0.00008	0.00023	0.02	0.00404	0.01153
FBB29	960.572	-2884447.99	-4074.25	-2886491.25	1588.46	1601.65	4.11	0.0008	0.050	0.143	0.00004	0.00011	0.02	0.00189	0.00540
FBB30	-145.053	-2887750.59	-4074.25	-2886491.25	1588.46	1601.65	-17.38	-0.0042	Above Gradient	Above Gradient	Above Gradient	Above Gradient	Above Gradient	Above Gradient	Above Gradient
FBB31	-2601.66	-2888877.57	-4074.25	-2886491.25	1588.46	1601.65	-3.69	-0.0013	Above Gradient	Above Gradient	Above Gradient	Above Gradient	Above Gradient	Above Gradient	Above Gradient
FBB32	-2611.67	-2888854.32	-4074.25	-2886491.25	1588.46	1601.65	-4.37	-0.0016	Above Gradient	Above Gradient	Above Gradient	Above Gradient	Above Gradient	Above Gradient	Above Gradient
FBB34	-5150.04	-2892085.7	-4074.25	-2886491.25	1588.46	1601.65	19.04	0.0033	0.050	0.143	0.00017	0.00048	0.02	0.00835	0.02384
FBB35	-7370.68	-2892764.81	-4074.25	-2886491.25	1588.46	1601.65	43.55	0.0061	0.050	0.143	0.00031	0.00088	0.02	0.01535	0.04383
FBB36	-7637.4	-2893200.37	-4074.25	-2886491.25	1588.46	1601.65	33.93	0.0045	0.050	0.143	0.00022	0.00064	0.02	0.01116	0.03186
FBB37	-7609.18	-2891878.62	-4074.25	-2886491.25	1588.46	1601.65	53.29	0.0083	0.050	0.143	0.00041	0.00118	0.02	0.02066	0.05899
FBB38	-8252.07	-2890496.36	-4074.25	-2886491.25	1588.46	1601.65	63.49	0.0110	0.050	0.143	0.00055	0.00156	0.02	0.02741	0.07825
FBB39	-6270.38	-2885161.84	-4074.25	-2886491.25	1588.46	1601.65	42.08	0.0164	0.050	0.143	0.00082	0.00234	0.02	0.04095	0.11692

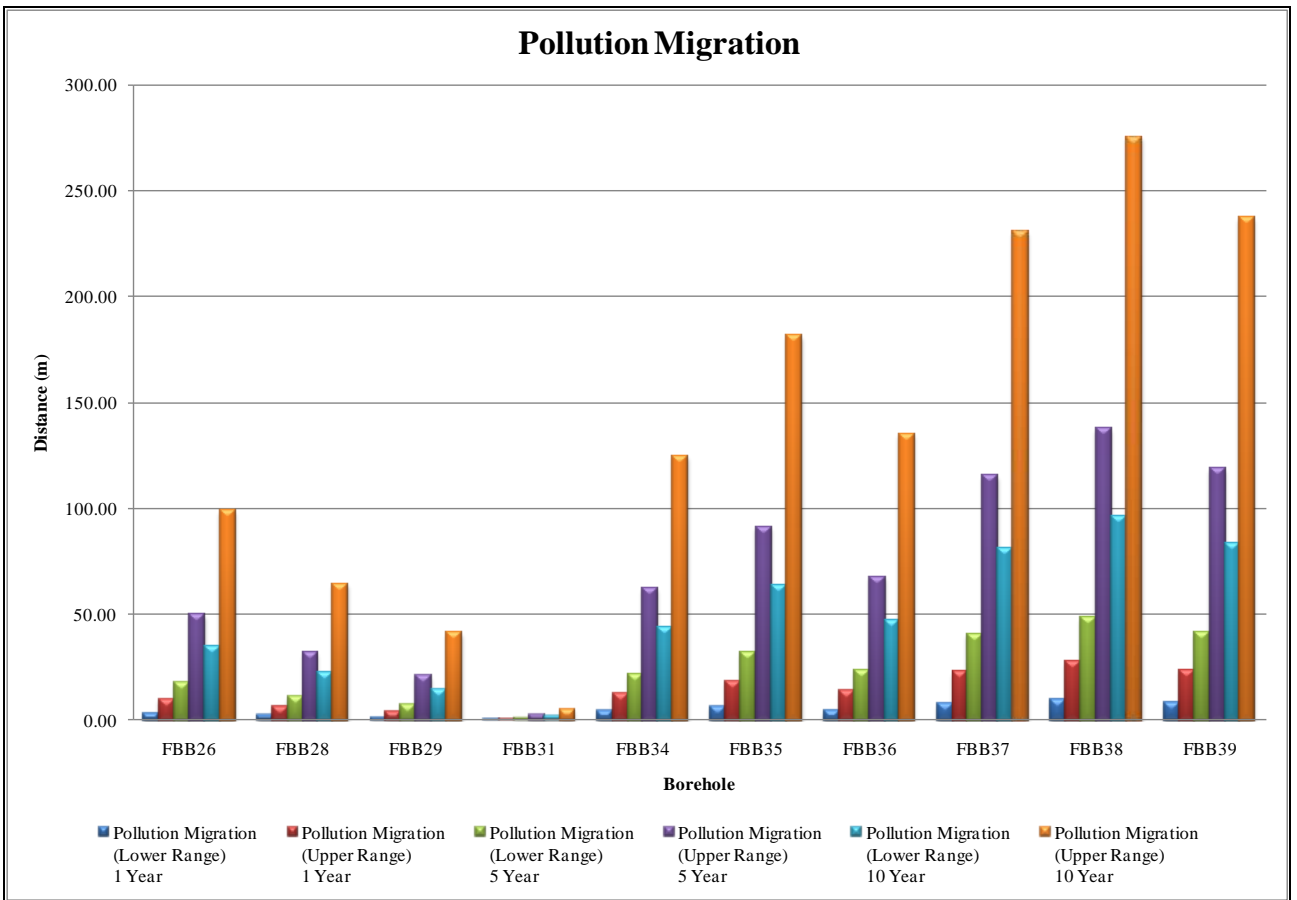
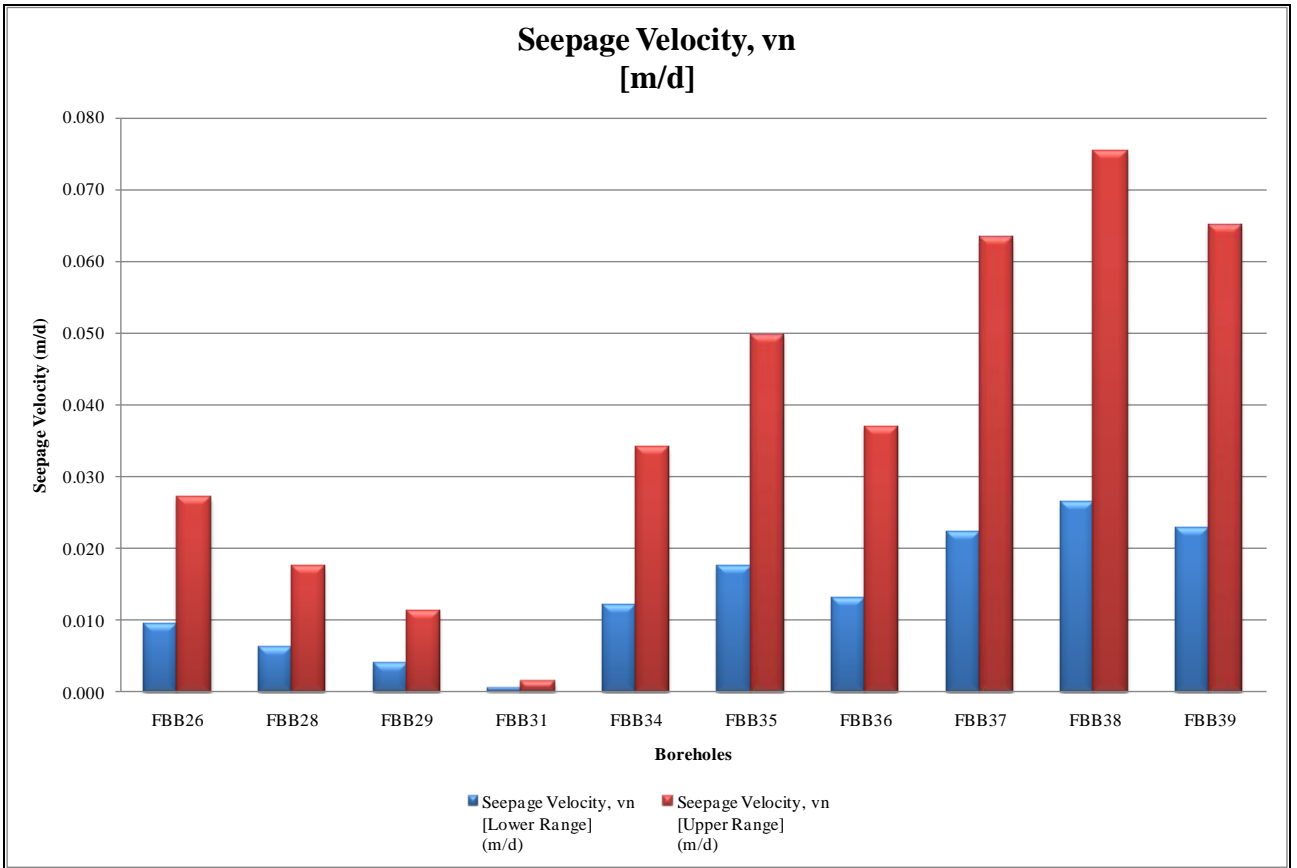
Borehole	Estimated Pollution Migration [Lower Range, 1 Year Period] (m)	Estimated Pollution Migration [Upper Range, 1 Year Period] (m)	Estimated Pollution Migration [Lower Range, 5 Year Period] (m)	Estimated Pollution Migration [Upper Range, 5 Year Period] (m)	Estimated Pollution Migration [Lower Range, 10 Year Period] (m)	Estimated Pollution Migration [Upper Range, 10 Year Period] (m)
FBB26	1.76	5.03	8.81	25.15	17.62	50.30
FBB27	Above Gradient	Above Gradient				
FBB28	1.47	4.21	7.37	21.03	14.73	42.07
FBB29	0.69	1.97	3.45	9.85	6.90	19.70
FBB30	Above Gradient	Above Gradient				
FBB31	Above Gradient	Above Gradient				
FBB32	Above Gradient	Above Gradient				
FBB34	3.05	8.70	15.24	43.51	30.48	87.01
FBB35	5.60	16.00	28.01	79.98	56.03	159.96
FBB36	4.07	11.63	20.37	58.15	40.73	116.29
FBB37	7.54	21.53	37.71	107.66	75.42	215.32
FBB38	10.00	28.56	50.02	142.80	100.03	285.61
FBB39	14.95	42.68	74.74	213.38	149.47	426.76



Pollution Source: Coal Stockyard Settling Dam

Borehole	Coordinate System (WGS84)			Water Level Elevation (mamsl)	Pollution Source Head (mamsl)	Piezometric Head difference (metres)	Gradient (i)	Hydraulic Conductivity [Lower Range, Average] (K)	Hydraulic Conductivity [Upper Range, Geomean] (K)	Darcy Velocity, q_h [Lower Range] (m/d)	Darcy Velocity, q_h [Upper Range] (m/d)	Effective Porosity (n_e)	Seepage Velocity, v_s [Lower Range] (m/d)	Seepage Velocity, v_s [Upper Range] (m/d)
	X (metres)	Y (metres)	Pollution Source (Coal Stockyard Settling Dam) X & Y Coordinates											
FBB26	1963.38	-2889679.58	-2286.25 -2888255.25	1588.46	1605.48	17.02	0.0038	0.050	0.143	0.00019	0.00054	0.02	0.00949	0.02708
FBB27	423.181	-2886714.72	-2286.25 -2888255.25	1614.26	1605.48	-8.78	-0.0028	Above Gradient	Above Gradient	Above Gradient	Above Gradient	Above Gradient	Above Gradient	Above Gradient
FBB28	771.476	-2884196.49	-2286.25 -2888255.25	1592.99	1605.48	12.49	0.0025	0.050	0.143	0.00012	0.00035	0.02	0.00614	0.01753
FBB29	960.572	-2884447.99	-2286.25 -2888255.25	1597.54	1605.48	7.94	0.0016	0.050	0.143	0.00008	0.00023	0.02	0.00396	0.01132
FBB30	-145.053	-2887750.59	-2286.25 -2888255.25	1619.03	1605.48	-13.56	-0.0062	Above Gradient	Above Gradient	Above Gradient	Above Gradient	Above Gradient	Above Gradient	Above Gradient
FBB31	-2601.66	-2888877.57	-2286.25 -2888255.25	1605.34	1605.48	0.14	0.0002	0.050	0.143	0.00001	0.00003	0.02	0.00050	0.00144
FBB32	-2611.67	-2888854.32	-2286.25 -2888255.25	1606.02	1605.48	-0.54	-0.0008	Above Gradient	Above Gradient	Above Gradient	Above Gradient	Above Gradient	Above Gradient	Above Gradient
FBB34	-5150.04	-2892085.7	-2286.25 -2888255.25	1582.61	1605.48	22.87	0.0048	0.050	0.143	0.00024	0.00068	0.02	0.01194	0.03410
FBB35	-7370.68	-2892764.81	-2286.25 -2888255.25	1558.11	1605.48	47.37	0.0070	0.050	0.143	0.00035	0.00099	0.02	0.01741	0.04972
FBB36	-7637.4	-2893200.37	-2286.25 -2888255.25	1567.72	1605.48	37.76	0.0052	0.050	0.143	0.00026	0.00074	0.02	0.01295	0.03697
FBB37	-7609.18	-2891878.62	-2286.25 -2888255.25	1548.36	1605.48	57.12	0.0089	0.050	0.143	0.00044	0.00127	0.02	0.02216	0.06327
FBB38	-8252.07	-2890496.36	-2286.25 -2888255.25	1538.16	1605.48	67.32	0.0106	0.050	0.143	0.00053	0.00151	0.02	0.02639	0.07535
FBB39	-6270.38	-2885161.84	-2286.25 -2888255.25	1559.57	1605.48	45.91	0.0091	0.050	0.143	0.00045	0.00130	0.02	0.02274	0.06492

Borehole	Estimated Pollution Migration [Lower Range, 1 Year Period] (m)	Estimated Pollution Migration [Upper Range, 1 Year Period] (m)	Estimated Pollution Migration [Lower Range, 5 Year Period] (m)	Estimated Pollution Migration [Upper Range, 5 Year Period] (m)	Estimated Pollution Migration [Lower Range, 10 Year Period] (m)	Estimated Pollution Migration [Upper Range, 10 Year Period] (m)
FBB26	3.46	9.89	17.31	49.43	34.62	98.85
FBB27	Above Gradient	Above Gradient				
FBB28	2.24	6.40	11.21	32.00	22.41	63.99
FBB29	1.45	4.13	7.23	20.65	14.47	41.31
FBB30	Above Gradient	Above Gradient				
FBB31	0.18	0.53	0.92	2.63	1.84	5.25
FBB32	Above Gradient	Above Gradient				
FBB34	4.36	12.45	21.80	62.24	43.60	124.48
FBB35	6.36	18.15	31.78	90.73	63.56	181.47
FBB36	4.73	13.49	23.63	67.46	47.26	134.92
FBB37	8.09	23.09	40.44	115.47	80.89	230.95
FBB38	9.63	27.50	48.16	137.50	96.32	275.01
FBB39	8.30	23.70	41.50	118.48	82.99	236.95



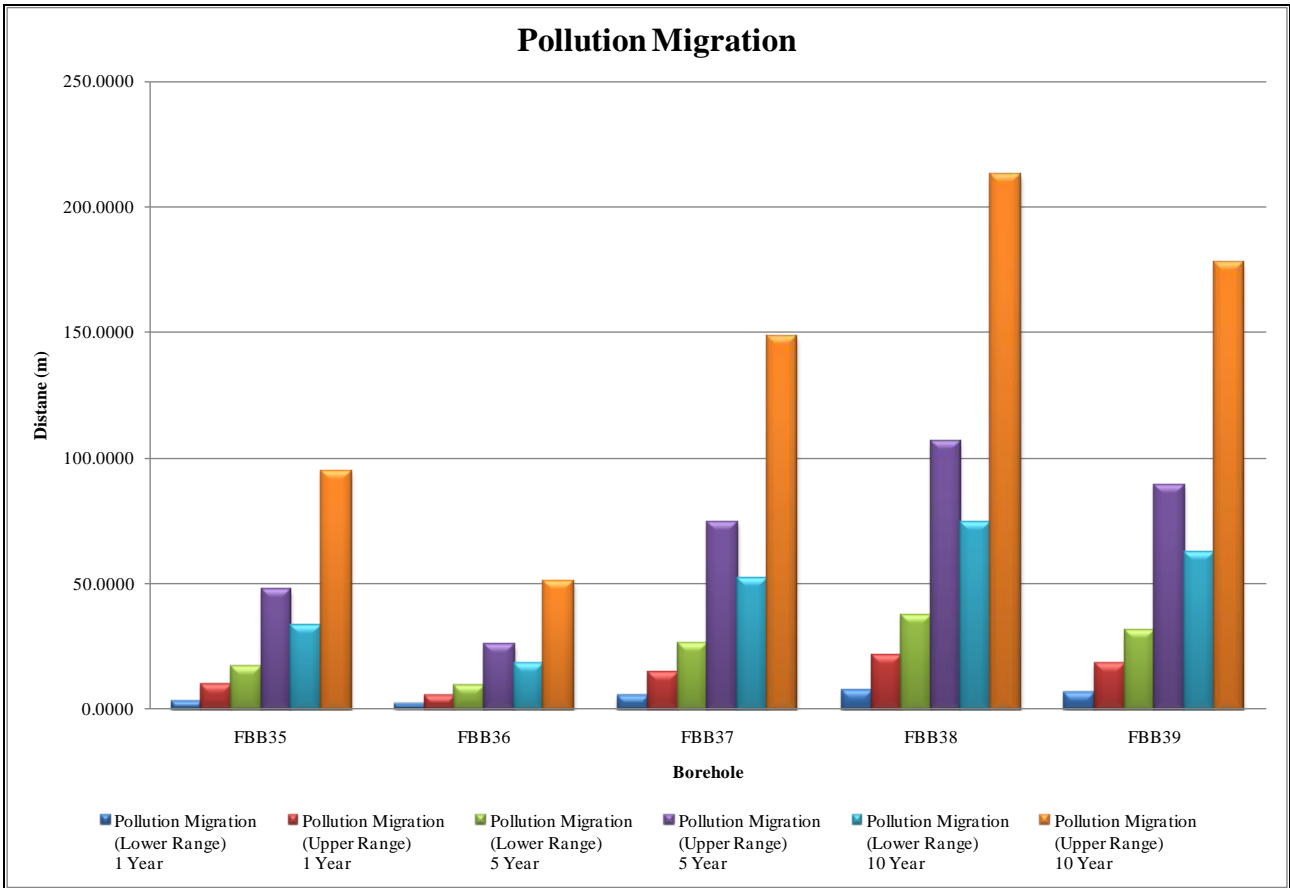
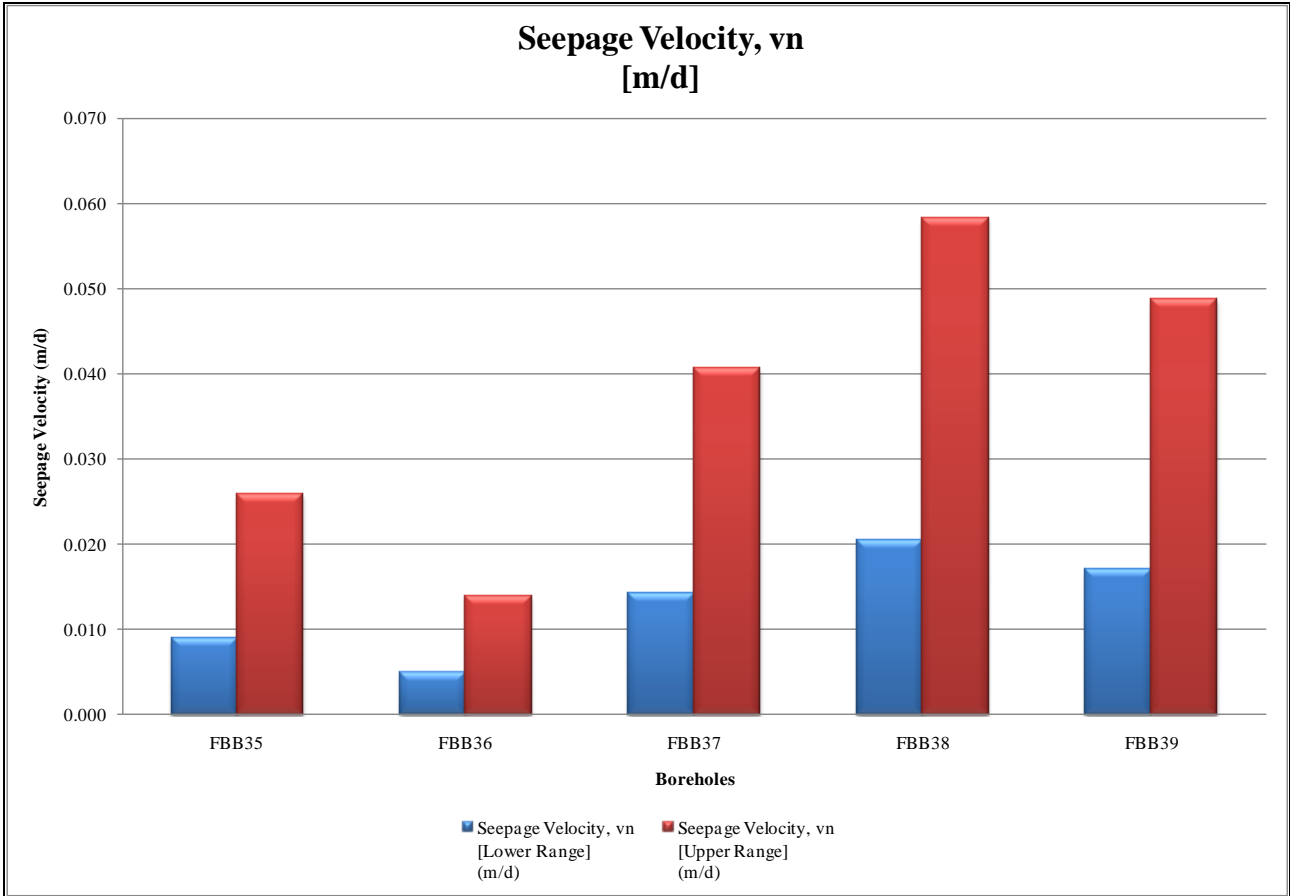
Pollution Source: Dam in Schoongezicht Spruit

Borehole	Coordinate System (WGS84)				Water Level Elevation (mamsl)	Pollution Source Head (mamsl)	Piezometric Head difference (metres)	Gradient (i)	Hydraulic Conductivity [Lower Range, Average] (K)
	X (metres)	Y (metres)	Pollution Source (Dam in Schoongezicht Spruit) X & Y Coordinates						
FBB26	1963.38	-2889679.58	-5668	-2886909	1588.46	1537.49	-50.97	-0.0063	Above Gradient
FBB27	423.181	-2886714.72	-5668	-2886909	1614.26	1537.49	-76.77	-0.0126	Above Gradient
FBB28	771.476	-2884196.49	-5668	-2886909	1592.99	1537.49	-55.50	-0.0079	Above Gradient
FBB29	960.572	-2884447.99	-5668	-2886909	1597.54	1537.49	-60.05	-0.0085	Above Gradient
FBB30	-145.053	-2887750.59	-5668	-2886909	1619.03	1537.49	-81.55	-0.0146	Above Gradient
FBB31	-2601.66	-2888877.57	-5668	-2886909	1605.34	1537.49	-67.85	-0.0186	Above Gradient
FBB32	-2611.67	-2888854.32	-5668	-2886909	1606.02	1537.49	-68.53	-0.0189	Above Gradient
FBB34	-5150.04	-2892085.7	-5668	-2886909	1582.61	1537.49	-45.12	-0.0087	Above Gradient
FBB35	-7370.68	-2892764.81	-5668	-2886909	1558.11	1537.49	-20.62	-0.0034	Above Gradient
FBB36	-7637.4	-2893200.37	-5668	-2886909	1567.72	1537.49	-30.23	-0.0046	Above Gradient
FBB37	-7609.18	-2891878.62	-5668	-2886909	1548.36	1537.49	-10.87	-0.0020	Above Gradient
FBB38	-8252.07	-2890496.36	-5668	-2886909	1538.16	1537.49	-0.67	-0.0002	Above Gradient
FBB39	-6270.38	-2885161.84	-5668	-2886909	1559.57	1537.49	-22.08	-0.0119	Above Gradient

Pollution Source: Dirty Water Dam

Borehole	Coordinate System (WGS84)				Water Level Elevation (mamsl)	Pollution Source Head (mamsl)	Piezometric Head difference (metres)	Gradient (i)	Hydraulic Conductivity [Lower Range, Average] (K)	Hydraulic Conductivity [Upper Range, Geomean] (K)	Darcy Velocity, q_h [Lower Range] (m/d)	Darcy Velocity, q_h [Upper Range] (m/d)	Effective Porosity (n_e)	Seepage Velocity, v_h [Lower Range] (m/d)	Seepage Velocity, v_h [Upper Range] (m/d)
	X (metres)	Y (metres)	Pollution Source (Dirty Water Dam) X & Y Coordinates												
FBB26	1963.38	-2889679.58	-4020.25	-2887374	1588.46	1581.12	-7.34	-0.0011	Above Gradient	Above Gradient	Above Gradient	Above Gradient	Above Gradient	Above Gradient	Above Gradient
FBB27	423.181	-2886714.72	-4020.25	-2887374	1614.26	1581.12	-33.14	-0.0074	Above Gradient	Above Gradient	Above Gradient	Above Gradient	Above Gradient	Above Gradient	Above Gradient
FBB28	771.476	-2884196.49	-4020.25	-2887374	1592.99	1581.12	-11.87	-0.0021	Above Gradient	Above Gradient	Above Gradient	Above Gradient	Above Gradient	Above Gradient	Above Gradient
FBB29	960.572	-2884447.99	-4020.25	-2887374	1597.54	1581.12	-16.42	-0.0028	Above Gradient	Above Gradient	Above Gradient	Above Gradient	Above Gradient	Above Gradient	Above Gradient
FBB30	-145.053	-2887750.59	-4020.25	-2887374	1619.03	1581.12	-37.91	-0.0097	Above Gradient	Above Gradient	Above Gradient	Above Gradient	Above Gradient	Above Gradient	Above Gradient
FBB31	-2601.66	-2888877.57	-4020.25	-2887374	1605.34	1581.12	-24.22	-0.0117	Above Gradient	Above Gradient	Above Gradient	Above Gradient	Above Gradient	Above Gradient	Above Gradient
FBB32	-2611.67	-2888854.32	-4020.25	-2887374	1606.02	1581.12	-24.90	-0.0122	Above Gradient	Above Gradient	Above Gradient	Above Gradient	Above Gradient	Above Gradient	Above Gradient
FBB34	-5150.04	-2892085.7	-4020.25	-2887374	1582.61	1581.12	-1.49	-0.0003	Above Gradient	Above Gradient	Above Gradient	Above Gradient	Above Gradient	Above Gradient	Above Gradient
FBB35	-7370.68	-2892764.81	-4020.25	-2887374	1558.11	1581.12	23.02	0.0036	0.050	0.143	0.00018	0.00052	0.02	0.00906	0.02586
FBB36	-7637.4	-2893200.37	-4020.25	-2887374	1567.72	1581.12	13.41	0.0020	0.050	0.143	0.00010	0.00028	0.02	0.00488	0.01394
FBB37	-7609.18	-2891878.62	-4020.25	-2887374	1548.36	1581.12	32.77	0.0057	0.050	0.143	0.00028	0.00081	0.02	0.01421	0.04058
FBB38	-8252.07	-2890496.36	-4020.25	-2887374	1538.16	1581.12	42.96	0.0082	0.050	0.143	0.00041	0.00117	0.02	0.02041	0.05827
FBB39	-6270.38	-2885161.84	-4020.25	-2887374	1559.57	1581.12	21.55	0.0068	0.050	0.143	0.00034	0.00097	0.02	0.01706	0.04872

Borehole	Estimated Pollution Migration [Lower Range, 1 Year Period] (m)	Estimated Pollution Migration [Upper Range, 1 Year Period] (m)	Estimated Pollution Migration [Lower Range, 5 Year Period] (m)	Estimated Pollution Migration [Upper Range, 5 Year Period] (m)	Estimated Pollution Migration [Lower Range, 10 Year Period] (m)	Estimated Pollution Migration [Upper Range, 10 Year Period] (m)
FBB26	Above Gradient	Above Gradient				
FBB27	Above Gradient	Above Gradient				
FBB28	Above Gradient	Above Gradient				
FBB29	Above Gradient	Above Gradient				
FBB30	Above Gradient	Above Gradient				
FBB31	Above Gradient	Above Gradient				
FBB32	Above Gradient	Above Gradient				
FBB34	Above Gradient	Above Gradient				
FBB35	3.31	9.44	16.53	47.20	33.07	94.40
FBB36	1.78	5.09	8.91	25.44	17.82	50.89
FBB37	5.19	14.81	25.94	74.05	51.87	148.10
FBB38	7.45	21.27	37.25	106.34	74.49	212.68
FBB39	6.23	17.78	31.14	88.91	62.28	177.82



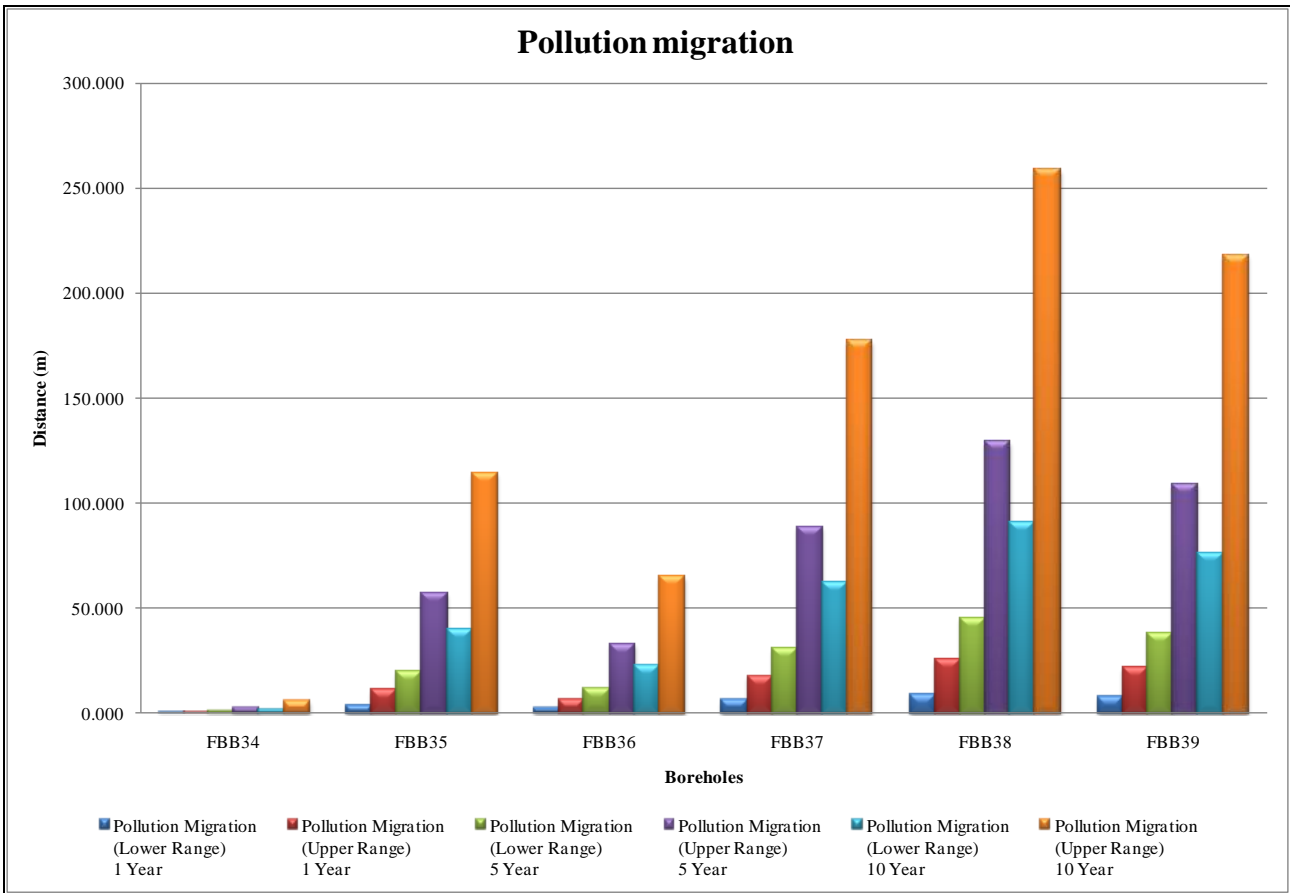
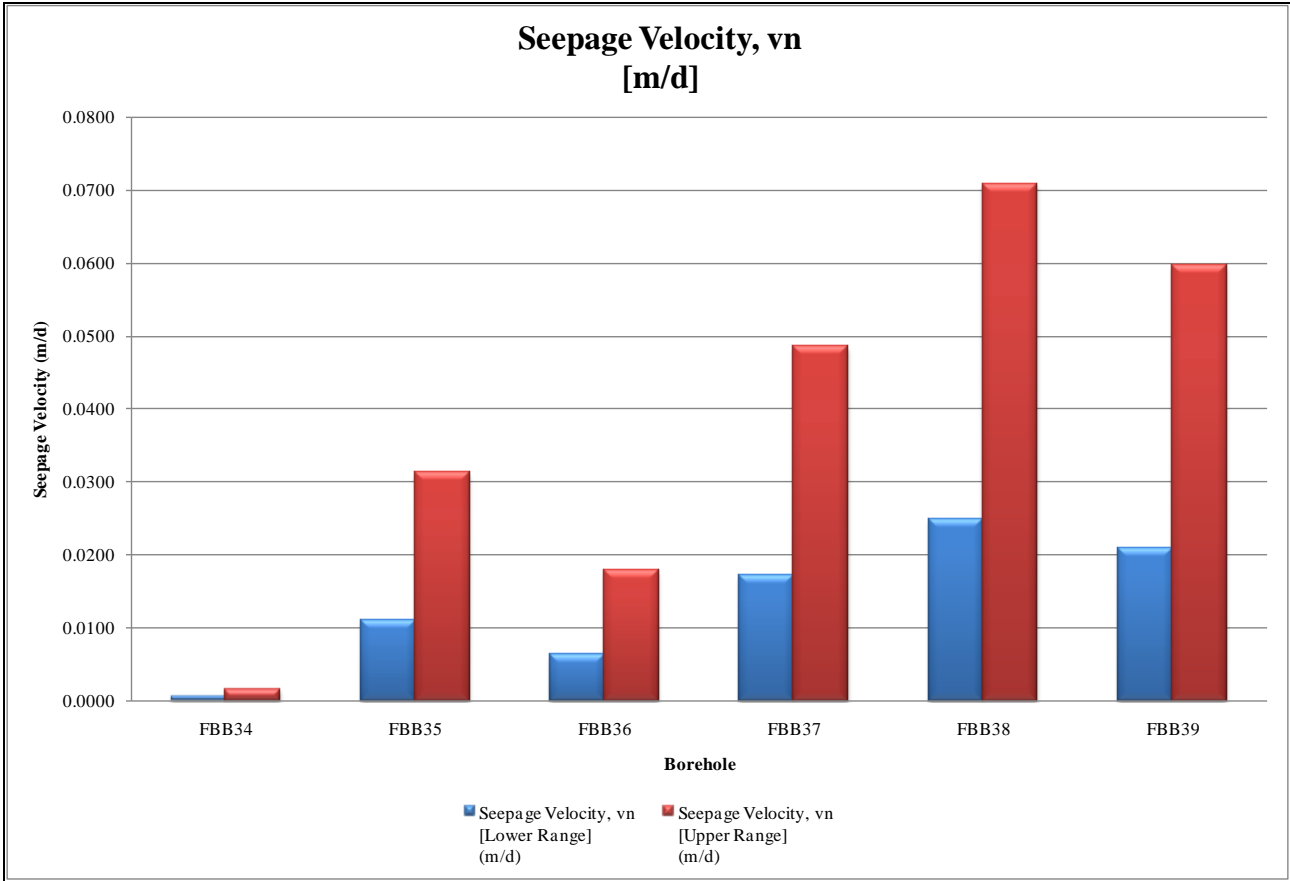
Pollution Source: Dam West of Ash Stack

Borehole	Coordinate System (WGS84)				Water Level Elevation (mamsl)	Pollution Source Head (mamsl)	Piezometric Head difference (metres)	Gradient (i)	Hydraulic Conductivity [Lower Range, Average] (K)
	X (metres)	Y (metres)	Pollution Source (Dam West of Ash Stack) X & Y Coordinates						
FBB26	1963.38	-2889679.58	-6752.5	-2887597.5	1588.46	1511.78	-76.68	-0.0086	Above Gradient
FBB27	423.181	-2886714.72	-6752.5	-2887597.5	1614.26	1511.78	-102.48	-0.0142	Above Gradient
FBB28	771.476	-2884196.49	-6752.5	-2887597.5	1592.99	1511.78	-81.21	-0.0098	Above Gradient
FBB29	960.572	-2884447.99	-6752.5	-2887597.5	1597.54	1511.78	-85.76	-0.0103	Above Gradient
FBB30	-145.053	-2887750.59	-6752.5	-2887597.5	1619.03	1511.78	-107.25	-0.0162	Above Gradient
FBB31	-2601.66	-2888877.57	-6752.5	-2887597.5	1605.34	1511.78	-93.56	-0.0215	Above Gradient
FBB32	-2611.67	-2888854.32	-6752.5	-2887597.5	1606.02	1511.78	-94.24	-0.0218	Above Gradient
FBB34	-5150.04	-2892085.7	-6752.5	-2887597.5	1582.61	1511.78	-70.83	-0.0149	Above Gradient
FBB35	-7370.68	-2892764.81	-6752.5	-2887597.5	1558.11	1511.78	-46.33	-0.0089	Above Gradient
FBB36	-7637.4	-2893200.37	-6752.5	-2887597.5	1567.72	1511.78	-55.94	-0.0099	Above Gradient
FBB37	-7609.18	-2891878.62	-6752.5	-2887597.5	1548.36	1511.78	-36.58	-0.0084	Above Gradient
FBB38	-8252.07	-2890496.36	-6752.5	-2887597.5	1538.16	1511.78	-26.38	-0.0081	Above Gradient
FBB39	-6270.38	-2885161.84	-6752.5	-2887597.5	1559.57	1511.78	-47.79	-0.0192	Above Gradient

Pollution Source: Ash Stack Settling Dam

Borehole	Coordinate System (WGS84)			Water Level Elevation (mamsl)	Pollution Source Head (mamsl)	Piezometric Head difference (metres)	Gradient (i)	Hydraulic Conductivity [Lower Range, Average] (K)	Hydraulic Conductivity [Upper Range, Geomean] (K)	Darcy Velocity, q _D [Lower Range] (m/d)	Darcy Velocity, q _D [Upper Range] (m/d)	Effective Porosity (n _e)	Seepage Velocity, v _s [Lower Range] (m/d)	Seepage Velocity, v _s [Upper Range] (m/d)
	X (metres)	Y (metres)	Pollution Source (Ash Stack Settling Dam) X & Y Coordinates											
FBB26	1963.38	-2889679.58	-4734.25 -2887582.5	1588.46	1583.57	-4.89	-0.0007	Above Gradient	Above Gradient	Above Gradient	Above Gradient	Above Gradient	Above Gradient	Above Gradient
FBB27	423.181	-2886714.72	-4734.25 -2887582.5	1614.26	1583.57	-30.69	-0.0059	Above Gradient	Above Gradient	Above Gradient	Above Gradient	Above Gradient	Above Gradient	Above Gradient
FBB28	771.476	-2884196.49	-4734.25 -2887582.5	1592.99	1583.57	-9.42	-0.0015	Above Gradient	Above Gradient	Above Gradient	Above Gradient	Above Gradient	Above Gradient	Above Gradient
FBB29	960.572	-2884447.99	-4734.25 -2887582.5	1597.54	1583.57	-13.97	-0.0021	Above Gradient	Above Gradient	Above Gradient	Above Gradient	Above Gradient	Above Gradient	Above Gradient
FBB30	-145.053	-2887750.59	-4734.25 -2887582.5	1619.03	1583.57	-35.46	-0.0077	Above Gradient	Above Gradient	Above Gradient	Above Gradient	Above Gradient	Above Gradient	Above Gradient
FBB31	-2601.66	-2888877.57	-4734.25 -2887582.5	1605.34	1583.57	-21.77	-0.0087	Above Gradient	Above Gradient	Above Gradient	Above Gradient	Above Gradient	Above Gradient	Above Gradient
FBB32	-2611.67	-2888854.32	-4734.25 -2887582.5	1606.02	1583.57	-22.45	-0.0091	Above Gradient	Above Gradient	Above Gradient	Above Gradient	Above Gradient	Above Gradient	Above Gradient
FBB34	-5150.04	-2892085.7	-4734.25 -2887582.5	1582.61	1583.57	0.96	0.0002	0.050	0.143	0.00001	0.00003	0.02	0.00053	0.00151
FBB35	-7370.68	-2892764.81	-4734.25 -2887582.5	1558.11	1583.57	25.46	0.0044	0.050	0.143	0.00022	0.00062	0.02	0.01094	0.03124
FBB36	-7637.4	-2893200.37	-4734.25 -2887582.5	1567.72	1583.57	15.85	0.0025	0.050	0.143	0.00013	0.00036	0.02	0.00626	0.01788
FBB37	-7609.18	-2891878.62	-4734.25 -2887582.5	1548.36	1583.57	35.21	0.0068	0.050	0.143	0.00034	0.00097	0.02	0.01702	0.04859
FBB38	-8252.07	-2890496.36	-4734.25 -2887582.5	1538.16	1583.57	45.41	0.0099	0.050	0.143	0.00050	0.00142	0.02	0.02484	0.07091
FBB39	-6270.38	-2885161.84	-4734.25 -2887582.5	1559.57	1583.57	24.00	0.0084	0.050	0.143	0.00042	0.00119	0.02	0.02091	0.05971

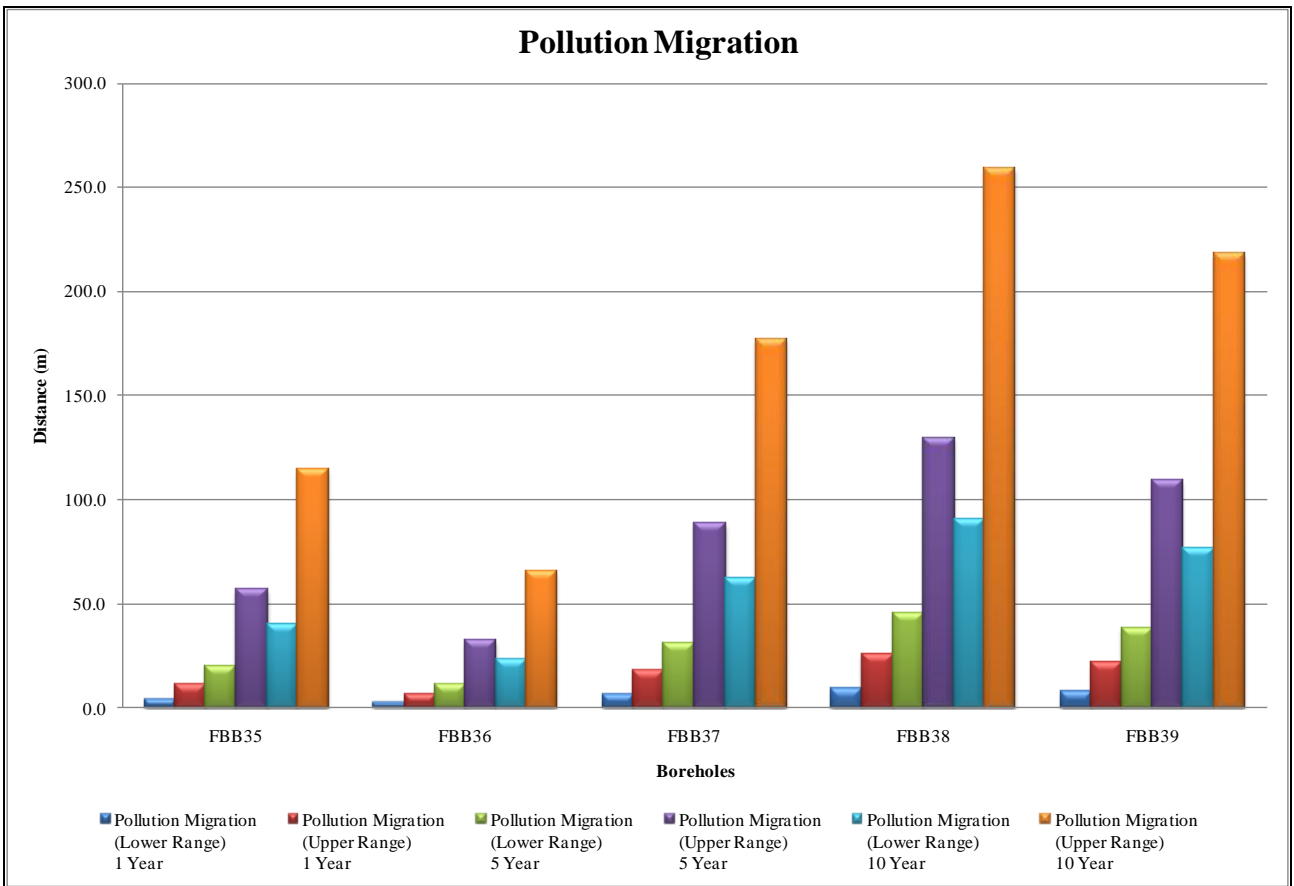
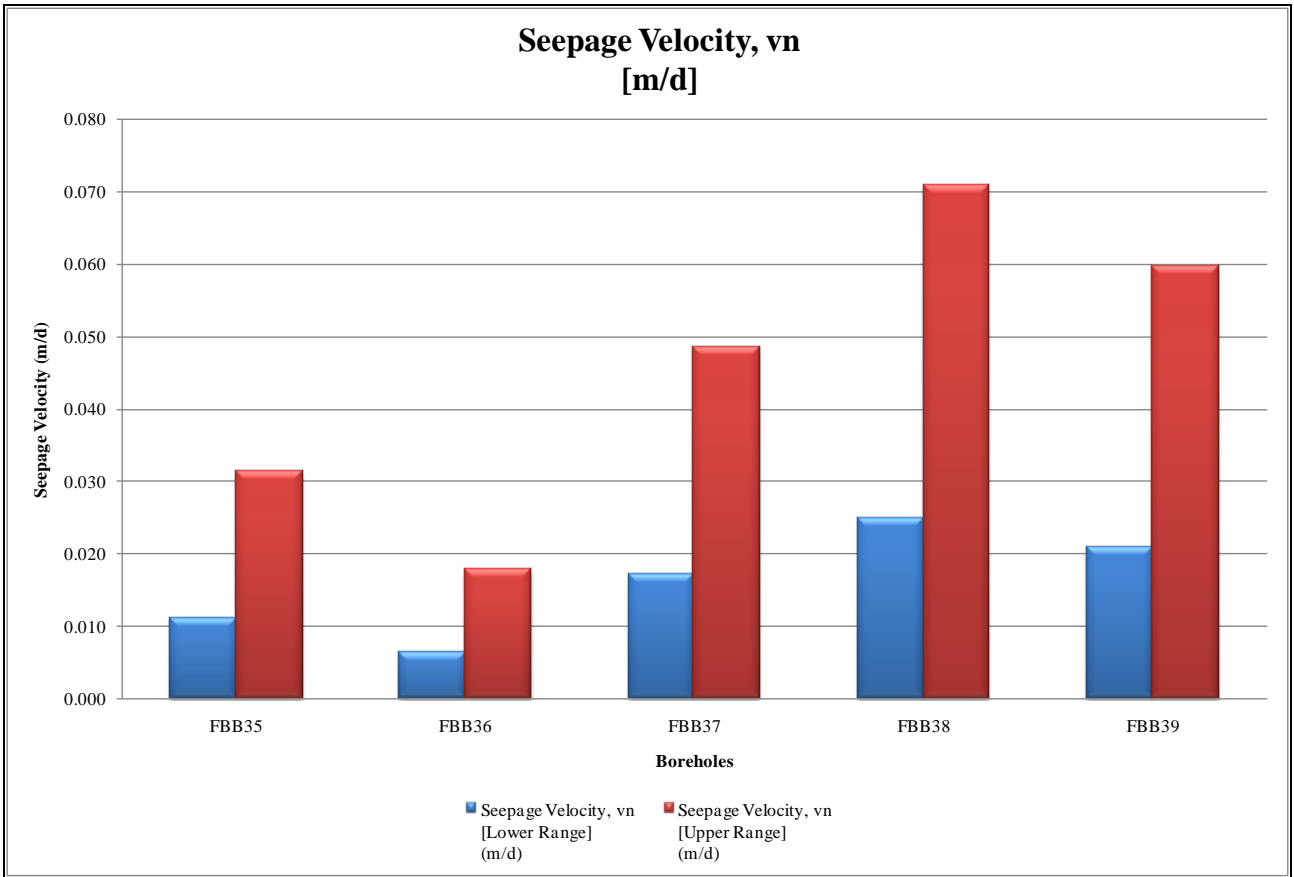
Borehole	Estimated Pollution Migration [Lower Range, 1 Year Period] (m)	Estimated Pollution Migration [Upper Range, 1 Year Period] (m)	Estimated Pollution Migration [Lower Range, 5 Year Period] (m)	Estimated Pollution Migration [Upper Range, 5 Year Period] (m)	Estimated Pollution Migration [Lower Range, 10 Year Period] (m)	Estimated Pollution Migration [Upper Range, 10 Year Period] (m)
FBB26	Above Gradient	Above Gradient				
FBB27	Above Gradient	Above Gradient				
FBB28	Above Gradient	Above Gradient				
FBB29	Above Gradient	Above Gradient				
FBB30	Above Gradient	Above Gradient				
FBB31	Above Gradient	Above Gradient				
FBB32	Above Gradient	Above Gradient				
FBB34	0.19	0.55	0.97	2.76	1.93	5.52
FBB35	3.99	11.40	19.97	57.01	39.93	114.01
FBB36	2.29	6.53	11.43	32.63	22.86	65.26
FBB37	6.21	17.73	31.06	88.67	62.11	177.34
FBB38	9.06	25.88	45.32	129.41	90.65	258.81
FBB39	7.63	21.79	38.17	108.97	76.33	217.94



Pollution Source: Settling Dam

Borehole	Coordinate System (WGS84)				Water Level Elevation (mamsl)	Pollution Source Head (mamsl)	Piezometric Head difference (metres)	Gradient (i)	Hydraulic Conductivity [Lower Range, Average] (K)	Hydraulic Conductivity [Upper Range, Geomean] (K)	Darcy Velocity, q_n [Lower Range] (m/d)	Darcy Velocity, q_n [Upper Range] (m/d)	Effective Porosity (n_e)	Seepage Velocity, v_n [Lower Range] (m/d)	Seepage Velocity, v_n [Upper Range] (m/d)
	X (metres)	Y (metres)	Pollution Source (Settling Dam) X & Y Coordinates												
FBB26	1963.38	-2889679.58	-4734.25	-2887582.5	1588.46	1583.57	-4.89	-0.0007	Above Gradient	Above Gradient	Above Gradient	Above Gradient	Above Gradient	Above Gradient	Above Gradient
FBB27	423.181	-2886714.72	-4734.25	-2887582.5	1614.26	1583.57	-30.69	-0.0059	Above Gradient	Above Gradient	Above Gradient	Above Gradient	Above Gradient	Above Gradient	Above Gradient
FBB28	771.476	-2884196.49	-4734.25	-2887582.5	1592.99	1583.57	-9.42	-0.0015	Above Gradient	Above Gradient	Above Gradient	Above Gradient	Above Gradient	Above Gradient	Above Gradient
FBB29	960.572	-2884447.99	-4734.25	-2887582.5	1597.54	1583.57	-13.97	-0.0021	Above Gradient	Above Gradient	Above Gradient	Above Gradient	Above Gradient	Above Gradient	Above Gradient
FBB30	-145.053	-2887750.59	-4734.25	-2887582.5	1619.03	1583.57	-35.46	-0.0077	Above Gradient	Above Gradient	Above Gradient	Above Gradient	Above Gradient	Above Gradient	Above Gradient
FBB31	-2601.66	-2888877.57	-4734.25	-2887582.5	1605.34	1583.57	-21.77	-0.0087	Above Gradient	Above Gradient	Above Gradient	Above Gradient	Above Gradient	Above Gradient	Above Gradient
FBB32	-2611.67	-2888854.32	-4734.25	-2887582.5	1606.02	1583.57	-22.45	-0.0091	Above Gradient	Above Gradient	Above Gradient	Above Gradient	Above Gradient	Above Gradient	Above Gradient
FBB34	-5150.04	-2892085.7	-4734.25	-2887582.5	1582.61	1583.57	0.96	0.0002	0.050	0.143	0.00001	0.00003	0.02	0.00053	0.00151
FBB35	-7370.68	-2892764.81	-4734.25	-2887582.5	1558.11	1583.57	25.46	0.0044	0.050	0.143	0.00022	0.00062	0.02	0.01094	0.03124
FBB36	-7637.4	-2893200.37	-4734.25	-2887582.5	1567.72	1583.57	15.85	0.0025	0.050	0.143	0.00013	0.00036	0.02	0.00626	0.01788
FBB37	-7609.18	-2891878.62	-4734.25	-2887582.5	1548.36	1583.57	35.21	0.0068	0.050	0.143	0.00034	0.00097	0.02	0.01702	0.04859
FBB38	-8252.07	-2890496.36	-4734.25	-2887582.5	1538.16	1583.57	45.41	0.0099	0.050	0.143	0.00050	0.00142	0.02	0.02484	0.07091
FBB39	-6270.38	-2885161.84	-4734.25	-2887582.5	1559.57	1583.57	24.00	0.0084	0.050	0.143	0.00042	0.00119	0.02	0.02091	0.05971

Borehole	Estimated Pollution Migration [Lower Range, 1 Year Period] (m)	Estimated Pollution Migration [Upper Range, 1 Year Period] (m)	Estimated Pollution Migration [Lower Range, 5 Year Period] (m)	Estimated Pollution Migration [Upper Range, 5 Year Period] (m)	Estimated Pollution Migration [Lower Range, 10 Year Period] (m)	Estimated Pollution Migration [Upper Range, 10 Year Period] (m)
FBB26	Above Gradient	Above Gradient				
FBB27	Above Gradient	Above Gradient				
FBB28	Above Gradient	Above Gradient				
FBB29	Above Gradient	Above Gradient				
FBB30	Above Gradient	Above Gradient				
FBB31	Above Gradient	Above Gradient				
FBB32	Above Gradient	Above Gradient				
FBB34	0.19	0.55	0.97	2.76	1.93	5.52
FBB35	3.99	11.40	19.97	57.01	39.93	114.01
FBB36	2.29	6.53	11.43	32.63	22.86	65.26
FBB37	6.21	17.73	31.06	88.67	62.11	177.34
FBB38	9.06	25.88	45.32	129.41	90.65	258.81
FBB39	7.63	21.79	38.17	108.97	76.33	217.94



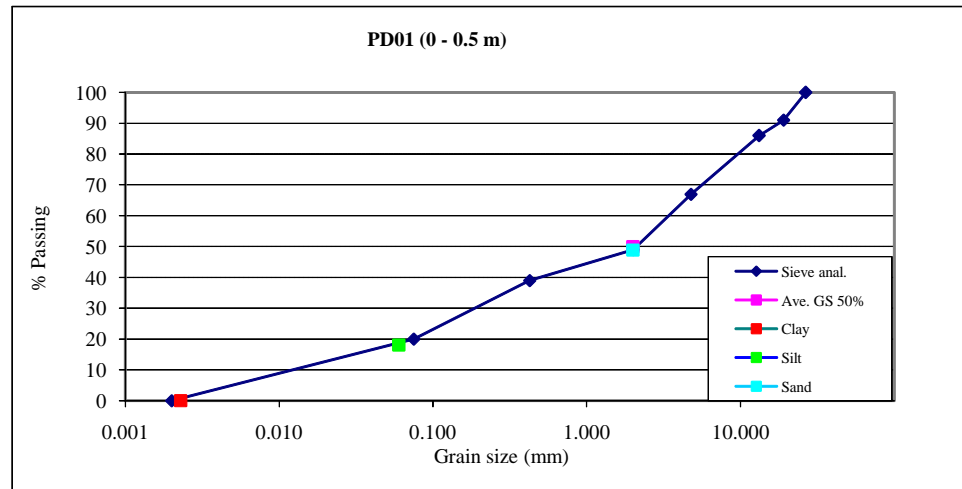
Appendix E
Soil hydraulic parameters

DETERMINATION OF SOIL HYDRAULIC PARAMETERS

Date: 18-Jan-10
Sample no.: PD01
Material Depth: (0 -0.5 m)
Classification: Brown Sand

Grain size d (mm)	Sieve anal. (%)	Hydraulic Conductivity		
		<u>Shephard (1989)</u> Calculated	(m/day)	(m/s)
26.5	100		85.9043	9.94E-04
19.00	91			
13.20	86			
4.760	67	<u>Rawls & Brakensiek (1985)</u> Calculated	(m/day)	(m/s)
2.000	49		0.1254	1.45E-06
0.425	39	<u>Brooks & Corey Parameters</u>		
0.075	20	Porosity	30%	Est.
0.002	0	Residual water saturation	0.1003	
2.00	Ave. GS 50%	Air entry head	0.1735	
		Pore size distr.	0.4468	

	Clay	Silt	Sand	Gravel
Grain Size (mm)	< 0.002	< 0.06	< 2	< 60
% Passing	0	18	48.8	100
% Fraction	0	18	30.8	51.2

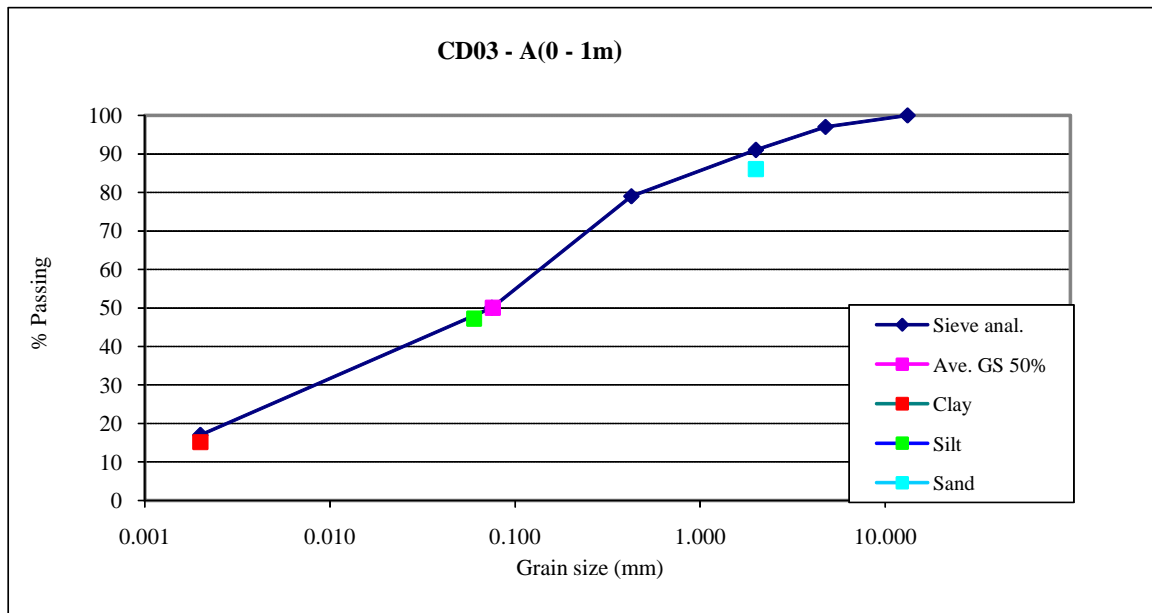


DETERMINATION OF SOIL HYDRAULIC PARAMETERS

Date: 18-Jan-10
Sample no.: CD03 - A
Material Depth: (0 - 1 m)
Classification: Red Clayey Sand

Grain size d (mm)	Sieve anal. (%)	Hydraulic Conductivity		
		<u>Shephard (1989)</u>	(m/day)	(m/s)
26.5		Calculated	0.6368	7.37E-06
19.00				
13.20	100	<u>Rawls & Brakensiek (1985)</u>	(m/day)	(m/s)
4.760	97	Calculated	0.0994	1.15E-06
2.000	91			
0.425	79	<u>Brooks & Corey Parameters</u>		
0.075	50	Porosity	30%	Est.
0.002	17	Residual water saturation	0.2286	
0.08	Ave. GS 50%	Air entry head	0.7607	
		Pore size distr.	0.3732	

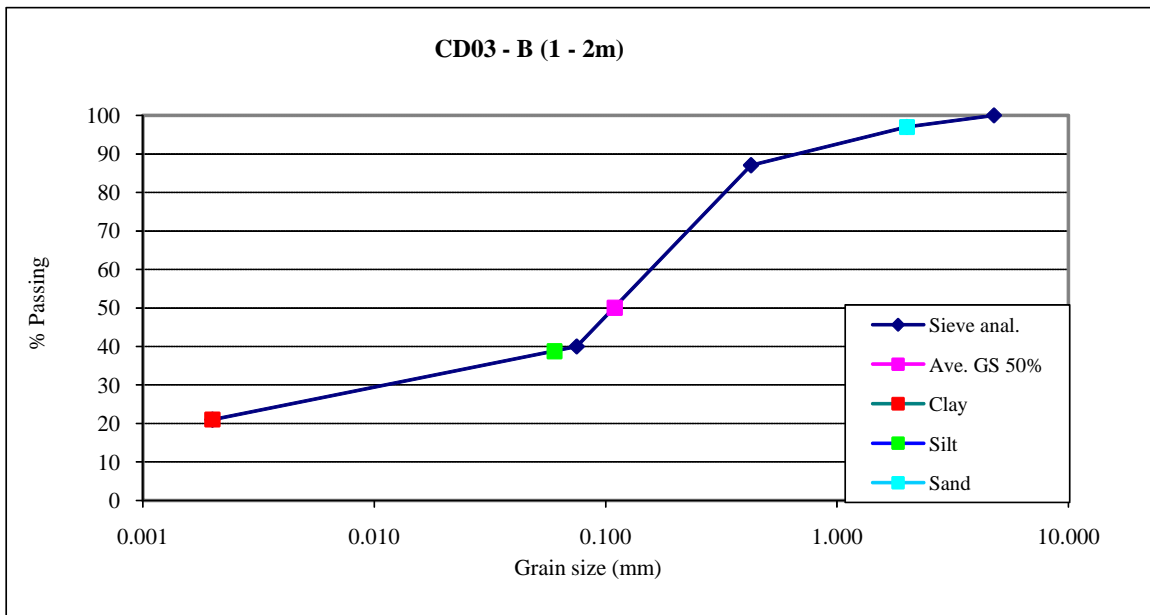
	Clay	Silt	Sand	Gravel
Grain Size (mm)	< 0.002	< 0.06	< 2	< 60
% Passing	15.2	47.2	86	100
% Fraction	15.2	32	38.8	14



DETERMINATION OF SOIL HYDRAULIC PARAMETERS

Date: 18-Jan-11
Sample no.: CD03 - B
Material Depth: (1 - 2m)
Classification: Red Clayey Sand

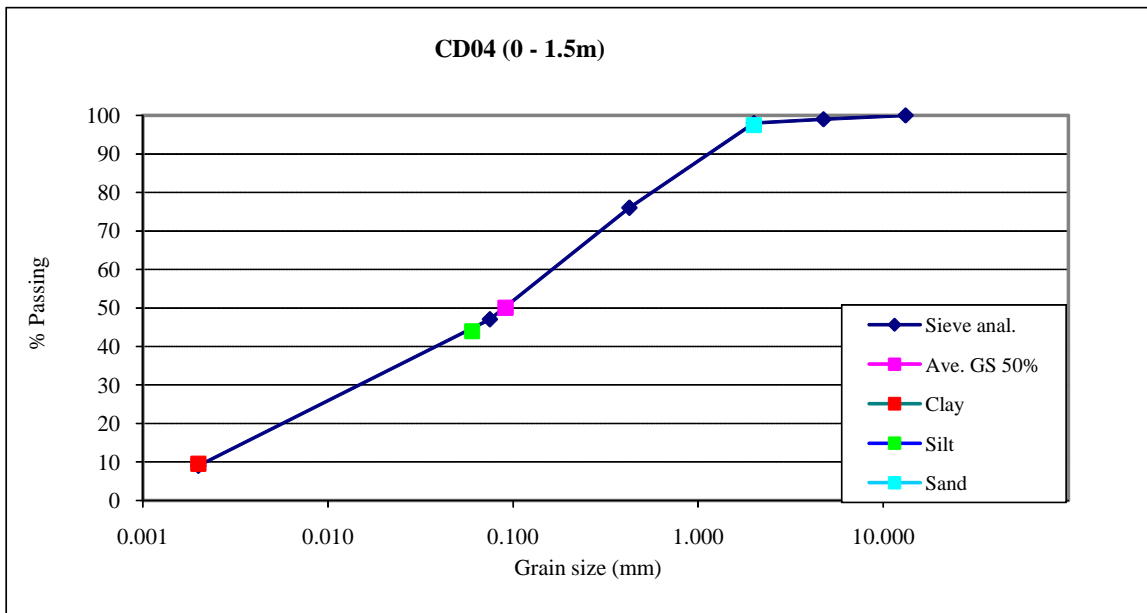
Grain size d (mm)	Sieve anal. (%)	Hydraulic Conductivity		
		<u>Shephard (1989)</u>	(m/day)	(m/s)
26.5		Calculated	1.1067	1.28E-05
19.00				
13.20		<u>Rawls & Brakensiek (1985)</u>	(m/day)	(m/s)
4.760	100	Calculated	0.2996	3.47E-06
2.000	97			
0.425	87			
0.075	40			
0.002	21			
0.11	Ave. GS 50%			
		<u>Brooks & Corey Parameters</u>		
		Porosity	30%	Est.
		Residual water saturation	0.3051	
		Air entry head	0.3621	
		Pore size distr.	0.3061	
<hr/>				
	Clay	Silt	Sand	Gravel
Grain Size (mm)	< 0.002	< 0.06	< 2	< 60
% Passing	21.1	38.7	97	100
% Fraction	21.1	17.6	58.3	3



DETERMINATION OF SOIL HYDRAULIC PARAMETERS

Date: 18-Jan-11
Sample no.: CD04
Material Depth: (0 - 1.5m)
Classification: Red Clayey Sand

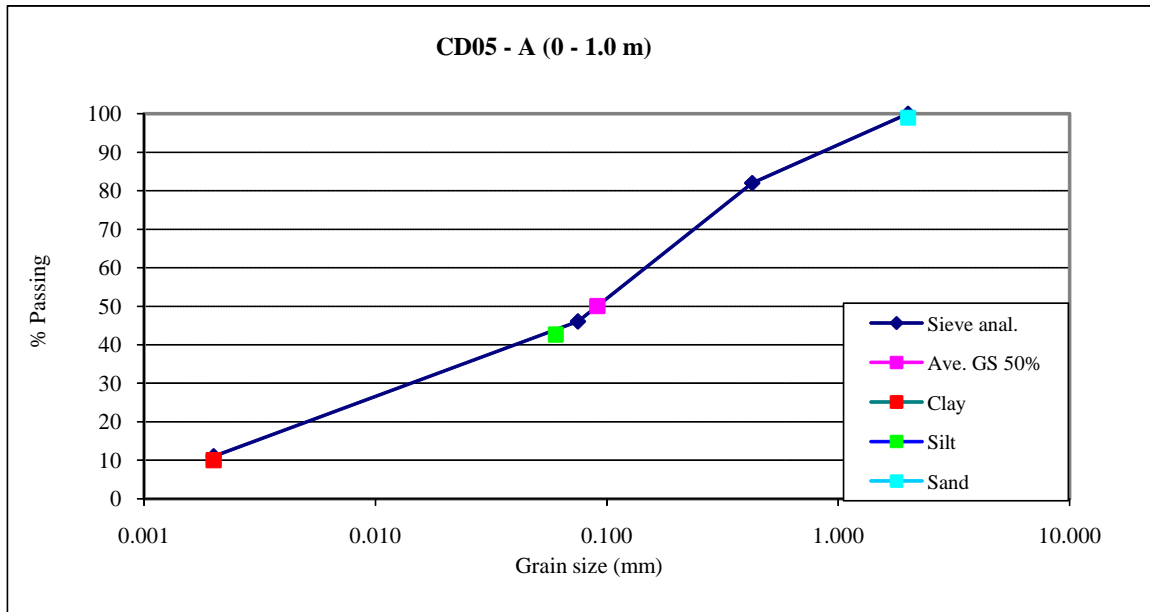
Grain size d (mm)	Sieve anal. (%)	<u>Hydraulic Conductivity</u>		
26.5		<u>Shephard (1989)</u>		(m/day)
19.00		Calculated		9.72E-06
13.20	100	<u>Rawls & Brakensiek (1985)</u>		(m/day)
4.760	99	Calculated		5.09E-06
2.000	98	<u>Brooks & Corey Parameters</u>		
0.425	76	Porosity	30%	Est.
0.075	47	Residual water saturation	0.1986	
0.002	9	Air entry head	0.4131	
0.09	Ave. GS 50%	Pore size distr.	0.4575	
		Clay	Silt	Sand
Grain Size (mm)	< 0.002	< 0.06	< 2	< 60
% Passing	9.5	44	97.5	100
% Fraction	9.5	34.5	53.5	2.5



DETERMINATION OF SOIL HYDRAULIC PARAMETERS

Date: 18-Jan-11
Sample no.: CD05 - A
Material Depth: (0 - 1m)
Classification: Red Clayey Sand

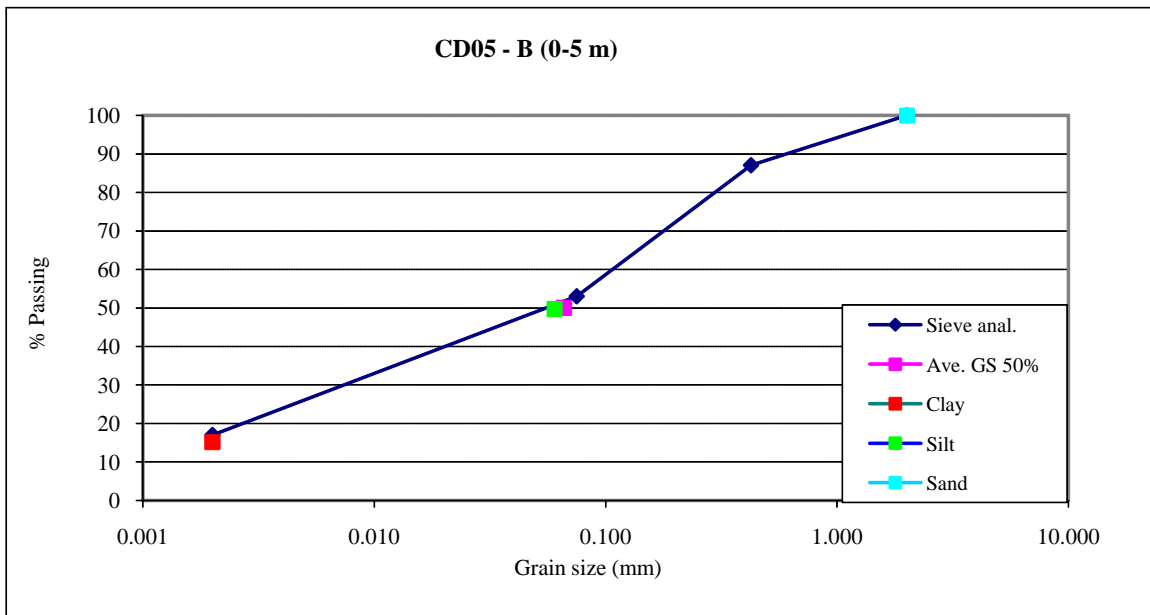
Grain size d (mm)	Sieve anal. (%)	<u>Hydraulic Conductivity</u>		
26.5		<u>Shephard (1989)</u>		(m/day)
19.00		Calculated		(m/s)
13.20				9.72E-06
4.760		<u>Rawls & Brakensiek (1985)</u>		(m/day)
2.000	100	Calculated		(m/s)
0.425	82			6.30E-06
0.075	46	<u>Brooks & Corey Parameters</u>		
0.002	11	Porosity	30%	Est.
0.09	Ave. GS 50%	Residual water saturation	0.2096	
		Air entry head	0.3735	
		Pore size distr.	0.4555	
		<u>Clay</u>	<u>Silt</u>	<u>Sand</u>
<u>Grain Size (mm)</u>	< 0.002	< 0.06	< 2	< 60
% Passing	10	42.6	99	100
% Fraction	10	32.6	56.4	1



DETERMINATION OF SOIL HYDRAULIC PARAMETERS

Date: 18-Jan-11
Sample no.: CD05 - B
Material Depth: (1 - 2m)
Classification: Red Sandy Clay

Grain size d (mm)	Sieve anal. (%)	Hydraulic Conductivity		
		<u>Shephard (1989)</u>	(m/day)	(m/s)
26.5		Calculated	0.5176	5.99E-06
19.00				
13.20		<u>Rawls & Brakensiek (1985)</u>	(m/day)	(m/s)
4.760		Calculated	0.2417	2.80E-06
2.000	100			
0.425	87			
0.075	53			
0.002	17			
0.07	Ave. GS 50%			
		<u>Brooks & Corey Parameters</u>		
		Porosity	30%	Est.
		Residual water saturation	0.2496	
		Air entry head	0.4968	
		Pore size distr.	0.3850	
		Clay	Silt	Sand
Grain Size (mm)	< 0.002	< 0.06	< 2	< 60
% Passing	15.2	49.7	100	100
% Fraction	15.2	34.5	50.3	0

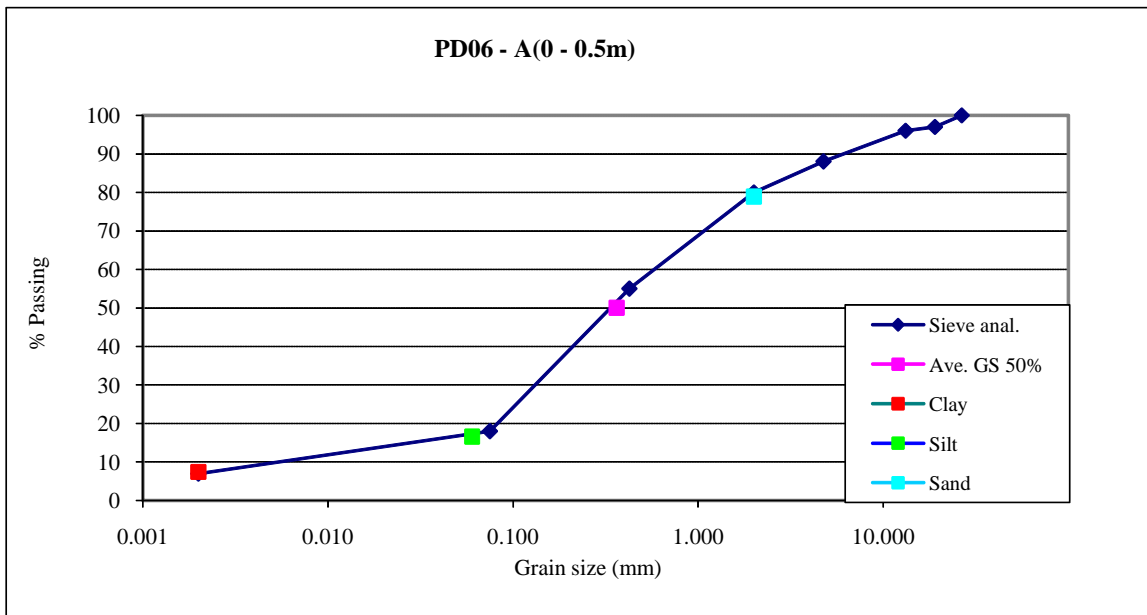


DETERMINATION OF SOIL HYDRAULIC PARAMETERS

Date: 18-Jan-11
Sample no.: PD06 - A
Material Depth: (0 - 0.5m)
Classification: Brown Clayey Sand and Calcrete

Grain size d (mm)	Sieve anal. (%)	Hydraulic Conductivity		
		<u>Shephard (1989)</u> Calculated	(m/day)	(m/s)
26.5	100		6.6683	7.72E-05
19.00	97			
13.20	96			
4.760	88	<u>Rawls & Brakensiek (1985)</u> Calculated	(m/day)	(m/s)
2.000	80		0.9388	1.09E-05
0.425	55	<u>Brooks & Corey Parameters</u>		
0.075	18	Porosity	30%	Est.
0.002	7	Residual water saturation	0.1907	
0.36	Ave. GS 50%	Air entry head	0.3007	
		Pore size distr.	0.4916	

	Clay	Silt	Sand	Gravel
Grain Size (mm)	< 0.002	< 0.06	< 2	< 60
% Passing	7.5	16.6	78.9	100
% Fraction	7.5	9.1	62.3	21.1

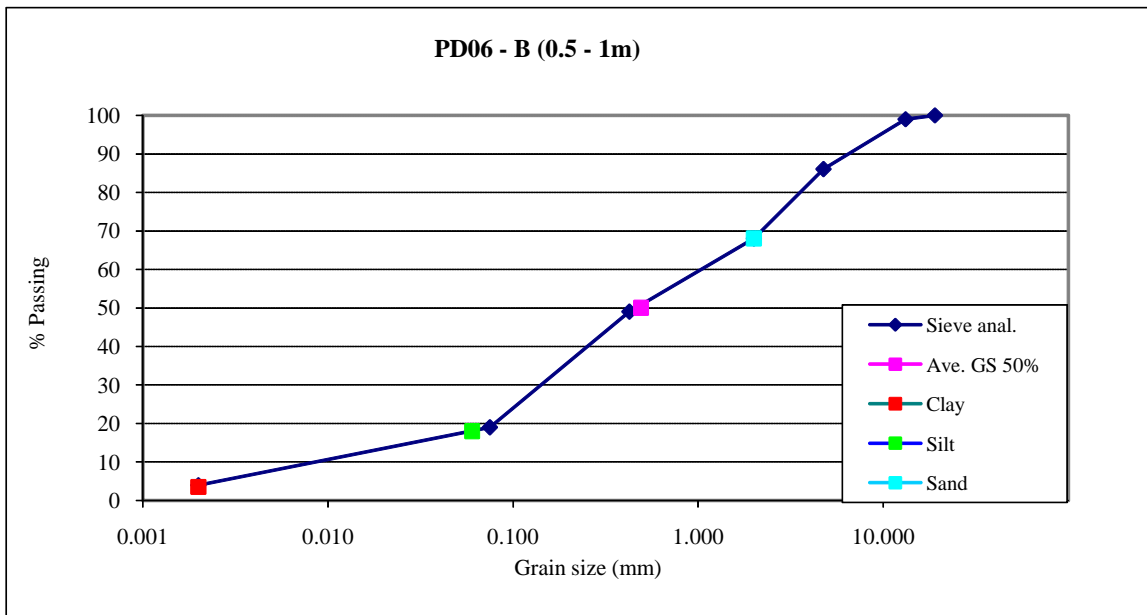


DETERMINATION OF SOIL HYDRAULIC PARAMETERS

Date: 18-Jan-11
Sample no.: PD06 - B
Material Depth: (0.5 - 1m)
Classification: Brown Clayey Sand

Grain size d (mm)	Sieve anal. (%)	Hydraulic Conductivity		
26.5		<u>Shephard (1989)</u>		
19.00	100	(m/day)	(m/s)	
13.20	99	Calculated	10.4476	1.21E-04
4.760	86	<u>Rawls & Brakensiek (1985)</u>		
2.000	68	(m/day)	(m/s)	
0.425	49	Calculated	0.3863	4.47E-06
0.075	19	<u>Brooks & Corey Parameters</u>		
0.002	4	Porosity	30%	Est.
0.49	Ave. GS 50%	Residual water saturation	0.1354	
		Air entry head	0.4395	
		Pore size distr.	0.4936	

	Clay	Silt	Sand	Gravel
Grain Size (mm)	< 0.002	< 0.06	< 2	< 60
% Passing	3.6	18	68	100
% Fraction	3.6	14.4	50	32

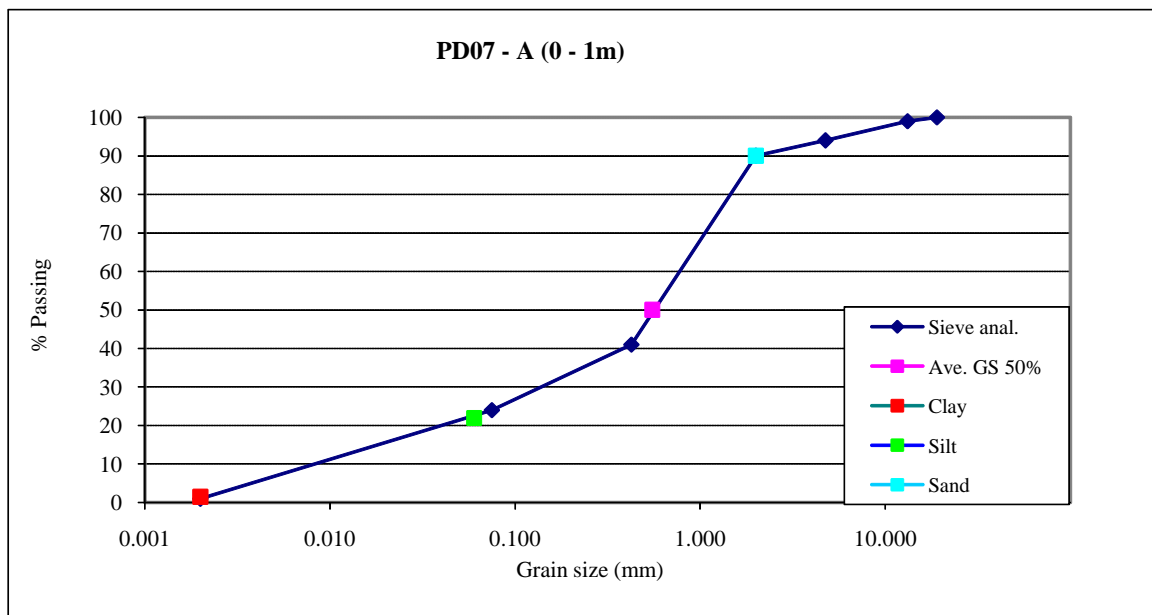


DETERMINATION OF SOIL HYDRAULIC PARAMETERS

Date: 18-Jan-11
Sample no.: PD07 - A
Material Depth: (0 - 1m)
Classification: Brown Sand

Grain size d (mm)	Sieve anal. (%)	Hydraulic Conductivity		
		<u>Shephard (1989)</u>	(m/day)	(m/s)
26.5		Calculated	12.4170	1.44E-04
19.00	100			
13.20	99			
4.760	94	<u>Rawls & Brakensiek (1985)</u>	(m/day)	(m/s)
2.000	90	Calculated	0.1358	1.57E-06
0.425	41			
0.075	24	<u>Brooks & Corey Parameters</u>		
0.002	1	Porosity	30%	Est.
0.55	Ave. GS 50%	Residual water saturation	0.1663	
		Air entry head	0.2614	
		Pore size distr.	0.5256	

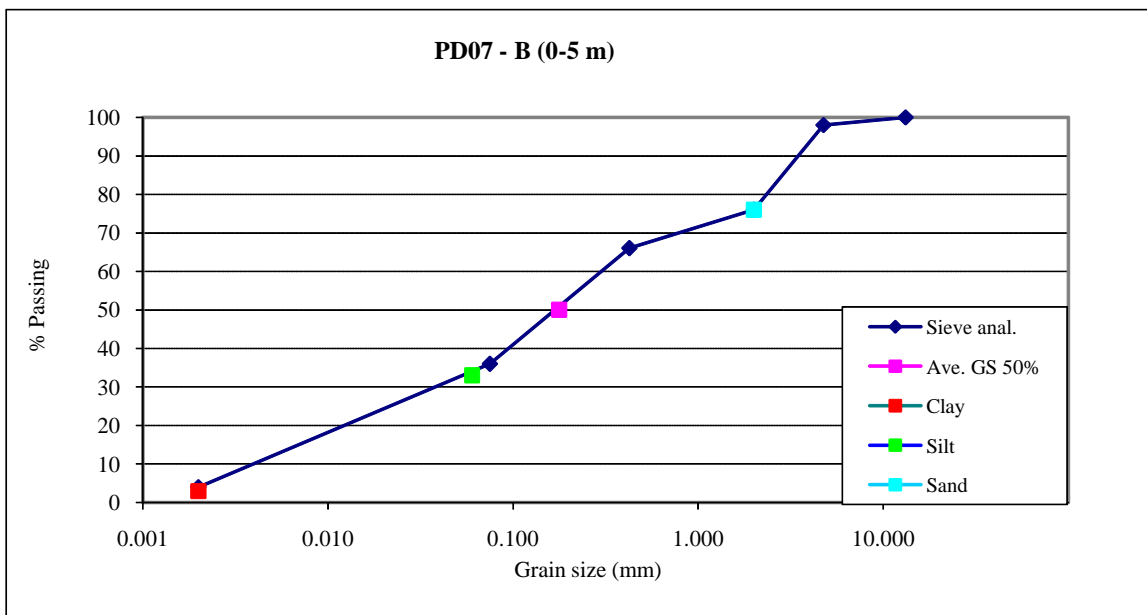
	Clay	Silt	Sand	Gravel
Grain Size (mm)	< 0.002	< 0.06	< 2	< 60
% Passing	1.5	22	90	100
% Fraction	1.5	20.5	68	10



DETERMINATION OF SOIL HYDRAULIC PARAMETERS

Date: 18-Jan-11
Sample no.: PD07 - B
Material Depth: (1 - 1.8m)
Classification: Dark Brown Sand

Grain size d (mm)	Sieve anal. (%)	<u>Hydraulic Conductivity</u>		
26.5		<u>Shephard (1989)</u>		(m/day)
19.00		Calculated		2.2857
13.20	100	<u>Rawls & Brakensiek (1985)</u>		(m/day)
4.760	98	Calculated		0.2469
2.000	76	<u>Brooks & Corey Parameters</u>		
0.425	66	Porosity	30%	Est.
0.075	36	Residual water saturation	0.1226	
0.002	4	Air entry head	0.5313	
0.18	Ave. GS 50%	Pore size distr.	0.4777	
		<u>Clay</u>	<u>Silt</u>	<u>Sand</u>
Grain Size (mm)	< 0.002	< 0.06	< 2	< 60
% Passing	3	33	76	100
% Fraction	3	30	43	24

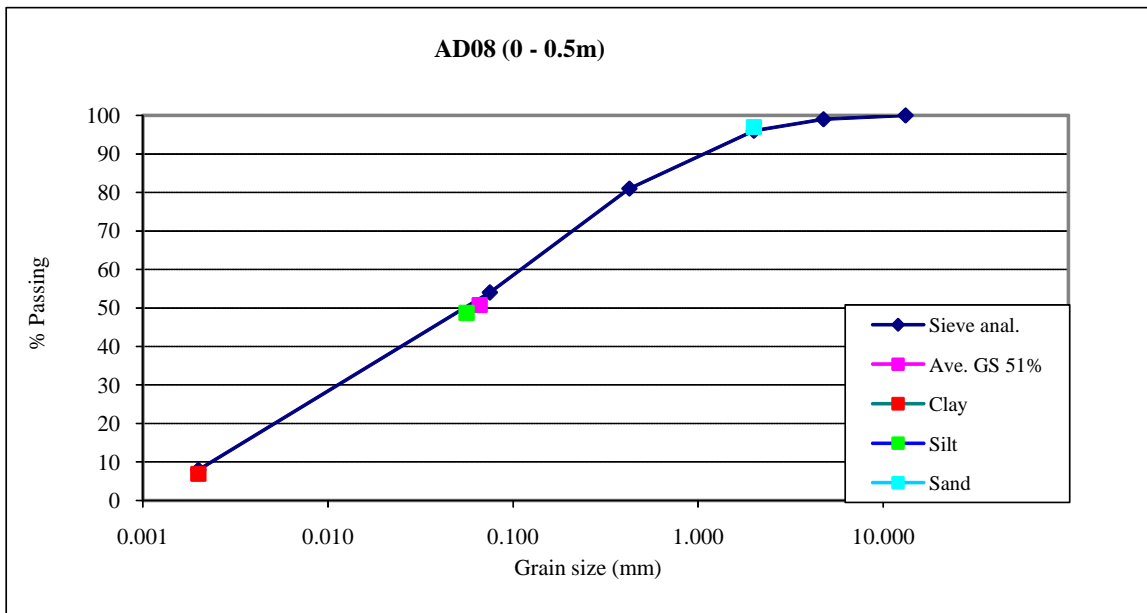


DETERMINATION OF SOIL HYDRAULIC PARAMETERS

Date: 18-Jan-11
Sample no.: AD08
Material Depth: (0 - 2m)
Classification: Brown Sandy Clay

Grain size d (mm)	Sieve anal. (%)	Hydraulic Conductivity		
		<u>Shephard (1989)</u>	(m/day)	(m/s)
26.5		Calculated	0.5176	5.99E-06
19.00				
13.20	100	<u>Rawls & Brakensiek (1985)</u>	(m/day)	(m/s)
4.760	99	Calculated	0.3280	3.80E-06
2.000	96			
0.425	81	<u>Brooks & Corey Parameters</u>		
0.075	54	Porosity	30%	Est.
0.002	8	Residual water saturation	0.1589	
0.07	Ave. GS 51%	Air entry head	0.4747	
		Pore size distr.	0.4738	

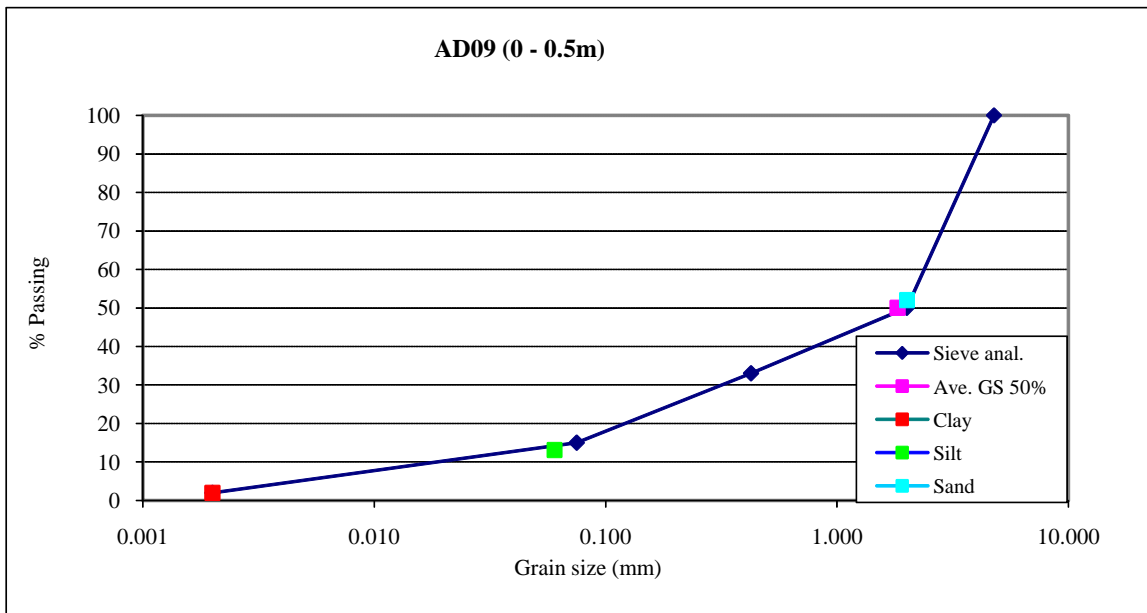
	Clay	Silt	Sand	Gravel
Grain Size (mm)	< 0.002	< 0.06	< 2	< 60
% Passing	7	48.7	97	100
% Fraction	7	41.7	48.3	3



DETERMINATION OF SOIL HYDRAULIC PARAMETERS

Date: 18-Jan-11
Sample no.: AD09
Material Depth: (0 - 0.5m)
Classification: Red Brown Clayey Sand

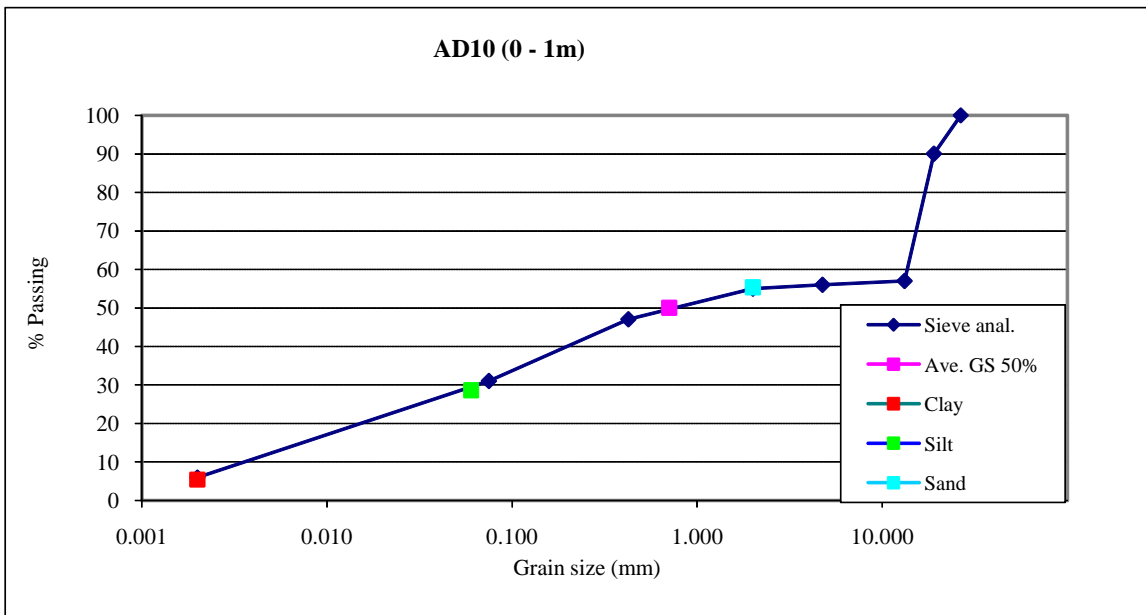
Grain size d (mm)	Sieve anal. (%)	<u>Hydraulic Conductivity</u>		
26.5		<u>Shephard (1989)</u>		
19.00		(m/day)	(m/s)	
13.20		Calculated	75.3382	8.72E-04
4.760	100	<u>Rawls & Brakensiek (1985)</u>		
2.000	50	(m/day)	(m/s)	
0.425	33	Calculated	0.1938	2.24E-06
0.075	15	<u>Brooks & Corey Parameters</u>		
0.002	2	Porosity	30%	Est.
1.83	Ave. GS 50%	Residual water saturation	0.1151	
		Air entry head	0.5896	
		Pore size distr.	0.4677	
	Clay	Silt	Sand	Gravel
Grain Size (mm)	< 0.002	< 0.06	< 2	< 60
% Passing	2	13.1	52	100
% Fraction	2	11.1	38.9	48



DETERMINATION OF SOIL HYDRAULIC PARAMETERS

Date: 18-Jan-11
Sample no.: AD10
Material Depth: (0 - 1m)
Classification: Orange Brown Clayey Sand, Ferricrete and Mudstone

Grain size d (mm)	Sieve anal. (%)	<u>Hydraulic Conductivity</u>		
26.5	100	<u>Shephard (1989)</u>		(m/day)
19.00	90	Calculated		2.10E-04
13.20	57	<u>Rawls & Brakensiek (1985)</u>		(m/day)
4.760	56	Calculated		1.16E-06
2.000	55	<u>Brooks & Corey Parameters</u>		
0.425	47	Porosity	30%	Est.
0.075	31	Residual water saturation	0.9968	
0.002	6	Air entry head	0.7933	
0.71	Ave. GS 50%	Pore size distr.	0.4332	
		<u>Clay</u>	<u>Silt</u>	<u>Sand</u>
Grain Size (mm)	< 0.002	< 0.06	< 2	< 60
% Passing	5.5	28.6	55.3	100
% Fraction	5.5	23.1	26.7	44.7

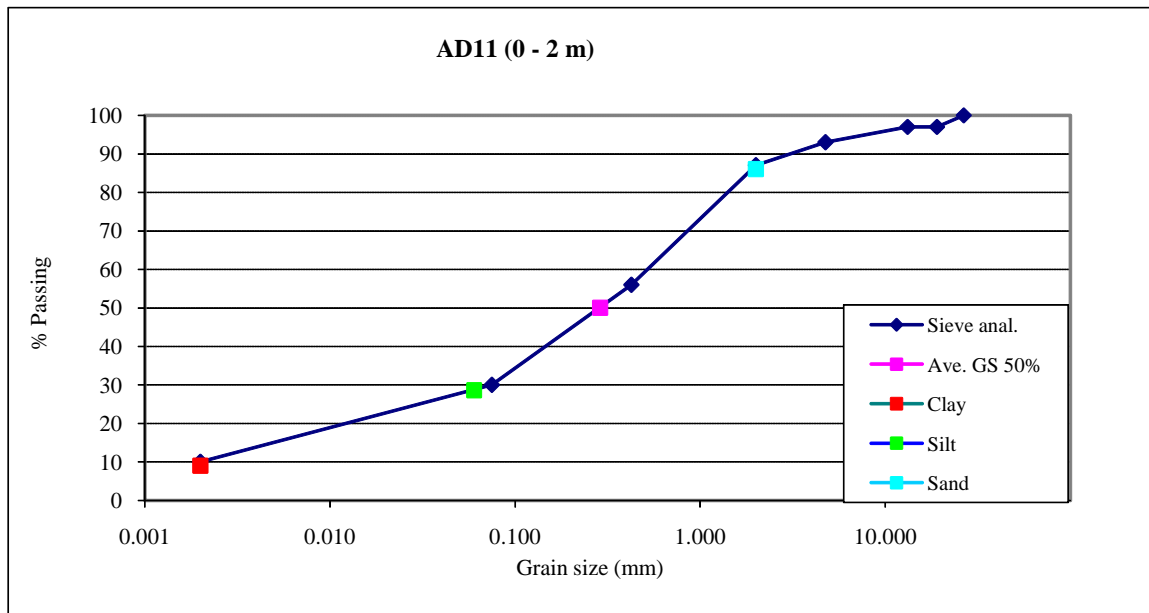


DETERMINATION OF SOIL HYDRAULIC PARAMETERS

Date: 18-Jan-11
Sample no.: AB11
Material Depth: (0 - 2m)
Classification: Red Clayey Sand

Grain size d (mm)	Sieve anal. (%)	<u>Hydraulic Conductivity</u>	
26.5	100	<u>Shephard (1989)</u>	(m/day) (m/s)
19.00	97	Calculated	4.7208 5.46E-05
13.20	97	<u>Rawls & Brakensiek (1985)</u>	(m/day) (m/s)
4.760	93	Calculated	0.6103 7.06E-06
2.000	87	<u>Brooks & Corey Parameters</u>	
0.425	56	Porosity	30% Est.
0.075	30	Residual water saturation	0.1999
0.002	10	Air entry head	0.3585
0.29	Ave. GS 50%	Pore size distr.	0.4683

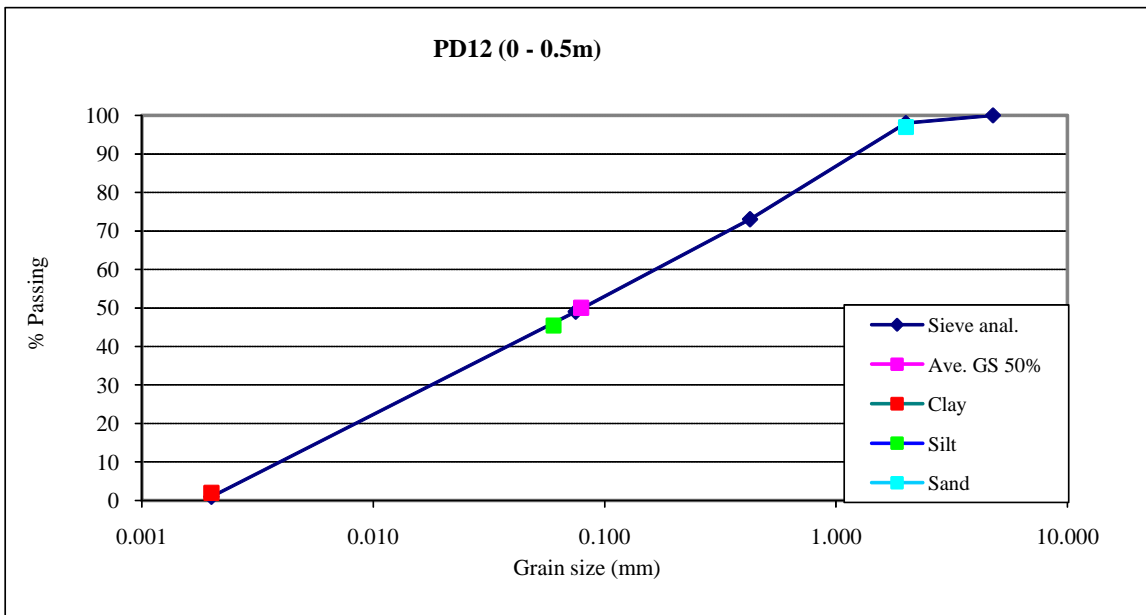
	Clay	Silt	Sand	Gravel
Grain Size (mm)	< 0.002	< 0.06	< 2	< 60
% Passing	9	28.6	86	100
% Fraction	9	19.6	57.4	14



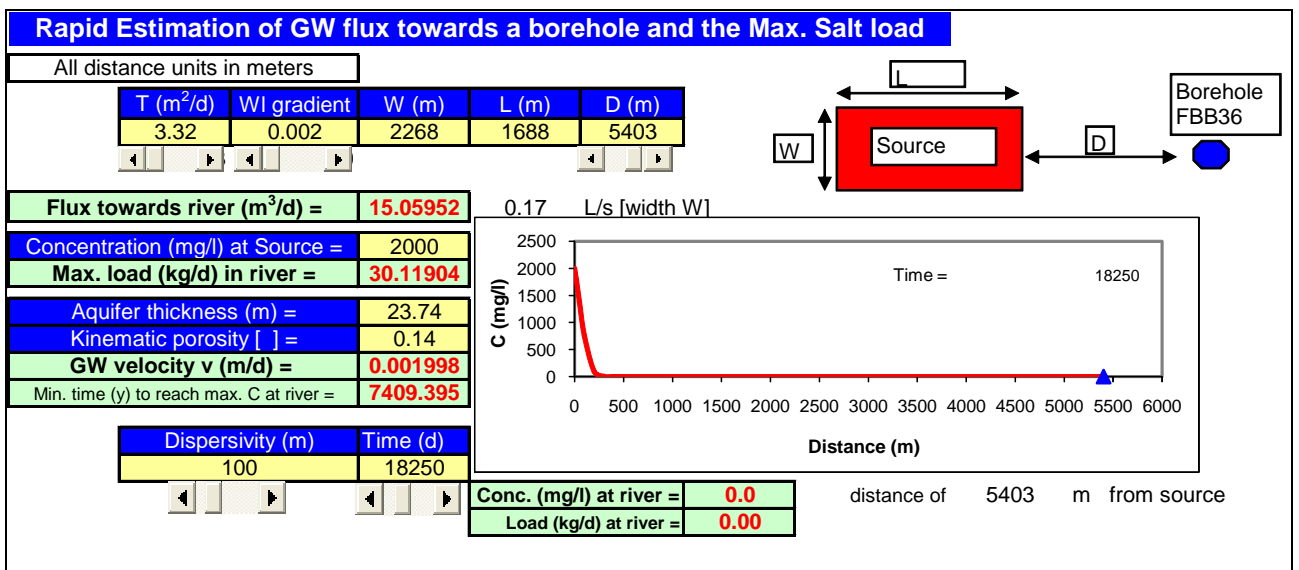
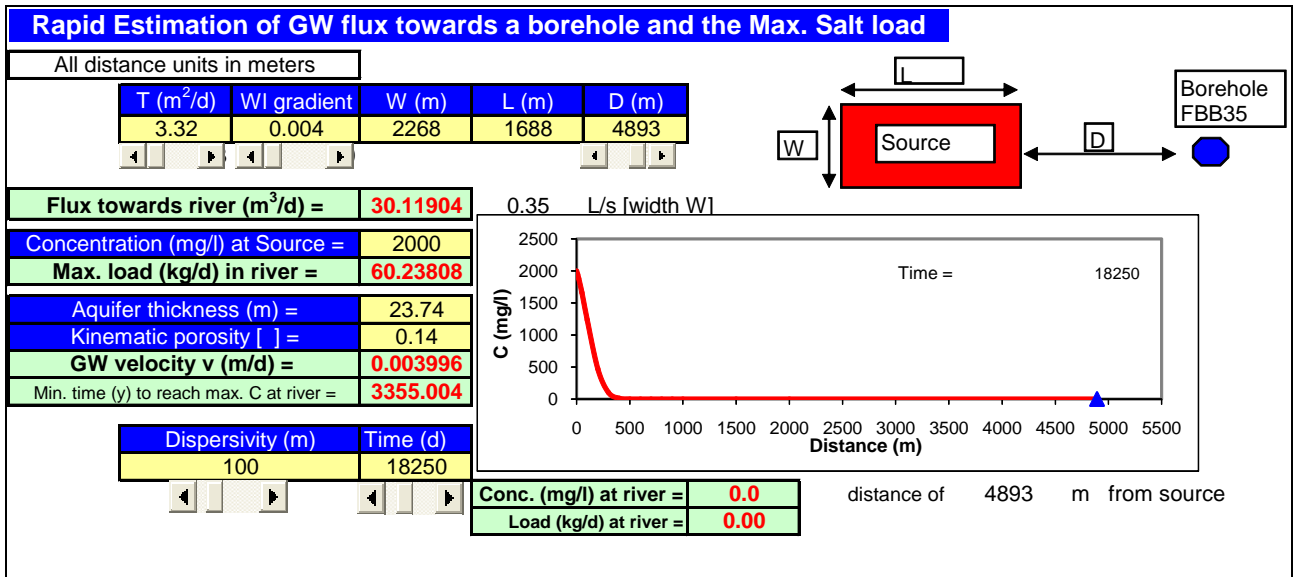
DETERMINATION OF SOIL HYDRAULIC PARAMETERS

Date: 18-Jan-11
Sample no.: PD12
Material Depth: (0 - 0.5m)
Classification: Light Brown Clayey Sand

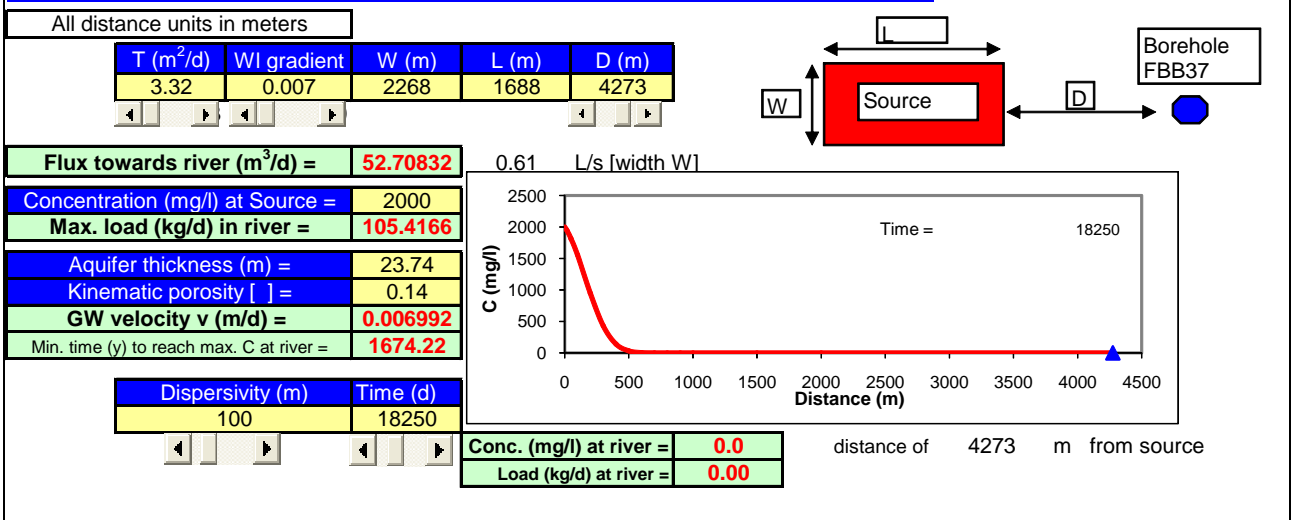
Grain size d (mm)	Sieve anal. (%)	<u>Hydraulic Conductivity</u>		
26.5		<u>Shephard (1989)</u>		(m/day)
19.00		Calculated		7.87E-06
13.20		<u>Rawls & Brakensiek (1985)</u>		(m/day)
4.760	100	Calculated		4.95E-06
2.000	98			
0.425	73	<u>Brooks & Corey Parameters</u>		
0.075	49	Porosity	30%	Est.
0.002	1	Residual water saturation	0.1381	
0.08	Ave. GS 50%	Air entry head	0.2411	
		Pore size distr.	0.4969	
		<u>Clay</u>	<u>Silt</u>	<u>Sand</u>
Grain Size (mm)	< 0.002	< 0.06	< 2	< 60
% Passing	2	45.5	97	100
% Fraction	2	43.5	51.5	3



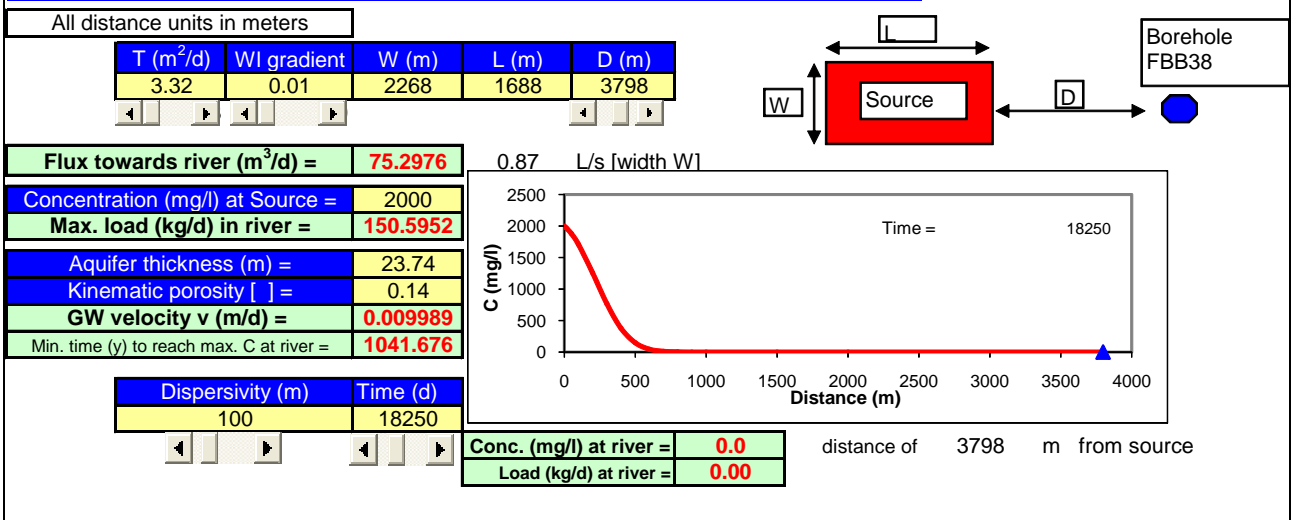
Appendix F
 Ogata Banks results
 Ash Stack



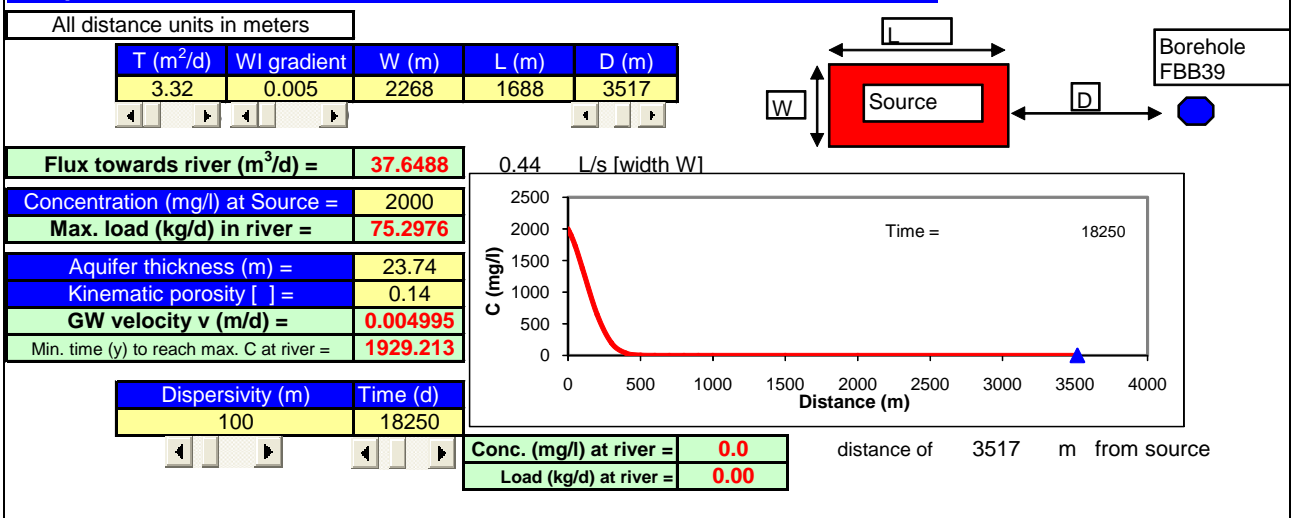
Rapid Estimation of GW flux towards a borehole and the Max. Salt load



Rapid Estimation of GW flux towards a borehole and the Max. Salt load



Rapid Estimation of GW flux towards a borehole and the Max. Salt load



Rapid Estimation of GW flux towards a borehole and the Max. Salt load

All distance units in meters

T (m ² /d)	WI gradient	W (m)	L (m)	D (m)
3.32	0.005	1045	320	4040

Flux towards river (m³/d) =	17.347
Concentration (mg/l) at Source =	2000
Max. load (kg/d) in river =	34.694
Aquifer thickness (m) =	23.74
Kinematic porosity [] =	0.14
GW velocity v (m/d) =	0.004995
Min. time (y) to reach max. C at river =	2216.099

Dispersivity (m)	Time (d)
100	18250

Borehole FBB26

0.20 L/s [width W]

Time = 18250

distance of 4040 m from source

Conc. (mg/l) at river =	0.0
Load (kg/d) at river =	0.00

Rapid Estimation of GW flux towards a borehole and the Max. Salt load

All distance units in meters

T (m ² /d)	WI gradient	W (m)	L (m)	D (m)
3.32	0.003	1045	320	4646

Flux towards river (m³/d) =	10.4082
Concentration (mg/l) at Source =	2000
Max. load (kg/d) in river =	20.8164
Aquifer thickness (m) =	23.74
Kinematic porosity [] =	0.14
GW velocity v (m/d) =	0.002997
Min. time (y) to reach max. C at river =	4247.523

Dispersivity (m)	Time (d)
100	18250

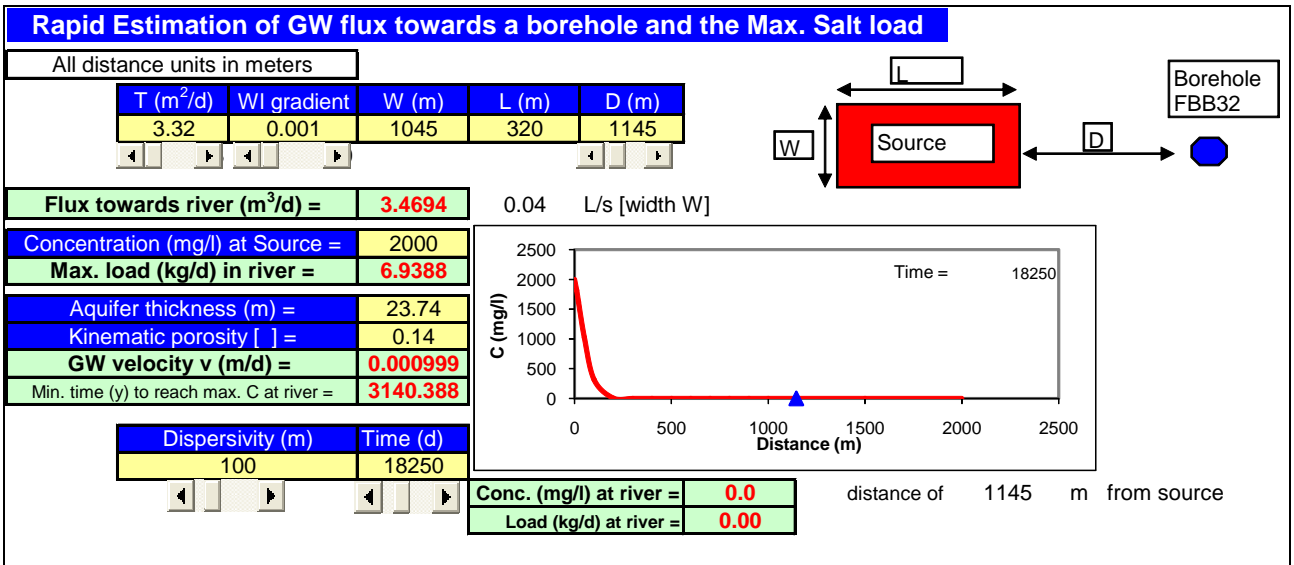
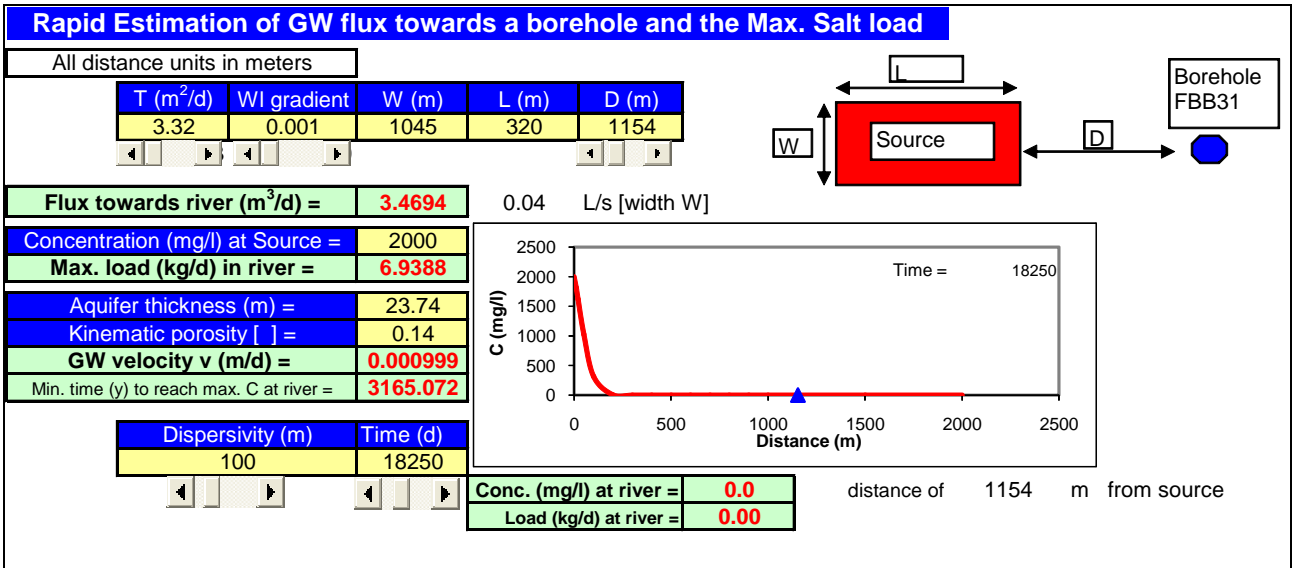
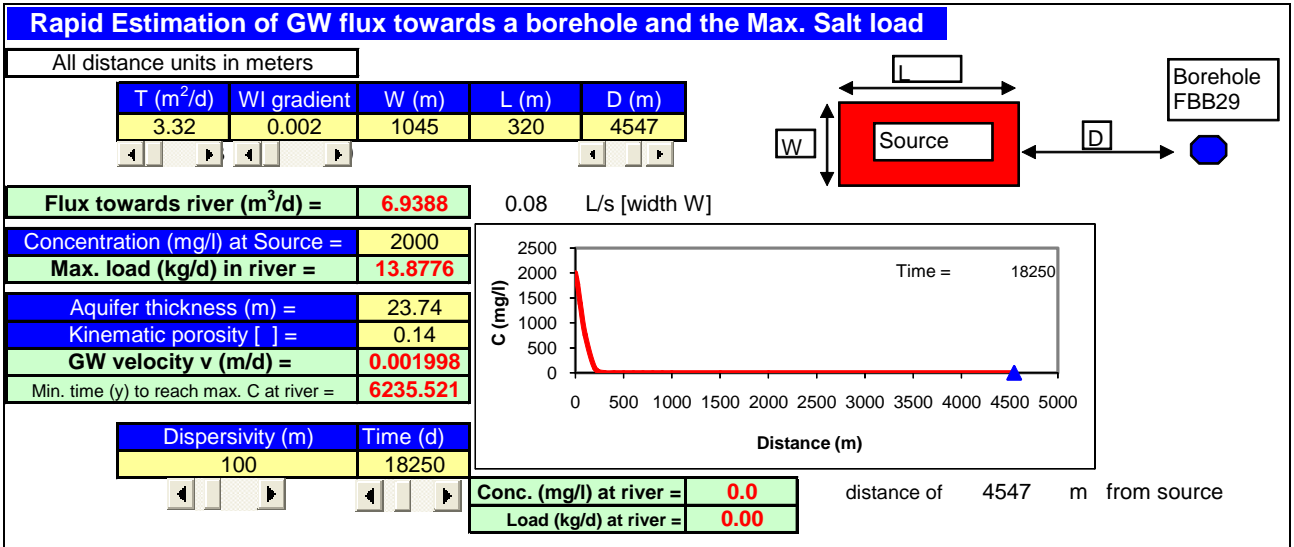
Borehole FBB28

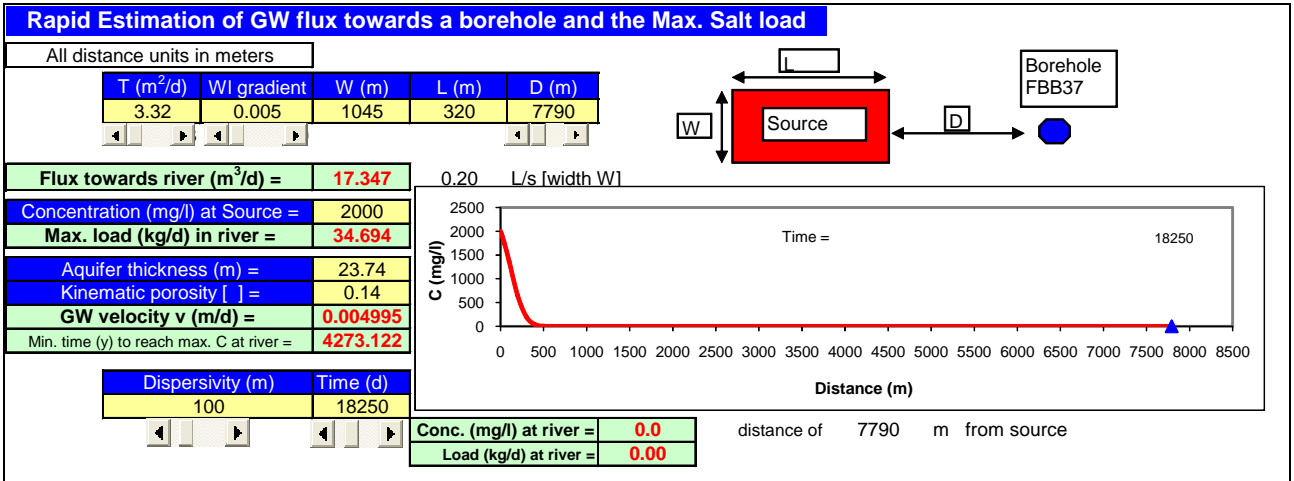
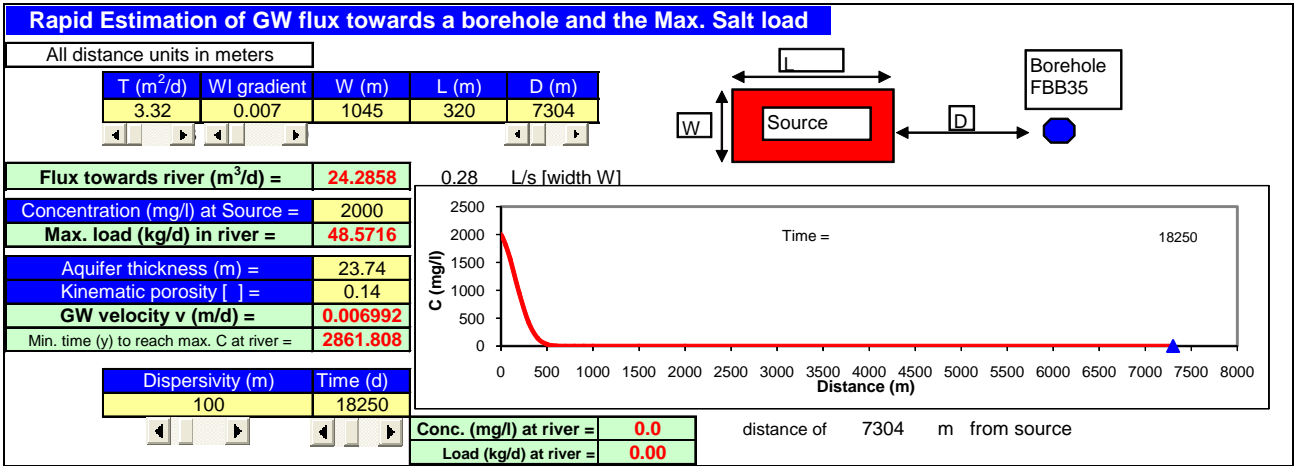
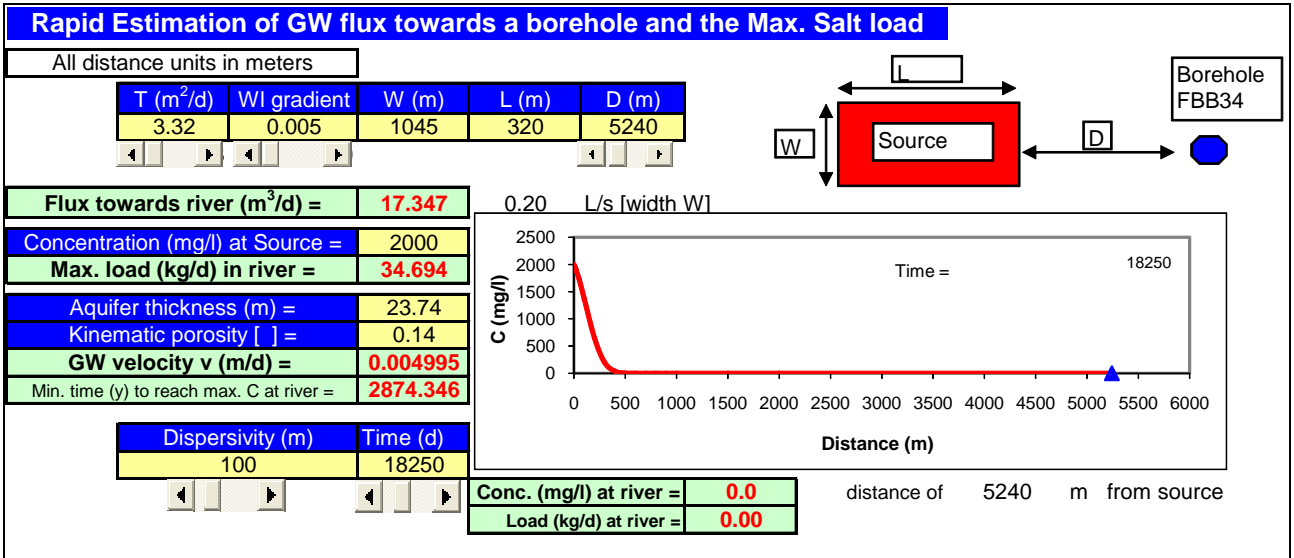
0.12 L/s [width W]

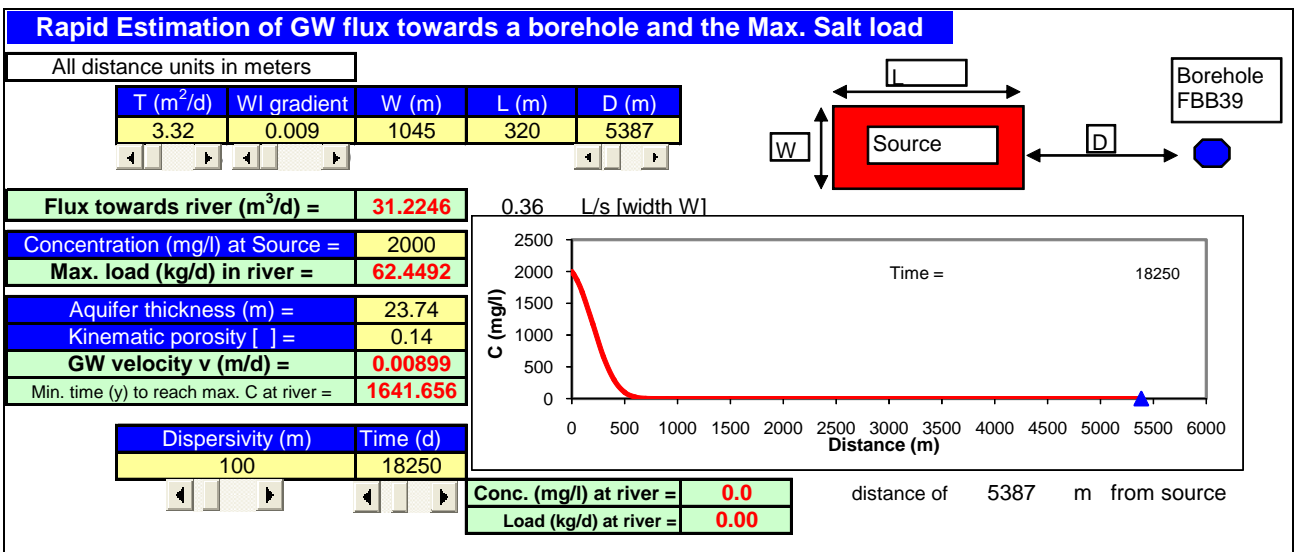
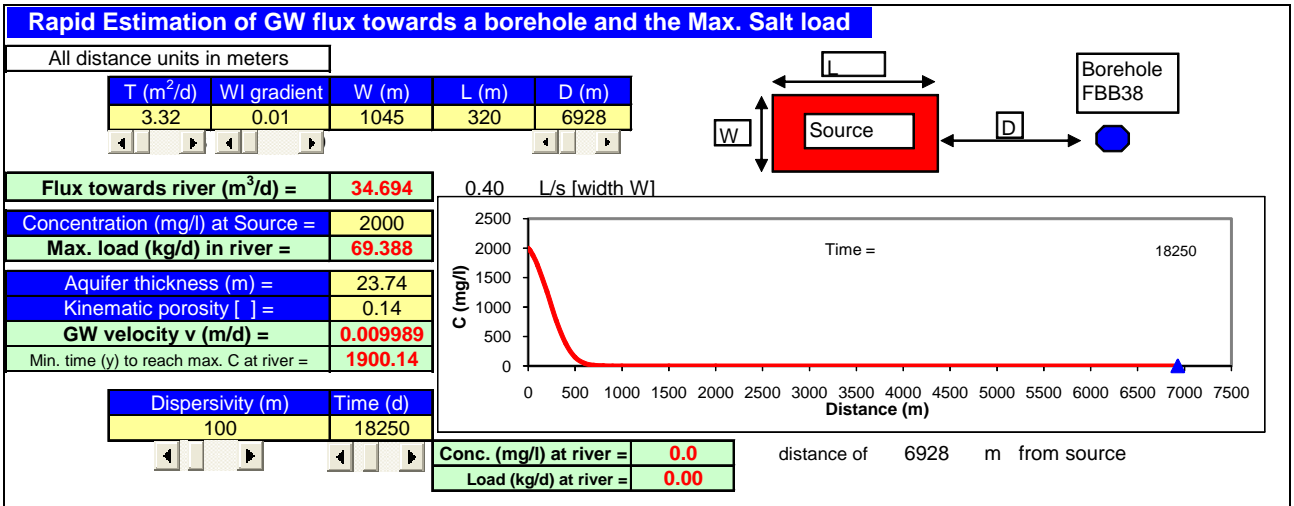
Time = 18250

distance of 4646 m from source

Conc. (mg/l) at river =	0.0
Load (kg/d) at river =	0.00







Emergency stack

Rapid Estimation of GW flux towards a borehole and the Max. Salt load

All distance units in meters

T (m ² /d)	WI gradient	W (m)	L (m)	D (m)
3.32	0.002	240	93	6828

Flux towards river (m ³ /d) =	1.5936
Concentration (mg/l) at Source =	2000
Max. load (kg/d) in river =	3.1872
Aquifer thickness (m) =	23.74
Kinematic porosity [] =	0.14
GW velocity v (m/d) =	0.001998
Min. time (y) to reach max. C at river =	9363.567

0.02 L/s [width W]

Time = 18250

Conc. (mg/l) at river = 0.0 distance of 6828 m from source
 Load (kg/d) at river = 0.00

Rapid Estimation of GW flux towards a borehole and the Max. Salt load

All distance units in meters

T (m ² /d)	WI gradient	W (m)	L (m)	D (m)
3.32	0.002	240	93	5362

Flux towards river (m ³ /d) =	1.5936
Concentration (mg/l) at Source =	2000
Max. load (kg/d) in river =	3.1872
Aquifer thickness (m) =	23.74
Kinematic porosity [] =	0.14
GW velocity v (m/d) =	0.001998
Min. time (y) to reach max. C at river =	7353.17

0.02 L/s [width W]

Time = 18250

Conc. (mg/l) at river = 0.0 distance of 5362 m from source
 Load (kg/d) at river = 0.00

Rapid Estimation of GW flux towards a borehole and the Max. Salt load

All distance units in meters

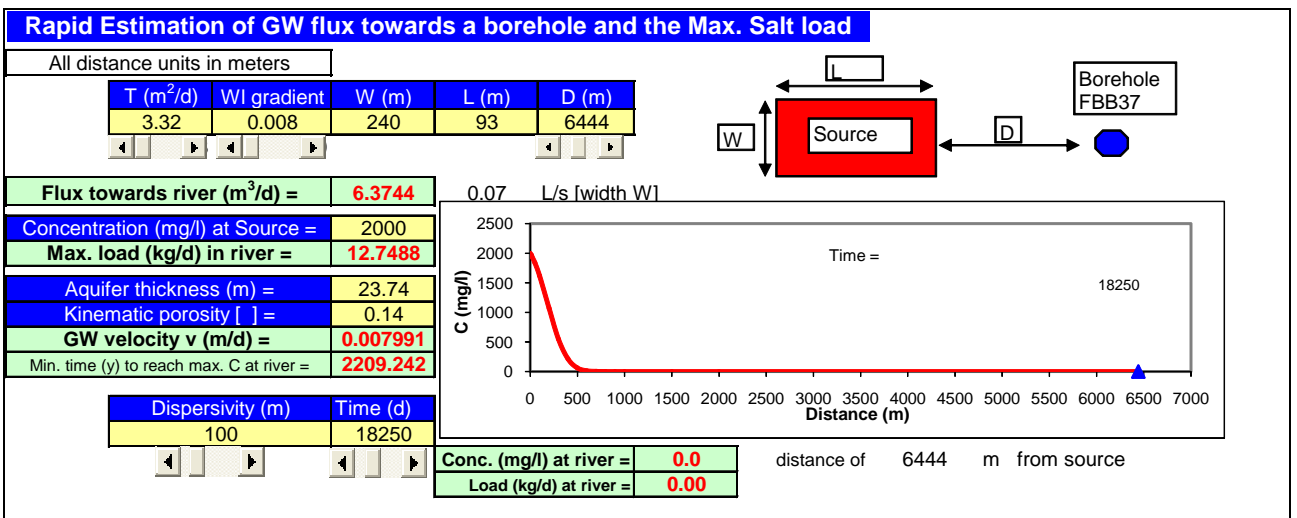
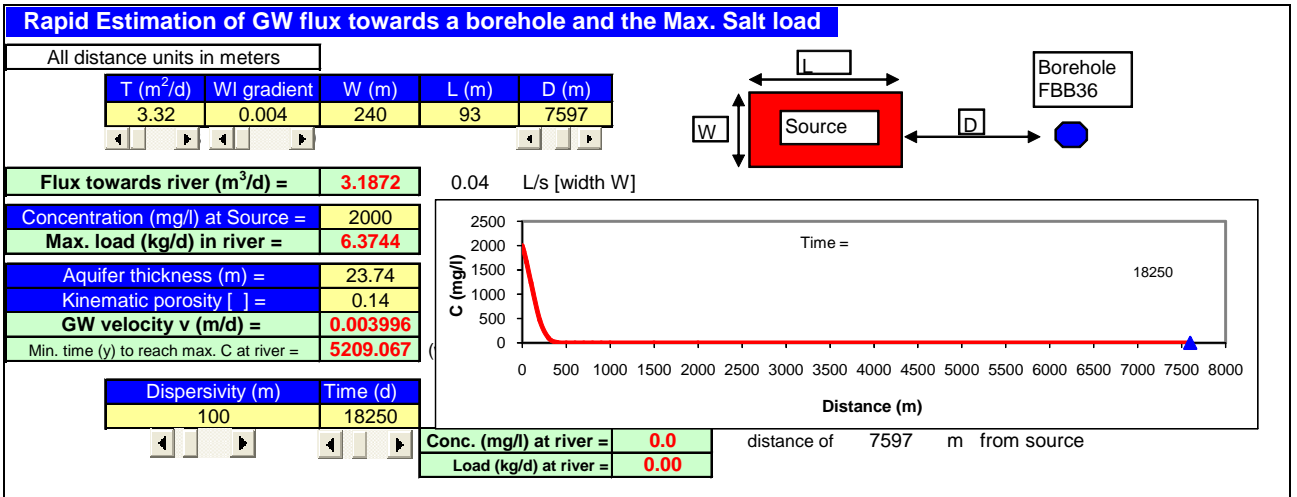
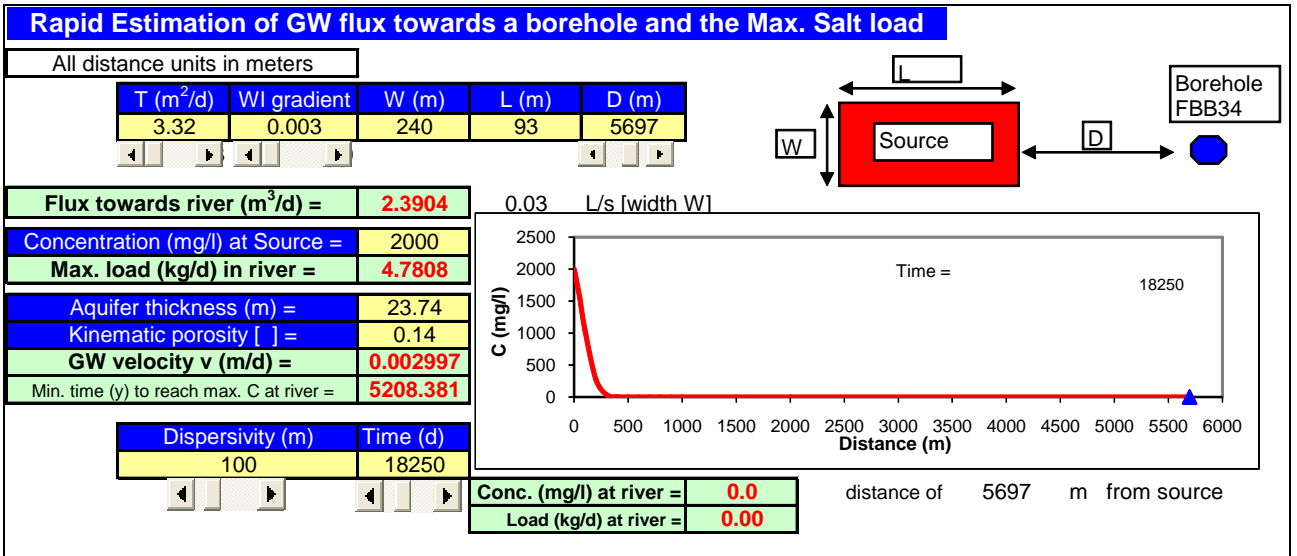
T (m ² /d)	WI gradient	W (m)	L (m)	D (m)
3.32	0.001	240	93	5434

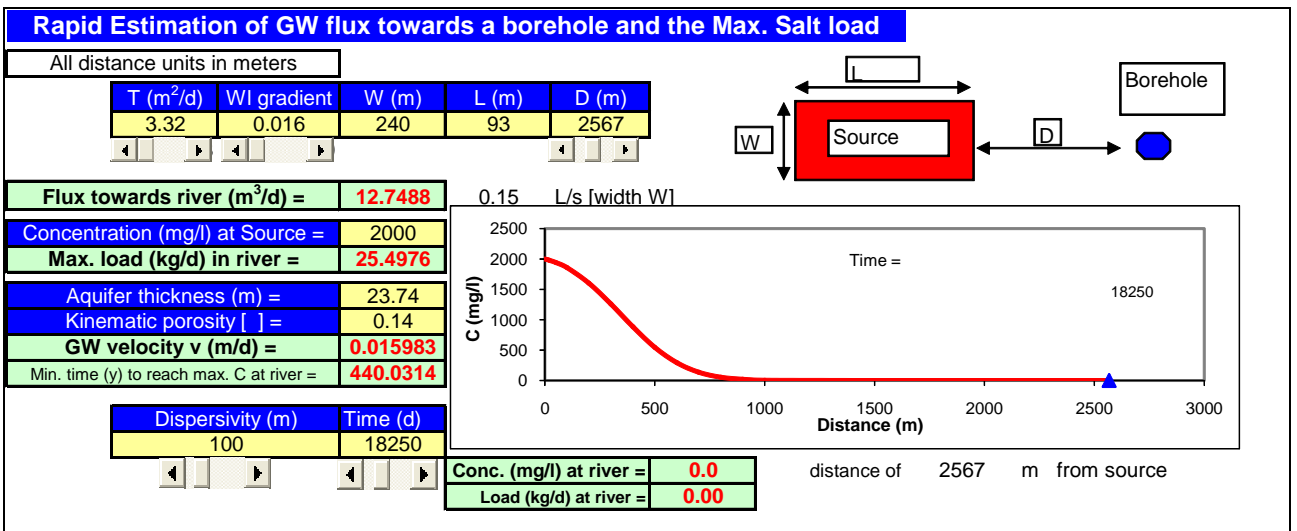
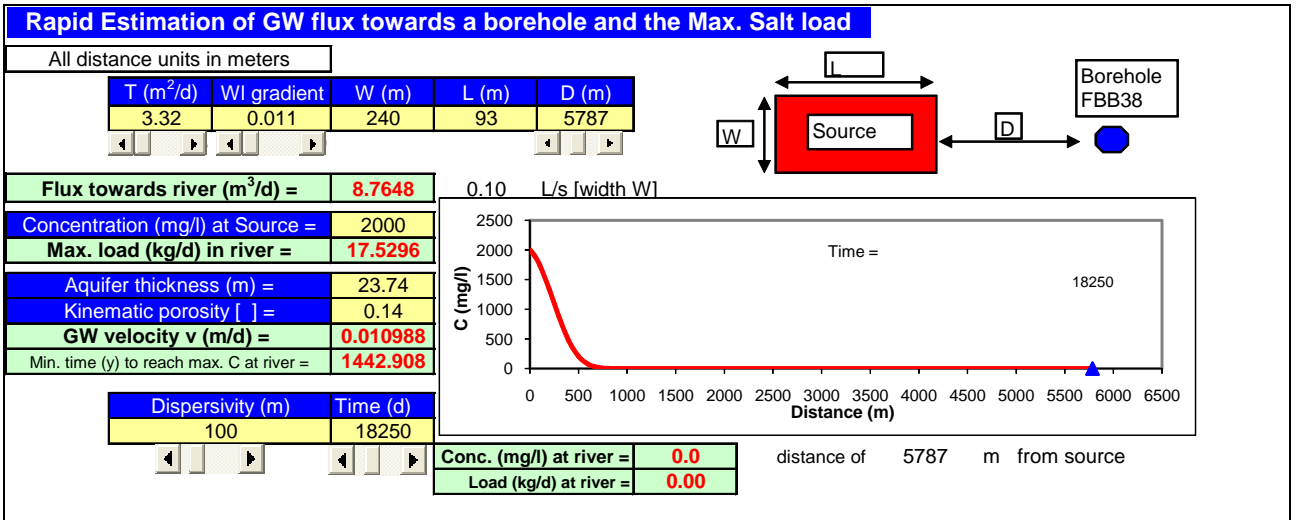
Flux towards river (m ³ /d) =	0.7968
Concentration (mg/l) at Source =	2000
Max. load (kg/d) in river =	1.5936
Aquifer thickness (m) =	23.74
Kinematic porosity [] =	0.14
GW velocity v (m/d) =	0.000999
Min. time (y) to reach max. C at river =	14903.81

0.01 L/s [width W]

Time = 18250

Conc. (mg/l) at river = 0.0 distance of 5434 m from source
 Load (kg/d) at river = 0.00





Ash stack settling dam

Rapid Estimation of GW flux towards a borehole and the Max. Salt load

All distance units in meters

T (m ² /d)	WI gradient	W (m)	L (m)	D (m)
3.32	0.004	143	142	5814

Flux towards river (m³/d) = **1.89904** 0.02 L/s [width W]

Concentration (mg/l) at Source =	326
Max. load (kg/d) in river =	0.619087
Aquifer thickness (m) =	23.7
Kinematic porosity [] =	0.14
GW velocity v (m/d) =	0.004002
Min. time (y) to reach max. C at river =	3979.793

Time = 18250

Conc. (mg/l) at river = **0.0** distance of 5814 m from source
 Load (kg/d) at river = **0.00**

Rapid Estimation of GW flux towards a borehole and the Max. Salt load

All distance units in meters

T (m ² /d)	WI gradient	W (m)	L (m)	D (m)
3.32	0.003	143	142	6324

Flux towards river (m³/d) = **1.42428** 0.02 L/s [width W]

Concentration (mg/l) at Source =	326
Max. load (kg/d) in river =	0.464315
Aquifer thickness (m) =	23.7
Kinematic porosity [] =	0.14
GW velocity v (m/d) =	0.003002
Min. time (y) to reach max. C at river =	5771.863

Time = 18250

Conc. (mg/l) at river = **0.0** distance of 6324 m from source
 Load (kg/d) at river = **0.00**

Rapid Estimation of GW flux towards a borehole and the Max. Salt load

All distance units in meters

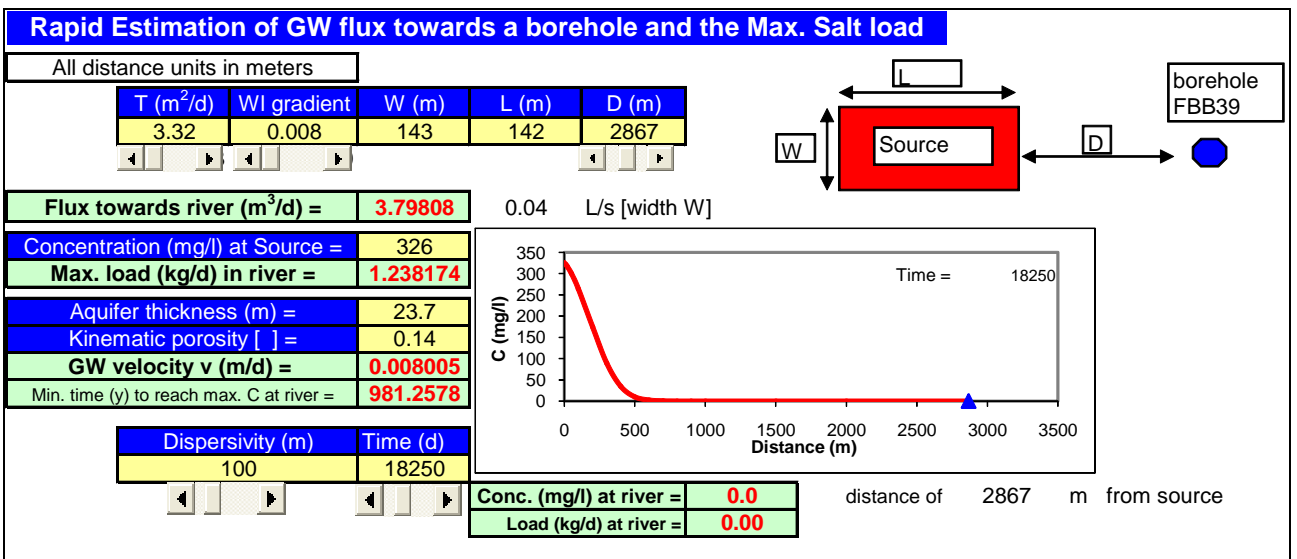
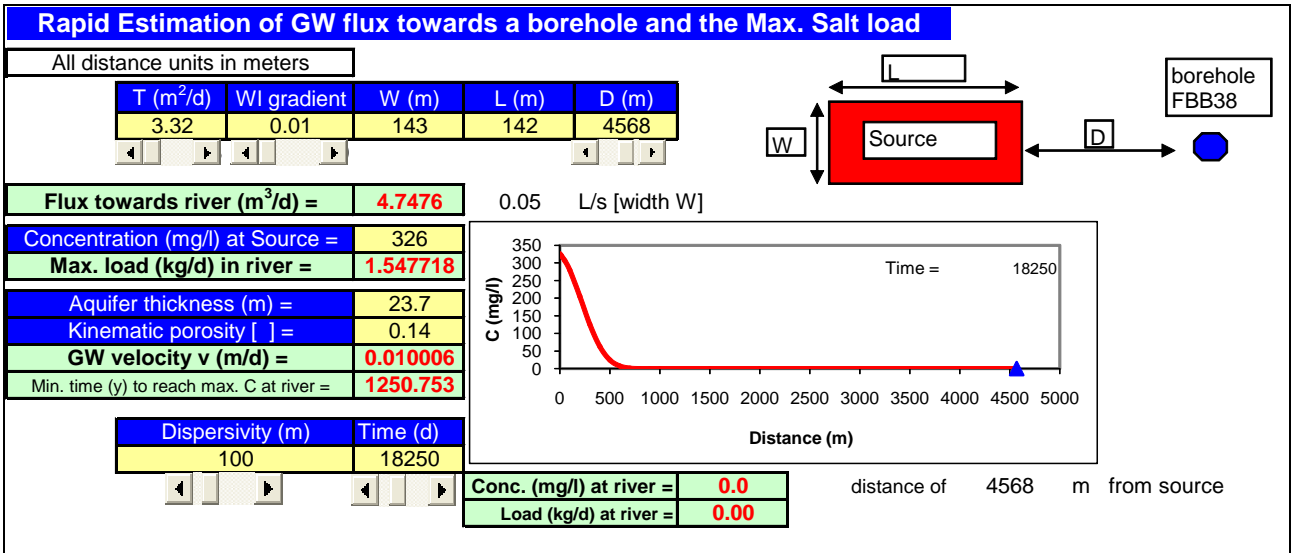
T (m ² /d)	WI gradient	W (m)	L (m)	D (m)
3.32	0.007	143	142	5169

Flux towards river (m³/d) = **3.32332** 0.04 L/s [width W]

Concentration (mg/l) at Source =	326
Max. load (kg/d) in river =	1.083402
Aquifer thickness (m) =	23.7
Kinematic porosity [] =	0.14
GW velocity v (m/d) =	0.007004
Min. time (y) to reach max. C at river =	2021.873

Time = 18250

Conc. (mg/l) at river = **0.0** distance of 5169 m from source
 Load (kg/d) at river = **0.00**



Coal stockyard settling dam

Rapid Estimation of GW flux towards a borehole and the Max. Salt load

All distance units in meters

T (m ² /d)	WI gradient	W (m)	L (m)	D (m)
3.32	0.004	118	98	4482

Flux towards river (m ³ /d) =	1.56704
Concentration (mg/l) at Source =	624
Max. load (kg/d) in river =	0.977833
Aquifer thickness (m) =	23.74
Kinematic porosity [] =	0.14
GW velocity v (m/d) =	0.003996
Min. time (y) to reach max. C at river =	3073.192

0.02 L/s [width W]

Time = 2670

Dispersivity (m)	Time (d)
100	2670

Conc. (mg/l) at river =	0.0
Load (kg/d) at river =	0.00

distance of 4482 m from source

Rapid Estimation of GW flux towards a borehole and the Max. Salt load

All distance units in meters

T (m ² /d)	WI gradient	W (m)	L (m)	D (m)
3.32	0.002	118	98	5082

Flux towards river (m ³ /d) =	0.78352
Concentration (mg/l) at Source =	624
Max. load (kg/d) in river =	0.488916
Aquifer thickness (m) =	23.74
Kinematic porosity [] =	0.14
GW velocity v (m/d) =	0.001998
Min. time (y) to reach max. C at river =	6969.193

0.01 L/s [width W]

Time = 18250

Dispersivity (m)	Time (d)
100	18250

Conc. (mg/l) at river =	0.0
Load (kg/d) at river =	0.00

distance of 5082 m from source

Rapid Estimation of GW flux towards a borehole and the Max. Salt load

All distance units in meters

T (m ² /d)	WI gradient	W (m)	L (m)	D (m)
3.32	0.002	118	98	5004

Flux towards river (m ³ /d) =	0.78352
Concentration (mg/l) at Source =	624
Max. load (kg/d) in river =	0.488916
Aquifer thickness (m) =	23.74
Kinematic porosity [] =	0.14
GW velocity v (m/d) =	0.001998
Min. time (y) to reach max. C at river =	6862.227

0.01 L/s [width W]

Time = 18250

Dispersivity (m)	Time (d)
100	18250

Conc. (mg/l) at river =	0.0
Load (kg/d) at river =	0.00

distance of 5004 m from source

Rapid Estimation of GW flux towards a borehole river and the Max. Salt load

All distance units in meters

T (m ² /d)	WI gradient	W (m)	L (m)	D (m)
3.32	0.005	118	98	4783

Flux towards river (m³/d) = **1.9588** 0.02 L/s [width W]

Concentration (mg/l) at Source = 624
 Max. load (kg/d) in river = **1.222291**

Aquifer thickness (m) = 23.7
 Kinematic porosity [] = 0.14
 GW velocity v (m/d) = **0.005003**
 Min. time (y) to reach max. C at river = **2619.243**

Dispersivity (m) = 100 Time (d) = 18250

Conc. (mg/l) at river = **0.0**
 Load (kg/d) at river = **0.00**

distance of 4783 m from source

Rapid Estimation of GW flux towards a borehole and the Max. Salt load

All distance units in meters

T (m ² /d)	WI gradient	W (m)	L (m)	D (m)
3.32	0.007	118	98	6796

Flux towards river (m³/d) = **2.74232** 0.03 L/s [width W]

Concentration (mg/l) at Source = 624
 Max. load (kg/d) in river = **1.711208**

Aquifer thickness (m) = 23.7
 Kinematic porosity [] = 0.14
 GW velocity v (m/d) = **0.007004**
 Min. time (y) to reach max. C at river = **2658.28**

Dispersivity (m) = 100 Time (d) = 18250

Conc. (mg/l) at river = **0.0**
 Load (kg/d) at river = **0.00**

distance of 6796 m from source

Rapid Estimation of GW flux towards a borehole and the Max. Salt load

All distance units in meters

T (m ² /d)	WI gradient	W (m)	L (m)	D (m)
3.32	0.009	118	98	7286

Flux towards river (m³/d) = **3.52584** 0.04 L/s [width W]

Concentration (mg/l) at Source = 624
 Max. load (kg/d) in river = **2.200124**

Aquifer thickness (m) = 23.7
 Kinematic porosity [] = 0.14
 GW velocity v (m/d) = **0.009005**
 Min. time (y) to reach max. C at river = **2216.624**

Dispersivity (m) = 100 Time (d) = 18250

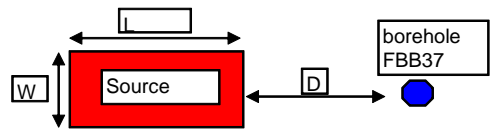
Conc. (mg/l) at river = **0.0**
 Load (kg/d) at river = **0.00**

distance of 7286 m from source

Rapid Estimation of GW flux towards a borehole and the Max. Salt load

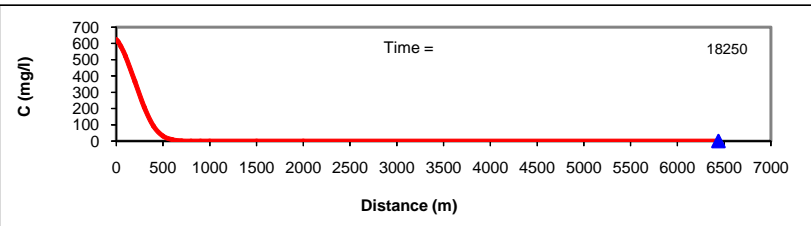
All distance units in meters

T (m ² /d)	WI gradient	W (m)	L (m)	D (m)
3.32	0.009	118	98	6439



Flux towards river (m³/d) = **3.52584** 0.04 L/s [width W]

Concentration (mg/l) at Source =	624
Max. load (kg/d) in river =	2.200124
Aquifer thickness (m) =	23.7
Kinematic porosity [] =	0.14
GW velocity v (m/d) =	0.009005
Min. time (y) to reach max. C at river =	1958.941



Time = 18250

Conc. (mg/l) at river = **0.0**
Load (kg/d) at river = **0.00**

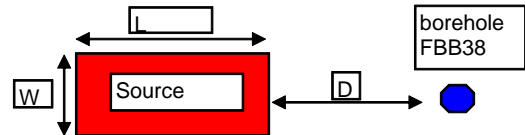
distance of 6439 m from source

Dispersivity (m)	Time (d)
100	18250

Rapid Estimation of GW flux towards a borehole and the Max. Salt load

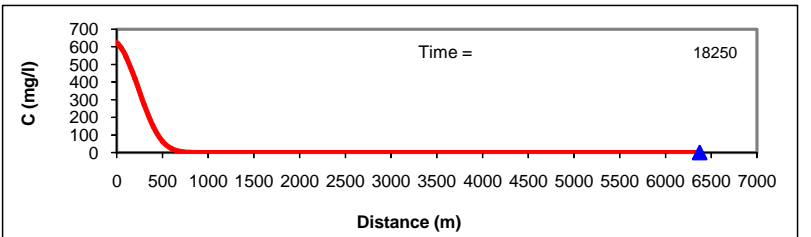
All distance units in meters

T (m ² /d)	WI gradient	W (m)	L (m)	D (m)
3.32	0.011	118	98	6373



Flux towards river (m³/d) = **4.30936** 0.05 L/s [width W]

Concentration (mg/l) at Source =	624
Max. load (kg/d) in river =	2.689041
Aquifer thickness (m) =	23.7
Kinematic porosity [] =	0.14
GW velocity v (m/d) =	0.011007
Min. time (y) to reach max. C at river =	1586.341



Time = 18250

Conc. (mg/l) at river = **0.0**
Load (kg/d) at river = **0.00**

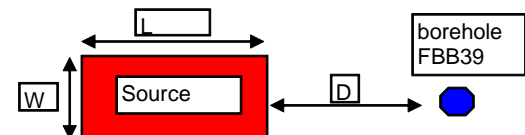
distance of 6373 m from source

Dispersivity (m)	Time (d)
100	18250

Rapid Estimation of GW flux towards a borehole and the Max. Salt load

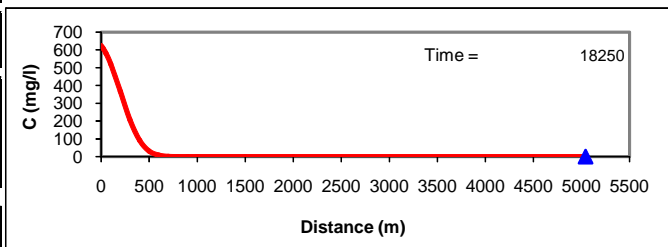
All distance units in meters

T (m ² /d)	WI gradient	W (m)	L (m)	D (m)
3.32	0.009	118	98	5044



Flux towards river (m³/d) = **3.52584** 0.04 L/s [width W]

Concentration (mg/l) at Source =	624
Max. load (kg/d) in river =	2.200124
Aquifer thickness (m) =	23.7
Kinematic porosity [] =	0.14
GW velocity v (m/d) =	0.009005
Min. time (y) to reach max. C at river =	1534.539



Time = 18250

Conc. (mg/l) at river = **0.0**
Load (kg/d) at river = **0.00**

distance of 5044 m from source

Dispersivity (m)	Time (d)
100	18250

Dirty water dam

Rapid Estimation of GW flux towards a borehole and the Max. Salt load

All distance units in meters

T (m ² /d)	WI gradient	W (m)	L (m)	D (m)
3.32	0.004	524	256	6347

Flux towards river (m³/d) = **6.95872** 0.08 L/s [width W]

Concentration (mg/l) at Source =	326
Max. load (kg/d) in river =	2.268543
Aquifer thickness (m) =	23.7
Kinematic porosity [] =	0.14
GW velocity v (m/d) =	0.004002
Min. time (y) to reach max. C at river =	4344.641

Conc. (mg/l) at river = **0.0**
Load (kg/d) at river = **0.00**

distance of 6347 m from source

Rapid Estimation of GW flux towards a borehole and the Max. Salt load

All distance units in meters

T (m ² /d)	WI gradient	W (m)	L (m)	D (m)
3.32	0.002	524	256	6858

Flux towards river (m³/d) = **3.47936** 0.04 L/s [width W]

Concentration (mg/l) at Source =	326
Max. load (kg/d) in river =	1.134271
Aquifer thickness (m) =	23.7
Kinematic porosity [] =	0.14
GW velocity v (m/d) =	0.002001
Min. time (y) to reach max. C at river =	9388.861

Conc. (mg/l) at river = **0.0**
Load (kg/d) at river = **0.00**

distance of 6858 m from source

Rapid Estimation of GW flux towards a borehole and the Max. Salt load

All distance units in meters

T (m ² /d)	WI gradient	W (m)	L (m)	D (m)
3.32	0.006	524	256	5760

Flux towards river (m³/d) = **10.43808** 0.12 L/s [width W]

Concentration (mg/l) at Source =	326
Max. load (kg/d) in river =	3.402814
Aquifer thickness (m) =	23.7
Kinematic porosity [] =	0.14
GW velocity v (m/d) =	0.006004
Min. time (y) to reach max. C at river =	2628.553

Conc. (mg/l) at river = **0.0**
Load (kg/d) at river = **0.00**

distance of 5760 m from source

Rapid Estimation of GW flux towards a borehole and the Max. Salt load

All distance units in meters

T (m ² /d)	WI gradient	W (m)	L (m)	D (m)
3.32	0.008	524	256	5259

Flux towards river (m³/d) =	13.91744
Concentration (mg/l) at Source =	326
Max. load (kg/d) in river =	4.537085
Aquifer thickness (m) =	23.7
Kinematic porosity [] =	0.14
GW velocity v (m/d) =	0.008005
Min. time (y) to reach max. C at river =	1799.942

Dispersivity (m)	Time (d)
100	18250

0.16 L/s [width W]

Time = 18250

Conc. (mg/l) at river = **0.0**

Load (kg/d) at river = **0.00**

distance of 5259 m from source

Rapid Estimation of GW flux towards a borehole and the Max. Salt load

All distance units in meters

T (m ² /d)	WI gradient	W (m)	L (m)	D (m)
3.32	0.007	524	256	3155

Flux towards river (m³/d) =	12.17776
Concentration (mg/l) at Source =	326
Max. load (kg/d) in river =	3.96995
Aquifer thickness (m) =	23.7
Kinematic porosity [] =	0.14
GW velocity v (m/d) =	0.007004
Min. time (y) to reach max. C at river =	1234.09

Dispersivity (m)	Time (d)
100	18250

0.14 L/s [width W]

Time = 18250

Conc. (mg/l) at river = **0.0**

Load (kg/d) at river = **0.00**

distance of 3155 m from source

Settling Dam

Rapid Estimation of GW flux towards a borehole and the Max. Salt load

All distance units in meters

T (m ² /d)	WI gradient	W (m)	L (m)	D (m)
3.32	0.003	163	116	6294

Flux towards river (m³/d) = **1.62348** 0.02 L/s [width W]

Concentration (mg/l) at Source =	315
Max. load (kg/d) in river =	0.511396
Aquifer thickness (m) =	23.7
Kinematic porosity [] =	0.14
GW velocity v (m/d) =	0.003002
Min. time (y) to reach max. C at river =	5744.483

Dispersivity (m)	Time (d)
100	18250

Conc. (mg/l) at river =	0.0	distance of 6294 m from source
Load (kg/d) at river =	0.00	

Rapid Estimation of GW flux towards a borehole and the Max. Salt load

All distance units in meters

T (m ² /d)	WI gradient	W (m)	L (m)	D (m)
3.32	0.002	163	116	6805

Flux towards river (m³/d) = **1.08232** 0.01 L/s [width W]

Concentration (mg/l) at Source =	315
Max. load (kg/d) in river =	0.340931
Aquifer thickness (m) =	23.7
Kinematic porosity [] =	0.14
GW velocity v (m/d) =	0.002001
Min. time (y) to reach max. C at river =	9316.302

Dispersivity (m)	Time (d)
100	18250

Conc. (mg/l) at river =	0.0	distance of 6805 m from source
Load (kg/d) at river =	0.00	

Rapid Estimation of GW flux towards a borehole and the Max. Salt load

All distance units in meters

T (m ² /d)	WI gradient	W (m)	L (m)	D (m)
3.32	0.005	163	116	5682

Flux towards river (m³/d) = **2.7058** 0.03 L/s [width W]

Concentration (mg/l) at Source =	315
Max. load (kg/d) in river =	0.852327
Aquifer thickness (m) =	23.7
Kinematic porosity [] =	0.14
GW velocity v (m/d) =	0.005003
Min. time (y) to reach max. C at river =	3111.549

Time = 18250

Conc. (mg/l) at river = **0.0** distance of 5682 m from source
 Load (kg/d) at river = **0.00**

Rapid Estimation of GW flux towards a borehole and the Max. Salt load

All distance units in meters

T (m ² /d)	WI gradient	W (m)	L (m)	D (m)
3.32	0.008	163	116	5129

Flux towards river (m³/d) = **4.32928** 0.05 L/s [width W]

Concentration (mg/l) at Source =	315
Max. load (kg/d) in river =	1.363723
Aquifer thickness (m) =	23.7
Kinematic porosity [] =	0.14
GW velocity v (m/d) =	0.008005
Min. time (y) to reach max. C at river =	1755.449

Time = 18250

Conc. (mg/l) at river = **0.0** distance of 5129 m from source
 Load (kg/d) at river = **0.00**

Rapid Estimation of GW flux towards a borehole and the Max. Salt load

All distance units in meters

T (m ² /d)	WI gradient	W (m)	L (m)	D (m)
3.32	0.007	163	116	2957

Flux towards river (m³/d) = **3.78812** 0.04 L/s [width W]

Concentration (mg/l) at Source =	315
Max. load (kg/d) in river =	1.193258
Aquifer thickness (m) =	23.7
Kinematic porosity [] =	0.14
GW velocity v (m/d) =	0.007004
Min. time (y) to reach max. C at river =	1156.641

Time = 18250

Conc. (mg/l) at river = **0.0** distance of 2957 m from source
 Load (kg/d) at river = **0.00**

Appendix G Borehole logs

